5-$HT_{2A/2C}$ receptor modulation of absence seizures and characterization of the GHB-model

A thesis submitted to Cardiff University for the degree of Doctor of Philosophy
by

Marcello Venzi (MSc)

School of Biosciences, Cardiff University, October 2014

Declaration and Statements

This work has not been submitted in substance for any other degree or award at this or any other university or place of learning, nor is being submitted concurrently in candidature for any degree or other award.

Signed …… (candidate) Date ……

STATEMENT 1

This thesis is being submitted in partial fulfillment of the requirements for the degree of PhD .

Signed …… (candidate) Date ……

STATEMENT 2

This thesis is the result of my own independent work/investigation, except where otherwise stated. Other sources are acknowledged by explicit references. The views expressed are my own.

Signed …… (candidate) Date ……

STATEMENT 3

I hereby give consent for my thesis, if accepted, to be available for photocopying and for inter-library loan, and for the title and summary to be made available to outside organisations.

Signed …… (candidate) Date ……

STATEMENT 4: PREVIOUSLY APPROVED BAR ON ACCESS

I hereby give consent for my thesis, if accepted, to be available for photocopying and for inter-library loans **after expiry of a bar on access previously approved by the Academic Standards & Quality Committee.**

Signed …… (candidate) Date ……

Summary

Absence seizures (ASs) are non-convulsive epileptic events which are common in pediatric and juvenile epilepsies. They consist of EEG generalized spike-and-wave-discharges (SWDs) accompanied by an impairment of consciousness and are expressed within the thalamocortical network. This thesis initially focused on investigating the modulation of ASs by two serotonin receptors (5-HTRs), 5-HT_{2A} and 5-HT_{2C}, in a polygenic (i.e. Genetic Absence Epilepsy Rats from Strasbourg, GAERS) and a pharmacological (i.e. γ-hydroxybutyrate, GHB) model of ASs. It was found that, in GAERS, pharmacological activation of 5-$HT_{2A/C}$Rs blocked ASs, whereas 5-HT_{2A}R antagonists increased seizure length. However, experiments on the GHB-model revealed that GHB induced not only ASs but also a period of sedation/hypnosis, a behavioural state that had been neglected in the literature. Thus, the rest of this thesis was devoted to further characterizing the GHB-model. The main result was that GHB-elicited ASs can be distinguished at the level of both EEG and behaviour. *In vivo* characterization of thalamic firing during GHB-elicited ASs and hypnosis via silicon probes in freely moving animals revealed that both states were accompanied by a decrease in firing rate. In particular, contrary to what was predicted by *in vitro* and *in vivo* experiments under neurolept anaesthesia, T-type Ca^{2+} channel-dependent burst firing in thalamic neurons was found in <10% of spike-and-wave complexes of SWDs. The prevalent activity of *nucleus reticularis thalami* neurons during ASs was either silence or tonic firing. Indeed, thalamic application of the potent T-type channel antagonist, TTAP-2, by reverse microdialysis did not affect GHB-elicited ASs. Finally, the development of an algorithm to classify GHB-elicited ASs demonstrated that the spectral properties of SWDs can be used to discriminate hypnosis and SWDs. Moreover, spectral coherence can be used in different experimental models of ASs to characterize SWDs according to their waveform regularity.

Collaborations

Animal implantations and data collection in Chapter 5 were performed together with Dr. François David.

Acknowledgements

First and foremost I would like to thank my supervisor, Vincenzo for his support throughout my PhD and for always having time for me no matter how busy he was. Secondly, I am grateful to all members of the Crunelli lab, in particular Cian and François: Cian for his help in teaching me surgery and for our discussions, which helped to keep alive my interest in science and Francois, for honing my matlab skills and teaching me spike sorting, and for showing me what it takes to stay at the top of the food chain. Also, Bill, for the chats about pharmacology, statistics, electrophysiology, and all the other areas of science in which my knowledge is sorely lacking, Tim, for his help with histological analysis, and Hannah, for giving me motivational treats whilst I was writing this thesis! Thirdly, I would like to thank Cristiano, for his expertise in 5-HT immunohistochemistry, and Giuseppe for helping me to find a serotinergic drug.

Table of contents

Abbreviations

aCSF	Artificial cerebrospinal fluid
AMPA	α-amino-3-hydroxy-5-methyl-isoxazolepropionic acid
AS	Absence seizure
CAE	Childhood absence epilepsy
CNS	Central nervous system
dLGN	Dorsal lateral geniculate nucleus
EPSC	Excitatory postsynaptic current
EPSP	Excitatory postsynaptic potential
EEG	Electroencephalogram
ETX	Ethosuximide
fMRI	Functional magnetic resonance imaging
FPGE	Feline penicillin generalised epilepsy
GABA	γ-aminobutyric acid
$GABA_AR$	γ-aminobutyric acid receptor type A
$GABA_BR$	γ-aminobutyric acid receptor type B
GAERS	Genetic absence epilepsy rats from Strasbourg
GAT-1	GABA transporter type 1
GBL	γ-butyrolactone
GHB	γ-hydroxybutyrate
GHBR	γ-hydroxybutyrate receptor
GPCR	G-protein coupled receptor
HVA	High voltage activated
ILAE	International League Against Epilepsy

i.m.	Intra-muscular
IPSC	Inhibitory postsynaptic current
IPSP	Inhibitory postsynaptic potential
i.p.	Intra-peritoneal
Ih	Hyperpolarisation-activated current
I_T	T-type Ca2+ current
i.v.	Intravenous
JAE	Juvenile absence epilepsy
JME	Juvenile myoclonic epilepsy
KCl	Potassium chloride
LFP	Local field potential
LTCP	Low-threshold calcium potential
LVA	Low voltage activated
MoCtx	Motor cortex
mGluR	Metabotropic glutamate receptor NEC Non-epileptic control
NMDA	N-methyl-D-aspartate
NRT	Nucleus reticularis thalami
PTZ	Pentylenetetrazol
S1po	Perioral region of the somatosensory cortex
stg	Stargazer mutant mouse
SWC	Spike-and-wave complex
SWD	Spike-and-wave discharge
TC	Thalamocortical
TTX	Tetrodotoxin
WAG/Rij	Wistar albino Glaxo rats from Rijswijk
WT	Wild-type

VB	Ventrobasal complex
VPL	Ventroposterolateral nucleus
VPM	Ventroposteromedial nucleus
VGCC	Voltage-gated Ca^{2+} channels
VGSC	Voltage-gated Na^{+} channels

Chapter 1 INTRODUCTION

In this chapter I will introduce the background information necessary to understand the aims of this thesis. In particular, I will outline the characteristics of typical absence seizures (ASs), the thalamocortical (TC) network within which they are generated and the animal models that have been used to study ASs experimentally. Finally, I will describe the serotoninergic system and its relevance to the modulation of ASs.

1.1 Classification of epileptic seizures and epilepsies

An epileptic seizure is defined as the manifestation of excessive, hypersynchronous, neuronal activity in the brain (Fisher et al., 2005). The classification of seizures and epilepsies has changes over the last few years to reflect advancements in genetics and in imaging studies (Berg et al., 2010; Berg and Scheffer, 2011). In this section this new terminology will primarily be adopted, although the old terminology (Blume et al., 2001; Engel, 2001), will still be used at times.

Epileptic seizures can be subdivided into two main groups (see **Table 1.1**): generalized and focal. Generalized epileptic seizures are defined as "originating at some point within, and rapidly engaging, bilaterally distributed networks" (Berg et al., 2010). Focal epileptic seizures are defined as "originating within networks limited to one hemisphere" (Berg et al., 2010). Various subtypes of generalized seizure have been described according to their EEG and behavioural manifestations (summarized in **Table 1.1**). Epileptic seizures are also grouped according to their etiology: seizures can have a genetic (formerly characterized as idiopathic) or a structural/metabolic origin (e.g. stroke, trauma).

Epilepsies, neurological disorders characterized by reoccurring seizures (Fisher et al., 2005), are grouped into electroclinical syndromes, constellations and structural/metabolic epilepsies (as the traditional distinction between epileptic syndromes and epileptic diseases has been officially dropped, Berg et. al., 2010). A summary of the current classification of epilepsies is presented in **Table 1.2**.

Table 1.1 Classification of seizures

Generalized seizures	Tonic–clonic (in any combination)	
	Absence	Typical
		Atypical
	Absence with special features	Myoclonic absence
		Eyelid myoclonia
	Myoclonic	Myoclonic
		Myoclonic atonic
		Myoclonic tonic
	Clonic	
	Tonic	
	Atonic	
Focal seizures		
Unknown	Epileptic spasms	

Modified from (Berg et al., 2010).

Table 1.2 Electroclinical syndromes and other epilepsies.

Electroclinical syndromes arranged by age at onset	
Neonatal period	Benign familial neonatal epilepsy (BFNE)
	Early myoclonic encephalopathy (EME)
	Ohtahara syndrome
Infancy	Epilepsy of infancy with migrating focal seizures
	West syndrome
	Myoclonic epilepsy in infancy (MEI)
	Benign infantile epilepsy
	Benign familial infantile epilepsy
	Dravet syndrome
	Myoclonic encephalopathy in nonprogressive disorders
Childhood	Febrile seizures plus (FS+) (can start in infancy)
	Panayiotopoulos syndrome
	Epilepsy with myoclonic atonic (previously astatic) seizures
	Benign epilepsy with centrotemporal spikes (BECTS)
	Autosomal-dominant nocturnal frontal lobe epilepsy (ADNFLE)
	Late onset childhood occipital epilepsy (Gastaut type)
	Epilepsy with myoclonic absences
	Lennox-Gastaut syndrome
	Epileptic encephalopathy with continuous spike-and-wave during sleep (CSWS)
	Landau-Kleffner syndrome (LKS)
	Childhood absence epilepsy (CAE)
Adolescence – Adult	Juvenile absence epilepsy (JAE)
	Juvenile myoclonic epilepsy (JME)
	Epilepsy with generalized tonic–clonic seizures alone
	Progressive myoclonus epilepsies (PME)
	Autosomal dominant epilepsy with auditory features (ADEAF)
	Other familial temporal lobe epilepsies
Less specific age relationship	Familial focal epilepsy with variable foci (childhood to adult)
	Reflex epilepsies
Distinctive constellations	
	Mesial temporal lobe epilepsy with hippocampal sclerosis (MTLE with HS)
	Rasmussen syndrome
	Gelastic seizures with hypothalamic hamartoma
	Hemiconvulsion–hemiplegia–epilepsy
Epilepsies attributed to and organized by structural-metabolic causes	
	Malformations of cortical development (hemimegalencephaly, heterotopias, etc.)
	Neurocutaneous syndromes (tuberous sclerosis complex, Sturge-Weber, etc.)
	Tumor
	Infection
	Trauma
	Angioma
	Perinatal insults
	Stroke
Conditions with epileptic seizures that are traditionally not diagnosed as a form of epilepsy per se	
	Benign neonatal seizures (BNS)
	Febrile seizures (FS)

Epilepsies that have ASs as part of their manifestation are shaded in grey. Modified from (Berg et al., 2010).

1.2 Typical absence seizures

A typical[1] ASs is a generalized, non-convulsive, seizure that consists of an impairment of consciousness accompanied in the electroencephalogram (EEG) by 2.5-4 Hz 'spike and slow-wave discharges' (SWDs) (Panayiotopoulos, 1999; Crunelli and Leresche, 2002) (**Figure 1.1**). Notably, it has become increasingly recognized that the EEG morphology of typical ASs can vary quite substantially compared to the 'textbook' representation, since often the spike component of the spike-wave complex (SWC) is reduced in amplitude or appears to be buried inside the wave, in particular during the terminal phase of a SWD (Sogawa et al., 2009) (**Figure 1.1**, see also **Figure 4.7A**).

Typical ASs are brief (9.4 ± 7 seconds; range 1–44 seconds, (Sadleir et al., 2006)) and start and end abruptly; there is no aura or postictal depression (Panayiotopoulos, 2001; Crunelli and Leresche, 2002). During a typical AS the patient stops any direct movement but some behavioural automatisms (e.g. lip smacking, eyelid flutters, chewing) can appear (Panayiotopoulos, 1999, 2001).

The extent of the impairment of consciousness is variable among individuals, and between seizures in the same individual. Clinically the impairment of consciousness is defined by a lack of responsiveness to external stimuli during the seizure, a temporary interruption of an ongoing task (although simple repetitive tasks can continue during ASs) and/or the inability to recall, after seizure termination, a stimulus that had occurred ictally (Panayiotopoulos, 1999; Blumenfeld, 2012). Typical ASs can be provoked by hypoventilation (Panayiotopoulos, 1999, 2001)

The pathophysiological mechanisms of ASs are only partly understood, but it is well established that ASs are generated by abnormal electrical activity in reciprocally connected

[1] Atypical ASs have also being described (DiMario and Clancy, 1988; Tenney and Glauser, 2013). The main differences with typical ASs are that during atypical ASs consciousness is sometimes preserved; moreover atypical ASs have a less abrupt onset and termination and they can last up to minutes. The frequency of the generalized SWDs is 1.5-2.5Hz, lower than for with typical ASs, and the ictal EEG patter is heterogenous, often asymmetrical and contains other fast EEG activities (Panayiotopoulos, 2008). Behaviourally they are accompanied by more pronounced motor symptoms (e.g. jerking).

thalamic and cortical territories, i.e. the thalamocortical (TC) network (Williams, 1953; Crunelli and Leresche, 2002; Blumenfeld, 2005). Imaging studies in humans have shown that the cerebellum and limbic structures (such as the hippocampus) are not involved in the expression of typical ASs (Moeller et al., 2008; Bai et al., 2010; Berman et al., 2010).

According to the current classification, typical ASs (hereafter simply referred as ASs for brevity) are found in three main types of epilepsies: childhood absence epilepsy (CAE) (where ASs are the only symptom), juvenile absence epilepsy (where in >80% of patients they co-occur with generalized tonic-clonic seizures) and Jeavons syndrome (where ASs are accompanied by a prominent eyelid myoclonia). In addition to these syndromes, ASs may also occur in other generalized epilepsies, where, however, they are not considered a distinctive feature of the disease (Panayiotopoulos, 2008) (see **Table 1.2**).

Due to the fact that in CAE ASs appear in the absence of other comorbidities, and that CAE is the best-characterized epilepsy displaying this type of seizures, in the next section this epileptic syndrome will be used to further explore the clinical and pathophysiological properties of human ASs.

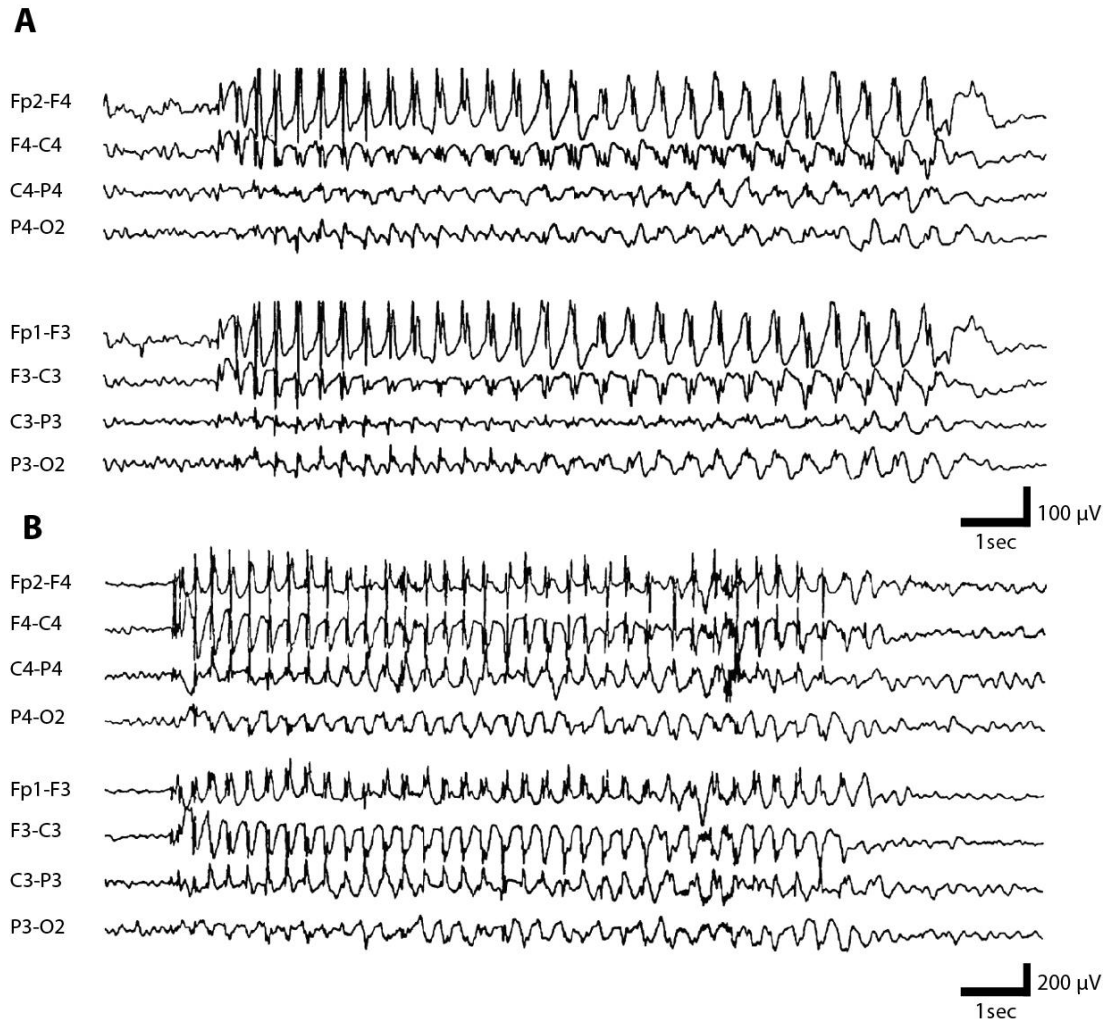

Figure 1.1. SWDs: the EEG hallmark of ASs. (A) Scalp EEG of a 14 year-old girl diagnosed with JME. (B) Scalp EEG of a 8 year old diagnosed with CAE. 4 channels are presented for each cerebral emisphere (FP= fronto-parietal; C= central; O=occipital; F=frontal; P=parietal). Adapted from (Panayiotopoulos, 2008).

1.2.1 Childhood absence epilepsy (CAE)

1.2.1.1 General features and epidemiology

CAE is the most common childhood epilepsy syndrome, occurring in 10-17% of children with epilepsy (Berg et al., 2000; Jallon et al., 2001). The onset is between 4 and 10 years (peaking between 5 and 7 years) (Fisher et al., 2005). Females are generally reported to be more affected than males (Matricardi et al., 2014). As mentioned above, ASs are the only symptom of this syndrome. The number of ASs is variable among patients and within the same patient, ranging from a few to several hundred per day (Crunelli and Leresche, 2002). The incidence of ASs in CAE depends on multiple factor such as the emotional state of the patient and the circadian rhythm (Leresche et al., 2011). In particular, ASs are observed more often during quiet wakefulness and light (NREM) sleep (Horita et al., 1991; Halász et al., 2002).

Importantly, CAE is not associated with any developmental or neurological abnormality (e.g. gross morphological alterations in the brain) (Crunelli and Leresche, 2002; Panayiotopoulos, 2008).

1.2.1.2 Neural substrates and generalized nature of CAE ASs

As mentioned above, CAE ASs are thought to be expressed within the TC network. In addition to invasive electrophysiological evidence (Williams, 1953), new studies using fMRI also indicate the involvement of thalamic territories in human ASs (Bai et al., 2010; Berman et al., 2010). A contribution of other regions such as the basal ganglia or the brainstem has been suggested by some studies, but the relevance of these areas to the expression of ASs is unclear (Motelow and Blumenfeld, 2009). Moreover, the blood-oxygen-level dependent (BOLD) signal of fMRI does not measure neuronal activity; thus, it is currently impossible to conclusively link patterns of increases or decreases in the BOLD signal to changes in neuronal excitability.

A long-standing claim in the field of ASs was that seizures are fully generalized from the start (Gloor, 1968); however, it is now accepted that this is not the case, as can be appreciated by the recent change in the definition of generalized seizures (section 1.1). The idea of a local initiation in generalized ASs stemmed from two studies in well-established polygenic rat models of ASs (Meeren et al., 2002; Polack et al., 2007) which suggested a cortical initiation site, in the perioral region of the somatosensory cortex (S1po). Since then, human EEG and MEG studies have confirmed this observation (Holmes et al., 2004; Tucker et al., 2007; Westmijse et al., 2009; Hu et al., 2011), although, due to the non-invasive nature of these studies, a putative thalamic initiation could not be investigated. fMRI studies further confirmed the idea of a cortical initiation site, in fact BOLD changes in the thalamus were observed only after seizure termination (Bai et al., 2010; Berman et al., 2010) (**Figure 1.2**).

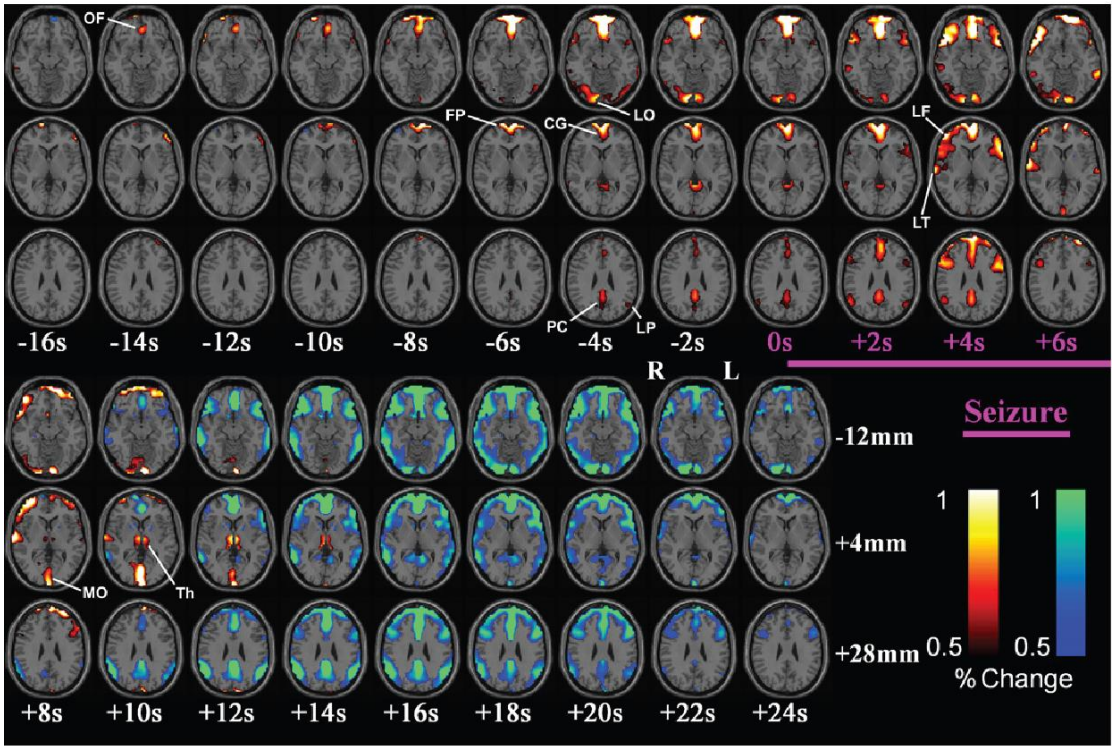

Figure 1.2. fMRI evidence of a cortical initiation site in ASs. Around 6 seconds before the initiation of ASs positive changes (warm colors) in the BOLD signal are detected in the frontal polar (FP), later parietal (LP), precuneus (PC), cingulate (FG) and lateral occipital (LO) cortex. An increase in the thalamus (Th) appears only after the end of the seizure. Decreases in the BOLD signal (cool colors) also follow seizure termination. Data is the group analysis over 8 subjects. Taken from (Bai et al., 2010).

Within the cortex, the initiation appears to vary both among patients and between seizures in the same patient, although frontal-lateral and medial-parietal cortices are the most common sources of seizure onset (Holmes et al., 2004; Westmijse et al., 2009; Bai et al., 2010).

1.2.1.3 **Etiology**

CAE is a genetically determined disease, with a complex polygenic inheritance (Crunelli and Leresche, 2002) and 15% to 44% of children diagnosed with CAE have a positive family history (Panayiotopoulos, 1999). Studies on monozygotic twins reveled a concordance of 70 % to 84%, which drops to 33% for first-degree relatives (Lennox, 1960; Berkovic et al., 1998).

Only few genes have been associated with CAE; most of these are involved in neurotransmission and neuronal excitability. Notable examples are genes coding for subunits of $GABA_A$ receptors or of voltage-dependent Ca^{2+} channels (Crunelli and Leresche, 2002; Yalçın, 2012).

Two different mutations have been found in the GABRG2 gene, which codes for the γ2 subunit of $GABA_A$ receptors (Wallace et al., 2001; Tian and Macdonald, 2012). These mutations were associated with a loss-of-function of the $GABA_A$ receptor (Wallace et al., 2001; Kang et al., 2004). Multiple mutations on the GABRB3 gene, which codes for the β3 subunit of the $GABA_A$ receptor, were also associated with CAE, although these findings were not replicated in all cohorts originating from different ethnic groups (Hempelmann et al., 2007; Heron et al., 2007b; Tanaka et al., 2008; Lachance-Touchette et al., 2010).

Interestingly, no association has been reported for $GABA_B$ receptors, which have been systemically implicated in the pathogenesis of experimental ASs (see section 1.4.1).

Associations between CAE and mutations in both P/Q-type (Cav2) and T-type (Cav3) Ca^{2+} channels have also been reported. Two mutations in the gene CACNA1A, coding for Cav2.1 channels, induce a loss-of-function in the protein, resulting in a reduced Ca^{2+} current (Jouvenceau et al., 2001; Imbrici et al., 2004). These mutations were linked in humans to ASs but also to ataxia. Importantly, two monogenic mouse models of ASs, tottering and leaner (see section 1.4.1), which display ASs together with ataxia, also have mutations on

the CACNA1A gene. Similarly to the human mutation, the Cav2.1 channels of these mice have a reduced Cav2.1-dependent Ca^{2+} current (Fletcher et al., 1996; Doyle et al., 1997; Wakamori et al., 1998).

Several mutations in the CACNA1H gene, coding for Cav3.2 channels, have been associated with CAE in Chinese cohorts (Chen et al., 2003; Liang et al., 2006). These mutations produced a gain-of-function of the channels, with an increase in Ca^{2+} current (Heron et al., 2007a). No link between CAE and either CACNA1G or CACNA1I has been found so far (Chen et al., 2003). Nonetheless, various experimental evidence suggests that T-type Ca^{2+} channels, and in particular Cav3.1 channels, could be involved in the pathogenesis of ASs. This evidence will be discussed in section 1.5.2.

In conclusion, the lack of a strong association between individual genes and CAE supports the polygenic nature of the disease. New genetic approaches, such as genome-wide association studies (GWAS), exome sequencing and copy number variants (CNVs) analysis have still not been applied to patients of CAE, partly due to the difficulty in recruiting large cohorts with a strict diagnosis (Heron et al., 2007b; Etter et al., 2011), but such approaches can be expected to shed new light on the etiology of the disease (Thomas and Berkovic, 2014).

1.2.1.4 **Treatment and prognosis**

The most common treatments for ASs are ethosuximide, valproate and lamotrigine. Patients that do not respond to the monotheraphy can be treated with a combination of two or three anti-absence drugs (Panayiotopoulos, 2001). In the past these treatments were generally perceived to achieve a high level of success in controlling ASs (Panayiotopoulos, 1999, 2001). However, up until recently only few studies had compared the relative efficacy of these treatments with a randomized, double-blind design (Glauser et al., 2006). Indeed, a systematic review highlighted that, due to small sample sizes and poor methodological quality, there was insufficient evidence to inform the clinical practice about the best treatment in CAE (Posner et al., 2005). Since then, a large (453 patients in total), randomized, double-blind trial, comparing the efficacy of the three drugs (in monotheraphy) in CAE patients, has been produced (Glauser et al., 2010). Ethosuximide and valproate were found to be more efficacious then lamotrigine, but still they achieved a freedom-from-failure rate of only 53 and 58%, respectively. Ethoximide was

recommended over valproate, as children presented less adverse effects (Glauser et al., 2010). After the initial characterization at 16 weeks, a follow-up study observed that the freedom-from-failure rates where 45 and 44% for ethosuximide and valproate, respectively (Glauser et al., 2013).

A notable characteristic of ASs is that antiepileptic drugs which are effective against convulsive seizures (such as carbamazepine and phenytoin) are generally reported to be either ineffective or to aggravate ASs (Snead and Hosey, 1985; Parker et al., 1998; Panayiotopoulos, 1999; Chaves and Sander, 2005), making the pharmacological profile of ASs unique.

The remission rate in CAE is generally reported to be between 21 and 74%, based on epidemiological cohort studies (Tenney and Glauser, 2013). Nonetheless, it has been reported that 35-60% of children suffering from CAE, develop generalized tonic-clonic seizures in adolescence (Currier et al., 1963; Livingston et al., 1965; Loiseau et al., 1983).

1.2.2 Summary

In summary, ASs are a type of non-convulsive epileptic seizures that are found in various generalized epilepsies. ASs are expressed within the TC network and have a cortical initiation site. ASs are associated with diseases with a polygenic inheritance and a several genes have been implicated in their etiology (including those coding for $GABA_A$ and voltage gated Ca^{2+} subunits). The best treatments available for ASs still work in only about 50% of the patients.

1.3 Thalamocortical Network

1.3.1 General features of the TC network

The term "thalamocortical network" is used to indicate a network of reciprocally connected thalamic and cortical territories (**Figure 1.3**). The functions of this network are multiple: it is believed that TC communication underlies arousal states, consciousness and the processing of sensory information, to name but a few (Alkire et al., 2008; Schiff, 2008; Jones, 2009; Crunelli et al., 2015). Moreover, all brain rhythms, e.g. the slow-oscillation, alpha, beta and gamma rhythms, are thought to be generated within the TC network (Hughes and Crunelli, 2005; Steriade, 2006; Crunelli et al., 2015).

The functional units of the TC network are: TC neurons (historically known as thalamic relay neurons), nucleus reticularis thalami (NRT) neurons and cortical neurons, organized in columns that consist of recipients of TC neurons and corticothalamic projecting neurons. In addition to this simplified description, it is important to note that TC processing also depends on cortical and thalamic interneurons and cortico-cortical connectivity.

Although the processing of information in the TC network happens as a holistic process (involving, for instance, high-order relay nuclei in the thalamus that connect multiple cortical areas), it is possible to identify individual thalamic nuclei and cortical areas which respond to specific sensory modalities (Nicolelis and Fanselow, 2002; Sherman and Guillery, 2002).

A well-characterized TC unit is that composed of the somatosensory nucleus of the thalamus, the NRT and the primary somatosensory cortex. Historically, this TC loop has been thoroughly investigated in absence epilepsy because, in several models of ASs, the amplitude of SWDs is highest at the level of somatosensory thalamus and cortex (while, for instance, the amplitude of SWDs is reduced in the visual thalamus and cortex (Marescaux et al., 1992a; Danober et al., 1998)). Importantly, it has also been recently reported that the somatosensory TC loop is important for the generation of ASs: in recent studies it was found that the initiation site of genetic ASs in the rat is located in the perioral region of the somatosensory cortex (see section 1.5.1). In the following section I will introduce the

functional anatomy and connectivity of these three areas, with a particular focus to the characteristics of VB and NRT, which are of relevance to the experiments presented in this thesis.

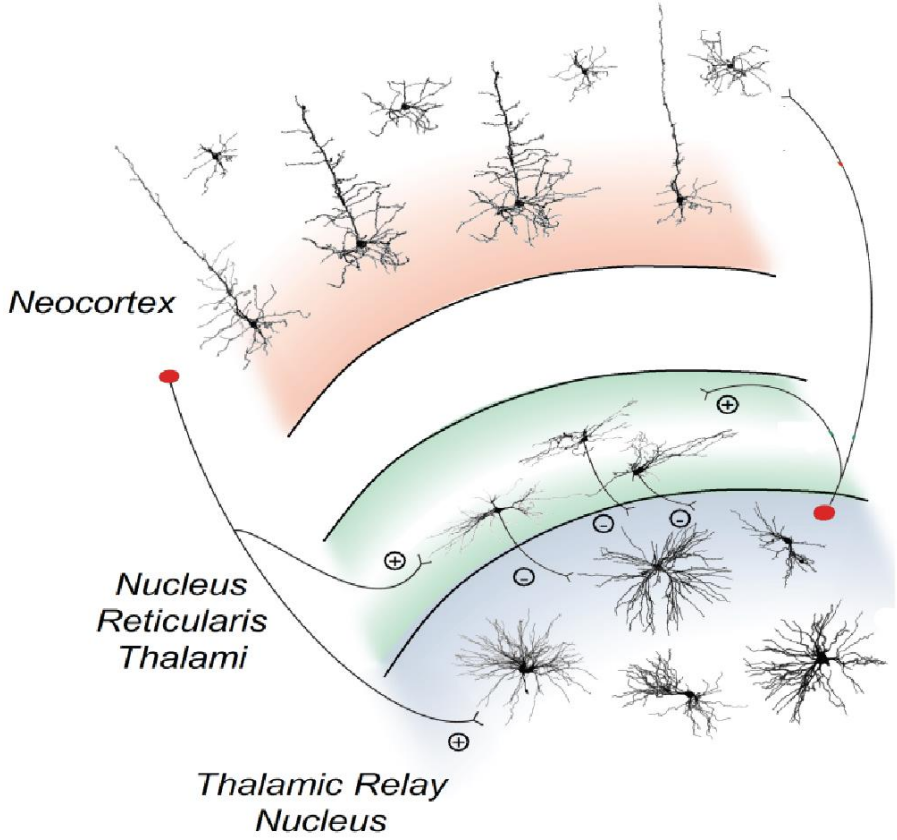

Figure 1.3. Diagram of the connectivity within the TC network. Connectivity between the neocortex, the NRT and TC nuclei (also called thalami relay): excitatory synapses are represented by a plus (+); inhibitory synapses by a minus (-). Adapted from (Crunelli and Hughes, 2010).

1.3.1.1 Ventrobasal nucleus of the thalamus

The ventrobasal nucleus (VB) nucleus is the primary somatosensory nucleus in the thalamus. It is located in the ventrolateral thalamus and is surrounded, ventrally and laterally, by the NRT (Groenewegen and Witter, 2004; Sherman and Guillery, 2006). The VB is composed of the ventral posterolateral nucleus (VPL), which receives somatosensory inputs from the spinal cord and the ventral posteromedial nucleus (VPM), which receives somatosensory inputs from face, head and neck via the trigeminal system (Groenewegen and Witter, 2004; Tracey, 2004). The main function of this nucleus is to convey somatosensory (i.e. tactile/proprioceptive and nociceptive) information to the primary

and secondary somatosensory cortex (Groenewegen and Witter, 2004; Oh et al., 2014). Both the VPM and VPL are organized somatotopically. In the VPM the information from whiskers is relayed to "barreloids", aggregates of TC neurons that code for individual whiskers though communication between barreloids is also thought to happen at the thalamic level, via dendritic branches of TC neurons that span multiple barreloids (Desîlets-Roy et al., 2002). VPL and VPM also receive inputs from layer VI corticothalamic neurons of the somatosensory cortex (see section 1.3.1.3), thus completing the TC loop.

Neurons of the VB are glutamatergic, medium-sized, TC projecting cells. Interneurons are not present in the rodent VB (Harris and Hendrickson, 1987; Sherman and Guillery, 2006) but see (Cavdar et al., 2014)), unlike in cats and primates.

In the case of the VPM (in the cat) it has been estimated that about 44% of the synapses on TC neurons are derived from corticothalamic neurons; 40% are derived from the NRT and 16% are sensory input from the periphery (Liu et al., 1995).

The VB is also innervated from the brainstem from which they receive monoaminergic (locus coeruleus), serotoninergic (dorsal raphe) and cholinergic (pedunctolopontine tegmental nucleus (PPTg) and laterodorsal tegmental nucleus (LDT)) neuromodulatory inputs (Groenewegen and Witter, 2004).

1.3.1.2 **Nucleus reticularis thalami**

The nucleus reticularis thalami (NRT) is a thin layer of GABAergic neurons that wraps around TC nuclei of the thalamus and is adjacent, on its lateral part, to the internal capsule (Crabtree and Isaac, 2002; Groenewegen and Witter, 2004). All NRT neurons are parvalbumin-positive, and a subset are also calbinding positive (Jones, 2002). Unlike TC nuclei, the NRT does not project to the cortex. Most axons connecting TC nuclei to cortex (and vice-versa) pass though the NRT and send collaterals to NRT neurons. Virtually all TC nuclei are connected to the NRT (Groenewegen and Witter, 2004; Oh et al., 2014).

The topographic organization of NRT neurons is complex and still only partially understood (Crabtree and Isaac, 2002; Sherman, 2004; Lam and Sherman, 2011). The majority of NRT neurons are topographically organized; these neurons are localized in

tiers that go from the outer (reticulocapsular) to the inner (thalamoreticular) border of the NRT (Lam and Sherman, 2007). The axons of these neurons synapse to TC neurons that are localized in TC nuclei distributed in roughly the same fashion (i.e. outer NRT neurons to outer TC neurons, inner NRT neurons to inner TC neurons). Therefore, these clusters of NRT neurons provide inhibitory feedback for specific sensory modalities. Nonetheless, about 25% of NRT neurons receive non-topographically organized inputs from various TC nuclei (Kimura et al., 2007; Lam and Sherman, 2011). This suggests that the NRT does more than provide inhibitory feedback to TC neurons and is, indeed, able to integrate information from different sensory modalities (Crabtree and Isaac, 2002; Pinault, 2004; Lam and Sherman, 2011).

Intra-NRT connections have also been described, both via chemical synapses and gap-junctions (Long et al., 2004; Pinault, 2004; Lee et al., 2014a). The role of this mutual GABAergic inhibition is not fully understood, but it has been suggested that it plays a role in generating spindle and hypersynchronous oscillations and in modulating sensory throughput (Fuentealba and Steriade, 2005; Deleuze and Huguenard, 2006; Huguenard and McCormick, 2007).The NRT also receives various neuromodulatory inputs from the brainstem (monoaminergic, serotoninergic, cholinergic) and the basal forebrain (cholinergic) (McCormick, 1992; Fuentealba and Steriade, 2005).

Considering the input received by NRT neurons that are connected to the somatosensory cortex, it has been observed that little less than 60-65% of the synapses that NRT neurons receive originate from corticothlamic neurons; thalamocortical collaterals make up about 20-25% and intra-NRT synapses 15-20% (Liu and Jones, 1999; Jones, 2002).

1.3.1.3 **Primary Somatosensory cortex**

The primary somatosensory cortex consists of 6 layers, which, in the rat, are comprised of an estimated 85% glutamatergic pyramidal cells and 15% GABAergic interneurons (Lin et al., 1985; Meyer et al., 2010b) . The barrel cortex is the part of the somatosensory cortex which receives somatotopically organized input from VPM. The connectivity and organization of the barrel cortex have been comprehensively described in recent years (Bruno and Sakmann, 2006; Wimmer et al., 2010; Feldmeyer et al., 2013), thus, in this brief description, a cortical column of the barrel cortex will be used as to describe the main features of the somatosensory cortex. A cortical whisker column (defined as a cortical

column receiving inputs from one VPM barreloid) is composed of ~20.000 neurons (Wimmer et al., 2010). The main input layer of TC afferents is generally considered to be layer IV, although collateral synapses are also found in deep layer V5 (Meyer et al., 2010a; Constantinople and Bruno, 2013) and in layer II/III (Feldmeyer, 2012). Only about 15% of the synapses on layer IV stellate neurons are TC and they generate large post-synaptic potentials in the recipient cells (Bruno and Sakmann, 2006), while the remaining 85% of the synapses derives mainly from cortico-cortical connections. After the TC inputs reaches layer IV, it spreads to the rest of the column, with the major output being to layer II/III (Feldmeyer, 2012; Feldmeyer et al., 2013). The major output layers for the barrel cortical column are layer II/III and layer V, which connect the column with other cortical columns belonging to different cortices (e.g. secondary somatosensory cortex, motor cortex) and (in the case of layer V) to subcortical targets. In addition, pyramidal cells of layer V also project to high-order thalamic nuclei (Sherman, 2007). Finally, layer VI is considered the major input to the thalamus, hence, corticothalamic neurons project back to VPM neurons (and collaterals to the NRT), completing the TC loop.

As mentioned in the previous sections on the VB and NRT, the somatosensory cortex also receives strong neuromodulatory inputs from basal forebrain and brainstem (Feldmeyer et al., 2013).

1.3.1.4 **Summary of the connectivity within a TC loop**

In this section a schematic summary of the anatomical connections that characterize a TC loop is presented. The main connectivity between thalamic and cortical territories is reciprocal (i.e. topographically organized), although more diffuse connections are also well-described (Jones, 2002; Sherman, 2007).

1) Thalamocortical: TC neurons project to layer IV of the cortex (and to a minor degree to other cortical layers).
2) Intra-cortical:layer IV project to layer II/III (and to a minor degree to other cortical layers), spreading intra-columnar connections.
3) Inter-cortical: inter-columnar connection are driven by layer V (and to a minor degree layer II/III).
4) Corticothalamic: layer VI (and to a minor extend layer V) project back to the TC neurons.
5) Thalamoreticular and corticoreticular: Collaterals from 1) and 4) input to the NRT.

6) Reticulothalamic: the NRT projects to TC neurons
7) Intra-reticular: reticular neurons have reciprocal $GABA_A$ synapses.

1.3.2 Electrophysiological properties of TC and NRT neurons

1.3.2.1 **Intrinsic currents of TC and NRT neurons**

1.3.2.1.1 Na+ and K+ currents

Like virtually all CNS neurons (Bean, 2007), TC and NRT neurons fire action potentials via voltage dependent TTX-sensitive Na+ channels (VGSCs) (Jahnsen and Llinás, 1984; McCormick and Huguenard, 1992). Moreover, TC neurons also have a Na+ persistent current (I_{NaP}), which does not inactivate and can modulate the firing mode of TC neurons (Parri and Crunelli, 1998).

TC and NRT neurons also posses various K^+ conductances, which have a pivotal role in controlling the resting potential and modulating the oscillatory activity of thalamic neurons (McCormick and Bal, 1997; Amarillo et al., 2014). The K^+ leak (I_{leak}) current (McCormick and Prince, 1987, 1988) stabilizes TC and NRT neurons to a relatively hyperpolarized potential. Recent work has shown that TASK1 and TASK2 channels underlie most of this current in TC cells (Meuth and Budde, 2003). Inward rectifying K^+ channels also contribute to maintaining the resting potential of TC cells via a distinct current (I_{KIR}) (Williams et al., 1997b). Finally a fast-activating, transient, A-type K^+ current (I_A), is also found in TC neurons (Huguenard et al., 1991). This current controls the onset, amplitude and duration of T-type channel mediated low-threshold bursts (see below) and is considered a "functional antagonist" of the T-type Ca^{2+} current (Pape et al., 1994; Meis et al., 1996; Tennigkeit et al., 1998).

1.3.2.1.2 Hyperpolarization activated mixed-cation current (I_h) and Ca^{2+} activated non specific cation current (I_{CAN})

I_h is a mixed K^+ /Na+ current generated by HCN channels (Wahl-Schott and Biel, 2009), found both in TC (McCormick and Pape, 1990) and NRT (Rateau and Ropert, 2006) neurons. Importantly, this current is unique because it is activated by membrane hyperpolarization (around -65mV). HCN channels are permeable to both K^+ and Na+ and

are modulated by cAMP. I_h does not inactivate and deactivates slowly and it has been shown to be fundamental for the generation of rhythmic activities in TC and NRT neurons (Wahl-Schott and Biel, 2009).

I_{CAN} is also a mixed K^+ /Na+ current, but it is activated by Ca^{2+} and is present both in TC (Hughes et al., 2002) and NRT neurons (Bal and McCormick, 1993). This current is responsible for producing a 'tail' of tonic spikes after a burst (see below) and has beem shown to be a key modulator of the slow oscillation (Hughes et al., 2002).

1.3.2.1.3 Voltage dependent Ca^{2+} currents

Voltage-gated Ca^{2+} channels (VGCCs) allow the influx of Ca^{2+} into neurons in response to membrane depolarization. Ca^{2+} entry via VGCCs in neurons is accompanied by a plethora of cellular responses, including neurotransmission, changes in synaptic plasticity, gene expression and membrane depolarization (Berridge, 1998; West et al., 2001; Pape et al., 2004; Neher and Sakaba, 2008).

VGCCs are composed of one pore-forming α subunit and various auxiliary subunits. The α subunit controls the kinetics and pharmacology of VGCCs and is organized into four domains with six transmembrane segments each (S1-S6); S4 is the voltage sensor (Hofmann et al., 1994).

VGCCs can be grouped according to the activation threshold of the associated Ca^{2+} current into high-voltage activated (HVA) and low-voltage activated (LVA), both of which are found in TC and NRT neurons (Hernández-Cruz and Pape, 1989; Budde et al., 1998; Perez-Reyes, 2003; Pape et al., 2004). HVA channels produce currents that are activated by a strong cellular depolarization (reaching a membrane potential of ~ -20mV) and are further subdivided into L-type (Cav1) and P/Q-, R-, N- type (Cav2) (Vacher et al., 2008). HVA channels are thought to mostly regulate tonic firing (see below) in TC and NRT cells (Guyon and Leresche, 1995; Kammermeier and Jones, 1997; Budde et al., 2000).

LVA channels are of particular interest for this thesis and have been proposed to be key players in the expression of ASs (see section 1.5), therefore they will be reviewed in some detail in the following section. In view of the experiments with systemic administration of a T-type channel antagonist (Chapter 4), the expression of T-type channels in cortical territories will also be briefly described.

1.3.2.1.4 LVA Ca^{2+} currents

LVA currents were first originally discovered in the starfish egg (Hagiwara et al., 1975). Since then they have been characterized in various mammalian tissues, including heart (Nilius et al., 1985), the adrenal gland (Cohen et al., 1988) and the CNS (Llinás and Yarom, 1981; Huguenard, 1996).

Experiments using whole-cell voltage clamp and single channel measurement to characterize the activation threshold of neuronal LVA currents have shown it to be far more negative (~-60mV) compared to that of HVA current. LVA channels were defined 'T-type' because of their fast kinetics (transient activation) and small unitary current (tiny, conductance in the order of 5-9 pS) (Carbone and Lux, 1984; Fedulova et al., 1985; Perez-Reyes et al., 1998). T-type Ca^{2+} channels also have faster inactivation and recovery-from-inactivation rates compared to HVA channels (Senatore et al., 2014).

The activation and inactivation kinetics of T-type Ca^{2+} are at the basis of the generation of low-threshold Ca^{2+} potentials (LTCPs), observed in various neurons of the CNS, including cortex (Friedman and Gutnick, 1987), TC (Jahnsen and Llinás, 1984) and NRT (Avanzini et al., 1989). LTCPs are generated by a hyperpolarizing input, which induces the recovery from inactivation (deinactivation) of a pool of T-type channels (mostly inactivated at the resting potential); influx of Ca^{2+} though T-type channels produces a depolarization of the cell membrane (lasting few tens of ms), which is often crowned by action potentials (see below).

The molecular identity of the channels underlying LVA currents was discovered by molecular cloning only towards the end of the 1990s. Three members of the T-type Ca^{2+} channels family are known to date, and are grouped based on the sequence similarity of their α subunit: Cav3.1 (α1G), Cav3.2 (α1H), Cav3.3 (α1I) (Perez-Reyes et al., 1998; Perez-Reyes, 1999). The three T-type Ca^{2+} channel (from now onwards "T-type channels" for brevity) isoforms have a sequence similarity of >90% (Senatore et al., 2012), nonetheless they possess varied gating properties (summarized in **Figure 1.4A**) which can influence the firing output of TC and NRT neurons (for instance by varying the properties of burst-firing, see section 1.3.2.4 and **Figure 1.4B**).

The expression of these three isoforms in the brain has been characterized both at the mRNA level and with immunohistochemistry techniques. There is a good concordance between the two approaches, indicating a high expression of T-type channels in the TC network (Vacher et al., 2008). In the cortex, Cav3.1and Cav3.2 are highly expressed in the soma and proximal dendrites of layers I-V (McKay et al., 2006). Cav3.3 has a similar expression pattern, but is also highly expressed in the mid and distal dendrites of LV pyramidal cells. In the thalamus, mRNA data suggests that the pattern of expression of the three isoforms is quite distinct: NRT neurons express Cav3.3 and Cav3.2 mRNA, but no Cav3.1. TC cells, and in particular the VB, strongly express Cav3.1, but none of the other isoforms (Talley et al., 1999). However, immunohistochemistry studies show discordant results according to the antibodies used (Craig et al., 1999; McKay et al., 2006). Importantly, electrophysiological recordings in knockout mice strongly support the differential distribution of T-type calcium channels observed in the mRNA study above (Kim et al., 2001; Lee et al., 2014b). In thalamic neurons, T-type channels are thought to be distributed in the soma and across proximal and distal dendrites, as suggested by calcium imaging studies (Zhou et al., 1997; Crandall et al., 2010; Errington et al., 2010, 2012).

The dendritic localization of T-type calcium channels underlies further roles of LVA currents in addition to the generation of LTCPs described above: various studies in TC (Crandall et al., 2010), NRT (Errington et al., 2010) and cortical neurons (Markram and Sakmann, 1994) suggest that T-type channels profoundly influence synaptic integration and synaptic plasticity (Senatore et al., 2012).

A

	Cav3.1	Cav3.2	Cav3.3
Activation constant (ms)	0.8 ± 0.1	1.34 ± 0.1	7.2 ± 0.8
Inactivation constant (ms)	18.8 ± 1.6	23.4 ± 0.3	122 ± 15
Deactivation constant (ms)	2.6 ± 0.2	3.6 ± 0.2	1.12 ± 0.1
Recovery constant (ms)	137 ± 5	448 ± 36	260 ± 30
Burst properties	Short and fast burst (typical of TC neurons)	Fast burst initiation (typical of NRT neurons)	Longest burst (typical of NRT neurons)

B

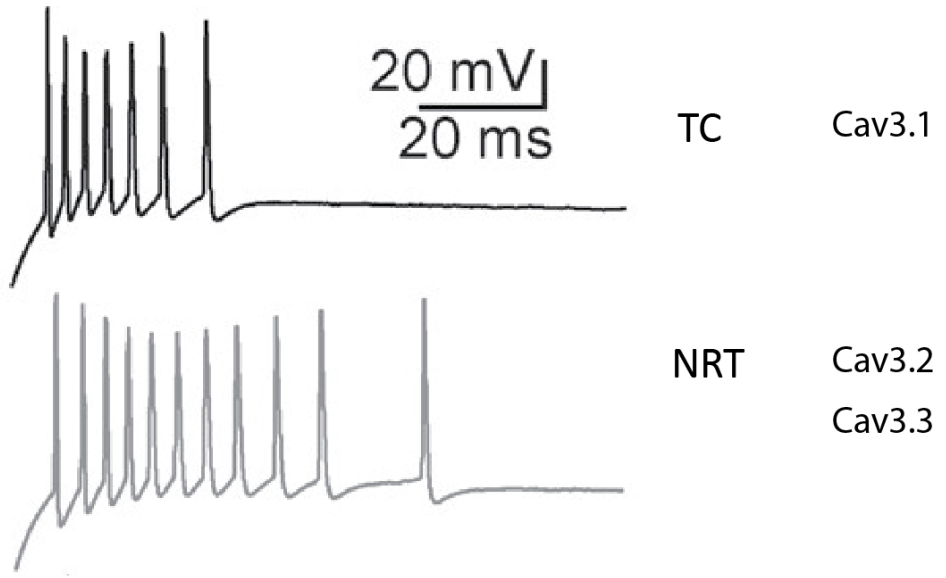

Figure 1.4. T-type Ca2+ subtypes properties and different burst firing of TC and NRT neurons. (A) Comparison of the critical kinetic parameters of T-type Ca2+ channels, adapted from (Cain and Snutch, 2010) and resulting effect on burst-firing. (B) Illustration of a typical TC burst (dependent on Cav3.1 channels) which show an accelerando pattern and a typical NRT burst (dependent on Cav3.2 and Cav3.3 channels) which show an accelerando-decelerando pattern. Adapted from (Tscherter et al., 2011)

Up until 2008, no selective agents were available to block T-type channels and isolate them from HVA currents. TTA-P2 (3,5-dichloro-N-[1-(2,2-dimethyl-tetrahydro-pyran-4-ylmethyl)-4-fluoro- piperidin-4-ylmethyl]-benzamide) was the first potent and selective T-type antagonist to be synthetized (Shipe et al., 2008). In TC neurons the IC_{50} for the T-type channel current (I_T) was 20nM. It was also observed that T-type channels are highly redundant in LTCP generation (Dreyfus et al., 2010): when I_T was blocked by 70%, LTCPs were still present and a full block of LTCP was reached only at 1μM TTA-P2 (>95% I_T block).

Another important property of T-type channels in thalamic neurons (and possible in cortical neurons) is that, at voltages close to the resting membrane potentials, a small fraction of channels (<1%) are open and produce a tonic Ca^{2+} influx in the cell (Williams et al., 1997a; Hughes et al., 1999). This "window current" is generated by the overlap of the activation and inactivation curves of T-type channels. Multiple physiological roles have been ascribed to the window current, including input signal amplification and the facilitation of bi-stable oscillations characteristic of the slow rhythm of NREM sleep (Hughes et al., 2002; Crunelli et al., 2005; Crunelli and Hughes, 2010; Lambert et al., 2014). Recent experiments with TTA-P2 allowed a direct experimental confirmation of the role of the window current in excitability of TC neurons. Bath application of 1μM TTA-P2, induced a hyperpolarization of TC neurons by ~3mV, highlighting the potential of the window current to powerfully modulate the activity of TC neurons in all behavioural states (Dreyfus et al., 2010).

1.3.2.2 **Synaptic (and extrasynaptic) neurotransmission: modulation of TC and NRT neurons**

The main neurotransmitters that produce excitation and inhibition in TC and NRT neurons are glutamate and GABA respectively. Glutamatergic inputs act on post-synaptic ionotropic receptors (AMPA/kainate and NMDA) located on corticothalamic, TC and NRT neurons (Jones, 2002). Glutamate also acts on metabotropic glutamate receptors (mGluRs). Group I mGluRs ($mGluR_1$ and $mGluR_5$) are located postsynaptically in TC, NRT and corticothalamic neurons where they produce a slow depolarizing response (Ngomba et al., 2011). Notably, activation of $mGluR_1$ in TC neurons modulates the intrinsic rhythmicity of these neurons and induces a slow-oscillation typical of NREM sleep (Hughes et al., 2002; Crunelli and Hughes, 2010). Group II and III mGluRs are instead generally found presynaptically, where they are thought to reduce neurotransmitter release (Alexander and Godwin, 2006). NRT

and TC both have a rich expression of Group III mGluRs, while group II mGluRs are mostly expressed at GABAergic terminal contacting TC cells (Ngomba et al., 2011).

In the VB (in rodents), GABAergic inhibition is uniquely driven by the NRT. Intra-NRT inhibition is mostly driven by ionotropic $GABA_A$ receptors ($GABA_ARs$), although a contribution of metabotropic $GABA_B$ receptors has also been suggested (Ulrich and Huguenard, 1996). In TC neurons, $GABA_B$ R1a/b and R2 appear to be co-localized postsynaptically (Kulik et al., 2002). $GABA_B$ receptors mediate a hyperpolarization on TC cells, via the opening of a K^+ channel (Williams et al., 1995). Nonetheless, presynaptic effects, induced by $GABA_B$ receptors, have also being described: the amplitude of sensory and corticothalamic EPSPs is reduced by application $GABA_B$ agonists (Emri et al., 1996; Gervasi et al., 2003). $GABA_A$ activation via synaptic receptors produced the classical fast hyperpolarizing IPSPs (Kim et al., 1997; Pinault, 2004).

In addition to synaptic $GABA_ARs$, $GABA_A$ Rs are also found at extrasynaptic locations (Brickley and Mody, 2012). Extrasynaptic $GABA_A$ Rs are activated by ambient GABA and generate a persistent Cl- influx in the neurons, dubbed "tonic current" (Farrant and Nusser, 2005). The kinetics of this current are due to the high affinity and slow desensitization of extrasynaptic $GABA_A$ Rs. The tonic current can profoundly influence cell excitability by decreasing the input resistance of a neuron, thus varying the neuron's input-output relationship (Farrant and Nusser, 2005; Farrant and Kaila, 2007). The $GABA_A$ tonic inhibition has been described in many areas of the CNS, including cortex and TC neurons (where extrasynaptic, but not synaptic, $GABA_ARs$ contain the δ subunit), but, notably, is not present in NRT neurons (Cope et al., 2005). Importantly, the thalamic tonic $GABA_A$ inhibition is a major player in the expression of ASs and will be discussed in section 1.5.2.

1.3.2.3 **Neuromodulatory inputs in TC and NRT neurons**

Thalamic neurons receive various inputs from arousal/sleep-promoting centers in the brainstem and basal forebrain (McCormick and Bal, 1997; Krout et al., 2002).

Cholinergic inputs from the PPTg and LDT, and noradrenergic inputs from the *locus coeruleus,* depolarize TC neurons by closing TASK channels and thus reducing I_{leak} (Varela and Sherman, 2007; Bista et al., 2012). This action has been shown, *in vitro,* to depend on muscarinic receptors and α1-adrenergic receptors, respectively (McCormick and Pape, 1990; McCormick and Bal, 1997). In addition, noradrenaline (acting on β-adrenergic

receptors) shifts the voltage curve of I_h to more depolarized potentials, facilitating membrane depolarization (Varela and Sherman, 2009; Coulon et al., 2012). The effect of 5-HT on TC cells is unclear. A small depolarization (McCormick and Pape, 1990; Varela and Sherman, 2009) or a prevalent hyperpolarization (Monckton and McCormick, 2002) have both been reported. Moreover, the effect of agonists and antagonists selective for different 5-HT receptors subtypes has not been tested to date (see section 1.6.2.1).

The effects of neuromodulators on the NRT are less well characterized, but generally seem to have a similar effect to that in TC cells (McCormick, 1992). 5-HT and noradrenaline are reported to depolarize NRT cells (McCormick and Wang, 1991). Cholinergic inputs to the NRT arise both from the brainstem, and from the basal forebrain (MESULAM et al., 1983; Steriade, 2004). Application of acetylcholine to NRT cells generated a biphasic response where a fast depolarization, induced by α4β2 nicotinic receptors, was followed by a long-lasting hyperpolarization, induced by activation of M2 muscarinic receptors (Sun et al., 2013; Beierlein, 2014).

1.3.2.4 **Firing dynamics of TC and NRT neurons: tonic and burst firing**

TC and NRT neurons exhibit two states of activity: tonic firing and burst firing, both of which have been extensively characterized *in vitro* and *in vivo* (Jahnsen and Llinás, 1984; Huguenard and Prince, 1992; Steriade et al., 1993b; McCormick and Bal, 1997).

Tonic firing (**Figure 1.5A**) is the characteristic firing mode normally associated with neurons: the firing of a steady stream of VGSC-dependent action potentials. In the thalamus, *in vivo,* this firing mode is predominantly found when the animal is awake and is associated with the transmission of sensory information to the cortex (Steriade et al., 1993b; Sherman, 2001). *In vitro* tonic firing can be produced at a relatively depolarized resting potential (e.g. >-65mV) when all the T-type channels (except for those which produce the window current) are inactivated. When the threshold to VGSCs is crossed (e.g. around -55mV), the neurons respond with a train of action potentials.

The burst firing mode (**Figure 1.5B**) is revealed *in vitro* when a TC neuron is hyperpolarized by at least -5mV from rest for a sufficient amount of time (~100ms) to deinactivate T-type channels (which remain closed at this hyperpolarized potential). A subsequent depolarizing stimulus induces the rapid opening of T-type channels and the

influx of Ca^{2+} into the cell that generates a LTCP. The LTCP generally lasts for less than 100 ms and is often sufficient for the membrane potential to cross the threshold and generate a 'burst' of 3-8 fast VGSC-dependent action potentials. The number of action potentials (and so the duration of a burst) is different in TC and NRT neurons. This difference arises from the different subtypes of T-type channels expressed in this neurons: Cav3.3 channels, expressed primarily in the NRT (see section 1.3.2.1.4) have the longest inactivation constant, therefore they give rise to a longer LTCP and associated burst with a characteristic accelerando-decelerando pattern (Domich et al., 1986; Cain and Snutch, 2010). TC neurons instead haveshorter bursts with a decelerando-only pattern (Domich et al., 1986) (see **Figure 1.4B**).

In addition to the low-threshold LTCP-mediated bursting described above, it has been observed that a subset (~25%) of TC cells in the cat lateral geniculate also produced another type of burst, called high-threshold (HT) burst (Hughes et al., 2004) (**Figure 1.5C**). HT bursting is observed when TC cells are at a relatively depolarized potential (~-55mV) and, *in vitro,* is dependent on mGLUR1A activation. HT bursts are commonly recorded as doublets or single spikes crowning a Ca2+ spike generated by T-type channels (possibly located in the dendrites and not inactivated even at a depolarized potentials) (Hughes et al., 2004). Since their discovery in the cat, HT bursts have also been described in several thalamic nuclei (including the VB) of rats (Hughes and Crunelli, 2005; Hughes et al., 2008).

The LTCP-mediated burst firing mode of thalamic neurons is normally associate with the slow waves of NREM sleep (Steriade et al., 1993b; Sherman, 2001). Neuromodulatory inputs (such as those described in section 1.3.2.3) have the main effect to switch the firing mode of thalamic neurons form burst to tonic firing (McCormick and Bal, 1997; Steriade, 1999). Nonetheless, it is currently recognized that bursts can also be detected during wakefulness, and may have a role in the processing of information in the TC network (Sherman, 2005). HT bursts have been shown to be important for the generation of the alpha rhythm (Hughes et al., 2004; Lorincz et al., 2009). Therefore the view that TC bursts are simply a means of interrupting the flow of sensory information to the cortex during NREM sleep should not be generalized.

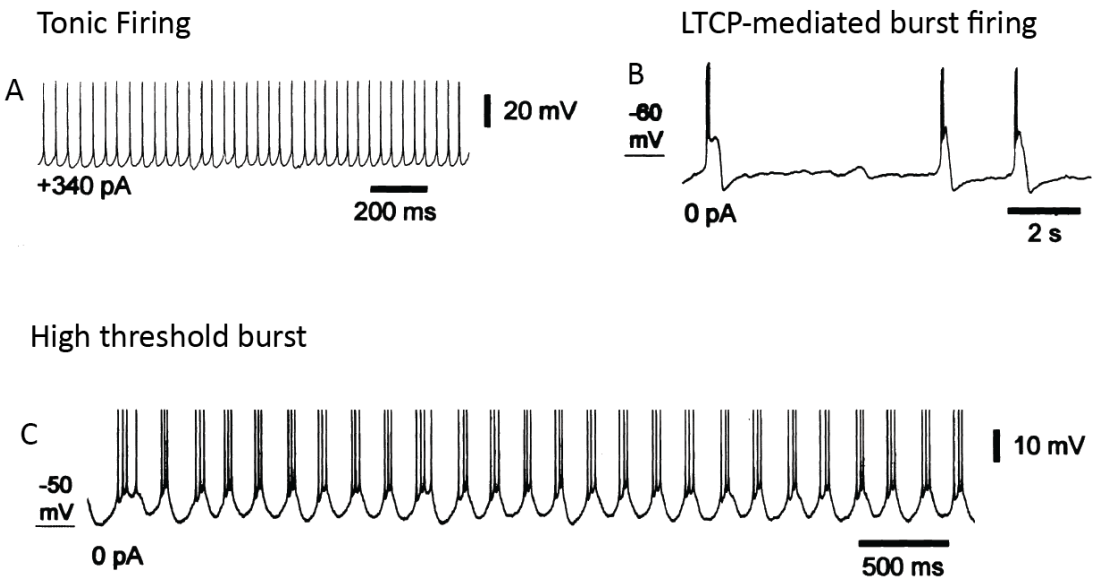

Figure 1.5 Tonic firing and burst firing in TC neurons. *In vitro* intracellular recordings of TC neurons in the cat lateral geniculate displaying single spike trains of action potentials (tonic firing, A), LTCP-mediated burst firing (B) and high-threshold burst (C). The current values (pA) underneath each panel represent the steady depolarizing current injected in each experiment. Adapted from (Hughes et al., 2004)

1.4 Experimental models of absence seizures

The pathophysiology of ASs has been investigated experimentally using two broad groups of models: genetic (spontaneous) and pharmacological (induced). Genetic models of ASs can be subdivided in monogenic and polygenic. To date, several monogenic mouse models of ASs have been described (Noebels, 1999, 2006), but only polygenic rat models are available for experimental use (Danober et al., 1998; Depaulis and Luijtellar, 2006). Polygenic rat models were obtained by selective inbreeding of rats, which displayed spontaneous ASs, to have a line which stably expresses ASs. Pharmacological models involve the acute administration of a substance to induce ASs in animals (Cortez and Snead, 2006), normally rodents, due to their ease of breeding, manipulation and broad availability of genetic tools (although the penicillin model in the cat has, historically, been instrumental in studying ASs (Avoli et al., 1983; Avoli, 2012)). The chronic administration of substances is only reported in models of atypical ASs (Cortez and Snead, 2006), and to the best of my knowledge has not been applied to generate models displaying typical ASs, therefore it will not be discussed in this thesis.

All established experimental models of ASs have a set of characteristics that define their similarity to human ASs, and which have been summarized as the following (Snead, 1992a; Danober et al., 1998; Coenen and Van Luijtelaar, 2003):

- presence in the EEG of SWDs accompanied by behavioural arrest, in the absence of convulsion;
- SWDs recorded in the TC network, but not in the hippocampus or other limbic structures;
- pharmacology similar to that of human ASs:
    - block of ASs by ETX and valproate;
    - aggravation of ASs by drugs effective treating convulsive seiures (e.g. carbamazepine and phenytoin);
    - aggravation by substances that increase the GABAergic tone (vigabatrin, tiagabine) or act as $GABA_B$ agonists (baclofen);
    - block of ASs via $GABA_B$ antagonists.

It can be noted that the "predictive validity" (i.e. response of experimental ASs to pharmacological manipulations) is the better-defined feature of ASs models. This reflects

the fact that assessing an impairment of consciousness in animals is even more problematic than it is in humans (see section 1.2) and, behaviourally, the experimenter can only detect a behavioural arrest. Moreover, the "face validity" (i.e. phenotypic similarity with the human disease) of experimental models of ASs is low in terms of their developmental profile. Spontaneous ASs in animals increase with ageing, in contrast to the remission rate found with CAE in adolescence. Notably, the degree of "construct validity" (i.e. commonality of genetic causes underlying the disease) of models of ASs is difficult to assess given that the etiology of the disease is not well understood (see section 1.2.1.3).

In the following sections I will give an overview of pharmacological and genetic models of experimental ASs, focusing on the two models employed in this thesis: Genetic Absence Epilepsy Rats from Strasbourg (GAERS) and the γ-hydroxybutyric acid (GHB) model. The pathophysiological mechanism that brings about ASs will be described in section 1.5.

1.4.1 Genetic models of absence seizures

Monogenic mouse models of ASs have a single gene mutation causal to the expression of spontaneous ASs along with other pathologies. To date no accepted mouse model of ASs has a pure ASs phenotype, in the absence of other comorbidities.

The three best-established monogenic mouse models of ASs are stargazer, lethargic and tottering (Noebels, 1999, 2006). The three mouse strains display 5-7Hz SWDs accompanied by behavioural arrest. Stargazers have a mutation in the CACNG2 gene (Letts et al., 1998), which codes for the γ2 subunit of L-type Ca^{2+} channels (also called stargazin); in addition to ASs they have a small body size, ataxic gait and abnormal head movements. Tottering mice have a mutation in the CACNA1A gene (Fletcher et al., 1996), which codes the Cav2.1 channels; in addition to ASs they display ataxia and spontaneous tonic-clonic seizures. Finally, lethargic mice have a mutation in the CACNB4 gene (Burgess et al., 1997), which codes for the β4 subunit of VGCCs; in addition to ASs they display hypolocomotion and are immunodeficient. Because of the abnormalities that accompany the ASs phenotype, these models of ASs have limitations compared to polygenic rat models, which, instead, display a pure ASs phenotype.

Two polygenic rat models of ASs are considered the best-established rodent models of ASs: GAERS and WAG/Rij (Wistar Agouti from Rijswijk). In these models a plethora of studies

have investigated, in detail, the circadian expression, pharmacological modulation, effect of neuromodulators, developmental and behavioural aspects of their ASs (Danober et al., 1998; Coenen and Van Luijtelaar, 2003; Depaulis and Luijtellar, 2006). Moreover, a thorough understanding of the mechanisms of ASs has been achieved via lesions, invasive electrophysiological recordings and fMRI (Pinault et al., 1998; Meeren et al., 2002; Polack et al., 2007; Mishra et al., 2011). GAERS and WAG/Rij originate from two independent strains of Wistar rats where an ASs phenotype was either discovered *a posteriori* in an inbred colony (WAG/Rij (van Luijtelaar and Coenen, 1986)), or purposely obtained by selective breeding of animals which displayed some ASs (GAERS, (Vergnes et al., 1982)) to obtain longer seizures with a more stable expression. Both strain express 7-11Hz SWDs accompanied by behavioural arrest and their ASs have comparable characteristics. Importantly, no lesions or gross structural changes in the brains of animals from either strain have been observed. The following section will describe, in some detail, the features of GAERS ASs, whilst mentioning some characteristics of WAG/Rij when appropriate. It is worth noting here some unique features of WAR/Rij that are not found in GAERS. In addition to the generalized SWDs found in both models, WAG/Rij also display rare focal SWDs in the frontal and parietal cortices (Coenen and Van Luijtelaar, 2003; Depaulis and Luijtellar, 2006). These SWDs have a lower frequency (6-7Hz) and no behavioural concomitants, and therefore do not represent true experimental ASs. In addition, WAG/Rij have recently been suggested to have a comorbity with depression (Sarkisova and van Luijtelaar, 2011).

1.4.1.1 **GAERS**

1.4.1.1.1 EEG and behaviour of GAERS ASs

GAERS rats display 7-11 Hz EEG SWDs that emerge abruptly from a normal EEG background (Vergnes et al., 1982; Marescaux et al., 1992a; Danober et al., 1998). In the original characterization, ASs were reported to last 17±10 seconds and to occur, when animals were in state of quiet wakefulness, about once per minute. Concomitantly to the EEG manifestation, the animals freeze while often displaying vibrissal twitching and facial myoclonus. During ASs animals would not respond to mild sensory stimulation, but ASs could be interrupted by a sudden and strong stimulus (e.g. handclap). Few attempts have been made to characterize the degree of impairment of consciousness during GAERS ASs. It has been observed that GAERS do not display any ASs whilst actively performing tasks

involving a reward. Instead, ASs appear only during inactivity or when the motivation to perform a task is reduced. In such instances, conditioned stimuli (e.g. sound) during SWDs never produce a behavioural response (Vergnes et al., 1991). Different results were obtained in WAG/Rij, were it has been shown that rats are able process and respond to different auditory stimuli during SWDs, suggesting that the degree of impairment of consciousness is moderate at the level of sensory processing, attention and memory (Drinkenburg et al., 2003). These results are consistent with the various degrees of impairment of consciousness found during human ASs (Killory et al., 2011; Blumenfeld, 2012; Blumenfeld and Meador, 2014).

Thorough investigations with depth EEG electrodes and lesions have shown that GAERS SWDs can be recorded in cortex and thalamus, but not in the hippocampus, and that the integrity of the TC is necessary for the expression of GAERS AS (Marescaux et al., 1992a; Danober et al., 1998). In particular, lesions of the NRT and VB fully suppress GAERS ASs (Avanzini et al., 1992; Vergnes and Marescaux, 1992).

Although it was originally thought that ASs were generalized from the start, it is now understood that GAERS (and WAG/Rij) ASs are initiated in the somatosensory cortex (Meeren et al., 2002; Polack et al., 2007). Details of seizure initiation will be described in section 1.5.1.

1.4.1.1.2 Pharmacology of GAERS ASs

GAERS ASs have a pharmacological profile strikingly similar to that of human ASs (see section 1.2.1.4). Acute administration of ETX and valproate blocks ASs, as do trimethatione and benzodiazepines (Marescaux et al., 1992a; Danober et al., 1998). Moreover, a recent paper showed that chronic oral administration of ETX (a situation that is more representative of the therapeutic dosing for CAE) produced a ~50% reduction in the total time spent in seizure that persisted up to three months after cessation of the treatment (Dezsi et al., 2013). A notable exception is lamotrigine, which is not effective in treating GAERS ASs (which is also the case in WAG/Rij) (Rijn et al., 1993; Danober et al., 1998). Anticonvulsants such as vigabatrine, tiagabin and gapentin, which are ineffective or even exacerbating human ASs, also exacerbate GAERS ASs (Marescaux et al., 1992a).

The effect of drugs acting on the GABAergic system has been systematically examined in GAERS (Danober et al., 1998). Agonists of the $GABA_B$ receptor (e.g. baclofen and GHB,

which also produce ASs on its own) exacerbate GAERS seizures, while $GABA_B$ antagonists suppress them (Liu et al., 1992; Vergnes et al., 1997). Drugs acting on $GABA_A$ receptors have a more complex effect: agonists of the $GABA_A$ receptors (e.g. THIP, muscimol) exacerbate GAERS ASs, but so do low doses of $GABA_A$ antagonists (PTZ, penicillin) (Marescaux et al., 1992a; Danober et al., 1998). It is noteworthy that THIP is a selective agonist of the extrasynaptic $GABA_A$ receptors, and that GAERS ASs are associated with an increase in tonic $GABA_A$ current in the thalamus (see section 1.5.2).

1.4.1.1.3 Genetics and developmental profile of GAERS ASs

GAERS rats were obtained by selective breeding of rats from a colony of Wistar rats in which 30% of the animals displayed short and irregular SWDs (Vergnes et al., 1982). A strain of non-epileptic controls (NECs) was also developed by the same group by selecting the non-epiletic Wistar rats from the same colony. GAERS start to display ASs at 1 month and 100% of the animals have ASs at 4 months. The number of ASs increases until 6 months, when it becomes stable (Marescaux et al., 1992a). NECs, instead, never develop ASs, even at 6 months (Marescaux et al., 1992a; Danober et al., 1998).

GAERS ASs are inherited as autosomal dominant, in fact 95% of animals in the first generation (F1) of the cross between GAERS and non-epileptic Brown Norway rats develop SWDs at 6 months (Marescaux et al., 1992a).

In 2004, a quantitative trait locus mapping study detected three broad chromosomal regions associated with the ASs phenotype, identifying several candidate genes, including stargazin (Rudolf et al., 2004). Stargazin was then found to be overexpressed in TC territories of GAERS compared to NECs, importantly, this was true across development, preceding seizure onset, suggesting that this was not a consequence of the ASs phenotype (Powell et al., 2008). Another study found that GAERS rats have a mutation in the Cav3.2 channels that segregates co-dominantly with the ASs phenotype. This point mutation induced a faster recovery from inactivation and increased the unitary current of the channel (Powell et al., 2009), which may explain why previous studies detected an increased T-type channel current in the NRT neurons of GAERS compared to NECs (Tsakiridou et al., 1995). A mutation in Cav3.2 channels is of particular interest because mutations in the orthologous human gene are also associated with ASs (see section 1.2.1.3).

1.4.1.1.4 Neurotransmitter and protein abnormalities in GAERS

Abnormalities in both glutamatergic and GABAergic systems have been observed in the brain of GAERS rats (Jones et al., 2011). Although the levels of glutamate in thalamus and cortex are reported to be comparable to NECs, GAERS have a reduce rate of glutamate reuptake in the cortex (Touret et al., 2007). mRNA data seems to support an alteration in the expression of glial glutamate transporters (Ingram et al., 2000), although confirmation at the protein level is still missing. As mentioned above, the expression of stargazin (which is known to regulate the synaptic trafficking of AMPA receptors (Deng et al., 2006)) is increased in the somatosensory cortex of GAERS , as is the expression of the AMPA receptors themselves (GLUA1 and GLUA2) (Kennard et al., 2011).

Evidence also links a dysfunction in the GABAergic system to the expression of ASs in GAERS. Levels of extracellular GABA are increased in the VB of GAERS compared to NECs (Richards et al., 1995), an effect that has been recently linked to a dysfunction of the thalamic GAT-1 transporter (Cope et al., 2009; Crunelli et al., 2011) expressed on glial cells. At the electrophysiological level, it has been observed that, in the NRT of GAERS, IPSPs have a larger amplitude and faster decay compared to NEC, while in cortex and VB IPSPs are not different to non-epileptic controls (Bessaïh et al., 2006). Changes in tonic $GABA_A$ inhibition will be discussed in section 1.5.2 in view of its broad involvement across various models of ASs (Cope et al., 2009; Errington et al., 2011). While, generally, the binding of GABA is reported to be unchanged in GAERS (except for the hippocampus, (Snead et al., 1992)), the expression of β2-β3 subunits of $GABA_A$ Rs was found to be decreased in the sensorimotor cortex and anterior thalamus of GAERS (Spreafico et al., 1993). $GABA_B$ receptors have long being implicated in the pathogenesis of ASs given that, in all experimental models, $GABA_B$ antagonists suppress ASs. Nonetheless, no abnormality has been observed in the expression of $GABA_B$ B receptors in GAERS. In WAG/Rij a marked reduction of some $GABA_B$ receptor subunits in the cortex has been detected at the mRNA level; moreover $GABA_B$ 1 receptors are not expressed in the distal dendrites of cortical cells in this model (Merlo et al., 2007).

1.4.1.1.5 Arousal dependence and role of neuromodulators in GAERS ASs

GAERS ASs arise most commonly during quiet wakefulness or during the transition between wakefulness and the early stages of NREM sleep. Seizures seldomly appear during

the deep stages of NREM (or REM) sleep (Lannes et al., 1988; Leresche et al., 2011). This suggest that, as in clinical ASs, GAERS ASs are under the control of the arousal state (Danober et al., 1998).

The historical view is that neuromodulatory inputs control the vigilance state, which in turn controls the probability of occurrence of an ASs, rather than having a direct effect on seizure generation, although no conclusive evidence exists to date (Danober et al., 1998).

In general, pharmacological treatments that increase noradrenergic tone decrease the occurrence of ASs, while the opposite holds true for antagonists of α and β adrenergic receptors (Micheletti et al., 1987; Marescaux et al., 1992b). Toxin lesions of the *locus coeruleus* produce only a transitory increase the occurrence of SWDs in GAERS (Lannes et al., 1991).

Chemical activation of the PPTg and the LDT markedly reduce absence seizures in the in GAERS. However, lesions of the PPTg and/or the LDTg in GAERS have been reported not to alter SWDs expression (Danober et al., 1995). Chemical lesions of the *nucleus basalis* completely suppress absence seizures (Danober et al., 1994).

In summary, although it is clear that neuromodulators control the expression of ASs, the use of non-specific chemical and electrolytic lesions (which target nuclei and passing fibers) and non-specific pharmacological agents have produced contradictory results regarding the specific role of each neuromodulatory system.

The role of serotonin will be described in section 1.6 in view of its importance for the experiments described in this thesis.

1.4.2 Pharmacological models of absence seizures

Pharmacological models of ASs were the first to be developed. All the pharmacological models known to date involve the systemic administration of substances that act on the GABAergic system: THIP and GHB are agonists at $GABA_A$ and $GABA_B$ receptors, respectively; penicillin and PTZ are weak antagonists at $GABA_A$ receptors (Cortez and Snead, 2006).

The feline penicillin generalized epilepsy (FPGE) was the first animal model of ASs to be characterized. Upon injection of large dose of peninicillin intra-muscularly, cats develop 3-5 Hz SWDs accompanied by behavioural arrest, staring and facial myoclonus (Prince and Farrell, 1969; Quesney et al., 1977; Avoli et al., 1983). Penicillin-elicited ASs are abolished by anti-absence drugs (Guberman et al., 1975). Notably, rats and mice do not respond in such a way to penicillin (Avoli, 1980; Snead, 1992a) and thus, in view of the practical and economic advantages of research using rodents, the FPGE is not commonly used at present.

PTZ has become the most commonGABA$_A$ antagonist used to induce ASs in rodents (Cortez and Snead, 2006). Low doses of PTZ (20-30mg/kg) induce ASs, while doses above 30mg/kg induce clonic and tonic-clonic seizures (Cortez and Snead, 2006; Lüttjohann et al., 2009). PTZ SWDs are expressed within the TC network and not in the hippocampus (Banerjee and Snead, 1994).

Finally, THIP, an agonist at extrasynaptic, δ-containing, GABA$_A$ receptors (see section 1.3.2.2) (Belelli et al., 2005; Drasbek et al., 2007), induces 7-9 Hz SWDs with behavioural arrest in rodents (Fariello and Golden, 1987; Cortez and Snead, 2006).

1.4.2.1 **The GHB-model**

1.4.2.1.1 General aspects of the GHB-model

GHB is a naturally occurring GABA metabolite which, when administered systemically, can induce EEG SWDs accompanied by behavioural arrest (i.e. experimental ASs) in various animal species including rodents, cats and primates (Cortez and Snead, 2006). Historically, the first evidence of the ability of GHB to elicit non convulsive, generalized seizures in a naïve animal came from a study in the cat (Winters and Spooner, 1964). This finding was then supported by studies in monkeys (Roth et al., 1966) and rats (Marcus et al., 1967), but it was mostly the work of Carter Snead's group which established GHB as a solid model of ASs (Snead, 1992a, 2002). Indeed, nowadays the GHB-model is considered the best established pharmacological model of ASs and is commonly used in rodent studies (Crunelli and Leresche, 2002; Snead, 2002)

In the current practice, γ-butyrolactone (GBL) is used as a GHB pro-drug because of its faster onset of action (Bearden et al., 1980). GBL is biologically inactive (Roth et al., 1966;

Snead, 1991; Carter et al., 2006) and is metabolized into GHB by a lactonase in the plasma and liver (Roth and Giarman, 1966). Nonetheless, to stress that GHB is indeed the active form of the drug, hereafter we will refer to the "GHB-model" or "GHB-elicited" ASs even if the administered drug is GBL.

In the rat, a dose of 100mg/Kg GBL reliably produces ASs for approximately one hour; behaviourally ASs are accompanied by vibrissal twitching and facial myoclonus (Snead, 1992a) but, apart from this , the animal is immobile for the duration of the EEG SWDs. ASs are initially isolated and then, about ~10 minutes after the injection of the drug, become continuous. The frequency of the GHB-elicited SWDs in the rat is somewhat similar to that of spontaneous SWDS genetic rat models of ASs: the frequency varies from 5-6Hz to 7-9Hz (Snead, 1992a; Cortez and Snead, 2006) .

GHB-elicited ASs can be recorded in the TC network, but are absent in the hippocampus and other limbic structures (Banerjee et al., 1993; Snead, 2002). While the mapping of GHB-elicited SWDs is mostly similar to that of polygenic rat models of ASs, some differences have emerged after comparing depth EEG recordings and thalamic electrolytic lesions with studies on GAERS rats (Banerjee et al., 1993; Banerjee and Snead, 1994). Firstly, in the GHB-model, SWDs could be recorded only in superficial layers (I-IV) of the fronto-parietal cortex and not in deep layers (V-VI), which were, instead, silent. Secondly, while SWDs could not be detected in intralaminar nuclei in GAERS (Marescaux et al., 1992a), they could be recorded in these nuclei in the GHB model. In fact, lesions of the intralaminar nuclei (ineffective in GAERS (Vergnes and Marescaux, 1992)) abolished SWDs in the GHB-model. Moreover, lesions of the ventrobasal complex and NRT, which abolish ASs in GAERS (Vergnes and Marescaux, 1992), only reduced ASs by 25% in the GHB model (Banerjee and Snead, 1994).

The ontogeny of GHB-elicited ASs was carefully studied in the rat using 200-400mg/kg of GBL (Snead, 1984). In young animals (< post-natal day 14, P14) GHB only produced a pronounced EEG slowing. Some intermediate spiking activity was evoked around P16, but full-blown SWDs were only observed after P28 (Snead, 1984). No differences were reported for GHB-evoked ASs amongst adult animals of different ages (P30-P90). Thus, in the GHB-model, SWDs can only be evoked in the adult brain, strengthening the similarity to other genetic models of ASs and the difference with humans.

1.4.2.1.2 Pharmacological manipulations of GHB-elicited ASs

The therapeutic profile of GHB-elicited ASs is similar to that of human absence. ETX and valproate block ASs, while carbamazepine and phenytoin exacerbate them (Snead, 1992a, 2002). Moreover, GHB ASs are also exacerbated by systemic administration of PTZ and penicillin (Snead, 1988).

The effect of drugs acting on the GABAergic and glutamatergic system has also been tested in the GHB-model, both with systemic and thalamic application. Systemic administration of both NMDA agonists and antagonists blocked the expression of GHB-elicited SWDs but also induced a burst suppression pattern (Banerjee and Snead, 1992). Bilateral infusion of NMDA in thalamic nuclei, and in the NRT, suppressed the expression of GHB-elicited SWDs (Banerjee and Snead, 1995a). As far as the GABAergic system is concerned, systemic administration of the $GABA_A$ agonist muscimol (Snead, 1990), or of weak $GABA_A$ antagonists (PTZ, penicillin), induces an increase in GHB-elicited ASs (Cortez and Snead, 2006). Systemic and intrathalamic administration of steroid modulators of $GABA_A$ receptors (alphaxalone, ganaxalone, tetrahydrodeoxycorticosterone) exacerbates GHB-elicited SWDs (Banerjee and Snead, 1998; Snead, 1998).

1.4.2.1.3 Genetic manipulations in the mouse

In the last decade, different genetic knockout mouse models have been used to investigate the role of specific genes in the expression of GHB-elicited ASs; interestingly, these experiments have highlighted differences between ASs elicited with $GABA_B$ agonists and $GABA_A$ antagonists. Metabotropic glutamate receptor 4 knockout mice were resistant to ASs induced by $GABA_A$ antagonists (PTZ, bicuculline), while GBL (100mg/kg) and baclofen elicited ASs as in wild-type littermates (Snead et al., 2000). Moreover, knockout mice for the AMPA subunit GluR2 had a lower latency of onset, and a decreased cumulative duration of GHB-elicited ASs (GBL 100mg/kg), compared to their wild-type littermates (Hu et al., 2001).

T-type Ca^{2+} channels have been systemically implicated in the expression of GHB-elicted ASs (Cheong and Shin, 2013a). Mice lacking the α1G T-Type Ca^{2+} channel gene, and which therefore do not express functional Cav3.1 channels, were resistant to GHB-elicited seizures (GBL i.p. 70mg/kg), while the susceptibility of these knockout mice to $GABA_A$ antagonist-elicited ASs was unchanged (Kim et al., 2001). $Ca_V2.3$ channel (R-type)

knockout mice displayed a reduced cumulative time spent in seizure and reduced seizure length after systemic application of GBL (70mg/kg) (Zaman et al., 2011).

Mice lacking the $GABA_A$ R α3 subunit had a reduced length and amplitude of GHB-elicited ASs (GBL 100mg/kg) compared to their wild-type littermates, and a similar result was found for systemic PTZ-induced ASs (Schofield et al., 2009). In contrast, mice lacking the δ subunit of the $GABA_A$ R were resistant to GHB-induced ASs (50mg/kg GBL) (Cope et al., 2009).

1.4.2.1.4 Molecular targets of GHB

GHB is known to bind to at least two populations of receptors in the brain: $GABA_B$ receptors ($GABA_B$Rs) and a putative GHB receptor (GHBR) (Crunelli et al., 2006; Bay et al., 2014). The overwhelming evidence suggests that the ictogenic activity of GHB is exclusively mediated by its activation of $GABA_B$ Rs, although for some years a role of the GHB receptors in ASs was also hypothesized (Snead et al., 1990; Snead, 1996a; Maitre, 1997). Recently, experiments in $GABA_B$ R knockout mice have provided compelling evidence that the effects induced by GHB are dependent on the presence of these receptors. At a wide range of doses (50-300 mg/kg GHB), no ASs or other behavioural effects were observed in these knockout mice (Kaupmann et al., 2003; Vienne et al., 2010). Moreover, it has long been known that GHB-elicited ASs can be fully blocked by $GABA_B$ R antagonists (Snead, 1992b, 1996b), although this property is common to all experimental models of ASs. Finally, it is worth mentioning that the potent and selective $GABA_B$ agonist baclofen induces similar EEG and behavioural effects which are indicative of an AS-like phenotype (Snead, 1996b). Nonetheless, the effects of systemic baclofen have not been fully characterized as an absence epilepsy model (e.g. pharmacological profile, anatomical substrates of SWDs, etc.), so the association of baclofen to an AS phenotype remains tentative.

GHB is a weak agonist at $GABA_B$ Rs: it displaces binding of the $GABA_B$ agonist baclofen with a Kd in the range of 30-500 μM (Maitre, 1997; Mathivet and Bernasconi, 1997) and activates heterologous $GABA_B$ Rs with an EC50 in the low mM range (Lingenhoehl et al., 1999). This is particularly significant considering the concentration of endogenous GHB in the brain is 1-4 μM (Doherty et al., 1978; Snead and Morley, 1981) and that the threshold brain concentration of GHB that correlates with the onset of an AS phenotype is 240 μM

(Snead, 1991). Therefore, only exogenously administered GHB is capable of activating $GABA_BRs$. Knowledge of the threshold brain concentration of a drug which evokes ASs is of particular use in interpreting the *in vitro* experiments presented in the next section.

1.4.2.1.5 Thalamic and cortical effects of GHB

Based on the observation that microinjection of 25 μg of GHB in the ventrobasal thalamus of Wistar rats produced brief SWDs with behavioural arrest (Snead, 1991), it was hypothesized that this area is one of the main sites of action the drug (Snead, 2002).

The effects of GHB on thalamic neurons have been characterized, i*n vitro,* in slice preparations of the cat and rat thalamus, and demonstrate multiple postsynaptic effects of GHB on TC neurons. GHB elicited a membrane hyperpolarization on TC cells; this effect was dose-dependent starting from 100μM (the lowest concentration tested) to 3mM (the plateau of the effect) (Williams et al., 1995). The effect was mediated by the opening of potassium channels and was blocked by $GABA_B$ R antagonists. Recent work has also produced evidence of another important thalamic postsynaptic effect of GHB: an increase in tonic $GABA_A$ inhibition (Cope et al., 2009) (see 0). This effect is postsynaptic and is mediated by $GABA_B$ Rs via a G-protein-dependent pathway that probably results in dephosphorylation of extrasynaptic $GABA_A$ Rs (Connelly et al., 2013).

Presynaptic effects induced by GHB on TC cells have also been described: GHB reduced the amplitude of sensory and corticothalamic EPSPs (Emri et al., 1996; Gervasi et al., 2003). The minimum concentrations of GHB to induce these reductions were 100μM and 250μM, respectively. Interestingly, GABA IPSPs originating from the NRT were only reduced by GHB concentrations ≥ 500 μM (Gervasi et al., 2003). All these effects were blocked by $GABA_B$ antagonists (Emri et al., 1996; Gervasi et al., 2003).

Finally, an *in vivo* study looked at the effects of GHB, injected systemically or in the ventrobasal thalamus by reverse microdialysis, on basal and K^+-evoked glutamate and GABA levels (Banerjee and Snead, 1995b). Starting from a concentration of 250 μM, GHB reduced basal GABA levels, leaving basal glutamate levels unchanged; both GABA and glutamate K^+-evoked levels were instead reduced. A similar effect on levels of these neurotransmitters in the ventrobasal thalamus was observed during GHB-induced ASs. These effects were fully blocked by systemic application of $GABA_B$ antagonists (Banerjee

and Snead, 1995b). Nonetheless, the significance of changes of basal and K^+ -evoked levels of neurotransmitters for local network activities are difficult to predict in the absence of electrophysiological data on neuronal firing dynamics.

Effects of GHB on cortical neurons are far less well characterized. An *in vivo* dialysis study investigated basal and K^+-evoked release of GABA and glutamate in the superficial layers of the cortex (Hu et al., 2000). While glutamate concentration was unchanged, there was a clear reduction of both basal and K^+-evoked GABA levels. It is worth noting that the effects on GABA release ended within 70 minutes, whilst ASs persisted for 2 hours. It is, therefore, unclear if these effects simply co-occur with ASs after GBL application or if they have a mechanistic role in their expression.

Experiments in slice preparations from the mouse frontal cortex have shown that, similar to the thalamus, GHB induces a hyperpolarization both of pyramidal cells and putative interneurons in layer II/III, although the threshold to obtain this effect was reported to be in the mM range (Jensen and Mody, 2001). In addition, GHB (1mM) caused a depression in both amplitude and frequency of miniature EPSPs and IPSPs, via a presynaptic mechanism. A more recent study (Li et al., 2007) in the rat prefrontal cortex demonstrated that 300μM of GHB was sufficient to reduce the amplitude of NMDA-EPSPs in layer II/III pyramidal cells. AMPA EPSPs and IPSPs were only depressed at a concentration of 1mM. All the aforementioned effects, either in mouse or rat, were fully antagonized by $GABA_B$ antagonists (Jensen and Mody, 2001; Li et al., 2007).

1.5 Mechanism of ASs: evidence from genetic and pharmacological models

It is well established that the integrity of all the elements of the TC network is necessary for the expression of ASs. Nonetheless, the mechanisms by which ASs are generated still remain an active area of investigation (Crunelli and Leresche, 2002; Meeren, 2005; Avoli, 2012). Historically, there have been two dichotomous theories: that either the thalamus lead the generation of ASs (centrencephalic theory, (Penfield and Jasper, 1947)) or that ASs were generated in cortex (cortical theory, (Bancaud, 1969; Niedermeyer, 1972)). Today it is widely believed that multiple cellular, molecular and pharmacological mechanisms in cortex and thalamus can independently lead to the generation of experimental and human ASs (Avoli, 2012). In the following sections I will review the evidence available regarding the activity of cortical and thalamic neurons during ASs, in light of the new discoveries about the abnormalities found in thalamic and cortical territories of genetic models of ASs (see section 1.4.1.1.4) and of the effects of drugs capable of inducing ASs in naïve and transgenic animals (see sections 1.4.2.1.3 and 1.4.2.1.5).

1.5.1 Cortex

The activity of cortical neurons during ASs was originally characterized in the FGPE model in animals under neurolept anaesthesia. Extracellular recordings have shown that the firing of cortical neurons exhibits a strong phase preference for the spike of each SWC (Fisher and Prince, 1977; Quesney et al., 1977; Avoli et al., 1983). During the wave neurons were silent, an activity that is attributed to Cl- influx into the cells in *in vivo* intracellular recordings (Giaretta et al., 1987). Since then, experiments in WAG/Rij (Inoue et al., 1993) and GAERS (Polack et al., 2007; Chipaux et al., 2013) have also demonstrated an association between pyramidal cell firing and the spike of each SWC.

A major discovery in the field was that, in WAG/Rij, seizures are not generalized from the beginning: there is a cortical initiation site of SWDs which is located in the S1po (Meeren et al., 2002). In particular, using nonlinear association analysis of the LFP, it was shown that other cortical sites lag behind this cortical focus and that, during the first 500 ms from the

beginning of the SWD, the cortex leads the thalamus. After 500ms the oscillation is established and cortex and thalamus can drive each other interchangeably (Meeren et al., 2002; Meeren, 2005).

This finding has since the been replicated in GAERS, where an initiation site in the same region was also identified; it was observed that SWDs could be detected in the somatosensory cortex before being detected in other cortical areas or in the thalamus (Polack et al., 2007). Intracellular recordings (under neurolept anaesthesia) of pyramidal cells within the initiation site demonstrated phase-locking to the EEG spike for both superficial and deep layers. Importantly, the firing of layer 5/6 pyramidal neurons around the EEG spike preceded that of neurons from other layers of the cortical column and was centered about 25 ms before the cortical EEG spike. These neurons were found to be hyperexcitable (i.e. they had more depolarized potential and fired more bursts) in GAERS rats compared to layer V/VI of other cortices, and to layer V/VI neurons of non-epileptic animals (**Figure 1.6**). The molecular or synaptic mechanisms underlying this hyperexcitability are currently unknown, although as noted in section 1.4.1.1.4, the somatosensory cortex of GAERS has an enrichment of stargazin and of AMPA receptors which could underlie the different excitability of these neurons (Jones et al., 2011). Nevertheless, it should be noted that similar molecular changes have not been found in the somatosensory cortex of WAG/Rij where, instead, a decrease in expression of some NMDA and AMPA receptor subunits has been observed (van de Bovenkamp-Janssen et al., 2006). Thus, to date it is still not understood what molecular changes underlie the ability of neurons of somatosensory cortex to initiate ASs. A functional confirmation of the importance of this area in the expression of ASs has come from experiments in GAERS and WAG/Rij, where local application of ETX or pharmacological inactivation of the somatosensory cortex was shown to block ASs (Manning et al., 2004; Sitnikova and van Luijtelaar, 2004; van Raay et al., 2012).

In summary, the current view is that, at least in genetic model of ASs, there is a cortical initiation site, as in humans, and that a subpopulation of pyramidal cells may be leading the initiation of SWDs. The role of different neuronal types, such as cortical interneurons, remains unexplored. During SWDs cortical neurons fire during the *spike* and are silent during the *wave* of a SWC.

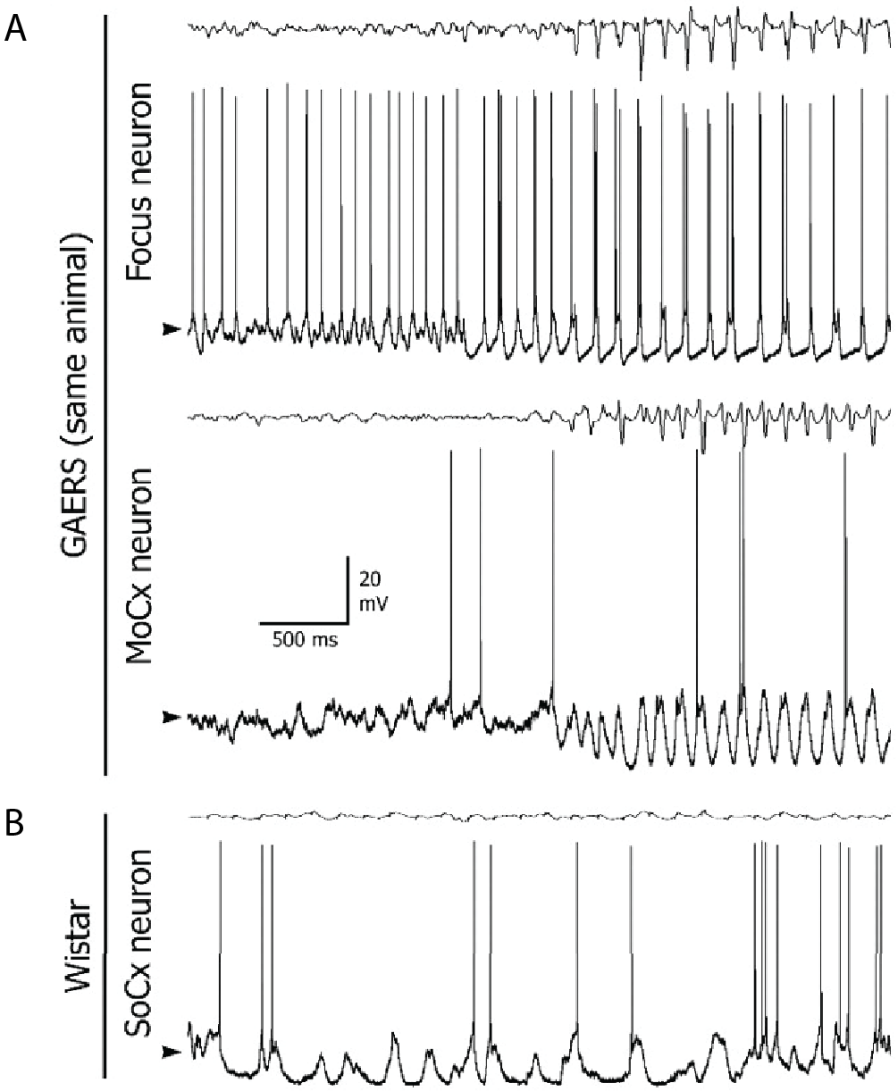

Figure 1.6. Intracellular activity of layer V cortical neurons during SWDs in GAERS
(A) Intracellular recording of a layer V pyramidal cell from the somatosensory cortex (focus, top) and from the motor cortex (MoCx; bottom) in the same GAERS, simultaneously with the corresponding EEG. Not how the focus neurons start firing rhythmically before the start of the EEG seizure. The pyramidal neurons fro motor cortex display rhythmic firing in correspondence to the SWD.
(B) Intracellular recording of a layer V pyramidal cell from the somatosensory cortex (SoCx) from a normal Wistar rat, and simultaneously recorded EEG.

1.5.2 Thalamus

Initial recordings in the FGPE model in animals under neurolept anaesthesia suggested that the firing of putative TC neurons was locked to the spike of the cortically recorded SWD (Avoli et al., 1983). Indeed, these neurons were less synchronous than cortical neurons and were divided in two groups: one composed of neurons firing about 45 ms before the cortical spike and one of neurons firing up to 45 ms after the cortical spike.

The discovery of T-type currents in the thalamus prompted *in vitro* studies that hypothesized a role of thalamic neurons as pacemakers of various oscillations including sleep spindles and SWDs (von Krosigk et al., 1993; Bal et al., 1995a, 1995b). In particular, it was shown that in ferret geniculate slices, the interaction between TC and NRT neurons could produce spindle-like waves, which were transformed into a 2-4 Hz SWD-like oscillation by the addition of the $GABA_A$ antagonist bicuculline. It was suggested that this activity was produced by a bicuculline-induced disinhibition of NRT neurons, which would result in the rhytmic inhibition of TC neurons via postsynaptic $GABA_B$ receptors. TC neurons were thus hyperpolarized, deinactivating T-type channels and generating robust bursting at each cycle of this SWD-like oscillation (Bal et al., 1995b; McCormick and Bal, 1997). TC bursting would then generate rebound bursting in NRT neurons, maintaining the paroxysmal oscillation.

Although this *in vitro* preparation is clearly different from ASs, which occur *in vivo* in the TC network of intact animals, the view that TC neurons act as pacemakers in ASs is still quite well represented in the literature (Buzsaki, 1991; McCormick and Contreras, 2001; Beenhakker and Huguenard, 2009).

More recent studies in GAERS rats *in vivo* strongly argue against the hypothesis arising from the *in vitro* experiments above. Intracellular recordings of TC neurons under neurolept anaesthesia showed that neurons which were silent fired single spikes during SWDs without any T-type channel dependent burst of action potentials (**Figure 1.7A**). This activity was accompanied by a tonic hyperpolarization (probably K^+ -mediated), and by rhythmic $GABA_A$ dependent IPSPs (Pinault et al., 1998). Notably, no rhythmic $GABA_B$ -mediated IPSPs were observed, although it was suggested that the tonic K^+-dependent hyperpolarization was mediated by a tonic activation of $GABA_B$ receptors. The intracellular

activity of NRT neurons in the same preparation (Slaght et al., 2002) instead displayed rhythmic hyperpolarization and LTCP-mediated bursts of action potentials at each SWC (**Figure 1.7B,C**). The firing of each NRT spike was ~20ms before the EEG spike, thus preceding the TC spike (~10ms before the EEG spike).

These *in vivo* results in genetic models of ASs have no counterpart in rodent pharmacological models of ASs. As far as the GHB-model is concerned, a partial support for the role T-type currents in TC neurons suggested by *in vitro* experiments comes from work in knockout mice for Cav3.1 channels. These animals display no bursting in TC neurons *in vitro* and are resistant to GHB-elicited ASs (Kim et al., 2001). Moreover, overexpression of Cav3.1 channels in the whole brain, which results in enhanced functional T-type current in TC neurons, produces mice with spontaneous ASs (Ernst et al., 2009). Nevertheless, a fundamental caveat of these studies is that deletion or overexpression of Cav3.1 channels was not restricted to TC neurons, therefore the resulting phenotypes could have been caused by changes in cortex (and it should be noted that T-type channels have other roles in addition to producing LTCPs, such as the generation of the window current, see section 1.3.2.1.4). *In vitro* experiments with bath application of GHB (see section 1.4.2.1.5) are also helpful understanding the potential mechanism of the generation of ASs via GHB. At brain concentrations relevant for the expression of ASs (i.e. 240 μM), GHB induces a postsynaptic hyperpolarization on corticothalamic and TC neurons and, both in the ventrobasal thalamus and in the frontal cortex, and presynaptically depresses EPSPs, therefore favoring phasic inhibition over phasic excitation. Without *in vivo* recordings after GHB administration it is not possible to predict what changes in thalamic neuron activity GHB would produce and how those changes would bring about ASs and the correspondent firing in TC and NRT neurons.

Recent work from our lab has shown that, at in TC neurons, a key player in the expression of ASs is an increase in the tonic $GABA_A$ inhibition (see section 1.3.2.2), which was shown to be sufficient for the expression of ASs (Cope et al., 2009). Importantly, this increased tonic inhibition has been found in both genetic (stargazer, lethargic and GAERS) and pharmacological models of ASs (the THIP and the GHB-model). In the genetic models, the increase in tonic inhibition was dependent on a malfunction of the GAT-1 transporter, which controls the level of ambient GABA (Cope et al., 2009). In the case of the GHB-model it was shown that GHB (300 μM) produced a ~30% increase in tonic $GABA_A$ current, an effect that is was later demonstrated to be mediated by a postsynaptic cross-talk between $GABA_B$ Rs and $GABA_A$ Rs (Connelly et al., 2013). It has been hypothesized that the increase

in tonic $GABA_A$ inhibition hyperpolarizes TC neurons (concomitantly with the activation of $GABA_B$ receptors described above) and increases the membrane conductance of the neurons, thus reducing the action potential output.

In summary, the current *in vivo* evidence suggests that, during spontaneous ASs in genetic models, TC neurons are mostly silent or fire single spikes, while NRT neurons burst at each SWC. This hypothesis is in opposition to *in vitro* data showing bursting in TC neurons at each cycle of the SWD-like oscillation. The activity of TC and NRT neurons during GHB-elicited ASs is not known, but there are at least three independent mechanisms by which GHB could facilitate/generate ASs: presynaptically, by an indirect increase in phasic $GABA_A$ inhibition, postsynaptically, by membrane hyperpolarization and by an increase in $GABA_A$ tonic inhibition.

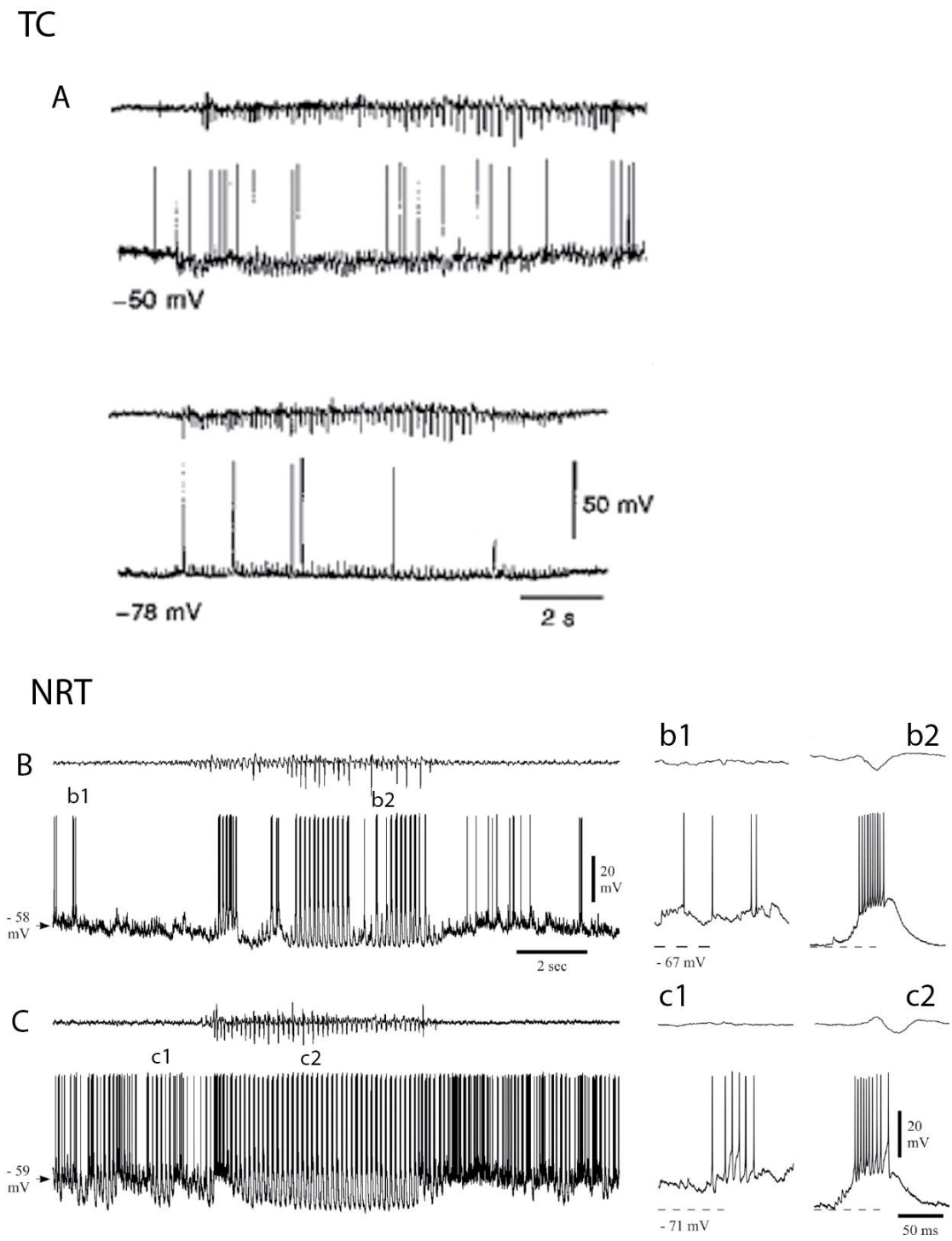

Figure 1.7 Intracellular activity of TC and NRT neurons during ASs in GAERS

(A) Intracellular recordings of two TC neurons (top and bottom) and simultaneously recorded EEG. Note how during SWDs neurons are tonically hyperpolarized and are either silent or fire single spikes during each SWC.

(B-C) Intracellular recordings of NRT neurons and simultaneously recorded EEG. During SWDs the neurons are tonically hyperpolarized and fire LTCP-mediated bursts (see enlargements b2, c2) during each SWC, while interictally they tonic firing is evident (see enlargements b1,c2).

A, adapted from (Pinault et al., 1998); B-C, adapted from (Slaght et al., 2002).

1.6 Serotonin and absence seizures

1.6.1 General aspect of the serotoninergic system

Serotonin (5-HT) belongs to the class of monoamine transmitters and has a broad range of functions in the CNS, in the peripheral nervous systemic and in non-neural tissues (e.g. gastrointerstinal, endocrine, blood) (Berger et al., 2009). 5-HT is recognized to modulate a plethora of activities in the CNS, including mood, cognition, sleep, memory, aggression, sex, respiration, vascular function to name a few (Hannon and Hoyer, 2008; Nichols and Nichols, 2008). The main source of serotoninergic innervation in the CNS arises from the raphe, a sparse structure distributed along the brainstem. Historically, the raphe was subdivided in 9 nuclei, B1-B9, based on formaldehyde histo-fluorescence (Dahlstroem and Fuxe, 1964). B7 and B8, known as the dorsal and median nuclei, provide the majority of serotonergic innervation to the forebrain and therefore to the TC network. One reason for the abundance of functions of 5-HT in the brain lies in the fact that although, 5-HT neurons make up less than 1% of the neurons in the brain, virtually no area of the CNS is devoid of serotoninergic innervation (Aghajanian and Liu, 2009). In the next sections we will first review the current classification of 5-HT receptors (5-HTRs), focusing especially on the 5-HT2 family, and describe the evidence available suggesting a role for 5-HT2 receptors in the modulation of seizures.

1.6.2 5-HT receptors subtypes

5-HT has a unique abundance of receptors, unrivaled by other neurotransmitters and neuromodulators systems. Indeed, 5-HT in one of the most ancient signaling molecules; the first 5-HTRs started to diverge about 700 million years ago, earlier than receptors for other neuromodulators (Nichols and Nichols, 2008).

Historically, the first sub-classification of 5-HTRs was based on non-specific drugs: two populations of 5-HTRs named ‘D’ type (blocked by application of dibenzyline) and ‘M’ type (blocked by application of morphine) were identified in the guinea-pig ileum (Gaddum and Picarelli, 1957). In subsequent years, new 5-HTRs were characterized with radioligand-

binding studies and by using selective antagonists (Peroutka and Snyder, 1979; Bradley et al., 1986) and a distinction between 5-HT1-like, 5-HT2 ('D' type) and 5-HT3 ('M' type) receptor families was proposed (Bradley et al., 1986).

Later, advancements in molecular biology allowed the cloning of multiple novel 5-HTRs subtypes. Therefore, a novel classification was introduced, integrating sequence homology information with the operational (i.e. pharmacological and binding) data (Humphrey et al., 1993). This classification consisted of five 5-HT_1 receptors subtypes (5-$HT_{1A/1B/1D/1E/1F}$), three 5-HT_2 receptor subtypes (5-$HT_{2A/2B/2C}$), a 5-HT_3 and a 5-HT_4 receptor. To date, the revised classification of 5-HTRs includes the newly discovered 5-HT_5, 5-HT_6 and 5-HT_7 receptors families and, therefore, totals 7 receptor families (Hoyer and Martin, 1997). This classification is based on the combined information available on sequence homology, pharmacology and transduction pathways (**Figure 1.8**); the nomenclature is based on human orthologues to avoid inter-species confusion (Hoyer et al., 2002). Interestingly, among the 14 receptors discovered so far, only the 5-HT_3 receptor is ionotropic, while all other serotonin receptors are metabotropic.

The repertoire of 5-HTRs is further enlarged by the presence of multiple splice variants (in particular, several have been characterized for 5-HT_4 and 5-HT_7 receptors (Bockaert et al., 2006; Coupar et al., 2007)) and with RNA editing, which, uniquely to the 5-HT_{2C} receptor, modifies the mRNA sequence, giving rise, post-transcriptionally, to functionally different 5-HT_{2C} receptors. Finally, 5-HT_3 receptors form homo/hetero pentamers (Thompson and Lummis, 2006) and G-protein coupled 5-HTRs can be found in neurons in the form of homo/hetero dimers (Millan et al., 2008).

1.6.2.1 **The family of 5-HT2 receptors**

In this section I will concentrate on the 5-HT2 family, which is been the focus of this thesis. I will first describe the common features of the three members of the 5-HT2 family (i.e. 5-HT_{2A}, 5-HT_{2B} and 5-HT_{2C}) and will move on to describe the specific properties of these receptors with respect to their signaling pathways, tissue localization and pharmacology.

5-HT2 receptors have a 46-50% sequence identity (>70% considering only the within-transmembrane sequence). To date, no high-resolution x-ray structure for any 5-HT2 receptor is available. Mutagenesis studies have identified the putative binding pocket for 5-

HT on the transmembrane α-helices 3, 5 and 6. The affinity of 5-HT2 receptors for 5-HT, measured in a binding study where each receptor was individually expressed in a heterologous expression system, is similar between subtypes and estimated to be in the nM range (Leysen, 2004).

5-HT2 receptors are clustered together in the current classification based mainly on common transduction pathways. 5-HT2 receptors are coupled to Gαq proteins; activation of these G proteins activates phospholipase C (PLC), which in turn hydrolyzes phosphatidylinositol biphosphate (PIP2) generating diacylaglicerol (DAG) and inositol trisphosphate (IP3). These second messengers can, respectively, activate protein kinase C and induce influx of intracellular Ca^{2+}. The 5-HT2 receptors are also reported to activate phospholipase A2 (PLA2) the main effect of which is the intracellular release of arachidonic acid (AA).

Importantly for this thesis, $5\text{-}HT_{2B}$ receptors are mostly localized in smooth muscle (in particular in stomach fundus where they were originally identified) and in other peripheral tissues, including endothelial cells of blood vessels and heart . The expression of this receptor in the brain is scarce (Leysen, 2004), thus they will not further discussed here. Nevertheless, it important to note that activation of $5\text{-}HT_{2B}$ receptor has been linked to pulmonary hypertension and valvulopaties (Berger et al., 2009), and therefore compounds produced for clinical applications are screened against agonist action at this receptor.

In recent years, it has become clear that different 5-HT2 receptors can activate a plethora of additional downstream pathways (Masson et al., 2012). This variety of outputs depends on receptor structure and intracellular (tissue-specific) binding partners but can also depend on the nature of the exogenous ligand used to activate the receptors. This latter property is defined as “functional selectivity” (sometimes called “agonist-directed trafficking of receptor stimulus” or “biased agonism” (Urban et al., 2007)) and has emerged as an important property of $5\text{-}HT_{2A}$ and $5\text{-}HT_{2C}$ receptors. The specific downstream pathways for each receptor subtype will be described in the relative paragraphs, focusing on examples pertinent to the CNS.

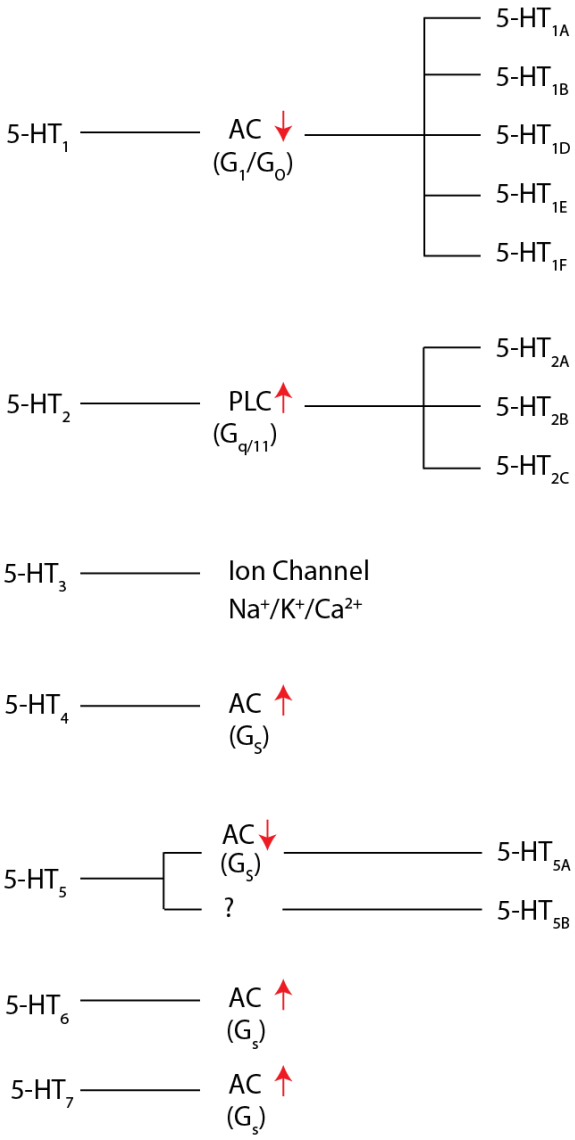

Figure 1.8 Classification of 5-HTRs subtypes. 5-HT receptors are grouped into 7 families, coupled to different G-proteins (i.e. $G_{q/11}$, G_S, $G_{i/o}$) and downstream effectors (AC, adenylate cyclase; PLC, phospholipase C), except for the 5-HT_3R which is ionotropic. Adapted from (Blackburn, 2009).

The desensitization and cellular trafficking of 5-HT2 receptors in response to chronic activation with agonists and antagonists has received a lot of attention because of their atypical properties (Van Oekelen et al., 2003a). Binding of agonists to 5-HT_{2A} and 5-HT_{2C} receptors induces their phosphorylation, β-arrestin binding and internalization in a classical agonist-induced desensitization. Nonetheless, paradoxically, chronic treatment with antagonists also induces a decrease in receptor density. This mechanism, dubbed antagonist-induced internalization, is atypical for G-protein coupled receptors and is thought to be partly responsible for the pharmacological properties of antipsychotics that bind to 5-HT2 receptors (see following paragraphs) (Van Oekelen et al., 2003a).

Finally the degree of constitutive (e.g. ligand-independent) activity of 5-HT2 receptors is also reported to be a major difference within the members of this family, with 5-HT_{2C} receptors having a constitutive activity 10 times higher than 5-HT_{2A} receptors *in vitro* (Millan et al., 2008). The constitutive activity of 5-HT2 receptors appear to have an important role in the physiological function of these receptors in the brain and will be discussed in the pertinent paragraphs.

1.6.2.1.1 5-HT_{2A} receptors

In the periphery, 5-TH2A receptors are localized on smooth muscles where they mediate muscle contractions. In addition, they are widely expressed in multiple CNS areas, including cortex, insula, limbic structures and in some brainstem nuclei (Li et al., 2004; Masson et al., 2012). Expression of 5-HT_{2A} in the thalamus is generally reported to be moderate to low (Cornea-Hébert et al., 1999; Li et al., 2004). In the cortex, 5-HT_{2A} staining is concentrated on layers IV-VI and the receptors are expressed both in interneurons and pyramidal cells. Within neurons, electron microscopy studies have shown that receptors are mostly concentrated on somas and apical dendrite shafts (Bockaert et al., 2006). Most studies agree that there is little expression of 5-HT_{2A} in the presynaptic terminals of cells projecting to the cortex (Miner et al., 2003) .

The effects of 5-HT_{2A} receptor activation have mainly been studied in cortical neurons, although, hampered by the lack of selective agonists and different experimental conditions, the net effect of 5-HT_{2A} activation is only partly understood. *In vivo*, iontophoretic application of 5-HT induced a decrease in firing of pyramidal cells, an effect which is

blocked by 5-HT_{2A} antagonists (Ashby et al., 1990), although, more recently, a prevalent excitation of pyramidal cells was reported (Puig et al., 2003). *In vitro*, 5-HT_{2A} receptor activation depolarizes pyramidal cells and induces an increase in spontaneous EPSCs (Araneda and Andrade, 1991; Aghajanian and Marek, 1997). 5-HT_{2A} receptor activation also greatly enhances the amplitude and frequency of spontaneous IPSCs recorded in pyramidal cells (Zhou and Hablitz, 1999) and depolarizes fast-spiking interneurons (Weber and Andrade, 2010). The effects of 5-HT_{2A} activation on neuronal excitability in pyramidal cells are thought to be mainly post-synaptic and to involve an increase in glutamate release in interconnected pyramidal cells (Andrade, 2011). At the electrophysiological level two main effects of 5-HT_{2A} activation in pyramidal cells have been identified: a slow membrane depolarization and the inhibition of the slow, K^+-dependent, afterhyperpolarizating current (Andrade, 2011; Celada et al., 2013). The downstream effectors of 5-HT_{2A} receptors that induce the above mentioned changes in cell excitability are at present unknown. No information is available on the role of 5-HT_{2A} receptors in the excitability of thalamic neurons.

As mentioned earlier, the level of constitutive activity of 5-HT_{2A} receptors is generally considered to be low *in vitro*. Nonetheless, *in vivo* studies have shown that constitutive activity of 5-HT_{2A} receptor has a role in controlling associative learning (Aloyo et al., 2009). Indeed while 5-HT_{2A} inverse agonists produce a strong retardation of learning, depletion of 5-TH is not effective in altering learning paradigms.

As mentioned earlier, part of the complexity of the effects of 5-HT_{2A} receptors is accounted for by functional selectivity. Most psychedelic drugs (i.e. phenethylamines and tryptamines) are thought to induce hallucinations via their agonist action at 5-HT_{2A} receptors. Interestingly, not all drugs that have an agonist activity at 5-HT_{2A} receptors are hallucinogenic (Nichols and Sanders-bush, 2001; Nichols, 2004). Functional selectivity is thought to be at least partly responsible for this discrepancy. Experiments in heterologous expression systems have shown that hallucinogenic drugs have a higher potency at activating the PLA2 than the PLC pathway (Kurrasch-Orbaugh et al., 2003). In particular, recent work has shown that, while the non-hallucinogenic, ergoline lisuride, activates only the Gq/PLC pathway, LSD is also coupled to the Gi/o proteins (González-Maeso et al., 2007). In rodents, the correlate of hallucination is a head-twitching response that is elicited by all drugs known to be hallucinogenic in humans (Fantegrossi et al., 2008). Moreover, 5-HT_{2A} and metabotropic glutamate 2 (mGlu2) receptors assemble into heterodimers and these complexes are thought to be partly responsible for the

hallucinogenic effects of 5-HT_{2A} agonists (González-Maeso et al., 2008; Moreno et al., 2011, 2012). Interestingly, the head-twitching response, which is abolished in 5-HT_{2A} R knock-out mice (González-Maeso et al., 2007), is only partly attenuated in knockout mice for the Gq subunit (Garcia et al., 2007).

The role of 5-HT_{2A} receptors in sleep has also been thoroughly investigated. Application of selective 5-HT_{2A} antagonist, M100,907, in wild-type mice increased NREM sleep and decreased REM sleep and wakefulness (Popa et al., 2005). Similar results were obtained by M100,907 injection in Wistar rats (Morairty et al., 2008). Interestingly, 5-HT_{2A} gene deletion had the opposite effect to the acute pharmacological block: 5-HT_{2A} knockout mice displayed an increase in wakefulness and a reduction in NREM sleep, while REM sleep was unchanged (Popa et al., 2005). This is indicative of adaptive mechanisms that take place in the global knockout mice. The efficacy of 5-HT_{2A} antagonists in promoting sleep in humans is less clear: various selective 5-HT_{2A} antagonists have been synthetized and tested in humans in last 20 years, including Volinanserin (M100,907), Pimavanserin (ACP-103,), Eplivanserin (SR-46,349), ritanserin, glemanserin (MDL11,939) andPruvanserin (LY-2,422,347), but none of these drugs have been approved for clinical use. Whether this is due to lack of efficacy or safety concerns remains unclear (Vanover and Davis, 2010).

An increased interest in the development of 5-HT_{2A} antagonists has arisen from the discovery that many atypical antipsychotics potently inhibit 5-HT_{2A} receptors and have a higher affinity for 5-HT2R relative to D2 receptors (Nichols and Nichols, 2008). Pimavanserin has recently undergone clinical trials to treat Parkinson's disease psychosis and is expected to go on the market in 2015 (Meltzer and Roth, 2013).

There is also clear evidence that the 5-HT_{2A} receptors are involved in the control of emotional states, in particular anxiety (Quesseveur, 2012). Indeed cortical disruption of 5-HT_{2A} receptors has been shown to reduce anxiety-related behaviours in mice without affecting depression or fear conditioning responses (Weisstaub et al., 2006).

1.6.2.1.2 5-HT_{2C}Rs

5-HT_{2C} receptors are found almost exclusively in the CNS. They are highly expressed in the epithelial cells of the choroidal plexus, where they were originally identified (Pazos et al., 1984). In addition, high levels of expression, confirmed both with immunocytochemistry

and *in situ* hybridization, are found in limbic structures (e.g. hippocampus, amygdala, olfactory nuclei, cingulate and piriform cortex), ventro-medial thalamus, basal ganglia, substantia nigra and in the arcuate nucleus of the hypothalamus (Leysen, 2004; Li et al., 2004). The expression of 5-HT_{2C} receptors in the cortex is low, although a transient upregulation during development has been identified (Li et al., 2004). The subcellular localization of 5-HT_{2C} receptors has not been thoroughly investigated, but in cortical areas the expression is presumed to be on pyramidal cells (Puig et al., 2010) (but see (Liu et al., 2007)) and, within them, on somato-dendritic compartments (Bécamel et al., 2004; Leysen, 2004).

Similarly to 5-HT_{2A}R, 5-HT_{2C}Rs also exhibit functional selectivity, and, therefore, equipotent synthetic ligands preferentially activate the PLC or PLA pathway (Stout et al., 2002; Urban et al., 2007). In contrast to other members of the 5-HT2 family, 5-HT_{2C} has also been reported to activate phospholipase D (PLD) via a $G\alpha^{13}$ dependent mechanisms, although this activity has only being described in the choroid plexus (Masson et al., 2012).

5-HT_{2C}Rs have a high constitutive activity, an effect that, *in vitro,* is specific for the activation of the PLC pathway (Aloyo et al., 2009). While the physiological roles of this constitutive activity are only starting to be elucidated, it is well known that 5-HT_{2C} constitutive activity is responsible for the inhibition of dopamine release in the striatum. Indeed, 5-HT_{2C} inverse agonists are more efficacious than 5-HT_{2C} antagonists in increasing dopamine release and the effect of inverse agonists is not influenced by the extracellular levels of 5-HT.

As mentioned earlier 5-HT_{2C} is the only metabotropic receptor which undergoes RNA editing. This process is catalyzed by enzymes of the class “adenosine deaminases acting on RNA” (ADARs) which, in the case of mammals, produce the deamination of an adenosine to an inosine. The transcription machinery reads an inosine as if it were a guanosine, thus resulting in amino acid substitutions. Humans have 5 adenosine-to-inosine mRNA editing sites, while rodents have 4. Editing is very commonly observed (Werry et al., 2008): >75% of the 5-HT_{2C} mRNAs in rats have been edited at 3 or more sites. About 15-20 different protein isoforms are obtained via RNA editing, which have regional expression differences within the brain (for instance editing in the position C’ is found only in the receptors expressed in the thalamus,). The functional consequences of this process are starting to be elucidated. In general, the more the 5-HT_{2C} mRNA is edited, the lower the constitutive activity of the receptor (Werry et al., 2008). The amount of editing also has an impact on

the downstream effectors recruited by the 5-HT_{2C} receptor: the unedited isoform of the receptor binds β-arrestin leading to constitutive internalization of the receptor, which is mostly found intracellularly. The fully edited isoform (which does not bind β-arrestin) is instead found on the cell membrane and is only endocytzed via agonist-dependent mechanisms. In parallel, editing also changes the receptor affinity for 5-HT and for other 5-HT_{2C} ligands. Overexpression of certain edited 5-HT_{2C} subunits in mice can produce disease phenotypes, such as Prader-Willi syndrome (Morabito et al., 2010) .

There is very little electrophysiological data regarding the effects of 5-HT_{2C} activation in thalamus or cortex (Celada et al., 2013). The depolarizing action of 5-HT on pyramidal cells seems to be produced only by 5-HT_{2A} receptors, given that it was blocked by selective 5-HT_{2A} antagonists but not by selective 5-HT_{2C} antagonists (Béïque et al., 2004). In the VTA, activation of 5-HT_{2C}Rs induces an increase in firing rate of VTA interneurons which then inhibits VTA dopaminergic neurons. The net effect is a decrease in dopamine release in the mesolimbic pathway (Matteo et al., 1999; Di Matteo et al., 2001; Di Giovanni et al., 2006). In the hypothalamus, 5-HT_{2C}Rs increase the excitability of central proopiomelanocortin (POMC) neurons (which control feeding behaviours) by inhibiting the M-current of K^+ channels.

Systemic administrations of 5-HT_{2C} agonists and antagonists was found to induce various effects in rodents, including changes in vigilance states, reward-mediated behaviours, emotional states (e.g. anxiety), network-excitability, feeding and locomotion (Giorgetti and Tecott, 2004; Di Giovanni et al., 2006; Monti and Jantos, 2010; Higgins et al., 2013a).

The role of 5-HT_{2C} receptor modulation in sleep has been studied using 5-HT_{2C} knockout mice (Frank et al., 2002) and by pharmacological approaches, leading to contradictory results. While REM sleep was unchanged in the knockout mice, the animals displayed increased wakefulness and decreased NREM sleep. These results are at odds with pharmacological manipulations that have shown that antagonism of 5-HT_{2C}Rs induces an increase in NREM sleep and a decrease in the REM sleep (Smith et al., 2002; Monti and Jantos, 2006). Conversely, other pharmacological experiments with the selective 5-HT_{2C} antagonist, SB202484, have found that inhibition of the 5-HT_{2C} receptor induces no changes in vigilance states but, rather, induces changes in theta spectral power during wakefulness (Kantor et al., 2005). Pharmacological activation of 5-HT_{2C} receptor was reported to increase wakefulness and decrease NREM sleep (Martin et al., 1998). Nonetheless, pharmacological manipulations have only been conducted with non-selective

5-HT_{2C} agonists and, therefore, a confirmation of the putative effect of 5-HT_{2C} receptor activation with selective agents is still needed. In conclusion, most studies confirm an effect of 5-HT_{2C}Rs on arousal states but the net effect is at the present unclear (Monti and Jantos, 2010).

Systemic administration of 5-HT_{2C} agonists is known to produce two peculiar phenotypes in rodents: hypolocomotion and penile grooming (Leysen, 2004). There is a general consensus that a decrease in locomotion is a stereotypical response of 5-HT_{2C} activation, as it is obtained with all known selective 5-HT_{2C} agonist and it is absent in 5-HT_{2C} knockout mice treated with 5-HT_{2C} agonists (Higgins and Fletcher, 2003; Fletcher et al., 2009). Nevertheless, the nature of the behavioural response and the mechanisms that bring about 5-HT_{2C} -elicited hypolocomotion are unclear. It has been suggested that 5-HT_{2C} induced hypolocomotion represents the effect of 5-HT_{2C} mediated inhibition of dopaminergic cells of the VTA and reduced activity of the mesolimbic pathways (described previously) which can modulate locomotor activity (Fletcher et al., 2004, 2009). Penile grooming and penile erections are also commonly observed after systemic administration of 5-HT_{2C} receptor agonists in rodents (Millan et al., 1997). This action is thought to reflect the activation of 5-HT_{2C}Rs present in parasympathetic preganglionic neurons in lumbo-sacral spinal cord (Leysen, 2004).

5-HT_{2C} receptor knockout mice are obese (Tecott et al., 1995), highlighting the role of this receptor in controlling feeding behaviour. Indeed, the 5-HT_{2C} agonists have long been known to be pro-anorexic and the selective agonist, lorcaserin, has been approved by the FDA in 2012 for the treatment of obesity (Thomsen and Grottick, 2008; Miller, 2013). This activity is partly mediated by increased excitability of POMC neurons in the hypothalamus, although modulation of 5-HT_{2C}Rs on cognitive-hedonic functions, via the mesocorticolimbic DA system, cannot be discounted (Higgins et al., 2013a). Indeed, 5-HT_{2C} receptor activation can reduce many reward-related behaviours, including the seeking of drugs of abuse (Higgins et al., 2013a).

5-HT_{2C}Rs also have a role in controlling mood states. In general pharmacological activation of 5-HT_{2C}Rs is thought to increase anxiety-like behaviours and a similar effect is obtained by overexpressing the 5-HT_{2C} receptor in the forebrain (Kimura et al., 2009; Quesseveur, 2012). Conversely, 5-HT_{2C} antagonists act as anxiolytics.

5-HT_{2C} knockout mice also have an increased susceptibility to seizures (seizure modulation by 5-HT_{2C}Rs will be discussed in section 1.6.3).

1.6.3 Serotonin and ASs: focus on 5-HT2 receptors

The idea that the 5-HT system is implicated in epilepsy dates back more than 50 years (Bonnycastle et al., 1957). In general, various studies have found that an increase in 5-HT levels (for instance produced by serotonin reuptake blockers) tends to inhibit seizure generation, while a decrease in 5-HT concentration in the brain lowers the threshold for various types of convulsive seizures (Bagdy et al., 2007).

The modern classification of 5-HTR subtypes, and the generation of selective pharmacological and genetic (i.e. knockout mice) tools to investigate the contribution of individual receptors, are fairly recent (see section 1.6.2). Within the family of 5-HT2 receptors, most evidence suggests an involvement of 5-HT_{2C}Rs in seizure generation and network excitability (Isaac, 2005). 5-HT_{2C} knockout mice display spontaneous tonic-clonic seizures which are occasionally lethal (Tecott et al., 1995). In addition, in these animals the threshold for various convulsant stimuli (e.g. kindling, PTZ, electroshock, audiogenic seizures) is decreased (Applegate and Tecott, 1998a; Heisler et al., 1998). A change in threshold for induction of non-convulsive, generalized seizures has not been investigated in 5-HT_{2C} knockout mice. Further evidence on the protective role of 5-HT_{2C} activation against convulsive seizures comes from experiments using non-selective 5-HT_{2C} agonists which raise the threshold for PTZ and electric shock-induced seizures in mice (Upton et al., 1998). Similarly to 5-HT_{2A} receptors, only a handful of studies have investigated the role of this receptor in convulsive seizures, leading to inconclusive results (Gharedaghi et al., 2014).

The evidence for the role of 5-HT2 receptors in non-convulsive, generalized seizures is scarce, and the interpretation of the results has been hampered by the lack of selective drugs.

Early experiments in GAERS excluded a contribution of 5-HT neurotransmission to the genesis or modulation of ASs (Danober et al., 1998). Indeed, treatments that increase serotoninergic tone, such as systemic administration of the 5-HT precursor 5-hydroxytryptophan or administration of non-selective 5-HT agonists, have no effect on SWDs (Marescaux et al., 1992b). Moreover, systemic administration of inhibitors of 5-HT

synthesis, broad spectrum 5-HT2 antagonists (ritanserin, ketanserin) or electrolitic lesions of the dorsal raphe also have no effect on SWDs (Marescaux et al., 1992b).

Instead, experiments on WAG/Rij rats have found that 5-HT_{2C} receptor activation decreased SWDs cumulative duration (Jakus et al., 2003). Importantly, while the 5-HT_{2C} agonist used, mCPP, is not selective for the 5-HT_{2C} receptor, the mCPP reduction of ASs was blocked with the selective 5-HT_{2C} antagonist SB242084 (Jakus et al., 2003). SB242084 had no effect on SWDs when administered on its own, suggesting that basal 5-HT_{2C} activity is not implicated in the generation of absence seizures.

In the AY-9944 model of atypical ASs, mCPP has no effect in modulating ASs, while the mixed 5-HT_{2A} /2C receptor agonist, DOI, dose-dependently reduced the cumulative time spent in seizure (Bercovici et al., 2006). The authors concluded the 5-HT_{2A} receptors were responsible for this effect, although no 5-HT_{2A} antagonist was used in combination with DOI to prove the selectivity of the decrease in seizures. The moderately selective 5-HT_{2A} antagonist, ketanserin, increased the cumulative time spent in seizure, but the effect was not dose-dependent (Bercovici et al., 2006).

In the groggy model of ASs (Tokuda et al., 2007), DOI dose-dependently reduced the cumulative time spent in seizure and, we note that, the same was true for the 5-HT reuptake inhibitors fluoxetine and clomipramine (Ohno et al., 2010). The non-selective 5-HT2 antagonist, ritanserin, had no effect on its own, but blocked the DOI-elicited decrease in ASs.

In summary, although there is clear evidence pointing to a role of 5-HT_{2C}Rs in the control of network excitability and seizures, the effect of modulation of 5-HT_{2C}R in ASs is still not fully understood.

1.7 Thesis Aims

The primary aims of this thesis were to investigate the role of 5-HT_{2A} and 5-HT_{2C}Rs on the expression of ASs in GAERS rats and in the GHB-model, via systemic and local pharmacological manipulations (Chapter 3)

However, in using the GHB-model of ASs it soon became evident that several aspects of the EEG and behaviour in this pharmacological model were poorly described in the literature. In particular, animals injected with GBL presented isolated, brief ASs but also a long-lasting state that resembled hypnosis/sedation. Given that the GHB-model is widely used in the absence-epilepsy literature and is generally considered a good model of ASs, the main focus of thesis was switched to further characterizing the GHB-model. Specifically, this was done by addressing the following points:

1) Investigating the role of T-type Ca^{2+} channels in the expression of GHB-elicited ASs and hypnosis (Chapter 4);
2) Studying the firing output of NRT neurons in the GHB-model via silicon probe recordings in freely moving rats (Chapter 5);
3) Developing an algorithm to classify different GHB-elicited activities and correctly identify GHB-elicited ASs (Chapter 6).

Chapter 2 **METHODS**

2.1 Animals and ethical statement

GAERS rats were bred in-house in the School of Biosciences (Cardiff University, UK). Wistar rats were purchased from Harlan (UK) and a minimum of 3 days was allowed from their arrival before starting any procedure in order to minimize stress. All rats had access to food and water *ad libitum.* The animals were moved to a time shifted housing room (10 a.m. lights-off; 10 p.m. lights-off) a week before the beginning of the recovery surgeries. The housing room had a temperature of 19-21 °C and a relative humidity of 45-65%. A minimum of 5 days post-recovery was allowed before commencing the experiments (unless otherwise stated). Only male rats at an age of 3-5 months were used for the experiments (unless otherwise stated). All animal procedures were approved by the Home Office and carried out in accordance with Cardiff University ethical guidelines.

2.2 Recovery Surgeries

All tools used during the surgery were autoclaved prior to the start of the surgery. When sterilization by autoclaving was not feasible (e.g. electrodes or probes that would be damaged by the high temperature) the devices were immersed in a 70% alcohol solution for at least 20 minutes before coming in contact with the animal or in the case of silicon probes, in a 4% solution of protein detergent (Contrad 70, Decon Labs, USA).

2.2.1 Anaesthesia, analgesia and post-operative care

General anaesthesia was induced in an induction box where 5% isofluorane was delivered in 2L/min 100% O_2. The animal was then transferred to a stereotaxic frame where initially received a concentration of 3.5% isofluorane in 1L/min 100% O_2. This concentration was gradually reduced over the course of the surgery to a final level of 2% isofluorane in 1L/min O_2, ensuring that the animal maintained a stable breathing pattern. The level of anaesthesia was judged by absence of hind leg withdrawal and tail pinch reflex. The

temperature of the animals was monitored with a rectal probe and maintained at 37° with a homoeothermic heat blanket (#507220F, Harvard Apparatus, Kent, UK)

To maintain the animal hydrated, 5mL/kg of sterile 0.9% saline was injected s.c. after one hour from the induction of general anaesthesia. Post-operative analgesia was ensured injecting s.c. 1mg/kg meloxicam (Metacam, Boehringer Ingelheim, Berkshire, UK), once the animal was transferred to the stereotaxic frame. After recovery from the surgery the animal was monitored for any sign of pain or dehydration and was further injected 1mg/Kg meloxicam or 5ml/Kg sterile 0.9% saline accordingly. Animals that did not recover 48-hours from the surgery or that showed signs of infection were culled.

2.2.1.1 **Surgical procedures: preparation for implantations**

On the day of the surgey, the rat was positioned on the stereotaxic frame and secured with non-traumatic ear bars in the auditory canals. The snout was clamped with a horizontal bar and enclosed into a custom-made mask for the delivery of the isoflurane/oxygen mixture.

The hair over the rat's head (eye-level to neck) was trimmed using electric clippers (Contura type HS61, Wella, UK). The skin was disinfected with a povidone-iodine solution (Betadine, Betadine Inc., UK) to ensure sterility. A paraffin-based eye lubricant (Lacrilube, Allegan Inc., USA) was carefully applied on both eyes and a custom-made mask was then used to cover the eyes and protect them from the lights used during surgery. A single incision was made from between the eyes to the back of the skull using a scalpel blade (Scalpel Blade No.10, Swann-Morton, UK) to expose the skull. The skin surrounding the incision was retracted using hemostatic forceps (Mosquito Forceps, WPI, USA) and the connective tissue over the skull was carefully removed using Dumont #7 forceps (WPI, USA) avoiding the muscles. The surface of the skull was further scrubbed with a cotton bud dipped into a solution of 5% H_2O_2 to remove all residual debris. The skull was then washed with ice-cold sterile 5% saline. The skull frontal, parietal and occipital bones and the skull landmarks bregma and lambda, were clearly visible at this stage. Any bleeding present on the skull surface was stopped either with ice-cold saline or using a cauterizer (Bovie Cauterizer, Bovie Medical Corp, USA).

From this point onwards, the implantation techniques differed according to the type of surgery and thus they will be described separately in the following sections.

2.2.2 Epidural EEG electrodes implantation

Six holes were drilled in the skull using either an electric drill or pin vice set (Maplin, UK) targeting, bilaterally, the frontal cortex, parietal cortex and the cerebellum for the EEG electrodes. In addition, two extra holes were drilled at the rostral part of the frontal bone and at caudal part of the cerebellar bone for the securing screws.

The EEG electrodes consisted of golden plated screws (1cm, Svenska Dentorama AB, Sweden) soldered to a 2-3 cm length insulated copper wire. The insulation was removed from the tips of the wire to allow current conduction. The anchor screws were 3mm stainless steel screws (M1.4 DIN 963, New Star Fastenings, UK).

The EEG electrodes and securing screws were screwed into the holes leaving the *dura mater* intact. To ensure long-term stability of the implant and appropriate electrical insulation of the EEG electrodes, all electrodes and anchor screws were painted with a small amount of metabond cement (C&B-Metabond, Parkell Inc., USA). Each copper wire was then soldered to an individual pin of a 6-pin PCB connector (Preci-Dip, Switzerland). The implant was further secured using acrylic cement (UNIFAST Trad, Minerva Dental, UK), fully coating the screws, wires and the sides of the PCB connector.

2.2.3 Epidural EEG electrodes and microdialysis probes implantation

The EEG electrodes and securing screws placement was the same as that described in section 2.2.2, but at the stage of drilling holes, two extra holes were drilled using an electric drill for bilateral implantation of the dialysis probes (**Figure 2.1**). The stereotaxic coordinates of the holes to target the VB were AP: -3.4 mm, ML ±2.8mm (Paxinos and Watson, 1997; David et al., 2013). The holes were frequently irrigated with ice-cold saline. The *dura mater* and remaining bone fragments were removed from the holes using 26-gauge needles (BD Microlance 3, Dickinsons & Co, UK) or fine tip forceps (Dumont #5, WPI, USA). Bleeding was stopped using ice-cold 0.9% saline. Each of the two guide cannulae for CMA 12 microdialysis probes (Linton Instruments, UK) was lowered into its hole at ~1mm per minute via a CMA 11/12 probe clip stereotaxic attachment (Linton Instruments, UK), until reaching the final position of DV: -4.4 mm (from the bottom of the guide cannula).

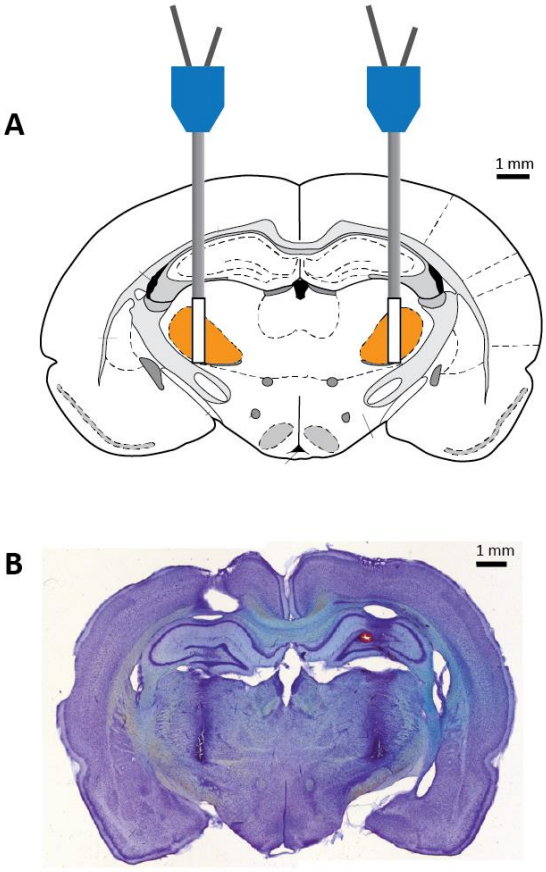

Figure 2.1. Implantation of dialysis probes in the VB thalamus. (A) Diagram of a coronal slice of the rat brain, showing the bilateral positioning of dialysis probes (guide cannulae not shown) in the VB (orange). (B) Thionin staining of a coronal slice (100 μm, approximately 3.3 mm from bregma) of a rat brain that was implanted with bilateral guide cannulae and dialysis probes targeting the VB. The probe's track is visible as a dark blue hue.

The guide cannulae inserted were filled with dummy probes (Linton Instruments, UK) that sealed the cannula, preventing contamination of the brain tissue. Once the bleeding stopped the guide cannulae were secured with acrylic cement. The coating of the implant with acrylic cement proceeded as described in section 2.2.2, and the sides of guide cannulae were also covered with cement to secure them.

2.2.4 Epidural EEG electrodes and thalamic silicon probe implantation

The design of silicon probe and microdrive and the implantation technique closely matched the one described in Vandecasteele et al. (2012) for cortical recordings, with the additional implantation of EEG electrodes. The silicon probes used in this surgery were four shank, linear, 32-site silicon probes (Buzsaki32, NeuroNexus, USA) attached to a HST/32V-G20 headstage (Omnetics, USA) via a 2cm-long flexible ribbon. The silicon probe was affixed to a custom-made microdrive build according to the design of Vandecasteele et al. (2012). Briefly, the microdrive was made of a plastic bridge on which the silicon probe was attached with dental cement; by turning the screw, the plastic bridge could be moved up and down between two fixed brass plates, allowing the probe to be moved over the course of the experiment. The drive range was approximately 8 mm and each half-turn of the screw moved the probe by 130 μm.

2.2.4.1 Surgical procedure for the implantation of EEG electrodes and silicon probe-microdrive

The muscle joining the right parietal bone was resected to allow drilling two holes in the parietal bone for the implantation of two stainless steel anchor screws. Before drilling holes for the EEG electrodes, the stereotaxic coordinates for the silicon probe implantation were calculated. The location of the silicon probe craniotomy was marked with a cross made with a scalpel blade at the position AP: -3.3 mm, ML: ±2.8 mm (Paxinos and Watson, 1997).

For the EEG electrodes, three holes were drilled on the left hemisphere, above the frontal cortex, parietal cortex and the cerebellum. The EEG electrodes described in section 2.2.2 were then screwed in position. On the right hemisphere, two holes were drilled above the cerebellum to accommodate the silicon probe ground and reference electrodes. In this case, stainless steel ground and reference screw posts (00-09, 1/8'', with soldered copper wires) were instead screwed in. All screw posts were painted with metabond cement while

leaving the area marked for silicon probe implantation on the right-hemisphere free of cement.

A craniotomy was carefully drilled to allow the silicon probe insertion. Using an electric drill and a round-head drill tip, the skull surrounding the area marked for the silicon position was thinned without damaging the brain surface. When the brain surface became visible throughout the thinned bone, using a bent 26-gauge the circle of bone remaining in the middle was lifted way. The *dura mater* was hooked with a curved insect needle and cut with scalpel blade. The pial surface was irrigated with sterile, ice-cold, 0.9% saline to stop any bleeding.

The microdrive was secured to the stereotaxic arm and positioned to the above mentioned AP and ML coordinates. The final probe position was adjusted slightly in order to avoid any major blood vessel present on the brain surface. The probe was then lowered into the brain, carefully checking that the silicon probe shanks did not bent whilst penetrating the tissue. The final DV position reached was -4.0 mm from the brain surface (i.e. above the thalamus). The craniotomy was sealed with a mixture of wax and paraffin oil and the bottom of the microdrive was secured to the skull using grip cement (Dentsply, USA).

A mini-Faraday cage was then built around the screw-post, enclosing the microdrive. Four copper mesh flaps were assembled and anchored with grip cement to the skull for this purpose, forming a cylindrical structure. The copper wires from the EEG electrodes were soldered to a PCB connector to record the EEG signal as described in section 2.2.2. The PCB connector was secured to the mini-faraday cage with grip cement. The ground and references wires from the screw posts were then soldered to the corresponding wires on the silicon probe headstage. Finally, the headstage ground was also soldered to the mini-faraday cage.

2.2.5 Conclusion of recovery surgeries

The skin rostral and caudal to the implant was sutured using braided 0.12 mm silk sutures and a X-8 needle (Cole Parmer, UK). The wound area was washed with sterile 0.9% saline and antiseptic powder (Battle Hayward and Bower Ltd, USA) was applied around the incision site. The animal was then removed from the stereotaxic frame and allowed to recover on the homoeothermic blanket until it regained his righting reflex. At that point the animal was returned to a housing cage.

2.3 Experimental protocols for *in vivo* recordings

2.3.1 Freely-moving EEG recordings

On the day of the experiment the animals were brought to the recording room at 10.00 am, and placed into individual plexiglas cages with access to food and water. The recording cages were surrounded by a custom made Faraday cage. To record the EEG signal, the PCB connector on the implant was connected to a pre-amplifier (0.08 Hz high-pass filter, impedance 10MOhm) via a stainless steel multistranded insulated wire; the preamplifier was in turn connected to an analogue EEG amplifier (4-channel BioAmp, SuperTech Inc., Hungary). The free movement of the animal was ensured by attaching the connecting wire to counterweighted swivel arm, positioned above the recording cage. The amplifier settings were 1000 gain and low-pass filter at 500Hz. The analogue EEG signal was digitized with a sampling rate of 1000Hz by a Cambridge Electronic Design (CED) Micro3 D.130 digitizer. The software interface used to acquire the date was CED Spike2 7.3. The EEG was recorded by differential between frontal and parietal EEG screws, using the electrode on the cerebellum as ground.

2.3.1.1 Systemic administration of 5-HT2A/2C drugs

For the experiments presented in Chapter 3, the following experimental protocol was used (Figure 2.2A). The GAERS were connected to the recording apparatus and left undisturbed for one hour (habituation phase). After that, the behaviour of the animal started to be monitored and a one-hour control EEG was recorded (control phase). If the experiment involved pre-treatment of a 5-HT2A/2C antagonist, the antagonist (or the corresponding vehicle) was injected (i.p.) 10 minutes before the end of the control EEG period. At the end of the control EEG period the animal was injected (i.p.) with the 5-HT drug of interest (or corresponding vehicle) and monitored for 2 hours (treatment phase).

In the case of the GHB-model of ASs, the protocol was the same as for GAERS rats except that Wistar rats received an injection of 5-HT2A/2C drugs 10 minutes before the i.p. injection of GBL 100mg/kg (Figure 2.2B).

2.3.1.2 Systemic administration of TTA-P2 and ETX in the GHB-model of ASs

For the experiments presented in Chapter 4, the following experimental protocol was used (Figure 2.2C). Wistar rats were connected to the recording apparatus and left undisturbed for one hour (habituation phase). The behaviour of the animal started to be monitored and a one-hour control EEG was recorded (control phase). At the 40 minutes mark, Wistar rats received an i.p. injection of TTA-P2 (10 mg/kg) or ETX (150 mg/kg) (or corresponding vehicles). At the end of the control phase the animals were injected with 100mg/kg GBL (or corresponding vehicle) and monitored for 2 hours (treatment phase).

2.3.2 Freely-moving EEG recordings and reverse microdialysis

Animals were restrained using a towel and the dummy probes were removed from the implant. Two microdialysis probes (CMA 12 MD Elite Probe 2mm) were slowly inserted in the guide cannulae. 18-24 hours after insertion of the microdialysis probes, the rat was placed in the recording chamber (at 10.00 a.m.) and connected to the EEG recording equipment. All EEG recording settings were the same as detailed in section 2.3.1.

Before initiation of recording, the microdialysis probes were connected via CMA FEP tubing (internal diameter 1.2uL/100mm) and B Braun catheter holders to 1ml syringes. A flow of 1µL/min was maintained with the CMA 400 syringe pump (Linton Instruments, UK). Animals were left undisturbed for one hour (habituation phase) while delivering via the microdialysis probe the vehicle solution (different vehicle solutions used are described in section 2.6.3) (Figure 2.2D).

At the one-hour mark the infusion of vehicle was either switched to the drug under study or maintained for control experiments. When using the GHB model of ASs (Figure 2.2E), animals received an i.p. of 100mg/Kg GBL after 40 minutes. Animals were recorded for a further hour (or two hours for GAERS). At the end of the recording session the dialysis probes were removed and replaced with dummy probes (cleaned with ethanol and rinsed in deionized water). A minimum of 6 days of rest was allowed between two consecutive recording sessions.

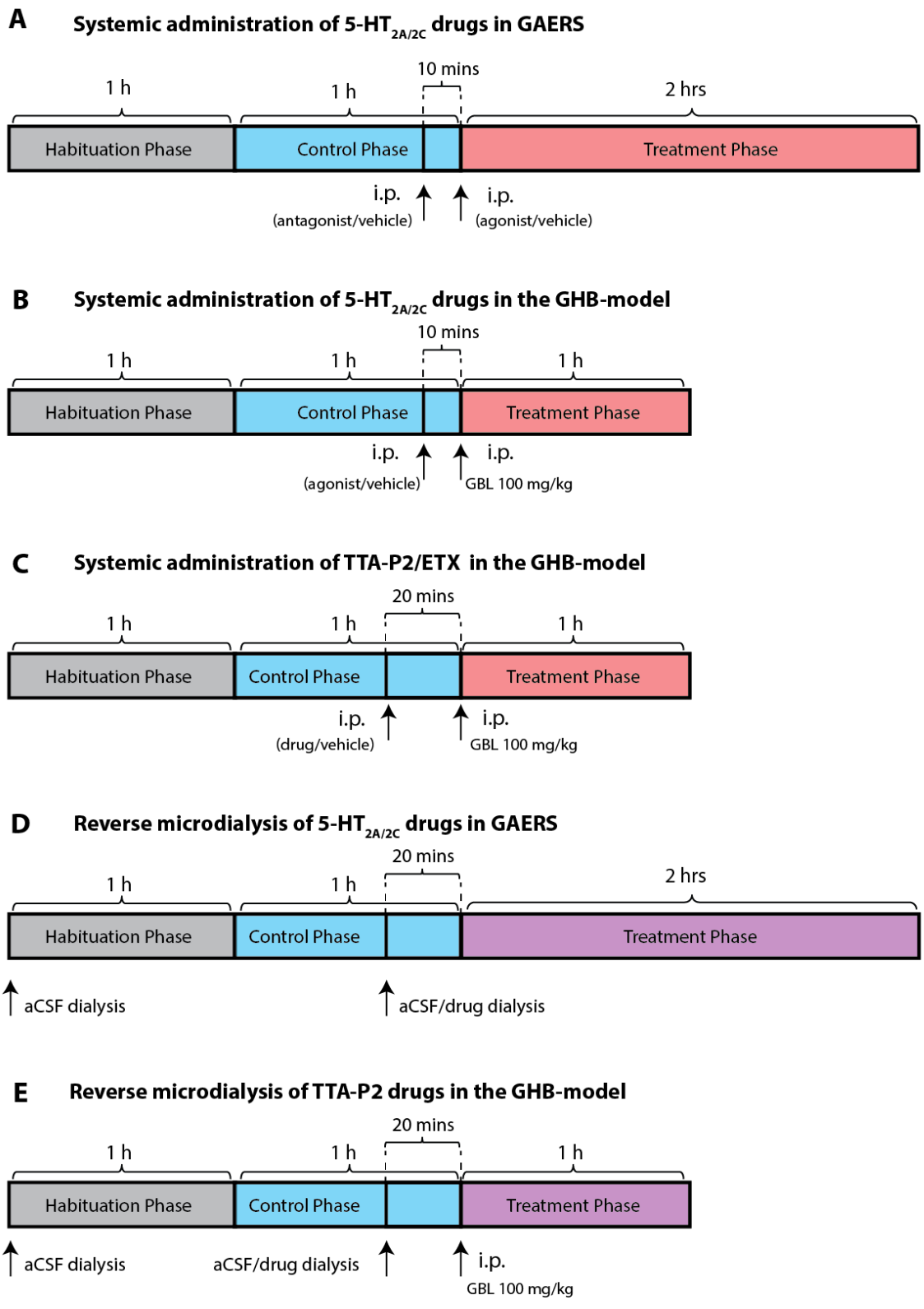

Figure 2.2 Protocols for the in vivo systemic and local administration of drugs. See main text for details.

2.3.2.1 **Principles of reverse microdialysis in the CNS**

Reverse microdialysis is a technique used that can be used for local administration of a substance in the brain (Höcht et al., 2007). The basic principles are the same that apply for conventional dialysis, normally used in CNS research to sample the interstitial concentration of endogenous compounds or drugs (Chaurasia, 1999): a dialysis probe that is permeable to the diffusion of water and other small molecules in inserted in a brain region. Substances that are small enough to cross the membrane diffuse (bi-directionally) according to their concentration gradient. To sample the concentration of a substance along time, a perfusion fluid pumped through the dialysis membrane is collected via an outlet tube.

It follows that if a substance is added to the perfusion fluid at a higher concentration to that of the interstitial fluid of the brain, the substance will diffuse into the brain. The ratio between the concentration of drug that diffuses into the interstitial fluid and that of the perfusion fluid is normally called 'relative recovery'. The relative recovery can be determined experimentally and depends on several factors in addition to the concentration gradient (although it often estimated in the range of 1/10 of the concentration gradient (Chaurasia, 1999; Höcht et al., 2007). Those include the weight cut-off and area of the dialysis membrane, the composition of the perfusion solution and the flow-rate (Plock and Kloft, 2005).

In the reverse microdialysis experiments presented in Chapter 3 and Chapter 4, drugs were administered to the center of the VB. A 2 mm dialysis probe was used to cover the full dorso-ventral extent of the VB (~1.5x1.7x1.5 mm) (Paxinos and Watson, 1997), similarly to previous experiments from the lab (David et al., 2013). A membrane with cut-off of 20 kDa was chosen to allow passage of the drugs administered, while blocking the passage of other substances and bacteria. The perfusion vehicles used for each drug (matching the CSF composition) are presented in section 2.6.3; the flow rate was 1μL/minute (David et al., 2013), in the range used for CNS application (i.e. 0.5 -2 μL/min, (Plock and Kloft, 2005).

Importantly, after the molecule of interest has diffused out of the dialysis membrane, the ability of the drug to reach the intended target (e.g. neurons of the VB or VB plus NRT in some experiments) via the extracellular space depends on the diffusion coefficient of the

molecule, the concentration gradient and rate of clearance of the molecule (Wolak and Thorne, 2013). Only the drug concentration in the perfusion solution can be altered experimentally and the dose selection was driven by different considerations for TTA-P2 (Chapter 3) and Ro60-0175 and MDL11,939 (Chapter 4).

In the case of the TTA-P2, previous experiments in the lab allowed to select the dose of TTA-P2 based on a physiological measure of its effect on VB neurons (David et al., 2013). These experiments measured, in anaesthetized Wistar rats, the efficacy of various doses of TTA-P2 in blocking low-threshold Ca^{2+} potential (LTCP) and associated high-frequency bursts of action potentials of TC neurons *in vivo*. A systemic injection of 3mg/Kg TTA-P2 produced a ~95% block of burst in the VB after 40 minutes, while with 10mg/kg the reduction reached 100% (Figure 2.3A). For local application of TTA-P2 in the VB, the distance and time of half-block of LTCP-mediated bursts were also calculated. Reverse microdialysis of 300 μM TTA-P2 produced a 90% block of burst firing compared to control at ~ 500 μm 1 hour after the beginning of the infusion, while for 1 mM a 90% block of burst firing compared to control was found at ~ 700μm 1 hour after the beginning of the infusion (Figure 2.3B). Considering that the membrane length is 2mm, the dimensions of the VB and NRT (~2.5x2x.1.7mm) (Paxinos and Watson, 1997), a concentration of 300 μM was therefore was chosen target the VB, while a concentration of 1mM was chosen to affect the VB and a large proportion of the NRT (Figure 2.3C). Finally, the distance of half block of LTCP-mediated bursts started to plateau after 40 minutes (Figure 2.3D). It was decided to inject GBL 40 minutes from the start of the TTA-P2 dialysis in order to maximize the time when the area of interest (VB alone or VB+NRT) would be affected by the drug without TTA-P2 reaching off-targets.

In the case of Ro60-0175 and MDL11,939, no information if available for the effects of the drugs on neuronal activity, so a similar approach to that described for TTA-P2 was not possible. The drug dosing approach and limitations in the reverse microdialysis of these drugs will be discussed in section 3.4.2.5.

2.3.3 Freely-moving EEG and thalamic silicon probe recordings

The animals were left at least 2 days to recover from the surgery. The recordings were performed in a recording room whilst leaving the animals freely moving in their own housing cage (which was moved into a Faraday cage for the duration of the experiments). The rat was connected via a head mounted HST/32V-G20 VLSI-based preamplifier to the

Plexon acquisition system (Recorder/64 amplifier and related software). The gain was set according to the SNR of the recording to 12.500x or 15.000x and maintained throughout the recording session. Data was sampled at 20.000 Hz using a 50Hz notch filter.

The animals were recorded throughout the day, starting from 09.00 a.m. The presence of thalamic neurons on each channel was judged via the software-based online high-pass filtered data. When high amplitude extracellular spikes were present, the recording commenced, otherwise the rat was restrained with a towel and the microdrive was moved by turning its screw (1/4 to 1 full turn, with a half-turn moving the silicon probe dorso-ventrally by ~130 μm). Once high amplitude extracellular spikes were identified and recorded for about one hour (which contained some light-sleep with high frequency bursting), the animals were injected with 100mg/kg GBL to induced ASs. After the wearing off of GBL's effect, the animal was unplugged from the recording apparatus and returned to the housing room.

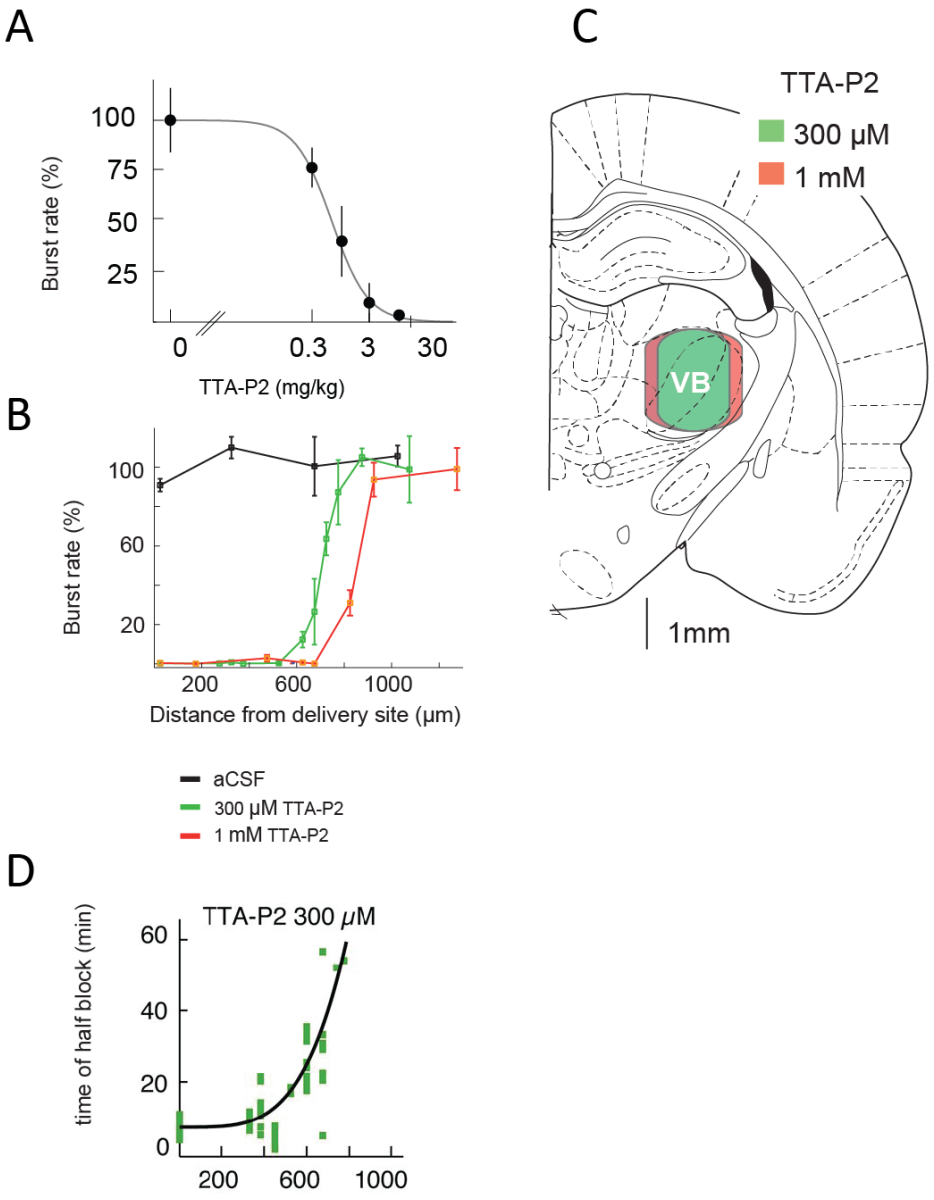

Figure 2.3. TTA-P2 blocks high-frequency burst firing in TC neurons *in vivo*.

(A) Plot of normalized change in burst firing (after 40 minutes from treatment) in TC neurons recorded via a silicon probe for different concentrations of TTA-P2 injected systemically. Note that at 3mg/Kg TTA-P2 burst firing is reduced by 95% compared to control conditions, while with 10mg/kg the reduction reaches 100%.

(B) Plot of normalized change in burst firing of TC neurons (after one hour of treatment) recorded via a silicon probe over distance of neuron from site of microdialysis for 300µM and 1mM TTA-P2. Note that with 300µM TTA-P2 burst firing is reduced to ~10% of control at up to 500µm from the microdialysis probe, while with 1mM TTA-P2 burst firing is reduced to ~10% at up to 700µm from the microdialysis probe

(C) Schematic brain drawing showing the area of burst firing block achieved with the dialysis of 300 µM TTA-P2 (green) which almost covers the entire VB. With 1 mM TTA-P2 the area of block is achieved (red) spans over the NRT.

(D) plot of the time of half-block of LCTP-mediated bursts for 300μM TTA-P2 at various distances from the dialysis probe. Note that the curve starts to reach a plateau around 40 minutes from the beginning of the dialysis.
(A-D reproduced with modification from David et. al, 2013)

2.4 Data analysis for *in vivo* recordings

Data analysis was performed using a series of custom–made Matlab (R2013b, The Mathworks Inc., USA) scripts, in conjunction with other freely available toolboxes described in the following sections.

2.4.1 Visual detection of behavioural states in the GHB-model of ASs

The EEG recordings after GBL injection were classified into different behavioural state (i.e. active wakefulness, light-sleep, GHB-elicited ASs and GHB-elicited hypnosis) by visual inspection according the criteria described in section 4.3.1. The times of each epoch were saved via a graphic interface modified from the signal-processing toolbox Fiedtrip (Oostenveld et al., 2011). A novel classification algorithm developed to distinguish between the different behavioural states generated by GBL administration is presented in Chapter 6.

2.4.2 Automatic detection of ASs in GAERS

The EEG detection of GAERS seizures was performed using the SeizureDetect script (kindly provided by Steve Clifford, CED), designed to discriminate between sleep spindles and ASs. The process involved DC removing the raw EEG signal and identifying a control epoch (baseline desynchronized EEG where the animals are awake). Then 5 parameters were used to identify SWDs in the recordings. An amplitude threshold (**Figure 2.4A**) was defined as 5-9 standard deviations (SD) from the mean amplitude of the control epoch. Every point crossing this threshold (defined hereafter as a 'peak') was used to identify SWD according to whether it fulfilled the criteria for onset (≤ 0.2 s; **Figure 2.4B**), maximum interval (≤ 0.4 s; **Figure 2.4C**), minimum duration (≤ 1 s; **Figure 2.4D**), minimum event interval (≤ 0.5 s; **Figure 2.4E**). After defining putative SWDs with these parameters, the script selected proper SWDs according to their frequency (by calculating the inter-peak

interval in the time domain). Only SWD which had ≥ 25% of its peaks in the 5-12Hz range were selected, resulting in sleep epochs and artifacts being excluded. The automatic selection was further refined by visual inspection.

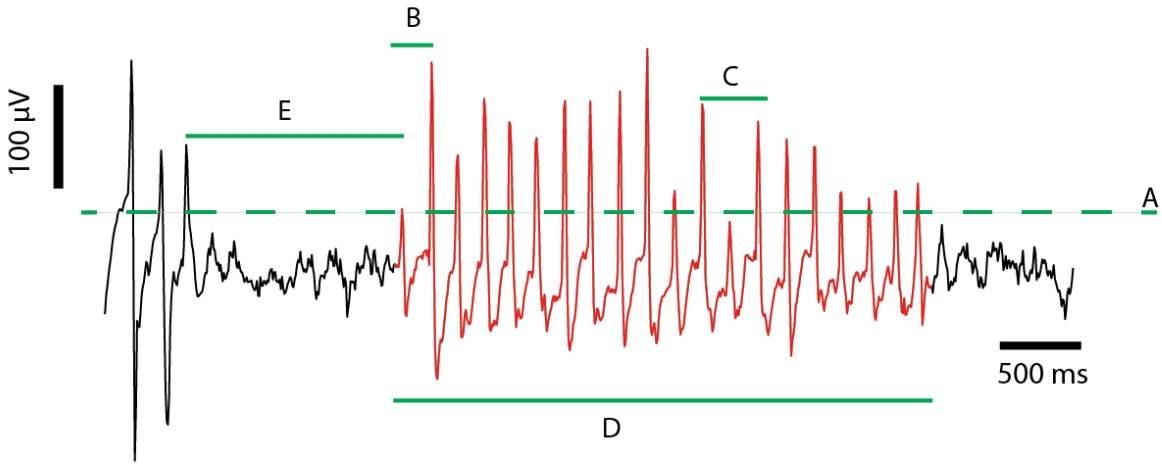

Figure 2.4. Seizure detection in GAERSs.
(A) Threshold: must be exceeded by a local maxima (hereafter 'peak') to be detected as a possible SWD peak.
(B) Onset: maximum time allowable between two peaks points in order for them to qualify as the initiation of a SWD.
(C) Maximum interval: maximum time allowable between two peaks in order for them to qualify as the continuation of a SWD .
(D) Minimum SWD duration
(E) Minimum event interval: maximum amount of time between two distinct SWDs that will not result in their merging into one event.

2.4.3 ASs quantification

ASs quantification was done on three parameters: total time spent in AS, average AS length and total number of ASs (Marescaux et al., 1992a). In the case of GAERS ASs the quantification was done in 20 minutes epochs and the value of each of the three parameters during the treatment phase was normalized to that of the control phase (see section 2.3.1.1). Normalization was employed because precedent work from the lab (Crunelli lab, unpublished) has shown that this results in a reduced variability in the baseline (e.g. systemic administration of vehicle), thus giving more power to detect a difference induced by the treatment.

In the case of the GHB-model no normalization to a pre-drug control period was possible because the effects of GBL administration are short-lived (i.e. in the order of 45 minutes, see chapter Chapter 4 for a full characterization of the GHB-model of ASs).

2.4.4 EEG spectral analysis

Only one of the two fronto-parietal EEGs was analyzed from each session. Spectral analysis of the EEG was performed on the raw signal after preprocessing the data with Fieldtrip. This involved resampling the data at 200Hz after applying an anti-aliasing (low-pass) FIR filter. Time-frequency decomposition and ridge extraction was performed using the scripts kindly provided by Dmytro Iatsenko (Leicester University, UK). Briefly, the signal was convolved with a Morlet Wavelet (ko=1) and analysed in the range 1-20Hz. The dominant frequency of the signal was extracted using the ridge extraction algorithm of WT script (Iatsenko et al., 2013a, 2013b) (freely available at: http://www.physics.lancs.ac.uk/research/nbmphysics/diats/tfr/). Illustration of this procedure, implemented for SWDs, will be presented in Chapter 6.

2.4.5 Analysis of extracellular ensemble recordings

The extracellular units data was analyzed with open-source NDManager, Neuroscope and Kusters suite of software (Hazan et al., 2006).

2.4.5.1 Spike sorting

Spike sorting involved three main steps: extracting extracellular spikes from the raw signal, reducing the dimensionality of the data via principal component analysis (PCA) and assigning each spike to 'clusters' that belong to putative neurons.

The extraction of spikes was done after high-pass filtering the data using the 'highpass' plugin of NDManager. Spike extraction was performed via the 'extractspikes' plugin, using an amplitude threshold of 2 standard deviation of the mean waveform. This resulted in extracting the spike waveform (i.e. 32-sample peak-centered waveforms) and spike time for each putative spike. The waveforms dimensionality was then reduced using the "PCA" plugin, recording the first three principal components of each putative spike on each of the 8 channels. This generated a 24-dimensional feature vector for each spike.

The final aspect of the spike sorting procedure was dealt with by first using the unsupervised clustering method offered by KlustaKwik (**Figure 2.5**A). This clustering method assumes that the variation between spikes belonging to the same neuron is due to Gaussian noise. To define which spike belongs to which clusters, KlustaKwik uses a Classification Expectation Maximization (CEM) algorithm (Harris and Henze, 2000). The total number of clusters is iteratively reduced via a Bayesian Information Criteria penalization procedure (Wild et al., 2012). Limitations of this approach arise from non-Gaussian sources of noise in the recorded waveforms. These include electrode drift, non-stationary noise, spike variations due to bursts (Pedreira et al., 2012). For this reason all spike sorting was refined manually (supervised clustering) using the 'Klusters' suite. In this stage of the analysis noisy clusters were discarded. Moreover, only clusters that that contained isolated units during ASs (**Figure 2.5B,C**) were kept for further analysis.

2.4.5.2 **Classification of neuronal firing output**

The firing output of neurons was classified into tonic firing, burst firing and doublet firing. Tonic firing included all spikes separated by at least 100ms; burst firng was defined as a group of 3 or more spikes with an inter-spike interval (ISI) ≤ 7ms (and preceded by a silence of minimum 100ms); doublets were defined as a group of 2 spikes separated by an ISI of ≤7 ms (and preceded by an silence of minimum 100ms) (Llinás and Jahnsen, 1982; Huguenard and Prince, 1992; David et al., 2013).

2.4.5.3 **Classification of neuronal type**

Neurons were classified as TC, NRT or as non-thalamic based on the basis of their burst signature during the control period (i.e. before the injection of GBL) (**Figure 2.6**). TC neurons have a characteristic decelerando pattern, while NRT neurons have a characteristic accelerando-decelerando pattern (Domich et al., 1986; Huguenard and Prince, 1992; Steriade et al., 1993a).

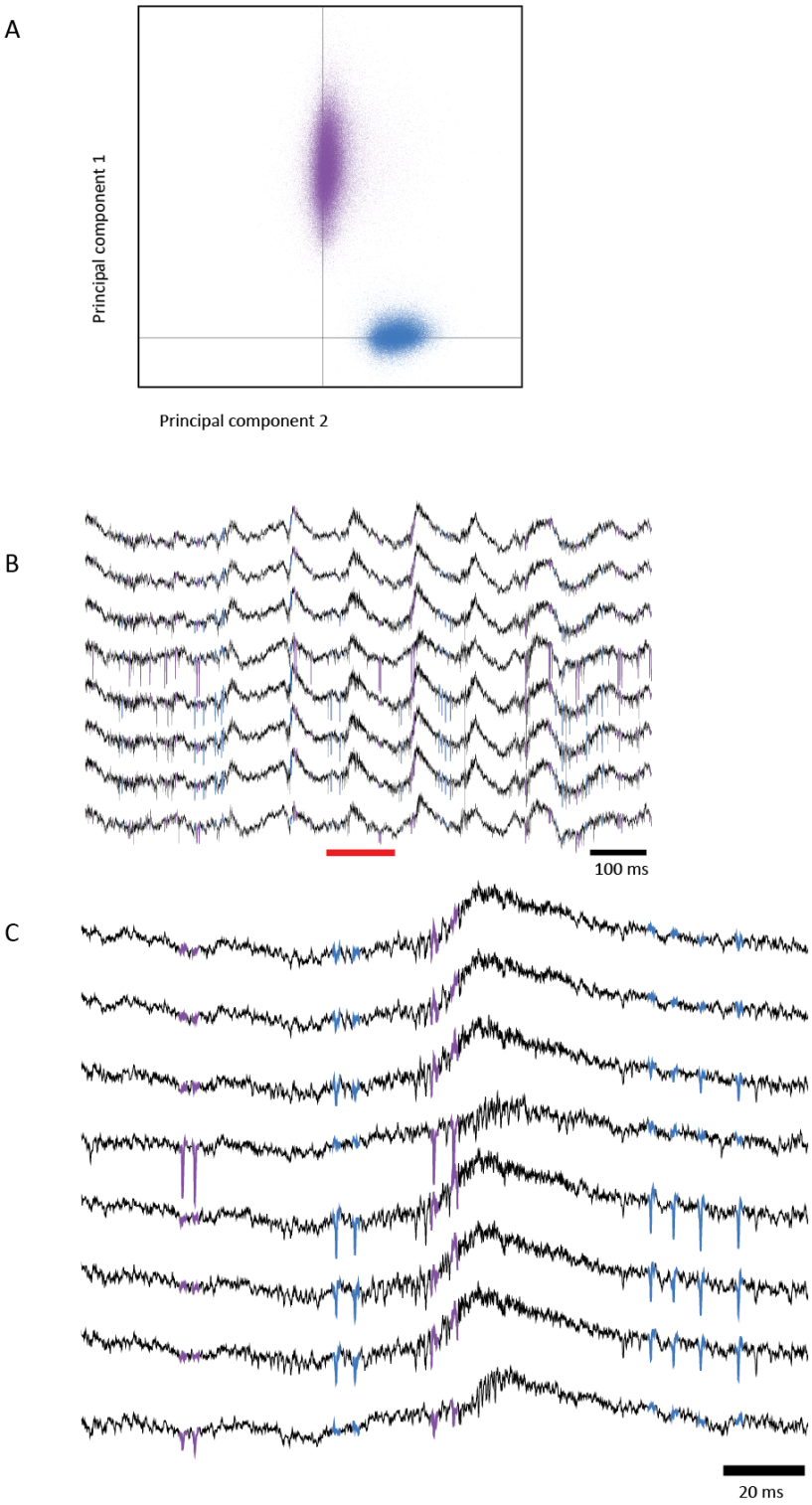

Figure 2.5 Extracellular recordings of NRT neurons during SWDs and neuronal clustering
(A) 2-D cluster plot of waveforms from two NRT neurons (violet and blue) subject to PCA analysis and clustered via KlustaKwik (see main text for details on this procedure). The principal component 1 reflects the amplitude of a spike, while principal component 2 reflects the shape.
(B) Raw extracellular recording of the same two NRT neurons in A, during a brief GHB-elicited SWDs. The recording is shown for 8 channels on one the 4 shanks of a Buzsaki32 silicon probe. An epoch (red mark) in further enlarged in C, highlighting how the units are distinguishable from the background noise.

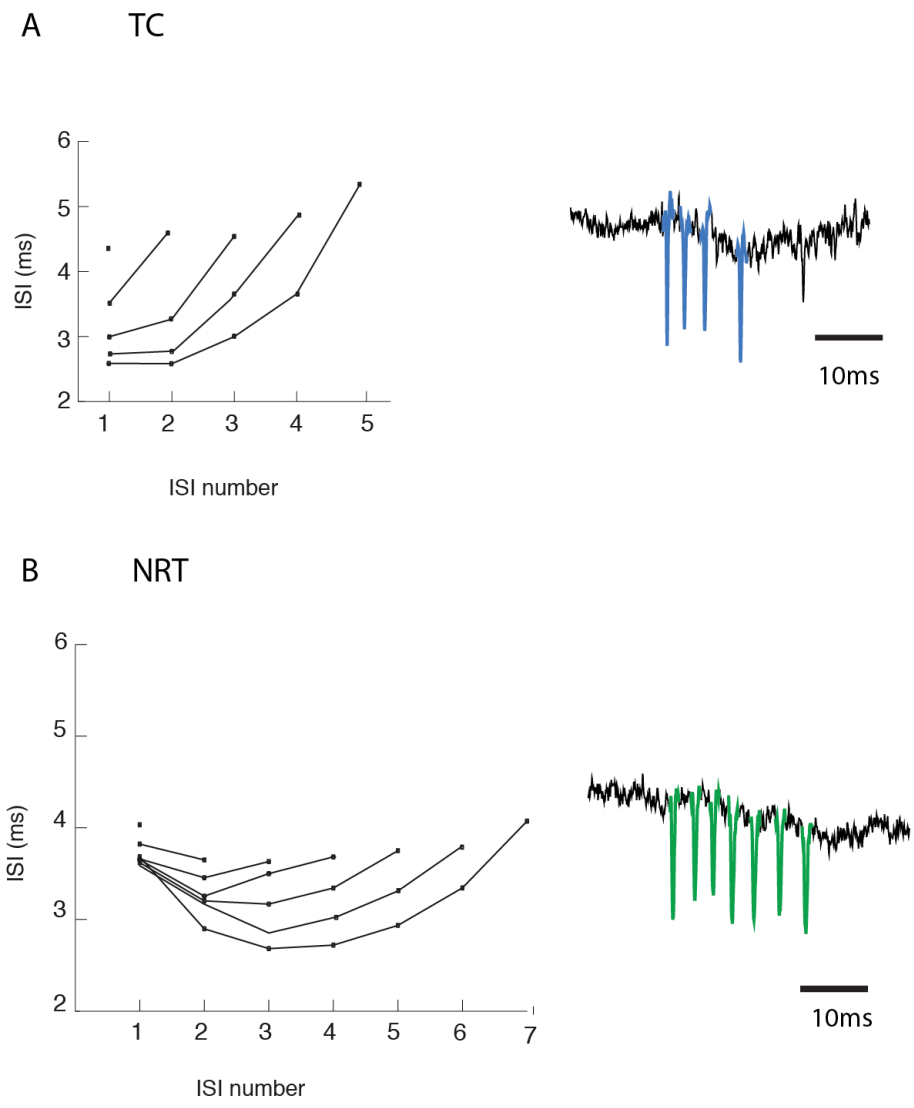

Figure 2.6. Burst signature of TC and NRT neurons.
(A) Characteristic decelerando pattern (increase in interspike intervals, ISI) of a TC neuron (average across the recording); an example of a TC burst is shown on the right.
(B) Characteristic accelerando-decelerando pattern of a NRT neuron. Note how burst tend to be longer than in TC neurons. An example of a NRT burst is shown on the right.

2.4.5.4 **Autocorrelograms and association of neuronal activity with EEG activity**

Autocorrelograms were calculated using the xcorr function in Matlab, using the 'coeff' normalization option (autocorrelations equal to 1 at 0 lag). Neuronal spike triggered EEG averages (window of 1 second, centered on the thalamic spike) for each behavioural state were calculated for the whole session and averaged for each neuron. EEG-spike triggered EEG average was calculated from a subset of GHB-elicited SWDs that presented high-amplitude peaks at each SWC. High-amplitude SWC peaks were identified on the DC-removed EEG trace as points exceeding a threshold of 3 SD from the average EEG amplitude for that seizure. If more local maxima were present in a given SWC, the greater local maximum was chosen to define the timing of SWC peak.

2.5 Histological procedures

Animals were deeply anaesthetized with 200 mg/kg sodium pentobarbital (Euthatal, Merial Animal Health Ltd, Essex, UK). 1 µL of thionine dye was injected inside the guide cannulae using a 10 µL Hamilton syringe in order to highlight the probe's tracks. Animals were then perfused intracardially using a peristaltic pump (flow rate 30-35 ml/min) as follows: 0.9% saline (+ 4°C) for 2 minutes, followed by a solution of 4% paraformaldehyde in 0.1 M sodium phosphate buffer, pH 7.4 (flow rate 10 ml/min) for 10 minutes. The brains were removed from the skull and postfixed in the final fixative for 6-8 hours. The brains were stored in phosphate buffered saline (PBS), pH 7.4 at +4C and cut in the coronal plane at 100 µm section thickness a sliding microtome (Leica VT 1000S vibratome). The sections were stored in PBS at room temperature until processed. Sections were taken out of the 10% formaldehyde solution, mounted on gelatin-coated slides, and dried overnight at 37°C. Sections were defatted 1 h in a mixture of chloroform/ethanol 100% (1:1), and then rehydrated through a graded series of ethanol, 2×2 min in 100% ethanol, 2 min in 96% ethanol, 2 min in 70% ethanol, 2 min in50% ethanol, 2 min in dH_2O, and stained 30 seconds in a 0.125% thionin (Fisher Scientific) solution, dehydrated and coverslipped with DPX (BDH Laboratory Supplies Poole, England). The slides were then visualized via an optic microscope (Nikon E100); animals where the tracks deviated from the VB or where brain damage was evident were excluded from the analysis.

2.6 Reagents

Drug name abbreviations that will be used in the main text are in bold.

2.6.1 Sources of drugs, antibodies and common reagents

Ethosuximide (**ETX**), pentylenetetrazol (**PTZ**), γ-butyrolactone **(GBL**), **M100907**, were purchased from Sigma-Aldrich (USA). **Ro60-0175**, **SB-242084, TCB-2, MDL11,939, Tocris aCSF** were purchased from Tocris Biosciences (UK).

3,5-dichloro-N-[1-(2,2-dimethyl-tetrahydro-pyran-4-ylmethyl)-4-fluoro-piperidin-4-ylmethyl]-benzamide (**TTA-P2**) was a kind gift from Merk Inc. (USA). APD-356 (**lorcaserin**) was a kind gift from Arena Pharmaceuticals Inc. (USA). SCA-136 (**vabicaserin**) was a kind gift from Pfizer Inc. (USA).

All common laboratory reagents were purchased from Sigma-Aldrich (USA).

2.6.2 Drug vehicles for systemic administration

GBL, PTZ, ETX, Ro60-0175, TCB-2, lorcaserin were dissolved in 0.9% saline. TTA-P2 was dissolved in 2% DMSO (v/v) in 0.9% saline. Vabicaserin was dissolved in 2% Tween 80. SB-242084 and M100907 were dissolved in 25mM citric acid, 8% (2-Hydroxypropyl)-β-cyclodextrin (w/v) in 0.9% saline. MDL11,939 was dissolved in 0.9% saline and 5% glacial acetic acid and then brought to pH 6 with NaOH.

2.6.3 Drug vehicles for reverse microdialysis

TTA-P2 was dissolved in 2% DMSO and then added to Tocris aCSF. Ro60-0175 was dissolved in Tocris aCSF.

MDL11,939 was dissolved according to the procedure described in Pehek et. al, 2006. Briefly, a modified Dulbecco's artificial cerebrospinal fluid (**mACSF**) buffer solution (137mM NaCl, 3mM KCl, 1.2mM $MgSO_4$, 0.4mM KH_2PO_4, with 1.2mM $CaCl_2$ and 10mM glucose; pH 7.4) was prepared and stored in fridge for a maximum a 5 days. On the day of the experiment MDL11,939 was dissolved in distilled water containing 1.5 µL of glacial acetic acid to make a 10mM stock solution. The solution was diluted to the necessary concentration in the mACSF solution described above and microfiltered via Whatman® GD/X syringe filters (Sigma, USA) with 0.4 µM pores to ensure sterility.

2.7 Statistical analysis

All statistical analysis was performed with Graphpad Prism version 5.00 for Mac (GraphPad Software, San Diego, USA).

For GAERS, the effect of systemic or thalamic administration of compounds was analyzed via non repeated measures two-way ANOVA with drug and time as factors. Dunnet's post hoc testing was employed to test for the simple main effect of drug vs. vehicle, both for the full treatment period and for each 20-minute bin. Full statistical tables are presented in Appendix A.

In the case of data from the GHB-model, t-test (paired or not paired, as stated in text) was employed to compare the effect of treatment vs vehicle, both in the case of reverse microdialysis and systemic administration of compounds. Due to to short duration of the effect of GBL and to the variability of the drug's onset (see chapter Chapter 4 for a full characterization of this parameters in the GHB-model of ASs) analysis on a shorter time scale was deemed not appropriate.

The comparison of the distributions of neuronal firing (Chapter 5), and of coherence and instantaneous frequencies (Chapter 6), non normally distributed, was done via the two-sample Kolmogorov-Smirnov test.

Chapter 3 Pharmacological modulation of 5-$HT_{2A/2C}$ receptors in spontaneous and pharmacological ASs

3.1 Introduction

As described in section 1.6.3, historically the serotoninergic modulation of ASs has been only partly investigated because of the lack of selective pharmacological agents. In particular, early experiments in GAERS with broad-spectrum agonists and antagonists had excluded a contribution of 5-HT to ASs (Marescaux et al., 1992b). Nonetheless, new evidence has pointed to an important role of the 5-HT_{2C}Rs : spontaneous ASs in WAG/Rij rats are blocked by application of 5-$HT_{2B/2C}$ agonist mCPP (Jakus et al., 2003). Moreover, 5-HT_{2C}Rs appear to be implicated in general network excitability given that 5-HT_{2C}R knockout mice have spontaneous tonic-clonic seizures and a lower threshold for seizures triggered by various convulsants (Tecott et al., 1995; Applegate and Tecott, 1998b).

Whether 5-HT_{2C} receptor modulation could alter ASs in GAERS was hitherto unknown, but preliminary *in vitro* work from the lab had shown that 5-HT_{2A} and 5-HT_{2C}Rs can modulate the thalamic tonic $GABA_A$ current (Cavaccini et al., 2012) (see section 1.3.2.2). In particular, in thalamic slices from GAERS rats, the 5-HT_{2C} agonist Ro60-0175 was found to the decrease the tonic $GABA_A$ current by ~42%, while the 5-HT_{2A} antagonist MDL11,939 was found to decrease the tonic $GABA_A$ current by ~36% (**Figure 3.1**).

Since an increased tonic $GABA_A$ inhibition has been shown to be a necessary and sufficient for the expression of ASs (Cope et al., 2009), I sought to investigate effects of pharmacological modulation of 5-HT_{2A} and 5-HT_{2C} on ASs in freely-moving GAERS and in the GHB-model of ASs. In addition to the aforementioned compounds, Ro60-0175 and MDL11,939, other drugs acting on 5-HT2 receptors have been tested based on their translational value, selectivity or biased agonism properties (see 1.6.2.1, summarized in **Table 3.1**).

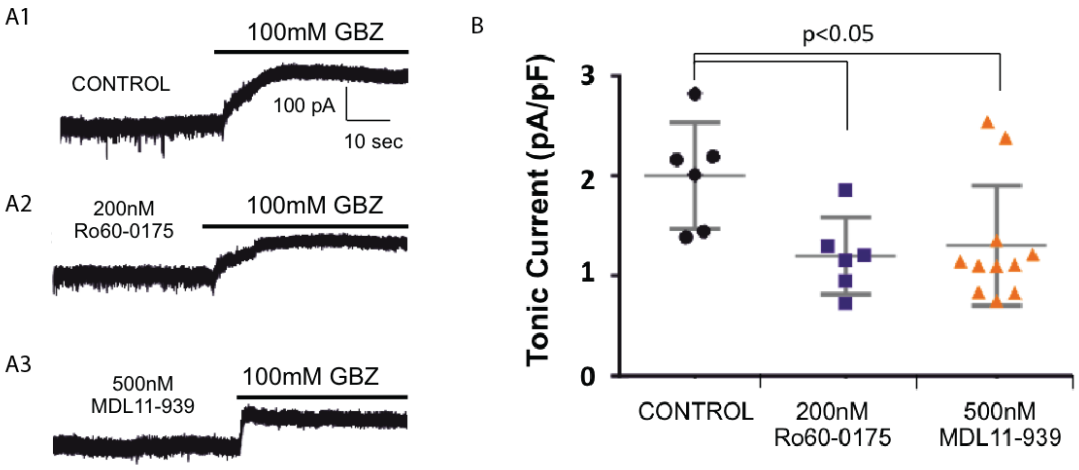

Figure 3.1 The 5-HT$_{2C}$ agonist Ro60-0175 and the 5-HT$_{2A}$ antagonist MDL11,939 decrease the tonic GABA$_A$ in TC neurons of the VB of GAERS. Representative patch-clamp recording of a TC neuron in voltage clamp. Upon addition of the GABA$_A$ antagonist gabazine (GBZ) (100mM) a shift in the holding current is observed, indicative of the presence of a tonic current (A1). Pre-treatment with the 5-HT$_{2C}$ agonist Ro60-0175 (200 nM) reduces the tonic current revealed by GBZ application (A2). In a different TC neuron, pre-treatment with the 5-HT$_{2A}$ antagonist MDL11,939 (500 nM) also reduces the tonic current revealed by GBZ application (A3). Quantification of the reduction in the tonic current induced by application of Ro60-0175 (n=6) and MDL11,939 (n=11) compared to control (n=6). All experiment in thalamic slices from GAERS rats at post-natal day 20-25.

The 5-HT_{2C} agonist lorcaserin (Thomsen and Grottick, 2008) has similar selectivity profile to that of Ro60-0175, but was selected because lorcaserin has been approved for human use (FDA, 2012), being the first-in-class 5-HT_{2C} agonist on the market. Vabicaserin (Dunlop et al., 2011) and CP809,101 (Siuciak et al., 2007), although not approved for human use, with their ~1000 fold selectivity for the 5-HT_{2C}R over 5-HT_{2A}R, represent the most selective 5-HT_{2C} drugs available for research use. SB242084 is the most selective 5-HT2C antagonist available for research use (Bromidge et al., 1997).

No selective 5-HT2A agonists have been synthetized to date, thus two potent 5-HT2A agonists, TCB-2 (McLean et al., 2006) and lisuride have been used, in combination with selective 5-HT2A antagonist MDL11,939 (Dudley et al., 1988). Notably, lisuride is not hallucinogenic and is approved for human use (Herrmann et al., 1977; Welsh et al., 1998). Finally, in some experiments the 5-HT2A antagonist M100,907 (Kehne et al., 1996) was used for comparative purposes with MDL11,939, in view of its wide use in published reports.

While all compounds were administered systemically, Ro60-0175 and MDL11,939 were also administered locally in the VB via reverse microdialysis in freely moving GAERS. The purpose of these experiments was to test whether any effect produced by these compounds was caused by a direct modulation of thalamic 5-$HT_{2A/2C}$ receptors.

Table 3.1 Selectivity profile of compounds used in the current chapter

Compound	**5-HT$_{2A}$**			**5-HT$_{2B}$**			**5-HT$_{2C}$**			**2C/2A** selectivity ratio
	Ki (nM) [a]	pEC$_{50}$ [b]	Efficacy [c]	Ki (nM)	pEC$_{50}$	Efficacy	Ki (nM)	pEC$_{50}$	Efficacy	
5-HT$_{2C}$ modulation										
Ro60-0175 [e]	37.1 [d]	6.4	6.4	4.3 [d]	9.1	0.79	9.1 [d]	7.5	7.5	13
Lorcaserin [f]	159 [d]	6.7	1	190 [d]	6.0	1	29 [d]	7.9	1	16
CP809,101 [g]	6 [d]	6.8	0.67	64	7.2	0.57	1.6	10	0.93	1585
Vabicaserin [h]	152 [d]	4.4	0.2	14	7.0	0.5	3	7.5	1	1258
SB242084 [i]	851 [d]	6.8	–	45 [d]	7.0	–	7.0 [d]	9	–	158
5-HT$_{2A}$ modulation										
TCB-2 [l]	0.73	6.8	–	–	–	–	–	–	–	–
Lisuride [m]	2.9 [d]	7.8		1.3 [d]	–	–	13.4 [d]	7		0.15
MDL11,939 [n]	2.8	–	–	1419	–	–	853	–	–	–
M100,907 [n]	1.9	8.9	–	261	6	–	88	7.7	–	0.06

Adapted from (Higgins et al., 2013a). Dash (-): information not available.

[a] Ki: binding affinity.

[b] pEC50, potency: negative logarithm of the EC50 (half-maximal effective concentration).

[c] Efficacy relative to response to a supramaximal concentration of 5-HT under the same assay condition.

[d] Ki Database (University of North Carolina at Chapel Hill). Average value for rat (when available) or human receptors.

[e] Porter et al. (1999) using h5-HT2 receptors expressed in CHO-K1 cells. 5-HT$_{2C}$ R isoform VSV, FLIPR (fluorescent imaging plate reader) assay.

[f] Thomsen et al. (2008) using h5-HT2 receptors expressed in HEK-293 cells. 5-HT$_{2C}$ R isoform INI, [3H]-inositol trisphosphate (IP3) assay. Receptor expression levels undisclosed

[g] Siuciak et al. (2007) using h5-HT2 receptors expressed in NIH3T3 cells. 5-HT_{2C} R isoform undisclosed, FL IPR assay. Receptor expression levels undisclosed.

[h] Dunlop et al. (2011) using h5-HT2 receptors expressed in CHO cells. 5-HT_{2C} R isoform undisclosed, [3H]-IP3 assay. Receptor expression levels undisclosed except h5-HT_{2B} receptor 1500 fmol/mg tissue.

[i] Bromidge et al. (1997) using h5-HT2 receptors expressed in HEK293 cells, radioligand binding assay.

[l] McLean et al. (2006) IP_3 accumulation in NIH-3T3 cells stably expressing rat 5-HT_{2A} receptors.

[m] Egan et al. (1998) IP_3 accumulation in NIH-3T3 cells stably expressing rat 5-HT_{2A} or 5-HT_{2C} receptors.

[n] Pehek et al. (2006).

3.2 Methods

The methods employed in this chapter are described in Chapter 2.

3.3 Results

3.3.1 Modulation of 5-$HT_{2A\ /2C}$Rs in GAERS rats

In the following sections I will present the results for systemic and local administration of 5-HT2C agonists on the expression of spontaneous ASs in GAERS rats. The behavioural effects of the systemic administrations of these drugs will be described in section 3.3.1.1.5.

3.3.1.1 Effect of 5-HT_{2C}Rs modulation on ASs in GAERS

3.3.1.1.1 Effect of systemic and local (VB) administration of Ro60-0175 on ASs

Figure 3.2A1-C1 shows the effect of systemic of administration of 3 mg/kg Ro60-0175 in a group of drug naïve GAERS rats (n=8). A repeated measures two-way ANOVA on the time spent in seizure revealed a significant effect of the drug ($F(5, 76) = 3.383$, $p = 0.0081$) reflecting a reduction in time spent in seizure in animals treated with Ro60-0175 compared to vehicle (overall 62.8% reduction, 2-hour window). Further analyses revealed a significant effect of drug for the number of seizures ($F(1, 78) = 53.50$, $p < 0.0001$), but not seizure length. Indeed, the number of seizures was overall decreased by 50.5%, underlying the decrease in time spent in seizure.

Ro60-0175 was also dialyzed locally in the VB (n=6) to test if the effect obtained by systemic administration was induced by activation of thalamic 5-HT_{2C}Rs (via modulation of the thalamic tonic $GABA_A$ current, see section 3.1). This did not appear to be case as no effect was observed on the time spent in seizure, seizure length and number of seizures with reverse microdialysis of 300 µM Ro60-0175 in the VB (n=6) (**Figure 3.2A2-C2**).

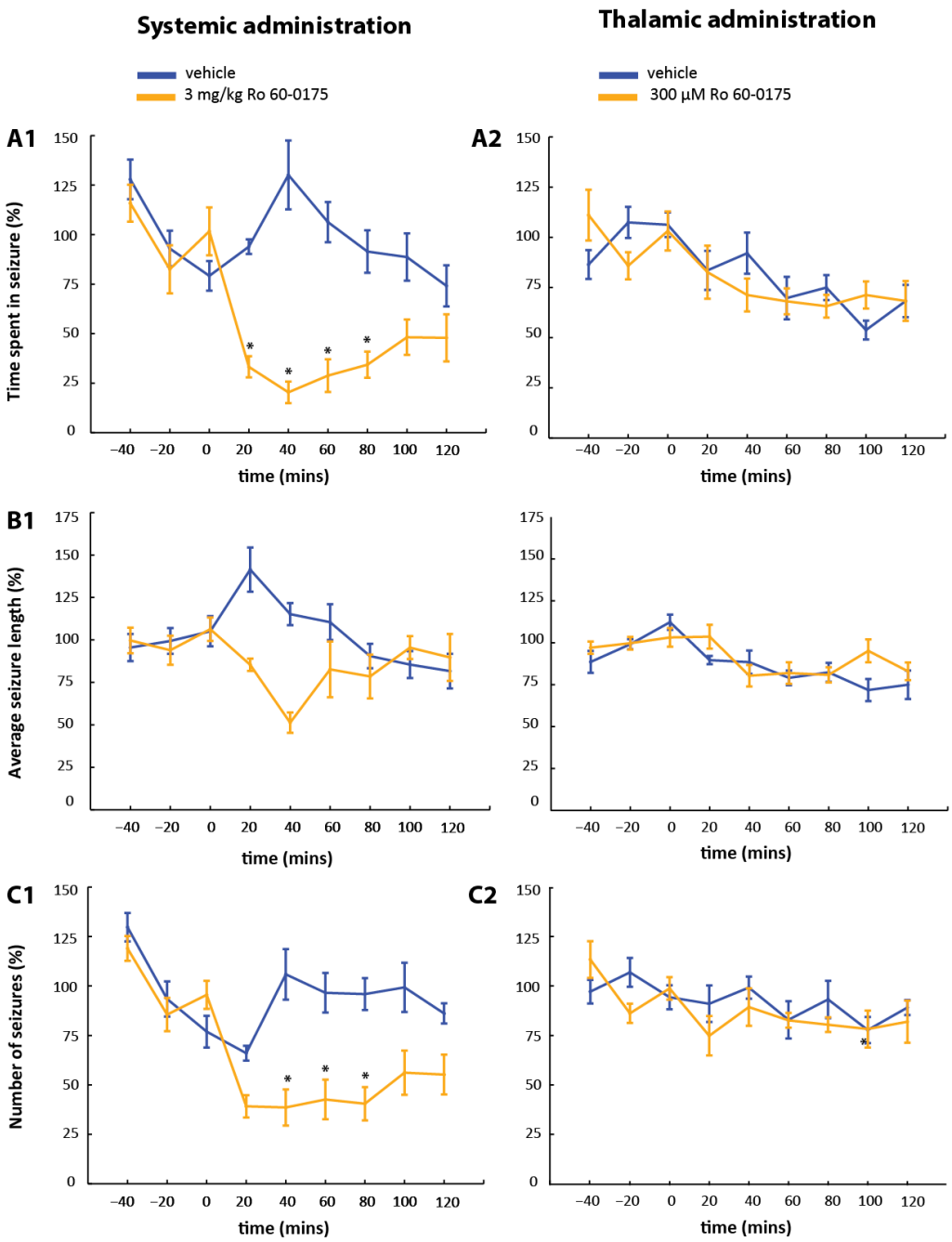

Figure 3.2. Effect of systemic and thalamic (VB) administration of the 5-HT$_{2C}$ agonist Ro60-0175 to the expression of ASs in GAERS. Systemic administration of 3mg/Kg Ro60-0175 decreased the time spent in seizure (A1, p<0.001), an effect driven by a decrease in the number of seizures (C1, p<0.001). The seizure length was unchanged (B1, ns). In contrast, microdialysis of 300 µM Ro60-0175 in the VB had no effect on time spent in seizure, seizure length or number of seizures (A2-C2, ns). In this figure and all subsequent figures of this chapter (unless otherwise stated), p-values in the figure legend refer to the main effect of treatment vs vehicle (two-way ANOVA). In this and in all figures in this chapter: *asterisks refer to a p-value <0.05 for a given time bin in the treatment group vs the corresponding time bin in the vehicle group (two-way ANOVA, Dunnet's multiple comparison test). All values are normalized to the control period (-40 to 0 minutes), lines and bars represent mean and SEM, respectively. Time zero indicates time of i.p. injection or of start of dialysis of the drug. For animal numbers see main text. See tables in appendix for exact p-values and simple main effects.*

3.3.1.1.2 Systemic administration of lorcaserin decreases ASs

To confirm the results of systemic administration Ro60-0175, which has a low selectivity for the 5-HT_{2C} R (see section 3.1), the 5-HT_{2C} agonist lorcaserin was used to test the effect of modulation of 5-HT_{2C}Rs on the expression of ASs in GAERS rats. Three doses of lorcaserin were used in three independent experiments with drug naive animals and a non-repeated measured design (0.3 mg/kg, n=8 vehicle, n=8 treatment; 3mg/kg, n=8 vehicle, n=8 treatment; 10mg/kg, n=8 vehicle, n=6 treatment). The data is presented in **Figure 3.3A1-C1**, with the vehicle groups pulled together for clarity. At 0.3 mg/kg there was no significant effect of drug on the time spent in seizure, seizure length and number of seizures. However at 3 and 10 mg/kg, lorcaserin induced a decrease in the time spent in seizure as revealed by a two-way ANOVA (3mg/kg: $F(1, 84) = 8.042$, $p = 0.0057$; 10mg/kg: $F(1, 72) = 53.67$, $p < 0.0001$). The effect was drastic, but short-lived, with post-hoc testing showing a significant effect for 40 minutes (3mg/kg, 84.2% decrease) and 80 minutes (10mg/mg, 86.9% decrease) post-injection. Analysis of the seizure length and number revealed a complex action of lorcaserin on these parameters. The drug had a significant effect on the number of seizures for both doses (3mg/kg: $F(1, 84) = 93.88$, $p < 0.0001$; 10mg/kg: $F(1, 72) = 106.6$, $p < 0.0001$) and the reduction of the number of seizures lasted for 80 minutes (3mg/kg) and 100 minutes (10mg/kg) post-injection (Dunnet's multiple comparison test). Lorcaserin had an effect on the seizure length only at the dose of 3mg/kg ($F(5, 83) = 6.068$, $p < 0.0001$) and, as can be seen in **Figure 3.3B1**, it induced a drastic increase in the seizure length for the second hour post-injection. A trend for the same behaviour was apparent for the dose of 10mg/kg.

To prove that the effect of lorcaserin on the expression of ASs was due to its action on 5-HT_{2C}Rs, another group of GAERS was tested with the 5-HT_{2C} antagonist SB242084. Rats received, 10 minutes apart, injections of either: SB242084-vehicle and lorcaserin 3mg/kg; SB242084 0.5 mg/kg and lorcaserin 3 mg/kg; SB242084-vehicle and lorcaserin-vehicle; SB242084 0.5 mg/kg and lorcaserin vehicle. The results of this experiments are shown in **Figure 3.3A2-C2**. While injection of 3mg/kg lorcaserin in animals pre-treated with SB242084-vehicle produced a similar effect as the one described above (see **Table A.1**), pre-treatment with the 5-HT_{2C} antagonist SB242084 blocked the effect of lorcaserin on time spent in seizure (simple main effect of SB242084 + lorcaserin vs vehicle, ns), but only partly attenuated the effect of the agonist on seizure length and number of seizures

(compare post-hoc testing results on **Figure 3.3B2,C2**). SB242084, at the concentration of 0.5 mg/kg, had no effect on his own on time spent in seizure (simple main effects of SB242084 vs vehicle, ns), but had a significant, albeit small, effect on seizure length (18.5% overall increase, $p \leq 0.001$) and number of seizures (17.5 % overall increase, $p \leq 0.01$). In particular, post-hoc testing revealed a small (30.2%), short-lived (40 minutes) decrease in average number of seizures compared to vehicle.

3.3.1.1.3 Systemic administration of CP-909,101 decreases ASs

Three doses of CP-909,101, 0.3-3-10 mg/kg, were selected consistent with other published reports (Higgins et al., 2012). In one set of experiments on group of animals was injected with either vehicle (n=10), 0.3 mg/kg CP-909,101 (n=10) or 10mg/kg CP-909,101 (n=6), in randomized order. Another group of 10 drug-naïve GAERs was injected with 3mg/kg CP-909,101 and tested against the antagonist SB242084 with the same design used in the lorcaserin experiment (section 3.3.1.1.2). **Figure 3.4** shows a summary of these experiments (the effect of 3mg/kg CP-909,101 from **Figure 3.4A2-C2** is also shown in **Figure 3.4A1-C1** for comparison).

At 0.3 mg/kg CP-909,101 a two-way ANOVA showed no significant effect of the drug on the time spent in seizure, seizure length and number of seizures (**Figure 3.4A1-C1**). However at 3 and 10 mg/kg, CP-909,101 induced a decrease in the time spent in seizure (3mg/kg: 24.4% decrease overall, $p < 0.001$; 10mg/kg: 78.2 % decrease overall, $p < 0.001$). For 3mg/kg the effect was drastic, but short-lived, with post-hoc testing showing a significant effect for 40 minutes (3mg/kg, 63.5% decrease); for 10 mg/kg the time spent in seizure was drastically reduced throughout the two-hour observation window.

Analysis on the seizure length showed that only in the case of 10mg/kg CP-909,101 there was a significant reduction of the seizure length (36.7% reduction overall, $p < 0.001$). The number of seizures was reduced for both 3 and 10 mg/kg CP-909,101, an effect that was significant for 60 and 100 minutes post-injection, respectively (see **Table A.2** in Appendix A).

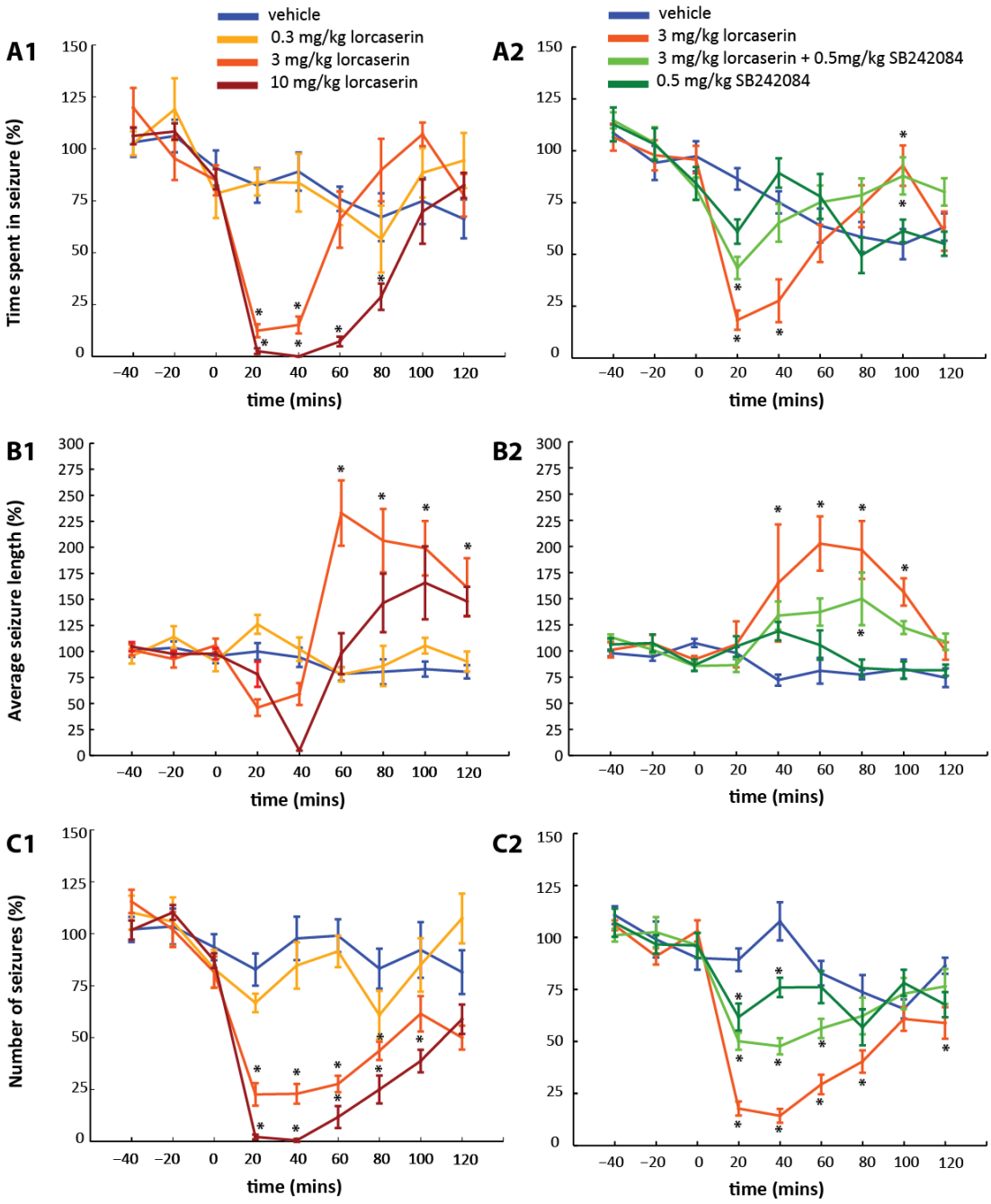

Figure 3.3. Systemic administration of the 5-HT$_{2C}$ agonist lorcaserin dose-dependently decreases ASs by acting on the 5-HT$_{2C}$R. Dose response curve for lorcaserin at 0.3-3-10 mg/kg with time spent on seizure (A1), seizure length (B1) and number of seizures (C1). Note the increase in seizure length in the second hour of the recording for lorcaserin 3-10 mg/kg (B1). Pre-treatment with the selective 5-HT$_{2C}$ antagonist SB-2402084 (0.5 mg/kg) partially blocked the effect of lorcaserin 3mg/kg on time spent on seizure (A2), seizure length (B2) and number of seizures (C2).

As shown in **Figure 3.4A2-C2,** pre-treatment with 0.5 mg/kg SB242084 blocked the effect of CP-909,101 on time spent in seizure (simple main effect of 0.5 mg/kg SB242084 + 3mg/kg CP-909,101 vs vehicle, ns), but only partly attenuated the effect of the agonist on seizure length and number of seizures (**Figure 3.4B2,C2**). As reported for the experiment presented in **Figure 3.3B2,C2**, SB242084 had no effect on its own on time spent in seizure (simple main effects of SB242084 vs vehicle, ns), but had a significant, albeit small, effect on seizure length (18.6% overall increase, $p \leq 0.001$) and number of seizures (22.8 % overall increase, $p \leq 0.01$). Post-hoc testing revealed a 38.2% decrease for the first 20 minutes post-injection in average number of seizures compared to vehicle.

3.3.1.1.4 Systemic administration of vabicaserin decreases ASs

Two doses of vabicaserin: 5 and 15mg/kg were selected, consistent with other published reports (Dunlop et al., 2011; Ogino et al., 2013). A group of 9 GAERS received injections of either vehicle or vabicaserin in randomized order. **Figure 3.5A** shows that vabicaserin had a bimodal effect on the time spent in seizure: first transiently decreasing and then increasing the time spent in seizure. Post-hoc testing reveled a significant increase in the time spent in seizure with 5mg/kg (30.9% overall increase, $p \leq 0.01$), but a trend for a decrease of the time spent in seizure with 15mg/kg (8.3% overall decrease, ns). Analyzing the data in separate 20 minute bins showed that with 15mg/kg vabicaserin there was indeed a significant decrease of the time spent in seizure for the first 40 minutes post-injection (54.5% decrease, $p \leq 0.05$). Similarly to the other 5-HT_{2C} drugs presented above, vabicaserin significantly decreased the number of seizures, at least at the higher dose (5mg/kg: 11.6%, ns; 15mg/kg: 40.0%, $p \leq 0.001$). Moreover, the drug significantly increased the seizure length (5mg/kg: 47.1%, $p \leq 0.001$; 15mg/kg: 62.9%, $p \leq 0.001$).

3.3.1.1.5 Behavioural effects of systemic administration of 5-HT_{2C} agonists and antagonists

The injection of 5-HT_{2C} agonists produced behavioural effects consistent with those reported in the literature (see section 1.6.2.1). In particular penile grooming was observed with each 5-HT_{2C} agonist injected at all doses. Hypolocomotion was also evident, especially at high doses (i.e. 10mg/kg lorcaserin, CP-909,101 and 15mg/kg vabicaserin).

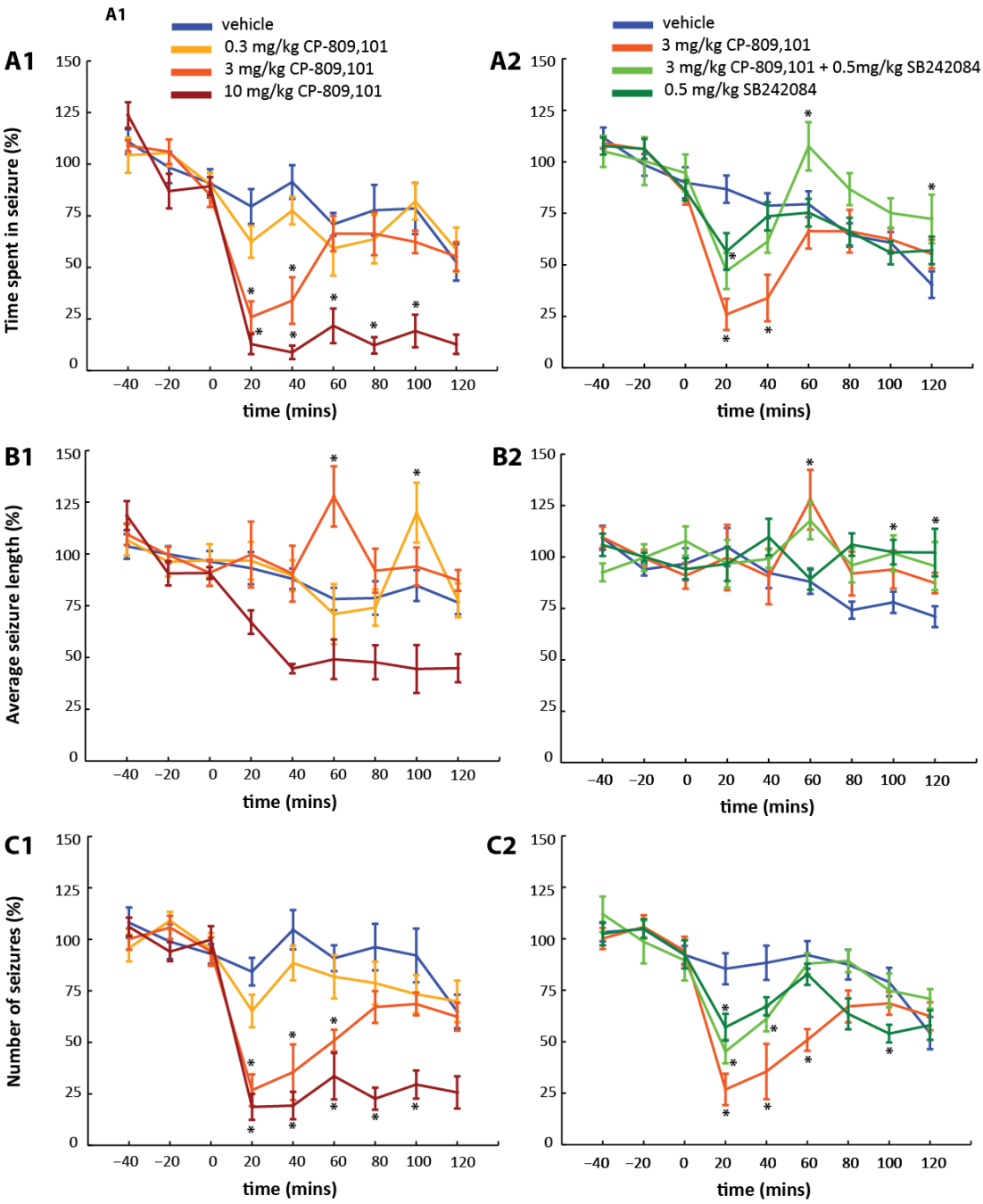

Figure 3.4. Systemic administration of the 5-HT$_{2C}$ agonist CP-809,101 dose-dependently decreases ASs in GAERS by acting of the 5-HT$_{2C}$ receptor. Dose response curve for CP809,101 at 0.3-3-10 mg/kg for time spent on seizure (A1), seizure length (B1) and number of seizures (C1). Pre-treatment with the selective 5-HT$_{2C}$ antagonist SB-2402084 (0.5mg/kg) partially blocked the effect of CP809,101 (3mg/kg) on time spent on seizure (A2), seizure length (B2) and number of seizures (C2).

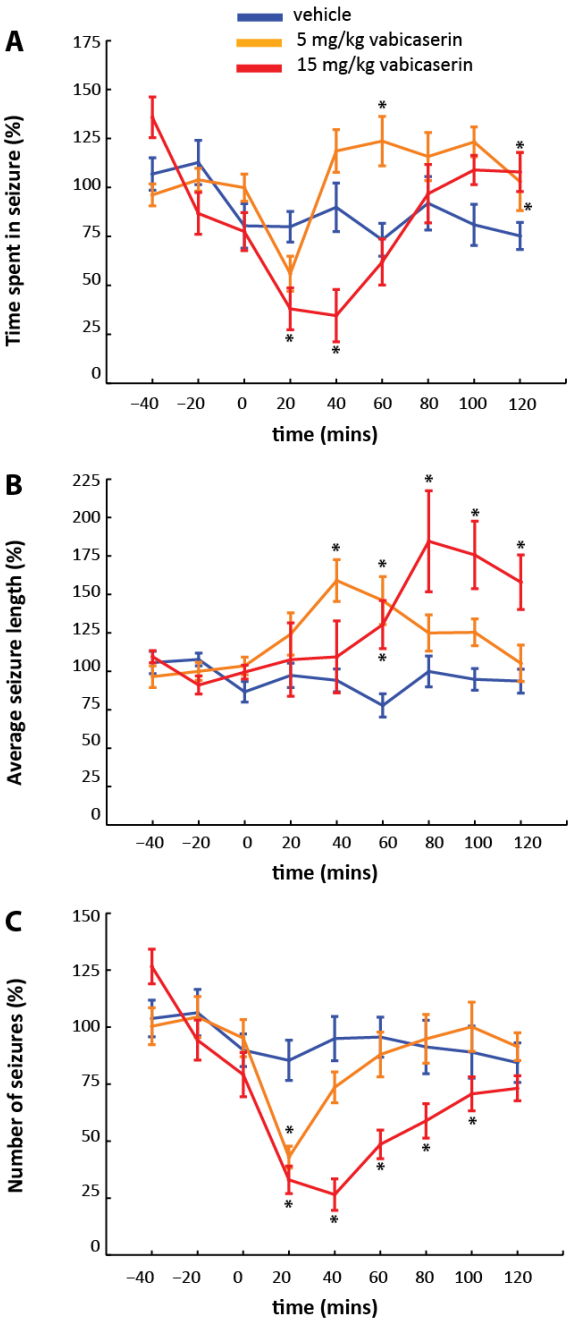

Figure 3.5. Systemic administration of the 5-HT$_{2C}$ agonist vabicaserin has a bimodal effect on ASs in GAERS. Effect of vabicaserin at 5-15 mg/kg on time spent on seizure (A), seizure length (B) and number of seizures (C). Note the transient (40 mins) decrease in time spent in seizure and prolonged decreased in number of seizures with vabicaserin 15mg/kg; also note the increase in seizure length in the second hour of the recording for both doses.

These effects were antagonized by pre-treatment with the selective 5-HT_{2C} antagonist SB242084, which instead had no overt effect on his own, consistently with previous reports (Kennett et al., 1997; Higgins et al., 2001).

3.3.1.2 **Effect of 5-HT_{2A} receptors modulation on spontaneous ASs in GAERS**

In the following sections I will present the results for systemic and local administration of 5-HT_{2A} agonists and antagonists on the expression of spontaneous ASs in GAERS rats. The behavioural effects of the systemic administrations of these drugs will be described in section 3.3.1.2.4.

3.3.1.2.1 Effect of systemic and thalamic (VB) administration of 5-HT_{2A} antagonists on ASs

Figure 3.6A1-C1 shows the effect of systemic of administration of 0.5 mg/kg MDL11,939 in GAERS rats. The data presented here was obtained in two different experiments (sections 3.3.1.2.2 and 3.3.1.2.3) and here is pulled together (n=17 rats treated with vehicle/0.5 mg/kg MDL11,939) for comparison with the case of microdialysis of MDL11,939 (see below). A repeated measures two-way ANOVA on the time spent in seizure revealed a significant effect of the drug ($F(1, 192) = 16.43$, $p < 0.0001$) reflecting a significant increase in time spent in seizure in animals treated with MDL11,939 compared to controls (overall 31.4% increase, 2-hour window). Further analyses revealed a significant effect of drug on seizure length ($F(1, 192) = 26.14$, $p < 0.0001$), but not on the seizure number. Indeed, the length of seizures was overall increased by 33.5%, driving the decrease in time spent in seizure.

MDL11,939 was also dialyzed locally in the VB to explain the discrepancy between the systemic administration the effects *in vitro* on the tonic $GABA_A$ current (section 3.1), which instead predicted a decrease in the expression of ASs. In the case of local dialysis of 50 μM Ro60-0175 there was no effect on time spent in seizure, seizure length and number of seizures (n=11) (**Figure 3.6A2-C2**).

To further confirm the effect of the 5-HT_{2A} antagonist MDL11,939, M100,907, another selective 5-HT_{2A} antagonist, was injected in a group of drug GAERS (**Figure 3.7**), which

received injections of vehicle (n=12), 0.5 mg/kg M100,907 (n=11) or 3mg/kg M100,907 (n=9), in a randomized order. A two-way ANOVA revealed a significant effect of drug on average time spent in seizure, seizure length and number of seizures. Post-hoc testing on the simple main effect of the drug showed that M100,907 induced a significant increase in time spent in seizure both at 0.5 mg/kg (28.9% overall increase, $p < 0.001$) and at 3mg/kg (21.6% overall increase, $p \leq 0.05$). Further analysis reveled that this effect was driven by a significant increase in the seizure length, both at 0.5 mg/kg (58.2% overall increase, $p < 0.001$) and at 3mg/kg (52.6% overall increase, $p < 0.001$). However, an effect on seizure number was also observed: M100,907 induced a small, but significant, decrease in the number of seizures both at 0.5 mg/kg (16.7% overall decrease, $p < 0.01$) and at 3mg/kg (18.9% overall decrease, $p < 0.01$). Post-hoc testing for each 20 minute bin is reported in **Table A.6** in Appendix A.

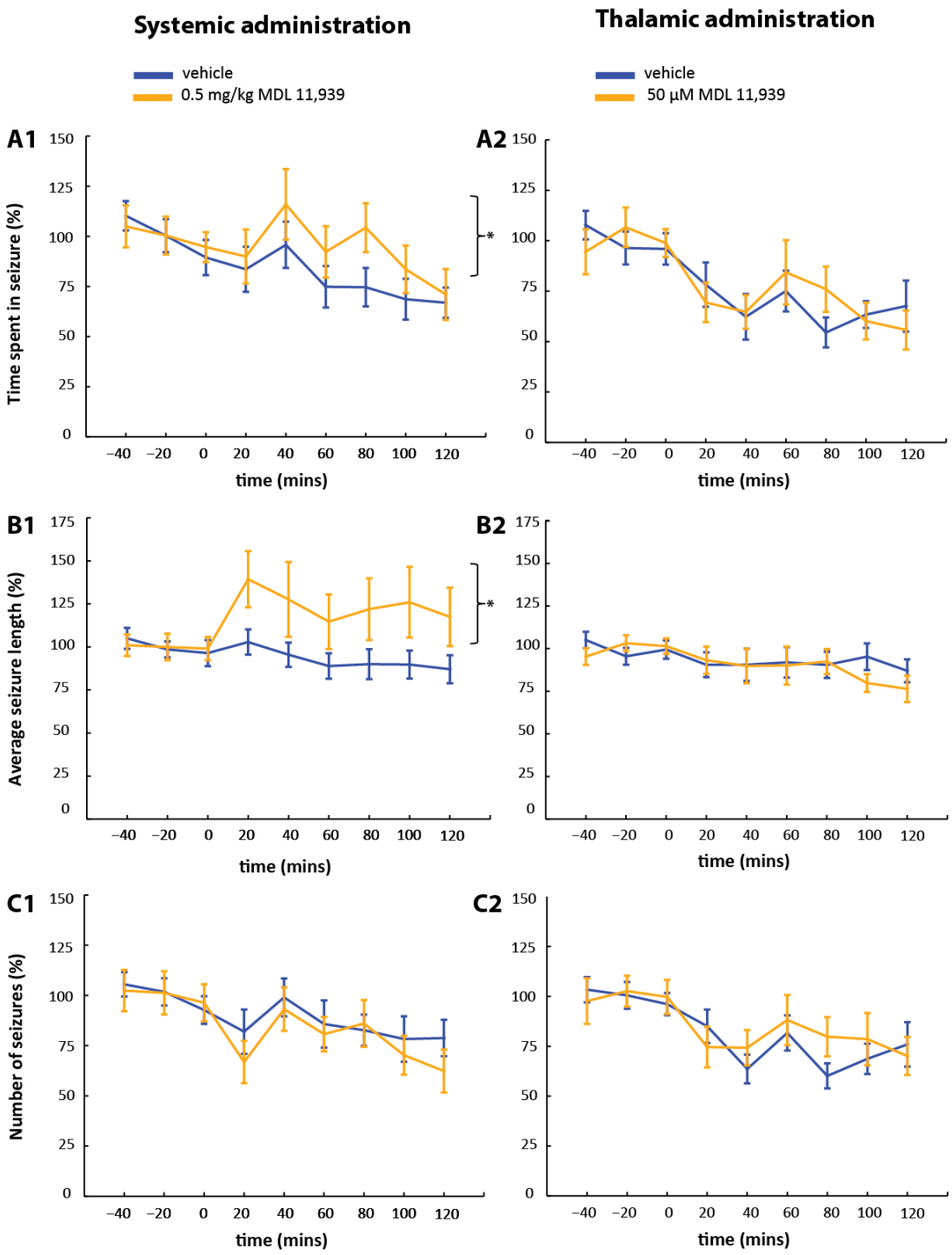

Figure 3.6. Effect of systemic and thalamic (VB) administration of the 5-HT$_{2A}$ antagonist MDL11,939 on ASs. Systemic administration of 0.5mg/Kg MDL11,939 increased the time spent in seizure ($p<0.05$) (A1), an effect driven by an increase in the length of seizures ($p<0.001$) (C1). The number of seizures was unchanged (ns) (B1). In contrast, microdialysis of 50 µM MDL11,939 in the VB had no effect on time spent in seizure, seizure length or number of seizures (A2-C2, ns). Asterisk with curly brackets in figure refer to a p-value <0.05 for the main effect of the drug (two-way ANOVA).

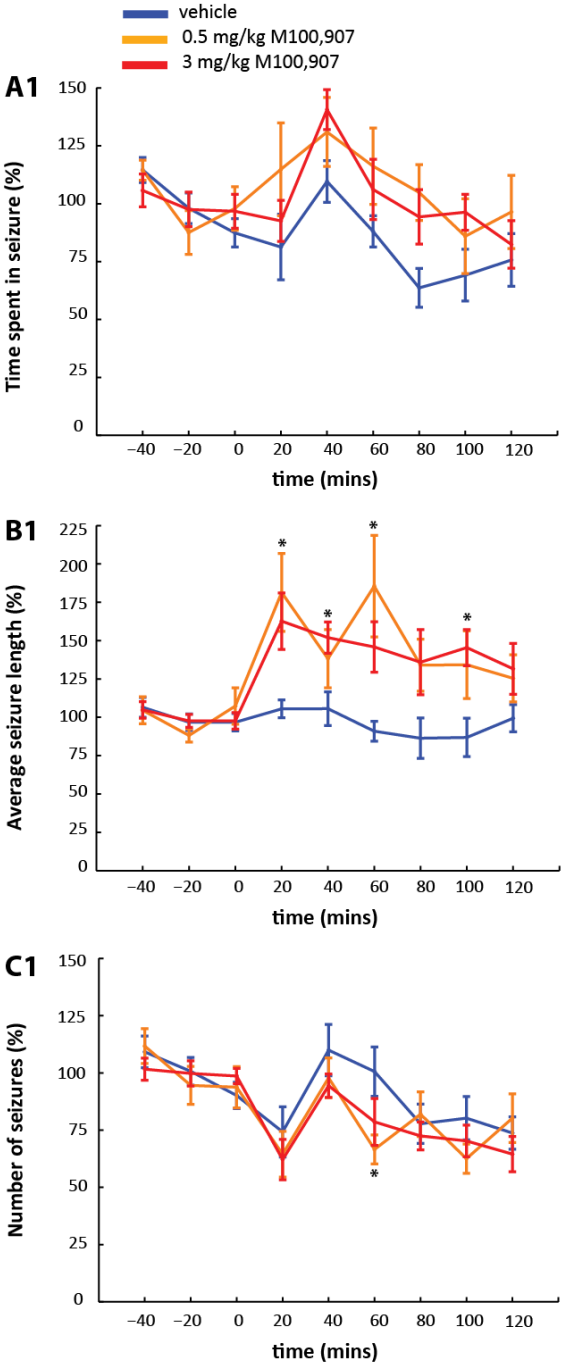

Figure 3.7. Systemic administration of the 5-HT$_{2A}$ antagonist M100,907 increases ASs average length. Effect of M100,907 at 5-15 mg/kg and effects on time spent on seizure (A), seizure length (B) and number of seizures (C). Note that with both doses there is a significant increase in the time spent in seizure and seizure length.

3.3.1.2.2 Systemic administration of the 5-HT$_{2A}$ agonist TCB-2 decreases ASs

Due to the surprising effect of 5-HT$_{2A}$ antagonists, the potent 5-HT$_{2A}$ agonist TCB-2 was used to investigate the role of activation of 5-HT$_{2A}$ receptors on the expression of ASs. Given that the selectivity profile of drug is currently unknown (see section 3.1), two separated set of experiments were conducted. In the first experiment, GAERS were injected with vehicle (n=9), 0.03 mg/kg TCB-2 (n=9) or 3 mg/kg TCB-2 (n=6) in a randomized order. In the second experiment, GAERS were injected with an intermediated dose 0.3 mg/kg TCB-2 and pre-treated with either the 5-HT$_{2A}$ antagonist MDL11,939 or MDL11,939-vehicle.

The effects of the three doses of TCB-2 are shown in **Figure 3.8A1-C1**, with vehicle groups pulled together for clarity (**Figure 3.8A1-C1**). As revealed by post-hoc testing for the simple main effect of the drug, TCB-2 dose-dependently decreased the time spent on seizure at all doses compared to vehicle (0.03mg/kg: 14.1% overall decrease, $p < 0.05$; 0.3mg/kg: 76.8% overall decrease, $p < 0.001$; 3mg/kg: 97.3% overall decrease, $p < 0.001$). Further analysis revealed that there was no effect on seizure length at 0.03 and 0.3 mg/kg, while there was a significant reduction of seizure length at 3mg/kg TCB-2 (72.5% overall decrease, $p < 0.001$). Note that from 40 to 60 minutes post-injection of 3 mg/kg TCB-2 there were no seizures, so no estimation of seizure length was possible (gap in **Figure 3.8B1**). The average number of seizures was also significantly decreased at all doses (0.03mg/kg: 25.6% overall decrease, $p < 0.001$; 0.3mg/kg: 75.1% overall decrease, $p < 0.001$; 3mg/kg: 94.1% overall decrease, $p < 0.001$).

As mentioned above, to prove that the effect of TCB-2 on the expression of ASs was due to its action on 5-HT$_{2A}$ receptors, the effect of 0.3mg/kg TCB-2 was tested against the 5-HT$_{2A}$ antagonist MDL11,939. The experimental design was the following: rats received, 10 minutes apart, injections of either: MDL11,939 vehicle and TCB-2 0.3mg/kg; MDL11,939 0.5 mg/kg and TCB-2 0.3 mg/kg; MDL11,939 vehicle and TCB-2 vehicle; MDL11,939 0.5 mg/kg and TCB-2 vehicle in a randomized order. The results of this experiment are shown in **Figure 3.8A2-C2**. Pre-treatment with 0.5 mg/kg MDL11,939 blocked the effect of TCB-2 on time spent in seizure and seizure length (simple main effect of 0.5 mg/kg MDL11,939 + 3mg/kg TCB-2 vs vehicle, ns) and greatly attenuated the effect of the agonist on number of seizures (simple main effect of 0.5 mg/kg MDL11,939 + 0.3mg/kg TCB-2 vs vehicle, 15.8%

overall decrease, p ≤0.05; compared to 75.1% overall decrease for 0.3mg/kg TCB-2 vs vehicle). The effect of MDL11,939 on his own are the same as described in section 3.3.1.2.1 (**Figure 3.6A1-C1**).

3.3.1.2.3 Systemic administration of the mixed 5-HT$_{2A}$ agonist lisuride has a bimodal effect on ASs, independently of 5-HT$_{2A}$ activation

Finally, the effect of the 5-HT$_{2A}$ agonist lisuride was also tested on the expression of ASs because, due to its functional selectivity, it is known to activate a different intracellular pathway than TCB-2 (see sections 1.6.2.1 and 3.1). Two doses of lisuride were selected: 0.1 and 0.5 mg/kg. The latter dose was also tested against the 5-HT$_{2A}$ antagonist MDL11,939 with the same experimental design presented in section 3.3.1.2.2. Analysis of the simple main effect of the drug after two-way ANOVA on the time spent in seizure revealed a significant effect of 0.1mg/kg lisuride (31.9% overall increase, p ≤0.05) but not of 0.5mg/kg. However, 0.5 mg/kg had a bimodal effect on ASs (**Figure 3.9A1**), first decreasing and then increasing the time spent in seizure. Indeed, post-hoc testing for each 20 minute bin revealed a drastic and significant reduction in time spent in seizure for the first 40 minutes post-injection (91.4% overall reduction, p<0.01), followed by a rebound increase (127% increase at 120 minutes, p<0.001). The rebound increase was driven by a significant increase in seizure length (95% increase at 120 minutes, p<0.01) (**Figure 3.9A2**). In the case of 0.1mg/kg there was a complex pattern of increase in seizure number during the first half hour and increase in seizure length in second half of the two-hour observation window.

Pre-treatment with the selective antagonist MDL11,939 did not a block the decrease in time spent in seizure during the first 40 minutes post-injection of 0.5 mg/kg lisuride, but attenuated the increase in seizure length evident in the second hour post-injection (**Figure 3.9A2-C2**). Nonetheless, pre-treatment with MDL11,939 had a complex interaction with lisuride, increasing significantly increase the seizure number at 60 minutes (257.2% increase, p<0.001).

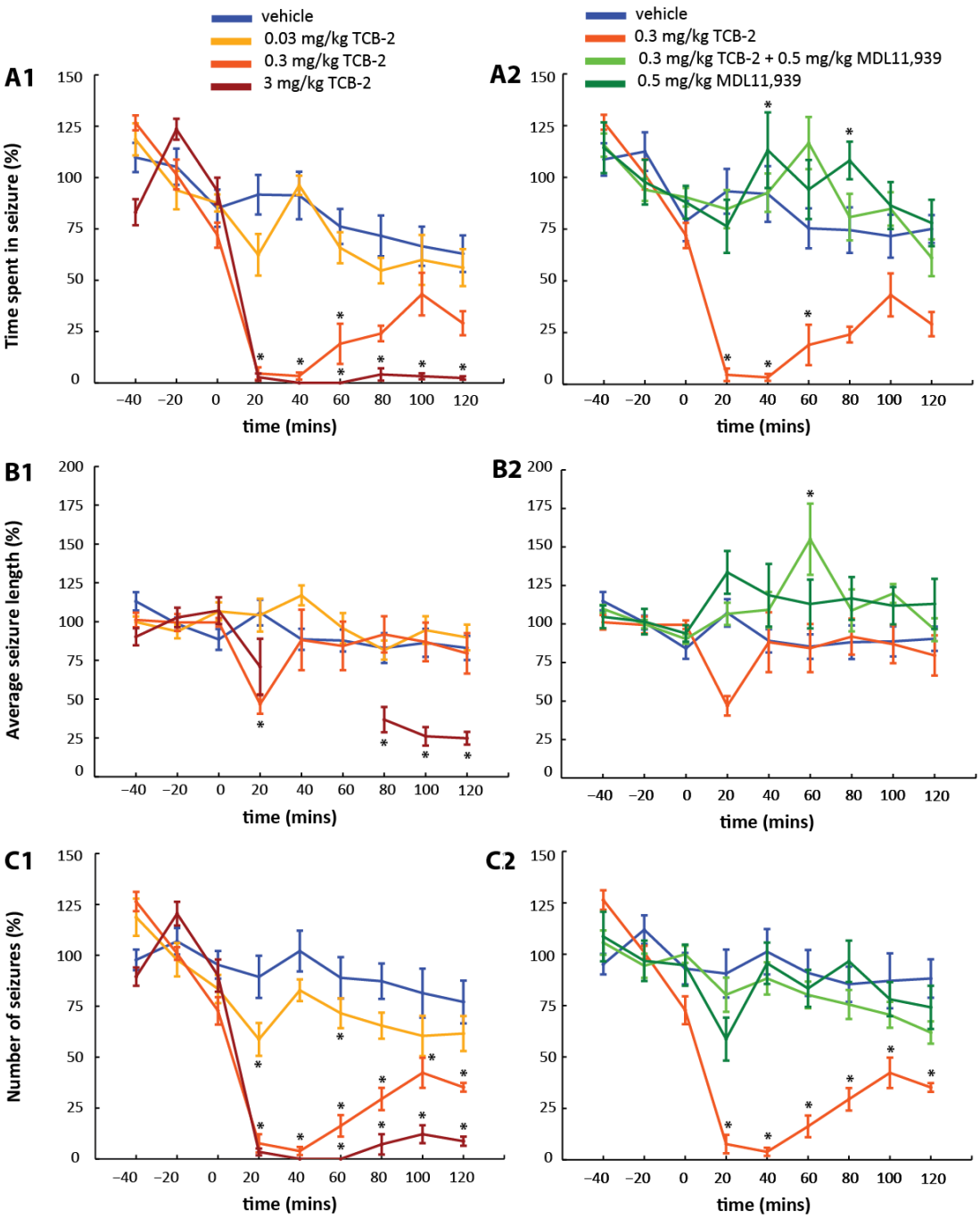

Figure 3.8. Systemic administration of the 5-HT$_{2A}$ agonist TCB-2 dose-dependently decreases ASs by acting on the 5-HT$_{2A}$ receptor. Dose response curve for TCB-2 at 0.03-0.3-3 mg/kg for time spent on seizure (A1), seizure length (B1) and number of seizures (C1). The gap in panel B1 is due to the absence of seizure in all animals for the 40-60 minutes time bins. pre-treatment with the selective 5-HT$_{2A}$ antagonist MDL11,939 (0.5mg/kg) partly blocked the effect of CP809,101 (3mg/kg) on time spent on seizure (A2), seizure length (B2) and number of seizures (C2).

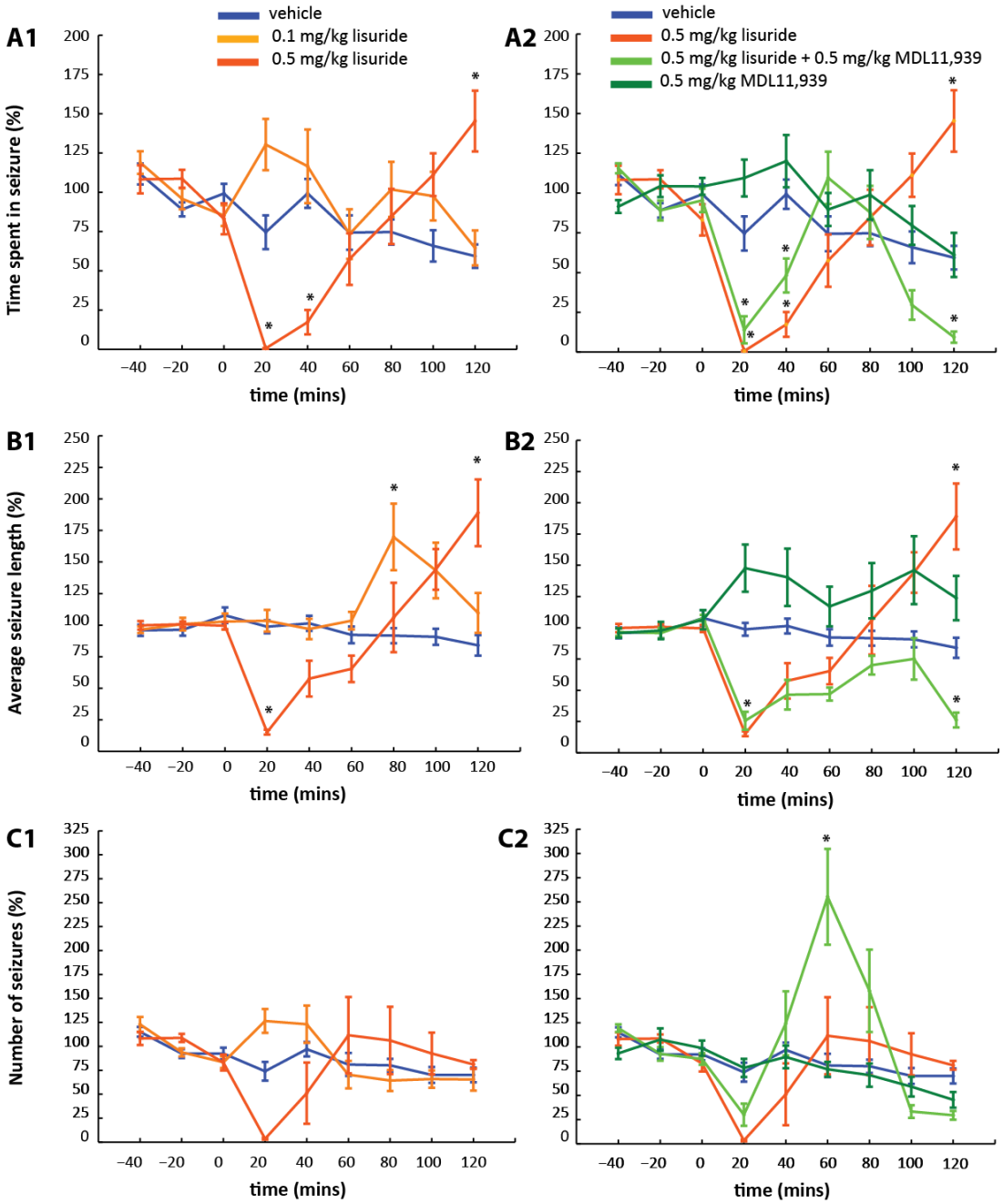

Figure 3.9. Systemic administration of the lisuride modulates ASs independently from 5-HT$_{2A}$ receptor activation. Dose response curve for lisuride at 0.1-0.5 mg/kg with time spent on seizure (A1), seizure length (B1) and number of seizures (C1). Note how lisuride 0.5 mg/kg has a bimodal effect on the time spent on seizure. Moreover, at both doses there is a tendency for an increase in seizure length in the second hour after lisuride injection. Right hand side: absence of block of lisuride 0.5mg/kg effects on time spent on seizure (A2), seizure length (B2) and number of seizures (C2) with pre-treatment with the selective 5-HT$_{2A}$ antagonist MDL11,939 at 0.5mg/kg.

3.3.1.2.4 Behavioural effects of systemic administration of 5-HT$_{2A}$ agonists and antagonists

The 5-HT$_{2A}$ antagonists MDL11,939 and M100,907 did not produce any overt change in behaviour.

The injection of 5-HT$_{2A}$ agonists instead produced behavioural effects consistent with those reported in the literature (see section 1.6.2.1). While no overt behavioural change was observed at 0.03 mg/kg TCB-3, head twitches were observed in response to 0.3 mg/kg. Importantly, the head twitches response was fully blocked by pre-treatment with 0.5 mg/kg MDL11,939. At 3 mg/kg instead the animals became immobile and displayed a decreased muscle tone.

In the case of lisuride instead, at both doses the animals appeared agitated and moved erratically in the cage, consistently with previous reports (Fink and Morgenstern, 1985). This hyperlocomotion was not altered by pre-treatment with 0.5 mg/kg MDL11,939.

3.3.2 Effect of 5-HT$_{2C}$Rs modulation by lorcaserin on pharmacological ASs in the GHB-model

After having characterized the effects of pharmacological modulation of 5-HT$_{2A/2C}$Rs in GAERS spontaneous ASs, a novel set of experiments was designed to characterize the role of these receptors in pharmacological ASs. The GHB-model was selected because it is generally considered the best-established pharmacological model of ASs (see section 1.4.2.1).

A group of drug-naive Wistar rats received i.p. injections of either 10 mg/Kg lorcaserin or vehicle, followed, after 10 minutes, by 100 mg/Kg GBL (n=8, **Figure 3.10**). Seizures were detected for one hour after injection of GBL. Lorcaserin had a significant effect on time spent on seizure (**Figure 3.10A**) (saline: 992.5 ± 247.9 s; lorcaserin: 69.7 ± 69.2 s; p= 0.0079) and number of seizures (**Figure 3.10C**) (saline: 60.9 ± 16.2; lorcaserin: 16.3 ± 16.1; p= 0.0325), but not a significant effect on the mean length of the remaining, lorcaserin-resistant seizures (**Figure 3.10B**) (saline: 35.86 ± 20.5 s; lorcaserin: 0.9 ± 0.6 s p= 0.1348). Effects of lorcaserin were clearly detectable notwithstanding the high

variability of the GHB model in control. Notably, in control conditions, the animals appeared to be in a sedated state, with behaviour remarkably different from the one with spontaneous ASs in GAERS rats (see chapter Chapter 4 for a detailed analysis of the GHB-model of ASs). When lorcaserin and GBL were combined the sedative state was further increased and the animals were immobile for the duration of the experiment.

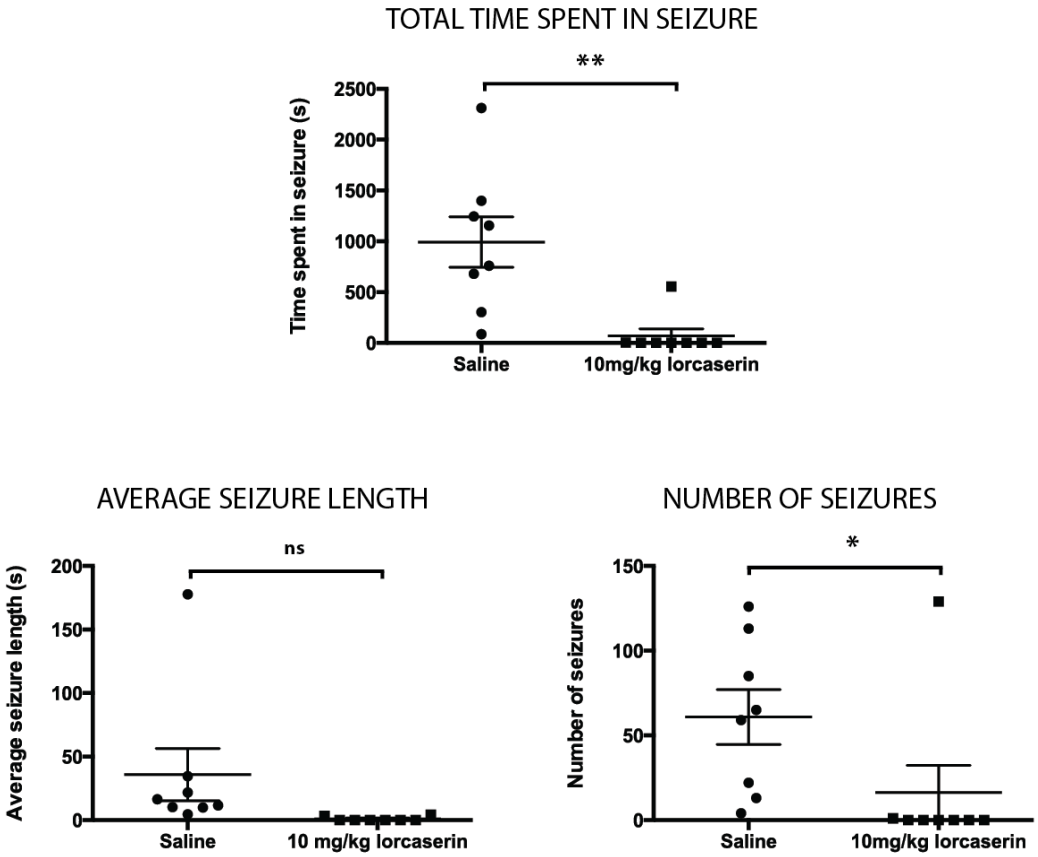

Figure 3.10. Effect of lorcaserin on GHB-elicited ASs. Pre-treatment with 10 mg/kg lorcaserin drastically reduced the time spent on seizure (A) and number of seizures (C) but did not have a significant effect on the mean length (B) of the remaining, lorcaserin-resistant seizures (n = 8; paired t-test, *, $P<0.05$, **, $P<0.01$, ns, not significant). Note the high variability of GHB-induced ASs for all parameters in control conditions (i.e. saline injection). Scatter plots with mean ± SEM.

3.4 Discussion

3.4.1 Summary of results

The main results of this chapter are:

1) global activation of 5-HT_{2C}Rs induces first a drastic decrease in ASs number followed, with certain compounds, by a rebound increase in seizure length;
2) global antagonism of 5-HT_{2C}Rs has no effect on the expression of ASs;
3) global activation of 5-HT_{2A}Rs via TCB-2 abolishes ASs;
4) global antagonism of 5-HT_{2A}Rs increases the seizure length;
5) local application of 5-HT_{2A} antagonists or 5-HT_{2C} agonists in the VB does not affect the expression of ASs.
6) systemic administration of lorcaserin in the GHB-model blocks ASs, although GHB-elicited ASs appear to be accompanied by a sedative/hypnotic state.

3.4.2 Methodological considerations

The first consideration to bear in mind with pharmacological manipulations of 5-HT_2 receptors is that, due to the similarity between 5-HT_{2A} and 5-HT_{2C}Rs (see section 1.6.2.1), very few compounds display a good (>1000 fold) selectivity for one receptor over the other (see also **Table 3.1**). This means that, to conclusively attribute one effect to the activation of a specific 5-HT2 receptor, the block of the same effect with pre-treatment of a selective antagonist is also necessary. In addition, another layer of complexity in the pharmacology of 5-HT2 receptors is due the functional selectivity exhibited by different ligands (1.6.3). It is well characterized in *in vitro* studies that different 5-$HT_{2A/C}$ agonists can preferentially activate IP accumulation or AA release (Berg et al., 1998, 1999; Stout et al., 2002; Moya et al., 2007). In the case of 5-HT_{2C}Rs agonists, it has been recently found that the level of receptor editing (see 1.6.2.1) can influence the efficacy of certain 5-HT_{2C} agonists (but not others, see below) to preferentially induce IP accumulation or AA release (Berg et al., 2008). Chemically different 5-HT2 agonists and antagonists can also differently modulate the rate of receptor internalization and desensitization (Schmid et al., 2008; Yadav et al., 2011). When comparing the effect of different 5-HT2 drugs on ASs these

factors need to be carefully considered, in addition to the differences in pharmacokinetic and pharmacodynamics that may influence experiments with systemic administration of drugs *in vivo*.

3.4.2.1 Systemic administration of 5-HT_{2C} agonists

Driven by the preliminary results *in vitro* on the reduction of the tonic $GABA_A$ current by 5-HT_{2C} agonists and by results in WAG/Rij rats (see section 1.6.3), the effect of various 5-HT_{2C} agonists was investigated on spontaneous ASs in GAERS.

In the current study four 5-HT_{2C} agonists have been used: Ro-60175, lorcaserin, CP809,101 and vabicaserin. Ro-60175 and lorcaserin have a poor (~10-20 fold) selectivity for 2C over 2A (**Table 3.1**). Nonetheless, lorcaserin has been approved for human use (FDA, 2012), so the compounds pharmacokinetic and pharmacodynamics have been thoroughly characterized. CP809,101 and vabicaserin display instead a high (>1000 fold) selectivity for 2C over 2A. The range of doses selected for the systemic administration are comparable to those used *in vivo* in rats for typical 5-HT_{2C} mediated behaviours, such as hypophagia (for instance Ro60175 0.1-10mg/kg (Martin et al., 1998); 0.5-10mg/kg lorcaserin (Thomsen and Grottick, 2008); 0.3-6mg/kg CP-809,101 (Higgins et al., 2013b)). Moreover, these three drugs have similar potency (at concentration ranging from 1-6mg/kg) at diminishing both food intake and nicotine self-administration (Higgins et al., 2013b). Vabicaserin is not available on the market and its effects have been mainly characterized *in vitro* (Dunlop et al., 2011). Nonetheless, a preliminary report on its efficacy against psychotic-like behaviours in rats employed doses of 1.7-10mg/kg (Marquis et al., 2014), comparable to the ones used in the current study.

In general, all 5-HT_{2C} agonists tested induced, dose-dependently, a decrease in the time spent in seizure for the first 40 minutes to 1 hour post-injection. This results are consistent with and extend those of Jakus et. al (2003) where the non-selective 5-HT2 agonist mCPP reduced the time spent in seizure in WAG/Rij rats, an effect blocked by the selective antagonist SB242084 (see section 1.6.3). In that case the effects were reported to last up to 60 minutes, consistently with the experiments presented in this chapter.

With all the compounds tested the decreases in ASs was due to a reduction in the number of seizures rather than of the seizure length. The acute effect for the first 40 minutes was drastic, especially at the highest dose testes, with lorcaserin 10mg/k and CP-809,101

inducing a decrease of >90% on the time spent in seizure. Importantly, whenever tested, this decrease was blocked by the selective antagonist SB-202484 suggesting that the acute effect of 5-HT_{2C} drugs is mainly due to their activation of 5-HT_{2C}Rs rather than a complex interaction with other 5-HT2 receptors. Interestingly, the decrease in the time spent in seizure and the duration of the effect did not correlate with the selectivity profile of the drug: CP-809,101 and vabicaserin, both of which have a selectivity greater than 1000 fold for 5-HT_{2C} over 5-HT_{2A} , were effective for 40 minutes and 120 minutes, at the highest dose tested. Similarly, Ro-60175 and lorcaserin which a ~10-20 fold selectivity for 5-HT_{2C} over 5-HT_{2A} were each effective for about 80 minutes post-injection. Whether this discrepancy is due to differences in pharmacokinetics or pharmacodynamics is unclear. The only drug for which pharmacokinetic studies are available is lorcaserin. With a 10mg/kg *per-os* administration in rats, lorcaserin reached peak concentration in the brain (Tmax) at 1 hour and had a half-life of 4.7 hours (Thomsen and Grottick, 2008). Interestingly, the mean brain concentration at two hours (where the effect of lorcaserin had disappeared in the current experiments) was the same as the mean brain concentration at 40 minutes (peak of the reduction of ASs). This results are similar to those of subcutaneous administration (s.c.) in rats, with lorcaserin 3mg/kg having a Tmax of 80 minutes in the plasma and the half-life 3.1 hours (Higgins et al., 2013b). Therefore, it appears that the short-lived effect of lorcaserin in blocking the expression of ASs is not due to the clearance of the molecule from the brain.

Instead, it is likely that receptor desensitization may play a role in the duration of the effect of 5-HT_{2C} agonists: the rapid desensitization of 5-HT_{2C}Rs after agonists-induced activation is a well characterized phenomenon, at least *in vitro* (Van Oekelen et al., 2003a; Martin et al., 2014). This process takes place within minutes from application of the agonist and its extent and kinetic vary according to the type of 5-HT_{2C} agonist employed and downstream pathway investigated (Stout et al., 2002). Unfortunately, for none of the 5-HT_{2C} agonist employed in this study information on desensitization rates is available. It is possible that desensitization of 5-HT_{2C}Rs would then unmask the activity of a moderately selective 5-HT_{2C} agonist at other targets (such as 5-HT_{2A} receptors). Indeed, in the case of lorcaserin, the brain concentration (1.7μM, (FDA, 2010)) reached by 10mg/kg *per-os* administration would be compatible with such action. Nonetheless, lorcaserin does not induce (at doses up to 18mg/kg) any activity in rats that is normally associated with 5-HT_{2A} receptor activation, such as wet-dog shakes and head twitches (FDA, 2010). The reasons for this discrepancy are at present unclear, but it has been suggested that the *in vivo* potency of lorcaserin is lower than the one measured in *in vitro* assays (FDA, 2012).

In the second hour post-injection, lorcaserin and vabicaserin induced a drastic increase in the seizure length, while no change was observed for Ro-60175 and CP-809,101. This discrepancy does not seem to be caused by differences in their 5-$HT_{2C/2A}$ selectivity profile of the drugs, but could arise from differences in functional selectivity. Unfortunately, Ro-60175 is the only 5-HT_{2C} agonist used in this study whose functional selectivity has been characterized to a certain extent. Ro-60175 is capable of inducing both IP accumulation and AA release when activating the unedited (INI) isoform of the 5-HT_{2C} receptor. In partially edited (VNI) 5-HT_{2C} receptor isoforms, Ro 60– 0175 is instead unable to activate the PLA-AA pathway, while its coupling with the PLC pathway was unchanged (Berg et al., 2008). There are too many unknown factors that could modulate the interplay between functional selectivity, desensitization rate and pharmacodynamics of the different 5-HT_{2C} agonists to conclusively explain their incongruent modulation of seizure length.

Nonetheless, the observation that some 5-HT_{2C} agonists are capable of both reducing seizure number and increasing seizure length is of interest on its own. 5-HT_{2C} drugs seem therefore to block seizure initiation and at later stage, to block seizure termination. It is difficult to pinpoint the brain target(s) of 5-HT_{2C} receptor agonists that at the basis of the modulation of ASs described in this chapter. 5-HT_{2C}Rs are diffusely expressed in thalamus and cortex, so a direct change in excitability in these areas could be hypothesized. No information is available for effect of 5-HT_{2C} agonist in cortex or thalamus in terms of changes in neuronal excitability (see section 1.6.2.1).

It should be borne in mind that 5-HT_{2C} activation is also generally linked to global changes in vigilance states, which in turn are known to modulate the expression of ASs (Danober et al., 1998). Unfortunately, no study has been conducted on 5-HT_{2C} regulation of arousal states using selective agonists for the 5-HT_{2C} receptor (such as CP-809,101 and vabicaserin) and the results obtained with non-selective agents are contradictory (see section 1.6.3). Moreover, 5-HT_{2C}Rs are also thought to control emotional states, in particular anxiety-like behaviours (Quesseveur, 2012). Although no change in the animals' behaviour was observed except for penile grooming and hypolocomotion (see section 3.3.1.1.5), a contribution of changes in anxiety levels to the modulation of ASs cannot be excluded.

3.4.2.2 **Systemic administration of a 5-HT_{2C} antagonist**

The administration of the selective 5-HT_{2C} antagonist SB242084 (0.5mg/kg) had no effect on the expression of ASs. This results is consistent to that reported by Jakus at. (2003) in WAG/Rij rats. The dose of 0.5 mg/kg was chosen because it selectively blocks 5-HT_{2C} -mediated behaviours *in vivo*, while higher doses can antagonize 5-HT_{2A}-mediated behaviours as well (Fletcher et al., 2004, 2009; Higgins et al., 2012).

Given that the global knockout mouse for the 5-HT_{2C} receptor has a high susceptibility to various forms of convulsive seizures (Tecott et al., 1995), an increase in ASs could have been expected. Nonetheless, the 5-HT_{2C} receptor has a high constitutive activity (Aloyo et al., 2009) and it is known that, at least in the striatum, the lack of effect of 5-HT_{2C} antagonists such as SB242084 can be unmasked by application of inverse agonists (De Deurwaerdère et al., 2004). Experiments with 5-HT_{2C} inverse agonists could reveal if this is the case also for the modulation of ASs in GAERS.

3.4.2.3 **Systemic administration of 5-HT_{2A} antagonists**

Although 5-HT_{2A}Rs have not previously implicated in the pathogenesis or modulation of ASs, the effect of systemic administration of 5-HT_{2A} antagonists was tested in GAERS rats driven by the preliminary results on their ability to decrease the tonic $GABA_A$ current, a key player in the expression of ASs (see section 3.1).

In the current study two moderately selective (~100 fold selectivity for 5-HT_{2A} over 50HT2C) 5-HT_{2A} antagonists were used: MDL 11,039 and M100,907. The concentration selected for both, 0.5 mg/kg, was chosen because it selectively blocks 5-HT_{2A} -mediated behaviours *in vivo*, while higher doses can antagonize 5-HT_{2C} -mediated behaviours as well (Fletcher et al., 2002).

Contrary to our hypothesis, both drugs induced a small, albeit significant increase in the time spent in seizure, driven by an increase in the seizure length. Although post-hoc testing revealed that no single 20 minute time point was significantly different to vehicle, the overall curves (simple main effects of drug) were highly significant, and the trend for the increase in seizure length was clearly visible for the whole observation window (see **Figure 3.6A1-C1** and **Figure 3.7**). Interestingly, when M100,907 was tested at 3mg/kg the magnitude of the effect some comparable to the lower dose. This suggests that antagonism

of 5-HT_{2A} receptors rapidly reaches a plateau, and reinforces the finding that 5-HT_{2C} antagonism has no effect on the expression of ASs.

This unexpected result is difficult to reconcile with the view that the constitutive activity of 5-HT_{2A} receptor is low, although little is known of the constitutive activity of these receptors *in vivo* (see section 1.6.2.1.1). Therefore, more than a change in excitability within the TC network, it is likely that the effect of 5-HT_{2A} antagonists reflects a global change in brain state. M100,907 has been shown to increase NREM sleep in rats (Morairty et al., 2008). Notably, the threshold concentration tested in the aforementioned report was 0.3 mg/kg and the effect was only evident after the second hour of treatment. Therefore, it is plausible that during the 2-hour observation window M100,907 induced an increase in drowsiness, the arousal state were GAERS ASs more commonly emerge from (Leresche et al., 2011). In addition, MDL11,939 and M100,907 are also have an anxiolytic effect in rats (Dudley et al., 1988; Kehne et al., 1996). It has been suggested that polygenic rats models of ASs, such as GAERS and WAG/rij have anxiety-like symptoms (Jones et al., 2008; Sarkisova and van Luijtelaar, 2011), but the effect of anxiolytics on seizure length has never been tested. Therefore, it cannot be excluded that changes in seizure length also reflect a modulation of emotional states driven by 5-HT_{2A} antagonists.

3.4.2.4 **Systemic administration of 5-HT_{2A} agonists**

Prompted by the results obtained with the systemic administration of 5-HT_{2A} antagonists, the effect of chemically different 5-HT_{2A} agonists were tested on the expression of GAERS ASs.

At present, no selective 5-HT_{2A} agonist is available for research use (Nichols, 2004; Roth, 2011), however several potent 5-HT_{2A} agonists have been used, in conjunction with selective 5-HT_{2A} antagonists, to investigate the role of this receptor. Two 5-HT_{2A} agonists have been used in the current study: TCB-2 and lisuride. The selectivity profile of TCB-2 is unknown (McLean et al., 2006), but the drug binds 5-HT_{2A} receptor with high (nM) affinity. Lisuride instead, while binding 5-HT_{2A} receptors in the nM range, is also known to activate several other 5-HT and dopamine receptors (Egan et al., 1998; Millan et al., 2002).

Activation of 5-HT_{2A} receptors is known for its ability to induce hallucinations in humans, although not all 5-HT_{2A} agonists are hallucinogenic (see section 1.6.2.1.1). Indeed, it has

been suggested that that hallucinogenic activity is better correlated with production of AA than with activation of PLC and IP accumulation, with some 5-HT_{2A} ligands preferentially activating one of the two pathways (Kurrasch-orbaugh et al., 2003). This is indeed the case for lisuride (González-Maeso et al., 2007; González-Maeso and Sealfon, 2009), which is approved for humans used and does not induce hallucinations even at high doses (Herrmann et al., 1977). TCB-2 was initially synthetized with the purpose of creating another non-hallucinogenic 5-HT_{2A} agonist, which could be used to ameliorate memory deficits (McLean et al., 2006), although it is currently understood that TCB-2 indeed induces hallucinations both in humans and in rodents (Fox et al., 2010).

To date, there are few published reports with systemic administration of TCB-2 in rats, therefore the three doses were selected at 10fold increments. Both 0.3 mg/kg and 3mg/kg produced a drastic decrease in the time spent in seizure which, at the higher dose, persisted through the 2-hour observation window. The block of ASs was accompanied by radical changes in behaviour (e.g wet dog shakes, head twitches), typical of hallucinogenic drug in rodents (see section 3.3.1.2.2). Importantly, the effect of TCB-2 on both ASs and the animal's behaviour was blocked by pretreatment with the 5-HT_{2A} antagonist MDL11,939, suggesting that the effect was indeed driven by the activation of 5-HT_{2A} receptors.

In the case of lisuride, the doses selected were consistent with a previous report in GAERS rats (Warter et al., 1988). Differently from the study, which reported no change in the expression of ASs at concentration between 0.25 and 0.5 mg/kg, in my hands lisuride modulated ASs in a bimodal way. In particular, at 0.5 mg/kg lisuride produced a drastic, but short-lived, reduction in the total number of seizures, which resulted in a decrease in the time spent in seizure. This was followed by a dramatic increase in the seizure length, which was maintained for the second hour-post injection. Importantly, the effect of lisuride was not blocked by pre-treatment with the selective 5-HT_{2A} antagonist MDL11,939. Moreover, the combination of lisuride with MDL11,939 induced a drastic increase in the number of seizures around 1 hour post-injection, an effect never observed with either the agonist or the antagonist on his own.

Given that lisuride acts on multiple receptors it difficult to conclusively establish what caused this complex modulation of ASs. It is possible that by blocking the 5-HT_{2A} receptor, effects of lisuride on other targets became evident. For instance lisuride binds the D1/D2 dopamine receptors, whose activation generally is reported to block ASs in GAERS (Warter

et al., 1988), and 5-HT_{1A} receptor, whose activation in WAG/Rij produces instead an increase in the number of seizures (Jakus et al., 2003).

3.4.2.5 Lack of effects of VB administration of 5-HT_{2C} agonists and 5-HT_{2A} antagonists

In the experiments with local administration of either the 5-HT_{2C} agonist Ro60-0175 and 5-HT_{2A} antagonist MDL11,939 no effect was observed on the expression of ASs. This lack of effect can be explained by a variety of technical and biological factors. With brain reverse microdialysis it is customary to select a drug concentration at least 10 times higher than the one bath-applied *in vitro* (Chaurasia, 1999; Höcht et al., 2007). In this case, considering the concentrations used in the *in vitro* experiments on the modulation of the thalamic tonic $GABA_A$ current presented in section 3.1, a concentration of 2μM for Ro60-0175 and 5μM for MDL11,939 should have been used. Nonetheless, the distance travelled by the drug from the outlet of the dialysis probe depends both on the diffusion coefficient of the molecule and is also proportional the total concentration of molecule added in the inlet (Höcht et al., 2007). The diffusion coefficients for the molecules used in the current experiment are unknown, therefore higher concentrations were used in the hope to reach a higher volume of the VB. The actual diffusion of a drug in the brain is difficult to measure without resorting to radioactively-labeled compounds or quantitative dual-probe microdialysis techniques (Chen et al., 2002). An estimation of the effective drug concentration can also be attempted if the effect of the drug on neuronal activity is known (see section 4.3.3 for a description of this technique), but in the case of the 5-HT drugs used in this study this is not possible because their net effect on neuronal excitability on thalamic neurons is unknown. Therefore it is impossible to conclude if the drug concentration used in this study was insufficient to affect the bulk of the VB and or if the lack of effect instead reflects a 'real' negative result in the experiment.

While it would be tempting to use higher concentrations of the compounds, this has not been attempted because of the scarce selectivity of the drugs employed. For instance, at 300μM Ro60-0175is already acting on all 5-HT2 receptors (the Ki for 5-HT_{2A}, 5-HT_{2B} and 5-HT_{2C} are (nM) 37.1, 4.3 and 9.1, respectively) and given that the diffusion rate of the drug is unknown, it is impossible to predict the extent of volume around the outlet where the three 5-HT2 receptor are activated at the same time. This is particularly problematic in the case of the thalamic tonic $GABA_A$ current, because it has been shown that while 5-HT_{2C} agonists decrease the tonic current, 5-HT_{2A} agonists increase it in Wistar rats (Cavaccini et al., 2012).

The reduction in the tonic current *in vitro* was ~42% for Ro60-0175 and ~36% for MDL11,939, which is comparable to the ~50% reduction obtained with antisense RNA for the delta subunit of $GABA_A$ receptors (Cope et al., 2009). Importantly, the 50% reduction of the tonic current *in vitro* was sufficient to block ASs *in vivo* (Cope et al., 2009). This suggests that the magnitude of reduction of the tonic current was compatible with observing an effect on ASs *in vivo*. Nevertheless, MDL11,939 and Ro60-0175 are likely to have other effects on the neuronal excitability other than modulating the tonic current. These changes in excitability could be strong enough to override any effect of the tonic current on ASs.

3.4.2.6 Therapeutic potential of 5-$HT_{2A/2C}$ drugs in ASs

The results with systemic administration of 5-HT_{2C} agonists indicate a therapeutic potential of these drugs for the treatment of human ASs. Nevertheless, the tendency of some 5-HT_{2C} agonists, such as lorcaserin (which is already approved for human use) to increase the seizure length suggests caution. Investigating the effect of chronic use of 5-HT_{2C} in pre-clinical models of ASs could be useful to further understand the role of receptor desensitization *in vivo* in controlling the duration of the block of ASs.

In the case of 5-HT_{2A} agonists, the results obtained suggest that the block of ASs was an effect downstream of the hallucinogenic activation of the 5-HT_{2A} receptor, precluding a therapeutic application of 5-HT_{2A} agonists in the treatment of ASs. Finally, 5-HT_{2A} antagonists, which have been the pipeline of various pharmaceutical companies for the treatment of insomnia or as anxiolytics, could potentially induce an increase in the seizure length in patients with ASs.

3.4.3 Effect of lorcaserin in the GHB-model of ASs

Pre-treatment with 10mg/kg lorcaserin blocked the expression of GHB-elicited ASs. Importantly, it was observed that the animals treated with 100mg/Kg GBL had peculiar changes in behaviour. Instead of displaying SWDs with behavioural arrest as GAERS, the animals stopped moving altogether and appeared in a sedated/hyopnotic state. Experimental ASs and defined by the occurrence of SWDs in the EEG, concomitantly with a

transitory behavioural arrest. A state of prolonged immobility, also accompanied an apparent loss of muscle tone, appeared to be distinct from GAERS ASs. It was therefore decided that before testing other 5-HT drugs in this pharmacological model of ASs, further characterization of the sedated/hypnotic state was needed. Thus, a thorough characterization of the GHB-model will be presented in the following chapter.

Chapter 4 Further characterization of the GHB-model: role of T-type Ca^{2+} channels

4.1 Introduction

Due to the fact that after systemic administration of GBL the animals appeared to be in a hypnotic/sedated state[2] (see section 3.4.3), I sought to further investigate the GHB-model. This was done by characterizing in detail the EEG and behaviour of rats injected with GBL and also by manipulating pharmacologically T-type Ca^{2+} channels which are thought to be fundamental for the expression of GHB-elicited ASs (Kim et al., 2001; Cheong and Shin, 2013b, 2014). Indeed, the role of T-type Ca^{2+} channels in the pathogenesis of ASs is supported both by the discovery of genetic mutations in these channels in humans with absence epilepsy and related syndromes and by genetic and molecular findings in experimental models of ASs (see sections 1.2.1.3 and 1.5).

Although T-type channels are highly expressed across the TC network, much attention has been devoted the role of T-type channels in thalamic territories, i.e. TC nuclei (such as the VB) and in the NRT. In particular, the most commonly accepted theories on the generation of ASs assume an essential role of T-type channel mediated bursting in both NRT and TC nuclei (McCormick and Contreras, 2001; Cheong and Shin, 2013a) or exclusively in the NRT (Crunelli and Leresche, 2002).

Since the first potent and selective T-type channel antagonist TTA-P2 has become available (Shipe et al., 2008), it has become possible to test experimentally these hypotheses, i.e. is the activity of T-type channels in the TC network and specifically in TC and NRT nuclei necessary for the expression of ASs?

[2] A sedated/hypnotic state (also sometimes defined as "light hypnosis") is a behavioral state induced by a drug (commonly compounds acting on the GABAergic system, such as benzodiazepines or low doses of anaesthetic agents such as propofol) that resembles drowsiness or natural sleep. This state is accompanied by an impairment of consciousness and a loss of muscle tone (Hinton and Johnston, 2009; Meerts and Absalom, 2013). The same compounds, at higher doses, can induce a loss of the righting reflex in rodents (stage normally dubbed 'deep hypnosis') and, eventually, surgical anaesthesia (Mendelson, 2002).

Recent experimental work has demonstrated that via reverse microdialysis of TTA-P2 it is possible to selectively block T-type channel dependent bursts locally in the VB and in the NRT (David et al., 2013). Moreover, preliminary data from the lab suggests that in GAERS the activity of T-type channels in the NRT is necessary for the expression of spontaneous ASs, while in the VB is not (McCafferty et al., 2012).

In contrast, a paper published at the time of writing of this thesis, suggests that this is not the case in the GHB-model, whereby a genetic downregulation of the main T-type channel subunit in the NRT produces an increase in the cumulative duration of GHB-elicited ASs (Lee et al., 2014b). To further investigate these controversial results, in this chapter I describe the effects of systemic and thalamic application of TTA-P2 on the expression of GHB-elicited ASs.

4.2 Methods

The methods employed are described in Chapter 2.

4.3 Results

4.3.1 EEG and behaviour in the GHB model and effect of ETX

A group of drug-naive Wistar rats received i.p. injections of either 150 mg/Kg ETX or saline, followed by 100 mg/Kg GBL. The effect of GBL in control conditions was similar to the one described in the literature (see section 1.4.2.1.1), with some important differences that will be highlighted in the following paragraphs. **Figure 4.1** shows a representative one-hour unilateral EEG trace starting at the time of injection of GBL. The wavelet power spectrum is also presented in order to illustrate the dominant frequency changes that occur in the EEG after GHB administration. After 6.7 ± 2.3 (n=8 rats) minutes from the i.p. injection, started to display bilateral synchronous SWDs (**Figure 4.1B**) in the EEG associated with behavioural arrest, facial myoclonus, and vibrissal twitching. The instantaneous maximum frequency of a SWD typically oscillated between 4 and 8Hz (**Figure 4.1B2**, bottom). Upon termination of the SWD animals resumed their previous motor behaviour.

The SWD length became progressively longer, and after 18.6 ± 5.0 minutes from i.p. injection, SWDs evolved into a continuous synchronized state (CSS). The frequency in the

CSS appeared to slow down to 3-4 Hz (**Figure 4.1C2**, bottom). In addition, spike and waves were not organized in orderly successions of spike-wave complexes, but appeared more disorganized and often only comprised of waves (**Figure 4.1C2**). During the CSS the animals were immobile, with their eyes half open in what appeared to be a sedated state. Occasional movements during this state were always accompanied by a desynchronized EEG. Importantly, the EEG and behaviour of the CSS was different from the one of natural sleep. **Figure 4.2** shows a one-hour unilateral EEG trace of a drug-naïve Wistar injected with saline. Periods of light-sleep were accompanied by behavioural immobility and an increase of delta waves in the EEG (**Figure 4.2A2,A3**). Behaviourally, natural sleep was accompanied by a curled up position, while the CSS behavioural state was characterized by a 'unnatural' change in posture with animals having their legs apart and the belly flat on the floor of the cage, indicative of a loss of muscle tone.

After 43.8 ± 4.9 minutes form i.p. injection a desynchronized EEG started to appear for gradually longer periods, interrupted by intermittent SWDs accompanied by behavioural arrest, similar to those observed in the initial period after the injection (**Figure 4.1D**). Finally, towards the end of the observation window (48.7 ± 3.6 minutes), the animals returned to display a desynchronized EEG and active behaviour. Over one hour post GBL injection the average total duration of the SWDs was 4.4 ± 3.5 minutes (mean ± SD); the average total duration of the CSS was 14.3 ± 11.4 minutes (mean ± SD).

Pre-treatment with ETX 150 mg/Kg completely blocked the expression of GHB-induced SWDs and CSS (n=8) (**Figure 4.3**). Given that both states were ETX sensitive, in the subsequent analysis we collated the two states together as "GHB-induced absence seizures" as suggested by other authors (Snead, 1988; Banerjee and Snead, 1992). ETX had a significant effect on time spent on seizure (**Figure 4.5A**) (saline: 992.5 ± 247.9 s; ETX: 69.7 ± 69.2 s; p= 0.0079) and number of seizures (**Figure 4.5B**) (saline: 60.9 ± 16.2; ETX: 16.3 ± 16.1; p= 0.0325), but not a significant effect on the mean length of the remaining, ETX-resistant seizures (**Figure 4.5A**) (saline: 35.86 ± 20.5 s; ETX: 0.9 ± 0.6 s p= 0.1348). Effects of ETX were clearly detectable notwithstanding the high variability of the GHB model in control (see spread of raw data points in control in **Figure 4.5A**).

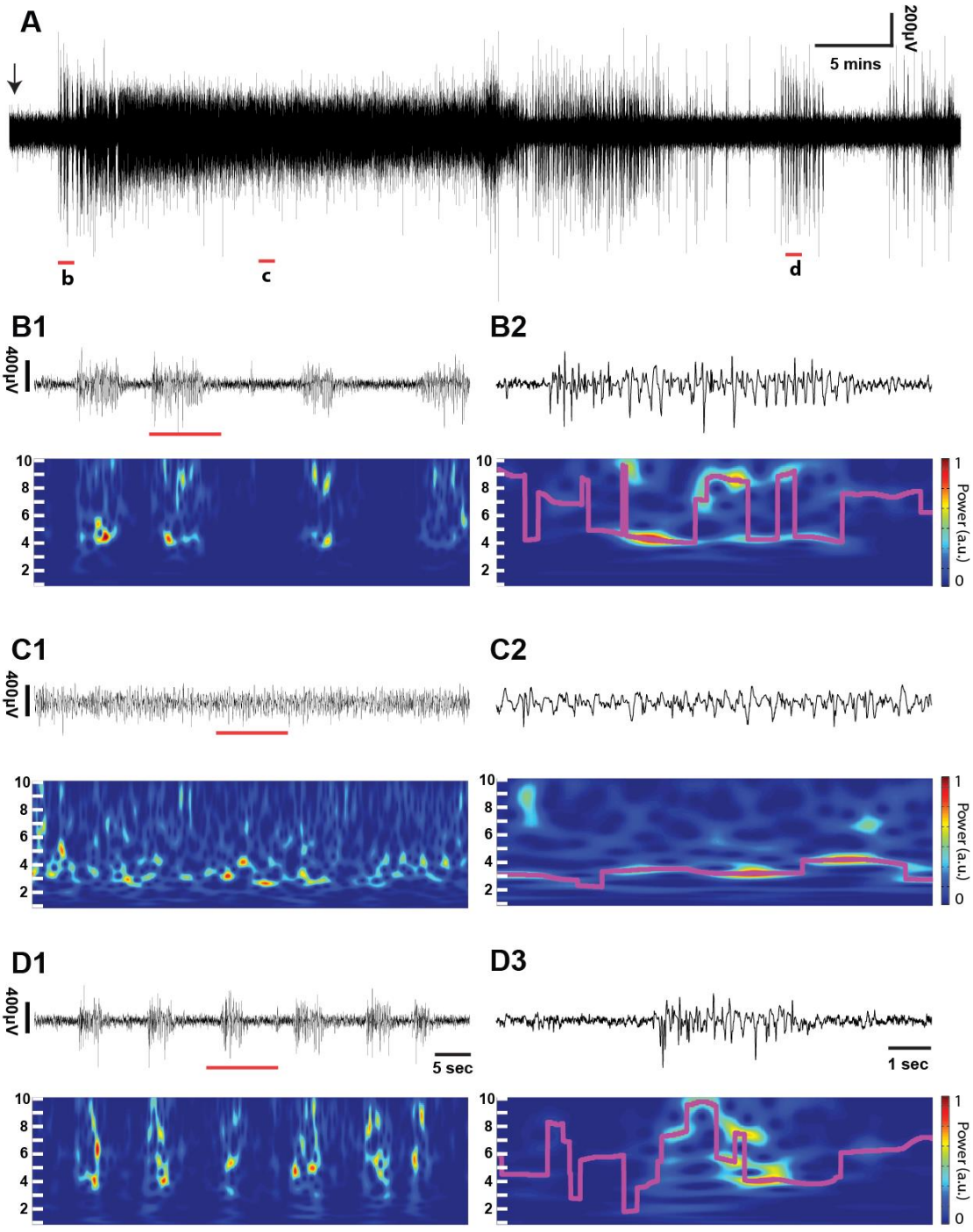

Figure 4.1. EEG after injection of GBL. (A, injection at arrow mark). Epochs b, c and d (red mark), one minute long, are shown with an extended time scale below. Each epoch is presented as EEG trace (top) and 1-10 Hz wavelet power spectrum (bottom). (C). Selected epochs of traces in B1, C1 and D1 (red mark, 10 seconds long) are further expanded on the right. The wavelet power spectrum (right, bottom) also shows the instantaneous maximum frequency of signal (magenta line). Two main EEG features are visible: SWDs (B, D) and a continuous synchronized state (C). See text for detailed description of EEG and corresponded behaviour.

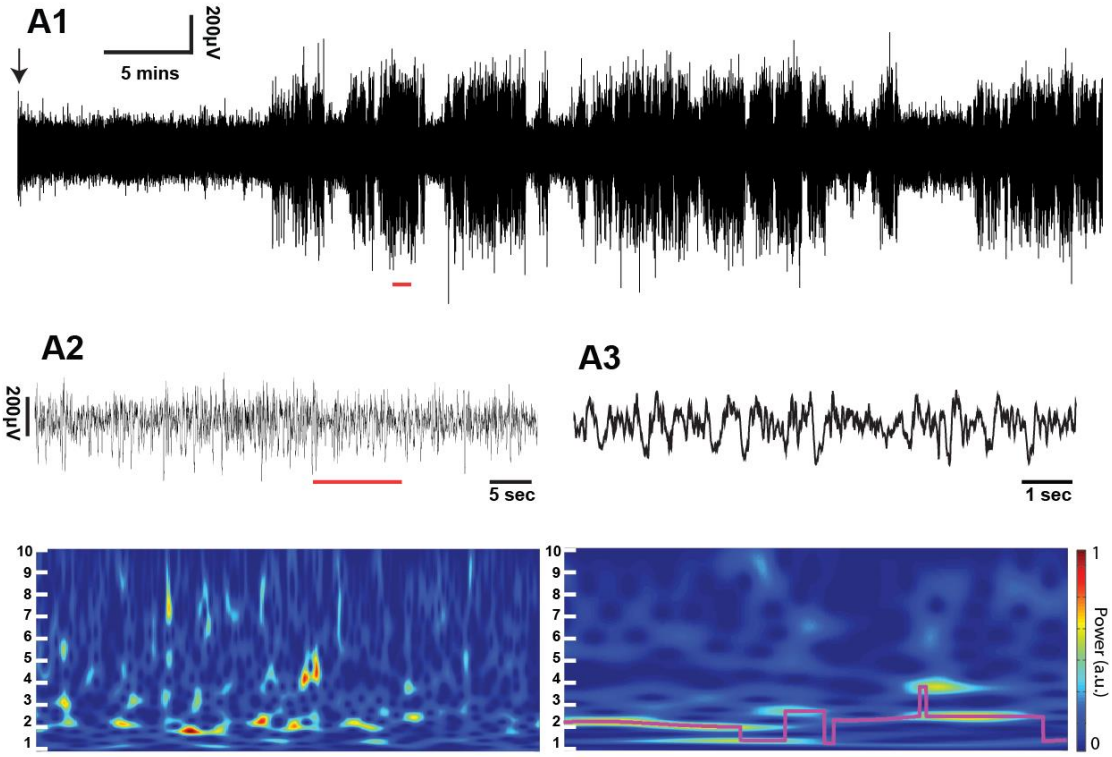

Figure 4.2. EEG after injection of saline. (A, injection at arrow mark) A one-minute long extract from a natural-sleep epoch, marked in red, is shown with an extended time scale below (A2) as EEG trace (top) and corresponding 1-10 Hz wavelet power spectrum (bottom). An epoch (red mark, 10 seconds long) is further expanded in the correspondent right side of the figure (A3, top). The wavelet power spectrum (A3, bottom) also shows the instantaneous maximum frequency of signal (magenta line) concentrated in the delta range. See text for detailed description of EEG and corresponded behaviour.

4.3.2 Systemic administration of TTA-P2 blocks GHB-elicited absence seizures

A group drug-naive Wistar rats received i.p. injections of either 10 mg/Kg TTA-P2 or saline, followed by 100 mg/Kg GBL. When the animals were pre-treated with TTA-P2, their locomotion decreased drastically, consistently with preliminary data from the lab (Orban et al., 2010). Since GBL also had a sedative/hypnotic state, it was not possible to pair SWDs with an associated behaviour; hence the subsequent seizure detection was based mainly on the EEG features. Pretreatment with TTA-P2 (n=9) had a significant effect on time spent on seizure (**Figure 4.5A**)(saline: 603.1 ± 83.9 s; TTA-P2: 12.8 ± 8.1 s, p= 0.0002), seizure length (**Figure 4.5B**) (saline: 5.9 ± 2.4 s; TTA-P2: 2.0 ± 3.2 s; p= 0.0352) and number of seizures (**Figure 4.5C**) (saline: 108.8 ± 16.9; TTA-P2: 2 ± 1.3, p=0.0003). As it can be see in **Figure 4.4A** pre-treatment with TTA-P2 completely blocked GHB-induced absence seizures. The EEG activity that was evoked after GBL injection had a comparable peak EEG power to that of animals treated with 10mg/kg TTA-P2 followed by injection of saline (compare **Figure 4.4A** and **Figure 4.4B**) and no SWDs were observed throughout the recording.

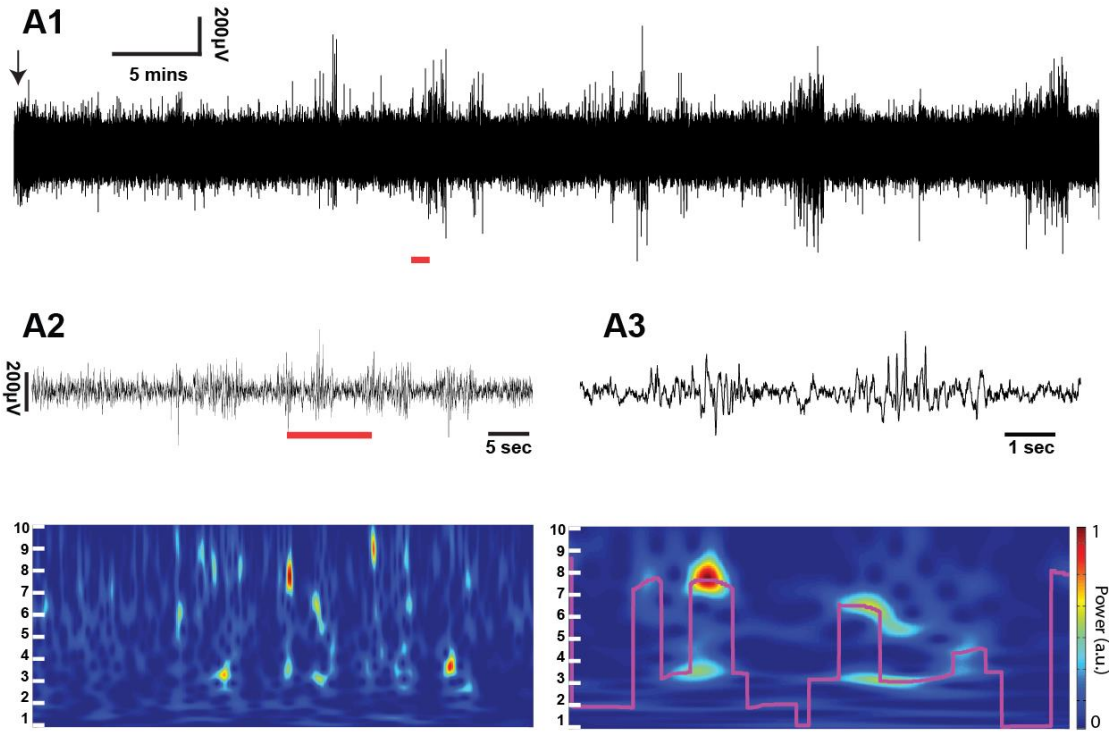

Figure 4.3. ETX abolishes GHB-elicited ASs. Representative one hour EEG recording with 100mg/kg of GBL pretreated with 150mg/kg ETX (A, injection at arrow mark). ETX fully blocks GHB-elicited ASs, with the exception of few isolated SWD-like activities (compare with **Figure 4.1** B and D) A one-minute long epoch, marked in red, is shown with an extended time scale below (A2) as EEG trace (top) and corresponding 1-10 Hz wavelet power spectrum (bottom). An epoch (red mark, 10 seconds long) is further expanded in the correspondent right side of the figure (A3, top) highlighting some remaining SWD-like activities of short duration. The wavelet power spectrum (A3, bottom) also shows the instantaneous maximum frequency of signal (magenta line) concentrated in the delta/spindle range. See text for detailed description of EEG and corresponded behaviour.

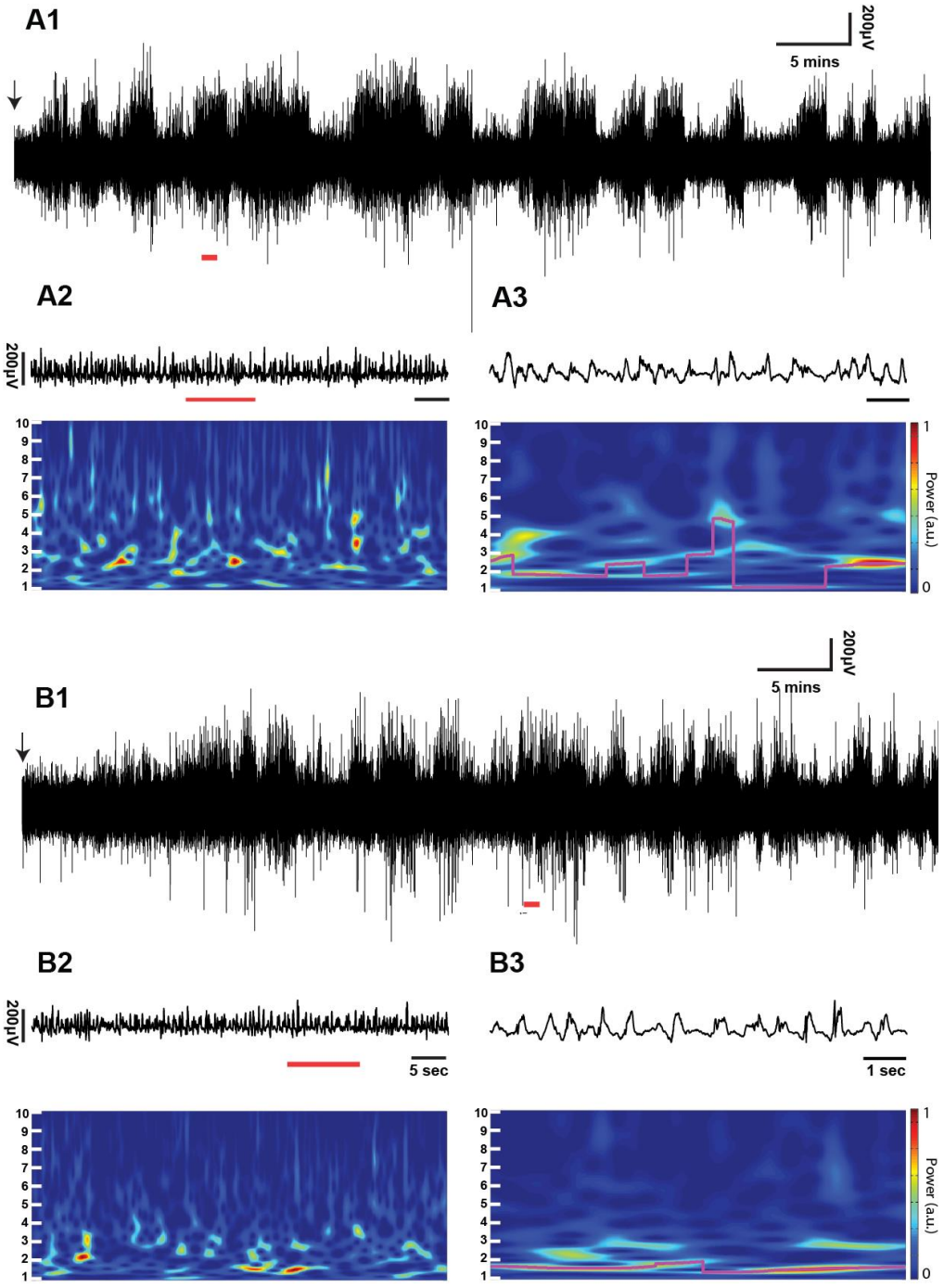

Figure 4.4. Systemic administration of TTA-P2 abolishes GHB-elicited ASs and induce an increase in delta/slow wave activity. Representative one-hour EEG recordings of GBL 100mg/kg pre-treated with 10mg/kg TTA-P2 (A, GBL injection at arrow mark) and of saline injection pre-treated with 10mg/Kg TTA-P2 (B, saline injection at arrow mark). One-minute long epochs, labeled with a red mark in A and B, are shown with an extended time scale in A1 and B1 respectively. Each epoch is presented as EEG trace (top) and 1-10 Hz wavelet power spectrum (bottom). Selected epochs of traces in A1 and B1 (red mark, 10 seconds long) are further expanded in the correspondent right side of the figure (A2, B2 top). The wavelet power spectrum (A2, B2, bottom) also shows the instantaneous maximum frequency of signal (magenta line). TTA-P2 fully blocked GHB-elicited ASs (A) and evoked low-delta band oscillations (A3, A4, bottom). The same low-delta band oscillations are evoked by TTA-P2 on his own (B).

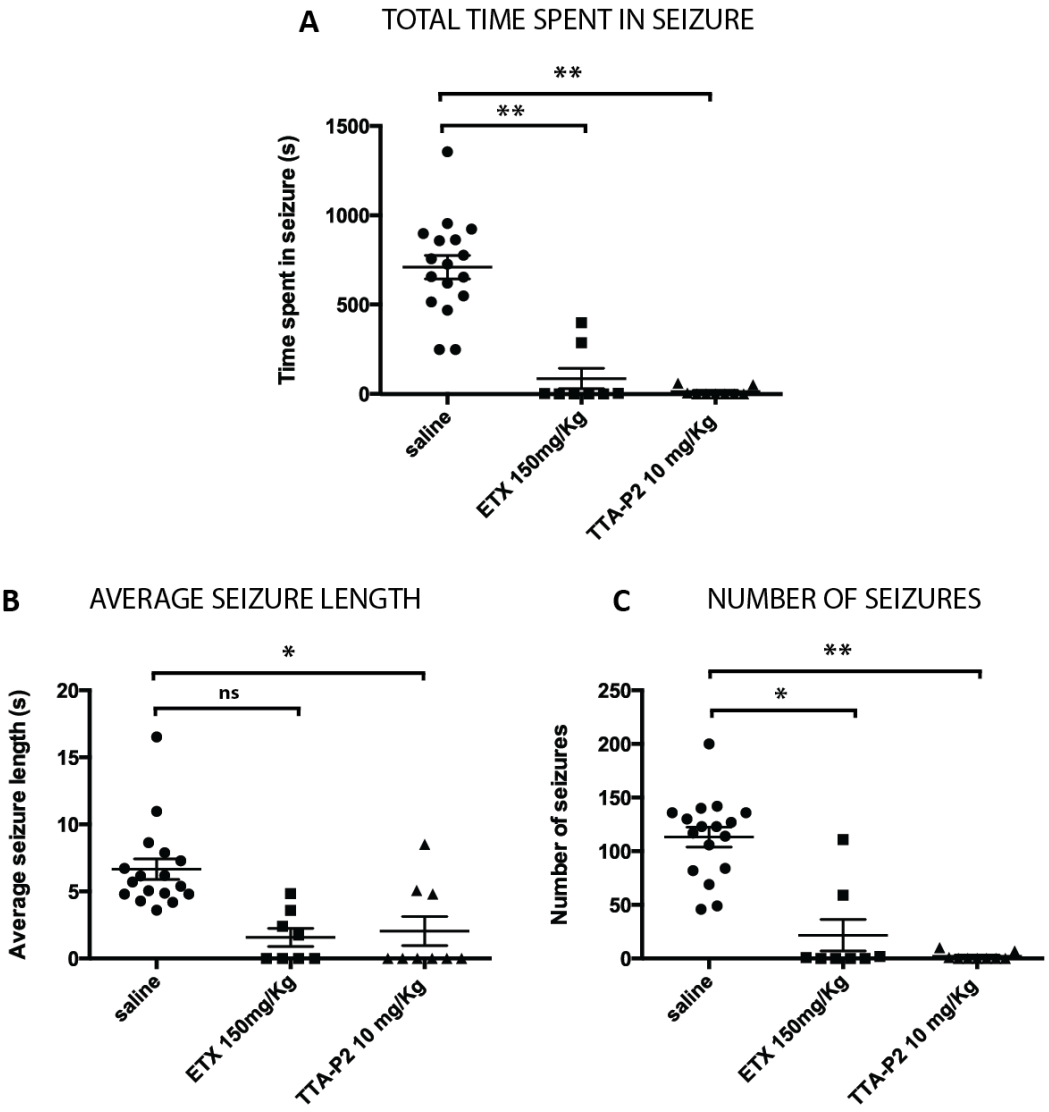

Figure 4.5. Systemic administration of TTA-P2 and ETX abolishes GHB-elicited absence seizures. Pre-treatment with 150 mg/Kg ETX drastically reduced the time spent on seizure (A) and number of seizures (C) but did not have a significant effect on the mean length (B) of the remaining, ETX-resistant seizures (n = 8; paired t-test, *, P<0.05, **, P<0.01). Similarly, pre-treatment with 10mg/Kg TTA-P2 had a significant effect on the time spent on seizure (A), seizure length (B) and number of seizures (C) (N=8; paired t-test, *, P<0.05, **, P<0.01). Controls for the TTA-P2 and ETX groups are plotted together for clarity. Observation window is one-hour post injection of GBL. Scatter plots with mean ±SEM

4.3.3 Microdialysis of TTA-P2 in the VB alone or in both VB and NRT does not reduce GHB-induced absence seizures

T-type Ca^{2+} channel are expressed throughout the CNS and the body, therefore systemic application of TTA-P2 is not suited to ascertain the role of T-type channels in specific areas of TC network. Bilateral reverse microdialysis of TTA-P2 was used to investigate the contribution of T-type Ca^{2+} channels located either in VB or VB plus NRT on the expression of GHB-induced absence seizures. In each experiment the coordinates for the dialysis probe placement where kept constant, but the concentration of TTA-P2 was varied in order to reach the sole VB (300 μM TTA-P2, n=11) or the VB and the NRT territories in conjunction (1mM TTA-P2, n=9) (see section 2.3.2.1 for details about the concentration dependent volume of TTA-P2-induced block of T-type channels).

GBL produced a comparable EEG and behaviour for the rats during the microdialysis experiments as for the i.p. experiments. Importantly, local application of TTA-P2 did not produce any overt change in locomotion and behaviour like the ones observed after systemic TTA-P2 administration. I noticed though that upon GBL administration in control conditions (aCSF dialysis) (n=20), the duration of the CSS was almost doubled compared to the equivalent control period of i.p. injections. Indeed, over one hour the average total duration of SWDs was 7.0 ± 1.15 minutes (not significantly different compared to I.P. control, p=0.0904) while the average total duration of the CSS was 24.3 ± 1.6 minutes, significantly longer then i.p. control (n=20) (p= 0.0146).

For neither dose of TTA-P2 we observed a net effect on the time spent in seizure, seizure length or number of seizures. In particular 300 μM TTA-P2 (n=11) elicited no significant change on time spent on seizure (**Figure 4.6B**) (aCSF: 1164 ± 225.8 s; TTA-P2: 921.5 ± 211.4 s, p= 0.3489), seizure length (**Figure 4.6C**) (aCSF: 6.5 ± 3.1 s; TTA-P2: 5.6 ± 3.1 s, p= 0.3059) or number of seizures (**Figure 4.6D**) (aCSF: 173.4 ± 25.6 ; TTA-P2: 153.7 ±, 28.4, p= 0.4505) compared to control.

For 1mM TTA-P2 (n=9) there was no significant change in time spent on seizure (**Figure 4.6B**) (aCSF: 1738 ± 115.1 s, TTA-P2: 1528 ± 277.3 s, p=0.4958), seizure length (**Figure 4.6C**) (aCSF: 14.37 ± 2.6 s, TTA-P2: 16.72 ± 2.9 s, p=0.5642) or number of seizures (**Figure 4.6D**) (aCSF: 139.8 ± 14.3, TTA-P2: 96.44 ± 15.0, p=0.0528) compared to control.

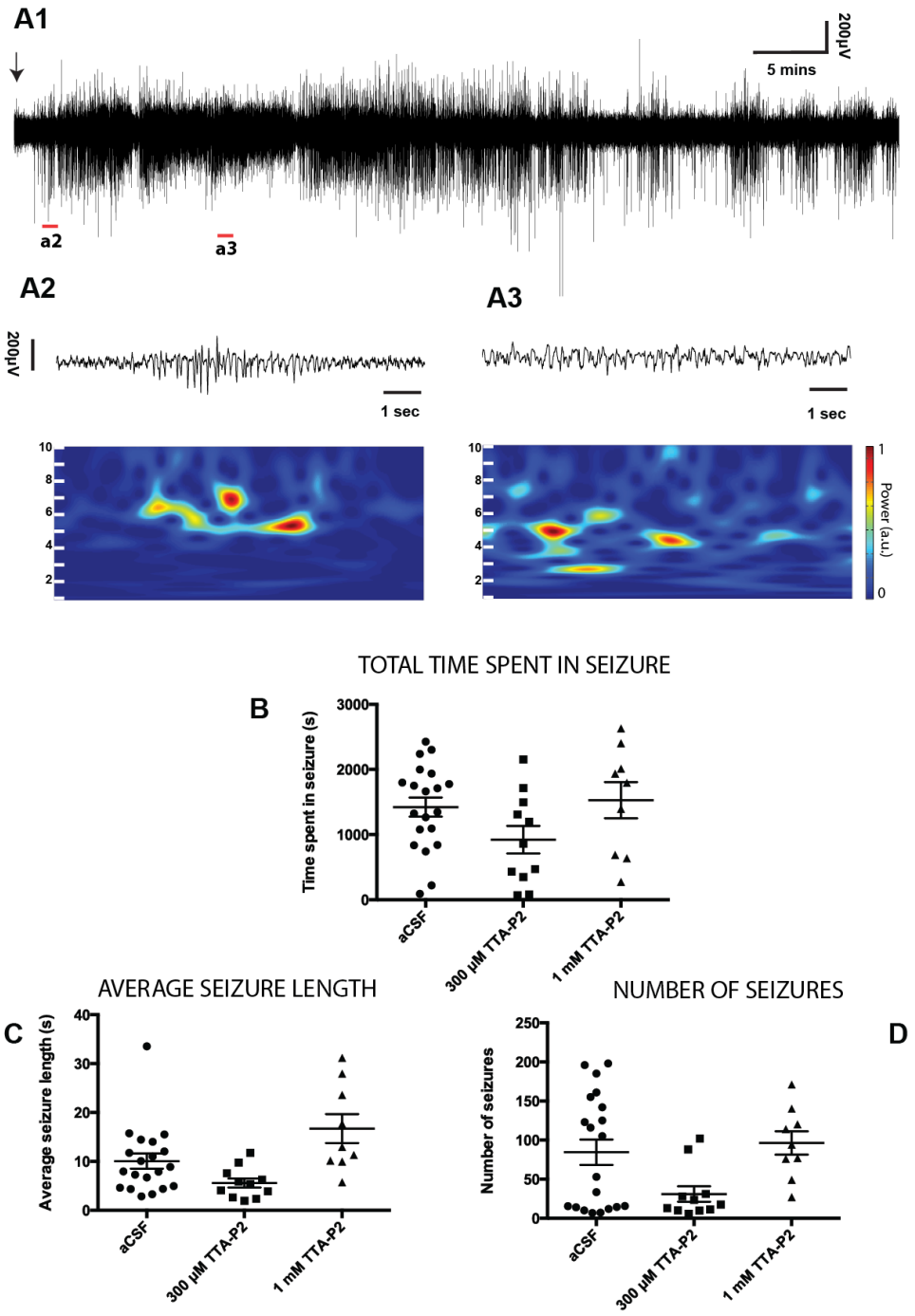

Figure 4.6. Administration of TTA-P2 in the VB alone or in VB and NRT, has no effect on GHB-elicited ASs. In control conditions (representative EEG recording, A) GBL administration in conjunction with microdialysis produced SWDs (A2) and a continuous synchronized state (A3). Microdialysis of either 300µM (targeting VB alone) or 1mM (targeting VB+NRT) has no significant effect on the time spent on seizure (B) and seizure length (C) or number of seizures (D) (paired t-test, ns, P>0.05). See text for details about dose selection. Dotted line separates two independent groups used for the experiment, n=11 (300µM) and n=9 (1mM). Observation window is one hour post injection of GBL. aCSF control groups are plotted together for clarity. Scatter plots with mean and SEM. Arrow represent the start of drug dialysis.

4.4 Discussion

4.4.1 Summary of results:

Two main results have been presented in this chapter:

- systemic administration of TTA-P2 blocks GHB-elicited ASs, whereas local application of TTA-P2 in the VB alone or in VB and NRT does not affect GHB-elicited ASs;

- the GHB-model is characterized by both SWDs and a CSS, each with different EEG and behavioural correlates.

4.4.2 Role of T-type channels in the GHB-model

The fact that systemic administration of a selective T-type channels antagonist abolishes GHB-elicited ASs is in agreement with findings in polygenic rat models of ASs both from our lab and others (Shipe et al., 2008; Orban et al., 2010; Tringham et al., 2012). The dose of 10mg/Kg TTA-P2 was selected because it is the threshold concentration of TTA-P2 that fully blocks T-type channels and T-type dependent high frequency bursting of TC neurons *in vivo* (David et al., 2013) (see also **Figure 2.3**). Nonetheless, detection of ASs after systemic pre-treatment with 10 mg/Kg TTA-P2 was made difficult by the fact that both TTA-P2 and GBL decrease locomotion (Carter et al., 2009; Orban et al., 2010). The detection of ASs was therefore based solely on the presence of SWDs in the EEG, ignoring the behavioural component of an experimental ASs. Moreover, systemic administration of TTA-P2 also produces a general shift of the EEG to slow-frequencies (David et al., 2013). It is well established that the occurrence of spontaneous ASs, both in humans and experimental models, is dependent on the arousal state and ASs most commonly arise from quiet wakefulness but are rare during sleep (Leresche et al., 2011). Consequently, the abolishment of GHB-elicited ASs could be explained by a global change in arousal state induced by TTA-P2 rather than a direct effect of antagonism of T-type channels on the generation of ASs. This situation is different from the case of pre-treatment with ETX, where instead rats treated with GBL maintained a normal awake EEG and locomotion pattern, i.e. ETX had a proper anti-absence effect on GHB-elicited ASs, as verified experimentally by others (Snead, 1988, 1992a).

Notwithstanding these caveats, it is worth comparing this result with those available for GHB-elicited ASs in global genetic knockouts of T-type channels.
Cav3.1 knockout mice were found to be completely resistant to GHB-elicited ASs (Kim et al., 2001). In contrast, the same group reported recently that global Cav3.3 knockout (but also Cav3.2/Cav3.3 double knockout) mice displayed an increase cumulative duration in the time spent in seizure (Lee et al., 2014b). This conflicting results could be explained by the different localization of T-type Ca^{2+} subtypes within the TC network: while all three subtypes are co-expressed in the cortex, TC neurons only express Cav 3.1 and NRT neurons express a combination of Cav3.2 and Cav3.3. Therefore, in order to understand the contribution of T-type Ca^{2+} to the expression of ASs is necessary to consider the effect of blocking these channels in different territories of the TC network in isolation.

4.4.2.1 **Role of TC and NRT T-type channels in the expression of GHB-elicited ASs**

The reverse microdialysis employed allowed to selectively block T-type calcium channels in the VB alone (300 μM TTA-P2) or in both NRT and VB (1mM TTA-P2). This targeting strategy was selected because of the shell-like shape of the NRT, which wraps around TC nuclei, thus imposing constrains on the nuclei that can be targeted in isolation. In particular, it is impossible to target the NRT in without affecting the VB or to target the full extent of the NRT with a single dialysis probe in each thalamus. Thus, the results in the dialysis experiments presented in this chapter should be interpreted with caution: it cannot be ruled out that by targeting a higher proportion of the NRT, the expression of ASs would have been affected. The insertion of two dialysis probes in each thalamus has not been performed because 1) it would have produce a higher damage in thalamic territories 2) the addition another probe to target the more medial part of the NRT would have resulted in targeting median nuclei thalamic (e.g. intralaminar and mediodorsal) as well, further complicating the interpretation of the results.

According to one theory on the generation of SWDs, TC neurons are thought to produce T-type channel dependent burst at each SWC (McCormick and Contreras, 2001). This hypothesis is mostly supported by *in vitro* evidence in thalamic slices (Bal et al., 1995a, 1995b), and contrasts strikingly with the *in vivo* evidence available in GAERS rats. Indeed, both *in vivo* recordings under neurolept anaesthesia (Pinault et al., 1998) and preliminary

recordings in freely moving GAERS (McCafferty et al., 2012) show that TC neurons are mostly silent or fire single spikes during each SW complex.

Therefore the current results of reverse microdialysis of TTA-P2 in the VB strongly support the hypothesis that T-type Ca^{2+} channels dependent burst are not required for the expression of GHB-elicited ASs. Notably, T-type channels are not only responsible for LTCPs but they also contribute to determine the resting potential of TC cells and, to some extent, their tonic firing output via the T-window current (Dreyfus et al., 2010; Deleuze et al., 2012). *In vitro* evidence has demonstrated that indeed only a small fraction of T-type Ca^{2+} channels is required to generate LTCP, suggesting that at the concentration of TTA-P2 that fully block T-channels dependent bursting, the T-window current would also be blocked (Dreyfus et al., 2010). Hence, this result suggest that presence of T-type Ca^{2+} channels in the TC neurons is not important for the generation GHB-elicited As. A similar conclusion has been reached in preliminary results in freely moving GAERS, whereby, using the same dialysis setup and coordinates, dialysis of 300 μM TTA-P2 in VB had no effect on the expression of ASs (McCafferty et al., 2012). No data is available for the local knockdown of Cav3.1 channels in the TC in the GHB-model, as is instead the case for the NRT (see below).

In the case of the dialysis in both NRT and VB, obtained by dialyzing 1mM TTA-P2 from the center of the VB, no effect was observed on the expression GHB-elicited SWDs. These results are in stark contrast with preliminary results from the lab, whereby, using the same dialysis setup and coordinates, dialysis of 1 mM TTA-P2 in VB drastically reduced GAERS spontaneous SWDs. This results is surprising considering that all current hypothesis on the mechanism of SWDs all assume that NRT neurons are bursting at each SW cycle (McCormick and Contreras, 2001; Crunelli and Leresche, 2002), an idea that is further supported by recordings in GAERS under neurolept anaesthesia (Slaght et al., 2002). Nonetheless, recent evince has shown that this may not be the case for GHB-elicited ASs. Indeed, local knockdown in the NRT of Cav3.3 channels (the main T-type channel expressed in this area) blocked LTCPs *in vitro* and produced a small but significant increase in the time spent in seizures in the GHB-model *in vivo* (Lee et al., 2014b). This points to a different role of the NRT activity in genetic and pharmacological ASs, as indeed it was suggested by early electrolytic lesion studies where lesions of the NRT in the GHB-model only attenuated ASs (Banerjee and Snead, 1994), while abolished ASs in GAERS (Vergnes and Marescaux, 1992). The lack of effects observed with 1mM TTA-P2 dialysis could be explained in two different ways. Firstly, given that effect observed by Lee et al.

(2014) for the local knockdown is small (in comparison to that for the global Cav3.3 knockout) it could be that because of high variability in the control aCSF dialysis there was not enough power to detect a small effect size. Secondly, because of intrinsic limitations in our targeting approach, the NRT could only be affected concomitantly with the VB. Therefore, it could be that blocking T-type channels in both nuclei has a different effect than targeting each nucleus in isolation.

In summary, T-type Ca^{2+} channel present in the NRT and the VB do no seem to play an important role in the expression of GHB-elicited ASs. Hitherto, there has been no *in vivo* recordings that has shown the output of TC and NRT neurons during GHB-elicited ASs, therefore is no conclusive evidence that indeed firing dynamic of these neurons during ASs involves T-type Ca^{2+} channels mediated bursts or any other T-type channels mediated activity. In order to explore this possibility, thalamic extracellular silicon probe recordings in freely moving rats were performed during GHB-elicited ASs (results will be presented Chapter 5).

4.4.3 A critical evaluation of the GHB-model

Having observed that GBL elicits different EEG states and concomitant behaviours, I sought to further understand the mechanism of GHB-elicited CSS and its relation to SWDs. To do so, I started by comparing at length the available data on GHB administration in the rat and in other species. What emerged from this analysis (which will be detailed in the following sections), is that, together with ASs, in all species GHB induces also a CSS which bears more resemblance to hypnosis than to ASs. This hypnotic state should therefore be considered a separate entity from the isolate SWDs with behavioural arrest (i.e. experimental ASs).

4.4.3.1 **GHB as an hypnotic agent**

It is seldom mentioned in literature of GHB and ASs that, originally, GHB was synthetized in an attempt to create a novel anaesthetic agent that would act as a GABA analogue still maintaining the ability to cross the blood-brain barrier (Laborit et al., 1960). In humans, GHB was never used as an anaesthetic agent in isolation; it was initially used as sedative/hypnotic agent, or as an adjuvant to other anaesthetics (Laborit et al., 1961; Laborit, 1964). Indeed, there still are some clinical applications where, to date, GHB is considered the hypnotic of choice (Kleinschmidt and Mertzlufft, 1995; Rousseau et al., 2012). In the next section I will critically review the evidence of hypnotic and seizure-like

activities evoked by acute administration of GHB in various animal species. Parts of this analysis were taken, with modification, from a review accepted for publication at the time of the writing of this thesis (Venzi et al., 2015).

4.4.3.2 EEG and behaviour following acute GHB administration: hypnotic and seizure-like activities

4.4.3.2.1 Species-specific effects of GHB administration

The effects of acute administration of GHB has been described in various species over the course of more than 50 years. Given that the terminology used to describe the EEG and behavioural effects of GHB varies markedly across studies I will try to be faithful to the original terminology used in each of the original reports (**Table 4.1**). In view of the peculiar pharmacological profile of human ASs (Snead, 1992a), special attention will be given to the sensitivity of the various GHB-elicited activities to anti-epileptic drugs (**Table 4.2**).

Humans

Early reports described the effect of GHB, administered intravenously (i.v.) in doses of 3g to 10g (~40-140mg/kg), on the EEG and behaviour of healthy volunteers (Laborit et al., 1960; Schneider et al., 1963). These early experiments are of particular interest because they show effects of GHB at higher doses than those currently used therapeutically.

Sedation appeared within 5-10 minutes from the beginning of the administration of the drug (Schneider et al., 1963; Lapierre et al., 1990; Van Cauter et al., 1997). This was accompanied by the disappearance of the alpha rhythm in the EEG along with an increase in theta activity, without any apparent change in behaviour (Schneider et al., 1963). This stage was followed by the occurrence of high-amplitude delta waves in the EEG (**Figure 4.7B3**) whilst the subject appeared to be drowsy. At a dose of 3g i.v. the subjects descended into a state of reversible sleep, but still responded to sensory stimulation which produced a temporary disappearance of the delta waves and EEG desynchronization for the duration of the stimulus. Furthermore the subjects had difficulty in performing mental calculations, pointing to a disruption of cognitive function (Schneider et al., 1963). Another study using GBL (20-30 mg/kg i.v.) also produced 2-5 Hz slow-waves, which appeared

initially as intermittent bursts (**Figure 4.7B2**)and then became continuous within 15 minutes of the injection (Yamada et al., 1967). Interestingly, the author of this study claims that consciousness was spared in these subjects, i.e. although the subjects felt mildly intoxicated, they were aware of their surroundings and could perform tasks such as counting light flashes. During this behavioural output the slow-waves were replaced by a desynchronized EEG (Yamada et al., 1967). At doses of 4-5g, the sensory threshold to awaken a subject who was in the delta wave stage was higher, and only painful stimulations could produce a desynchronized EEG and a behavioural response (e.g. movement). With doses of 7-8g of GHB, the appearance of delta waves was followed by another characteristic stage: the EEG displayed cortical silence, interrupted by K-complexes (**Figure 4.7B4**)whilst behaviourally, the subject was unresponsive to external stimuli, including nociceptive ones, i.e. the subject was anaesthetized (Schneider et al., 1963). This EEG manifestation, called "burst suppression pattern", is also characteristic of the anaesthetic state induced by thiopental, propofol and isoflurane (Akrawi et al., 1996; Huotari, 2004; Amzica, 2009). In summary, in healthy volunteers there is no evidence that GHB induce SWDs or ASs, and, importantly, no anti-absence drug has been tested against the GHB-elicited slow/delta waves, burst suppression pattern and respective behaviours that are elicited by GHB.

However, GHB has been shown to have a pro-epileptic effect in patients with a history of (non-identified) generalized seizures (Schneider et al., 1963). Indeed, in these patients SWDs were observed in the EEG within 2 minutes of an i.v. bolus injection of 3g of GHB. These SWDs, however, were short lived: within few minutes the spikes started to slowly disappear and the frequency of the EEG large amplitude waves became progressively slower eventually giving rise to full blown delta waves similar to those observed after administration of an equivalent dose of GHB to healthy subjects. Unfortunately, no description of the behavioural correlates (e.g. impairment of consciousness) that accompanied the EEG expression of SWDs was provided and no anti-absence drug was tested against the GHB-elicited SWDs (Schneider et al., 1963).

Table 4.1 EEG activities evoked by GHB in different species

Species	Drug and dose	Route	Stage2a		Stage2b		References
			Frequency	Description	Frequency	Description	
Human							
Human	GHB 3-6g	i.v.	?	?	2-3Hz	Monomorphic delta waves	(Schneider et al., 1963)
Human	GBL 25-30mg/Kg	i.v.	2-5 Hz	Slow waves	2-2.5 Hz	Slow waves	(Yamada et al., 1967)
Non-human primate							
Rhesus Monkey	GHB 200-400mg/kg	i.v.	?	?	2.5 -3 Hz	High-voltage slow waves often associated with spikes (note spikes are not visible in the figures)	(Snead, 1978a)
Marmoset Monkeys	GBL 200mg/Kg	s.c.	?	?	3Hz	SWDs with spikes that are not discernible	(Tenney et al., 2004)
Cat							
Cat	200-400mg/Kg	i.p.	2-3Hz	Intermittent hypersynchronous bursts	2.5 Hz	Continuous hypersynchronous waves composed of one of three complexes, i.e., slow waves, a slow wave followed by a spike or a slow wave followed by a short polyphasic burst discharge.	(Winters and Spooner, 1964)
Rat							
Sprague-Dawley	500mg/Kg GHL/700mg/Kg GHB	i.p.	?	Intermittent hypersynchronous waves	2-3Hz	Continuous hypersynchrony	(Winters and Spooner, 1965)
Sprague-Dawley	400mg/Kg GBL	i.p.	?	Brief bursts of spikes	?	Continuous spiking and/or spike and slow wave	(Snead, 1984)
Sprague-Dawley	100mg/Kg GBL	i.p.	4-6 Hz	SWDs	?	Continuous SWDs	(Snead, 1988)
Sprague-Dawley	100mg/Kg GBL	i.p.	5-6 Hz	Bursts of spikes	?	Continuous spiking	(Banerjee and Snead, 1995a)

Sprague-Dawley	150mg/Kg GBL	i.p.	7-9 Hz	SWDs	?	?	(Tenney et al., 2003)
Sprague-Dawley	100mgkg GHB	i.p.	6-9 Hz	SWDs	?	?	(Banerjee et al., 1993)
Sprague-Dawley	200mg/Kg GBL	i.p.	6-7 Hz	SWDs	?	?	(Snead et al., 1980)
Wistar	200mg/Kg GHB	i.p.	5-6Hz	Bursts of hypersynchronous waves	4-5Hz	Continuous hypersynchrony	(Godschalk et al., 1976, 1977)
Wistar	100mg/Kg GBL	i.p.	4-5 Hz	SWDs	?	?	(Danober et al., 1994)
Wistar	200mg/Kg GBL	i.p.	4-5 Hz	SWDs	?	Continuous SWDs	(Danober et al., 1994)
Mouse							
Ddy	100mg/Kg GHB or GBL	i.p.	3-6 Hz	SWDs	3-6 Hz	SWDs	(Ishige et al., 1996)
C57BL/6J	70mg/Kg GBL	i.p.	3-5 Hz	SWDs	3-5 Hz	SWDs	(Kim et al., 2001)
BALB/cJ	100-150mg/Kg GBL	i.p.	?	Burst of hypersynchronous slow waves	?	Hypersynchronous slow waves and/or spiky EEG	(Black et al., 2014)
C57BL/6	100-150 mg/Kg GBL	i.p.	?	Hypersynchronous slow waves and/or SWD	?	Hypersynchronous slow waves and/or SWD	(Vienne et al., 2010)

The description of stage 2a and 2b reports the wording used in the original papers. For further details of the classification of stage 2a and 2b see section 4.4.3.2.2. i.p. intraperitoneal; i.v. intravenous; s.c. subcutaneous; ?: data not available. Adapted from (Venzi et al., 2015).

Table 4.2 Comparison of the pharmacological profile of human ASs and GHB-elicited stage 2 activities (ASs and hypnosis)

	Anti-absence drugs			Drugs ineffective or worsening ASs		Refs.
	Ethosuximide	**Valproate**	**Lamotrigine**	**Carbamazepine**	**Phenytoin**	
Human ASs (CAE)						
	↓	↓	↓	↓/=	↑/=	[1]
GHB-elicited stage 2 activities						
Human	?	?	?	?	?	NA
Monkey	↓	?	?	?	↑/=	[2]
Cat	?	?	?	?	?	NA
Rat	↓	↓	?	↑	↑	[3]
Mouse	↓	=	?	?	?	[4]

Adapted from (Venzi et al., 2015).

For further details of the classification of stage 2 activities into hypnosis and ASs see section 3.2.

↓: decrease of ASs; ↑: exacerbation of ASs; =: no effect on ASs; ?: data not available.

[1] (Snead and Hosey, 1985; Panayiotopoulos, 1999, 2008; Crunelli and Leresche, 2002).

[2] (Snead, 1978a, 1978b; Tenney et al., 2004).

[3] (Godschalk et al., 1976; Snead et al., 1980; Snead, 1988; Kumaresan et al., 2000).

[4] (Ishige et al., 1996; Kim et al., 2001)

Non-human primates

I.v. administration of GHB in non-human primates elicited similar patterns of EEG activity to those seen in healthy humans(**Figure 4.7C**). In rhesus monkeys, a low dose of GHB (100-200mg/kg) induced low-voltage slowing of the EEG, accompanied by drowsiness (Snead, 1978c). At a dose of 400 mg/kg (Snead, 1978b) a continuous activity, characterized by 2-3 Hz high-voltage slow waves, appeared in the EEG. Animals were unresponsive to sensory stimulation and displayed occasional stereotyped movements and myoclonic jerks. At even higher doses (> 500 mg/kg), animals started to display generalized myoclonic jerks accompanied by a burst suppression EEG pattern (**Figure 4.7C3**) (Snead, 1978c). These EEG and behavioural effects were blocked by ethosuximide, given both acutely (100mg/kg i.v.) and chronically (serum concentration: 140µg/ml), and were worsened by chronic treatment with phenytoin (serum concentration: 14 µg/ml) (**Table 4.2**) (Snead, 1978a, 1978b). These results have recently been replicated in marmoset monkeys with i.v. injection of 200mg/kg GBL producing a similar slow-wave EEG pattern (**Figure 4.7C2**) and associated behaviour, both of which were reversed by chronic treatment with ethosuximide (30mg/kg/day) (Tenney et al., 2004).

On the basis of the co-occurrence, and unique pharmacological profiles, of the behavioural output and EEG paroxysm, it was argued that the GHB-elicited activity in monkeys modeled the spontaneous ASs of idiopathic generalized epilepsy. However, as in healthy humans treated with GHB, the presence of spikes superimposed to the slow/delta waves is not discernible in the EEG recordings of GHB-treated monkeys, and in contrast to spontaneous ASs in humans, the slow/delta wave activity could be evoked by auditory stimulation (Snead, 1978c).

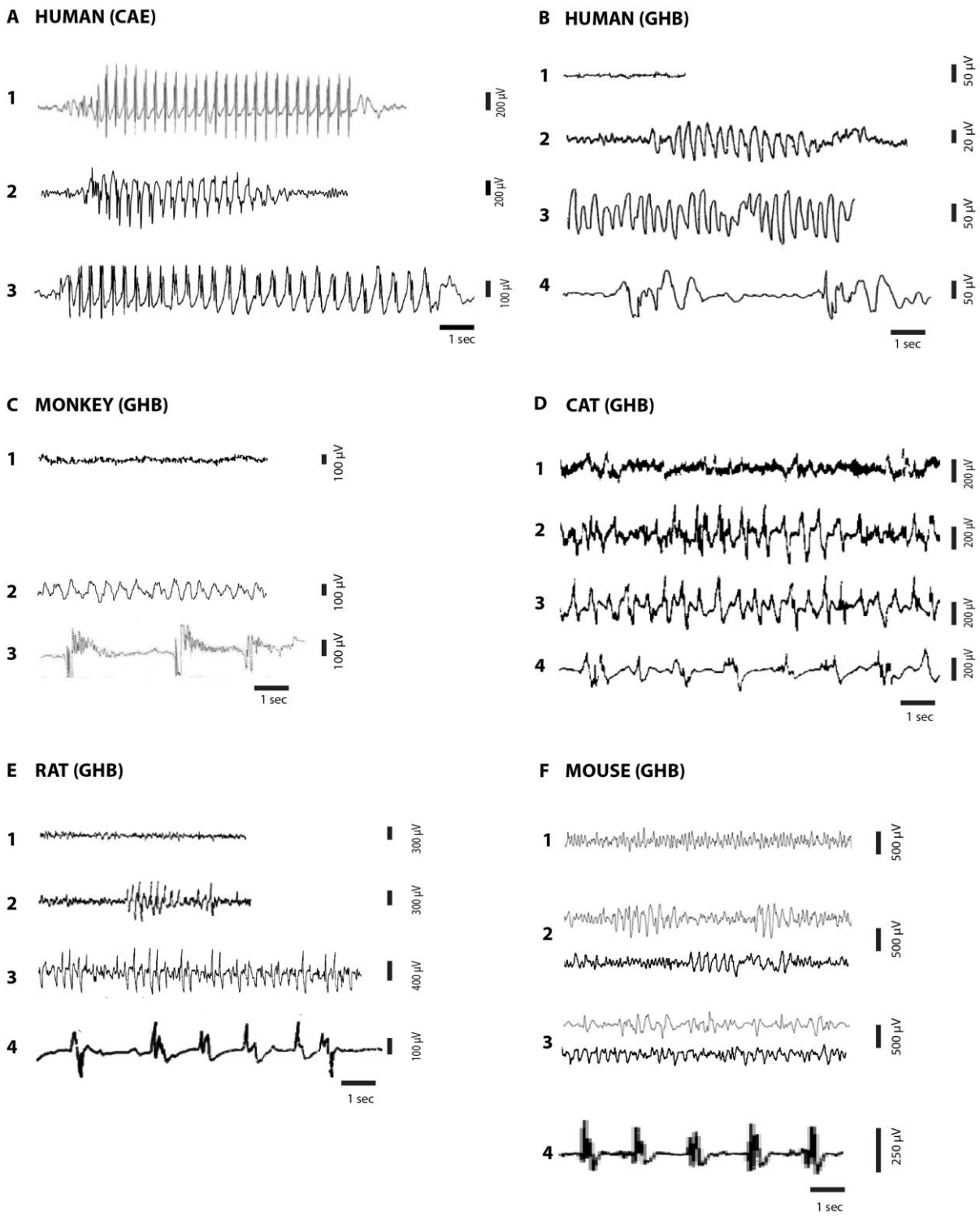

Figure 4.7. EEG recordings of human ASs and EEG activities elicited by GHB in various animal species. A Scalp EEG recordings from three Childhood Absence Epilepsy (CAE) patients showing the characteristic 3-4 Hz SWDs, the EEG hallmark of ASs. Note the sudden onset and termination of the SWDs from a desynchronized EEG background, and the different SWD morphology among patients (i.e. different amplitude of the spike component both within a SWD (2,3) and in different patients (1-3). B Administration of GBL (30mg/kg i.v.) to healthy human volunteers produces 2-3 Hz delta waves (2) that appear suddenly from a desynchronized EEG background (1). After 10-15 minutes the delta waves

become continuous (3). This EEG output can be obtained for a range of GBL and GHB doses (3-6 g GHB i.v.). Doses exceeding 7-8 g i.v. produce, following the EEG manifestations shown in (2) and (3), a burst suppression pattern (4) where bursts of slow EEG waves interrupt cortical silence. This EEG activity is invariably accompanied by a state of deep hypnosis/anaesthesia. (See Figure 2 for a comparison of the effect of GHB in a patient with generalized epilepsy). C In monkeys, the desynchronized EEG (1) evolves into an EEG pattern of 3 Hz slow/delta waves following administration of 200 mg/kg/s.c. of GBL (2). High doses of GHB (500 mg/kg/i.v.) produce, in addition to the EEG manifestations shown in (2), a clear burst suppression pattern (3). D In cats, an i.p. injection of GHB 200 mg/kg induces first an intermittent (2) and then a continuous hypersynchronous EEG (3). The EEG is punctuated with spikes that are found either alone or within 2-3Hz SWCs. GHB 400mg/kg i.p. induces, in addition to the EEG manifestations shown in (2) and (3), a burst suppression pattern (4). E In rats, a dose of 200mg/kg GHB i.p. elicits at first isolated 5-6 Hz SWDs (2) that emerge from a desynchronized EEG background (1). Within 10-15 minutes this EEG activity becomes continuous and its frequency slows down to 4-5 Hz (3). Note that SWCs are not always discernible and slow waves without spikes are sometimes prevalent. A dose of 400mg/kg GBL induces, subsequently to the EEG manifestations shown in (2) and (3), a burst suppression pattern (4). F In mice, a dose of 70mg/kg GBL i.p. induces first the appearance of 4-5Hz SWDs (2, top trace) or 4-5 Hz waves (2, bottom trace) that appear intermittently in the EEG. This EEG activity gradually becomes continuous and its frequency slows down (3), still exhibiting spike and waves (top trace) or waves only (bottom trace). A dose of 150mg/kg GBL elicits, following the EEG manifestations shown in (2) and (3), a burst suppression pattern (4). Adapted from (Venzi et al., 2015).
Reproduced (with and without modification) from (Panayiotopoulos, 2008) A1; (Nevado-Holgado et al., 2012) A2; (Panayiotopoulos, 1999) A3; (Schneider et al., 1963) B1-2-4; (Yamada et al., 1967) B3; (Tenney et al., 2004) C1-2; (Snead, 1978c) C3; (Winters and Spooner, 1964) D; (Godschalk et al., 1977) E1-2-3; (Snead, 1984) E4; (Zaman et al., 2011) F1, F2-3 (top); (Kim et al., 2001) F2-3 (bottom); (Ishige et al., 1996) F4.

Cats

Injection of GHB, either i.v. or i.p., produced EEG and behavioural changes similar to those that have been described in primates (Winters and Spooner, 1964, 1965; Snead et al., 1976), with some important differences: no drowsiness was observed at low doses (e.g. 60mg/kg) and the EEG slowing was accompanied by the presence of spikes in the EEG (Winters and Spooner, 1964). Upon i.p. administration of 200-400mg/kg of GHB, the animal first produced an EEG pattern defined as "2-3 Hz intermittent hypersynchronous bursts" (**Figure 4.7D2**) (Winters and Spooner, 1964), while it was in a crouching position with its eyes open. This gradually progressed into a pattern of "2.5 Hz continuous hypersynchrony, where each complex is composed of either a slow wave, a slow wave followed by a spike or a slow wave followed by a polyphasic burst discharge" (**Figure 4.7D3**) (Winters and Spooner, 1964). During this EEG state, the animal had fixed gaze and made repetitive head movements. Sensory stimulation disrupted the EEG synchrony and awakened the cat. Following a dose of 400-600 mg/kg, the EEG progressed through the previously described continuous and intermittent EEG stages and then showed a burst-suppression pattern (**Figure 4.7D4**) that was accompanied by myoclonic jerks (Winters and Spooner, 1964). No anti-absence drugs were tested against the EEG and behavioural phenotype elicited by GHB in cats.

Rats

The effects of GHB in rats are by far the best described among all species. Systemic administration of GHB (25-100mg/kg) in Wistar rats produced an increase in slow wave sleep (Godschalk et al., 1977; Monti et al., 1979) that persisted for up to 4 hours. Higher doses (200mg/kg) in Wistar rats were reported instead to induce two types of activity, distinguishable both at the EEG and behavioural level (Godschalk et al., 1976, 1977). At first intermittent bursts, i.e. short (5-8 sec) periods of hypersynchronous 5-6 Hz "spikes and waves", appeared on the EEG (**Figure 4.7E2**). Concomitantly with the start and end of these intermittent bursts of "spike and waves" the animals froze with their eyes open. These intermittent bursts gradually increased in length and within 10 minutes evolved into a continuous hypersynchronous state at a lower frequency (4-5Hz) (**Figure 4.7E3**). This state lasted for about 20 minutes during which the animal stopped moving altogether and appeared to be in a sedated state. As shown in **Figure 4.7E3**, the EEG activity in this continuous hypersynchronous state appeared to be less regular than during the intermittent bursts, with slow waves and spikes not always associated into spike-wave

complexes (SWCs). After 20 minutes the intermittent bursts, and their associated behavioural output, gradually reappeared on the background of a desynchronized EEG. The authors of this study posited that the intermittent bursts of "spike and waves", with their clear transitory interruption of directed movement, paralleled spontaneous ASs (Godschalk et al., 1977). No attempt was made to correlate the continuous synchronized state with human pathology. A similar progression between an intermittent synchronized EEG state and a continuous synchronized EEG state had been described in an early study (Marcus et al., 1967) where equimolar doses of 5.8mM GHB or GBL (equivalent to ~700mg/kg GHB and ~500mg/kg GBL) were administered to Sprague-Dawley rats. In addition, these higher doses of GHB and GBL produced a reversible burst suppression pattern (for 50-80 minutes) that was concomitant with a loss of the righting reflex (**Figure 4.7E4**). During the intermittent bursts with behavioural arrest, rats were seen to display facial myoclonus and vibrissal twitching (Snead, 1992a), features that are also present in genetic rat models of ASs (Coenen et al., 1992; Marescaux et al., 1992a). These manifestations are said to represent the correlates of some behavioural automatisms (e.g. lip smacking, eyelid flutters, chewing) that are observed during spontaneous ASs in humans (Panayiotopoulos, 2008). Importantly, the intermittent and continuous hypersynchronous EEG states in the rat (**Figure 4.7E2,E3**) had a pharmacological profile strikingly similar to the one of humans ASs, being blocked by drugs that are effective against spontaneous human ASs (e.g. ethosuximide and valproate) and exacerbated by drugs that are effective on convulsive seizures (e.g. carbamazepine and phenytoin) (Godschalk et al., 1976; Snead et al., 1980; Snead, 1992a; Kumaresan et al., 2000). In addition, ethosuximide was ineffective in blocking the burst suppression pattern (**Figure 4.7E4**), suggesting that this state is distinct from GHB-elicited ASs (Snead, 1984).It is noteworthy that even though the initial study posited that only GHB-elicited SWDs, accompanied by behavioural arrest with sudden onset and termination (**Figure 4.7E2**), could model spontaneous human ASs (Godschalk et al., 1977), in the subsequent literature all of the activities evoked by GHB in the rat (with the exclusion of the burst suppression pattern), were said to reproduce ASs (Snead, 1984, 1988, 1992a, 2002). Nonetheless the EEG and behavioural effects of GHB-elicited ASs seem to vary amongst experiments and even within the same experiment (Banerjee and Snead, 1995b). This is also apparent in the frequencies of GHB-elicited SWDs and continuous hypersynchrony, which have been reported to vary across the range 3-9Hz, and in the different terminology that researchers have used to describe these EEG manifestations (**Table 4.1**). It is currently unclear how much these differences are related to rat strain (with experiments being conducted mainly on Wistar and Sprague-Dawley rats) (**Table 4.1**) or doses of GHB/GBL.

Mice

EEG (Aizawa et al., 1997) and, in contrast to rats, failed to induce slow wave sleep (Meerlo et al., 2004; Vienne et al., 2010). Instead a slightly larger dose (70mg-100mg/kg GBL) induced a state that was generally described as EEG hypersynchrony (Meerlo et al., 2004; Vienne et al., 2010) or SWDs (Ishige et al., 1996; Snead et al., 2000; Kim et al., 2001). The frequencies reported for the GHB-elicited EEG activities are generally lower than in the rat and they vary around 3-6 Hz (**Table 4.1**). In addition, although it is never discussed directly in the literature, it appears that the so-called SWDs in the mouse are often less regular than in the rat, and clearly discernible SWCs (where spikes and waves are phase-locked) are seldom observed (**Figure 4.7F2**). Indeed, the most prevalent EEG activity appears to be a general shift of EEG activity to lower frequencies with occasional spikes (**Figure 4.7F3**). Higher doses of GBL (200-400 mg/kg) induced an EEG burst suppression pattern and, behaviourally, a loss of the righting reflex (**Figure 4.7F4**) (Aizawa et al., 1997), as observed in other species. The pharmacological profile of GHB-induced SWDs in mice has not been characterized as thoroughly as in the rat. Notably, GHB-induced continuous hypersynchrononous events and SWDs were reduced by ethosuximide (200mg/kg), while valproate (100mg/kg) was ineffective (Ishige et al., 1996). Moreover, no data is available on the effects of carbamazepine or phenytoin on GHB-elicited responses in mice.

4.4.3.2.2 Classification of GHB-elicited effects: which stage models human ASs?

From the description provided in the previous sections, it is clear that the effects of GHB on the EEG and behaviour of different species vary dose-dependently on a spectrum from drowsiness/sleep-facilitating effects, to activities that resemble spontaneous human ASs, to hypnosis and anaesthesia. Expanding on the classification originally introduced by Schneider for humans (Schneider et al., 1963) and by Snead for rats (Snead, 1982, 1984), here we propose a structured classification of GHB-elicited activities into three stages, each with characteristic EEG and behavioural correlates across all animal species (**Figure 4.8**). These three stages are reached in succession and with different thresholds of GHB concentration, and the wearing off of the drug follows the same stages but in the reverse order (**Figure 4.8**).

Stage 1: drowsiness/sleep-facilitation

GHB produces drowsiness and a slowing down of the EEG and/or facilitates an increase in slow wave sleep. This stage is generally not observed in cats and mice, but is present in primates and rats (**Figure 4.8**).

Stage 2: absence seizures/ light hypnosis

High amplitude slow waves and/or spikes appear in the EEG. Primates have very prominent 2-3Hz slow/delta waves but no clear spikes in the EEG. Rats display a range of activities from SWCs (at 4-9Hz) to slow/delta waves. Cats, in addition to 2-3 Hz SWDs and slow waves, also present intermittent trains of spikes. Generally, slow-waves/SWDs start to occur intermittently in well isolated short periods (~5 seconds in humans and cats; ~5-8 seconds in rats) from a background of desynchronized EEG, and are invariably concomitant with a behavioural arrest and, in some species, behavioural automatisms (stage 2a) (**Figure 4.8**). Then, in all species, the EEG slow-waves/SWDs become continuous, their frequency tends to slow down (humans 2-5 Hz to 2-2.5 Hz; cats 2-3Hz to 2.5 Hz; rats 5-6Hz to 4-5Hz) and immobility sets in (stage 2b) (**Figure 4.8**). This continuous EEG activity is reversible and can be temporarily interrupted by sensory stimulation, which producing both a behavioural output and a desynchronized EEG. The behaviour (e.g. body posture and muscle tone) observed in stage 2b is suggestive of a light hypnotic state (**Figure 4.8**).

Stage 3: deep hypnosis/anaesthesia

The slowing down of the EEG frequency progresses and, in all species, evolves into an EEG burst-suppression pattern similar to what is observed in propofol or isofluorane anaesthesia, i.e. electrical silence interrupted by bursts of spikes (**Figure 4.8**) (Akrawi et al., 1996; Huotari, 2004). Behaviourally, this state is similar to deep hypnosis/anaesthesia. In rodents, there is a characteristic loss of the righting reflex. Myoclonic jerks are sometimes observed in monkeys and cats.

4.4.3.3 Does GHB induce ASs in all animal species?

In all animal species examined, concentrations of GHB that reach stage 2 and stage 3 induce a behavioural phenotype that is indicative of impairment of consciousness. However, many hypnotic drugs besides GHB, such as barbiturates (Winters and Spooner, 1964), also produce an impairment of consciousness. To model an AS, the impairment of consciousness should be sudden, transient and devoid of convulsion. Moreover, an impairment of consciousness can be inferred by an external observer only if it has a behavioural correlate, such as a transient behavioural arrest; so, only the intermittent EEG paroxysms found in stage 2a fully meet these requirements (**Table 4.3**). In addition, the EEG paroxysm of human ASs has a unique SWD morphology. However, this human EEG morphology can vary quite substantially compared to the 'textbook' representation, since often the spike component of the SWC is reduced in amplitude or appears to be buried inside the wave, in particular during the terminal phase of a SWD (**Figure 4.7A2,A3**) (Sogawa et al., 2009). Nonetheless, an EEG spike component can always be observed, in at least some SWCs.

In the case of primates, several observations challenge the classification of stage 2 GHB-induced activities as being similar to spontaneous human ASs. In both healthy humans and monkeys, the EEG of stage 2 GHB-induced activities is characterized by high amplitude 2-3 Hz slow waves with no spike component. It is unlikely that this is due to technical limitations in the original EEG recordings (Snead, 1978c), as the same results have been recently replicated in marmoset monkeys (Tenney et al., 2004).

Moreover, in an earlier human study (Schneider et al., 1963), GHB was able to trigger proper SWDs but only in patients with a history of generalized seizures. This effect was temporally restricted to the transition between stage 1 and stage 2 of the GHB action. Upon cessation of the SWDs, the usual stage 2 GHB-induced delta waves (devoid of EEG spikes) appeared in the EEG (Schneider et al., 1963). Finally, in humans (Yamada et al., 1967) and in monkeys (Snead, 1978c) the delta waves could also be triggered by auditory or visual stimulations, a feature that is not present in typical human ASs.

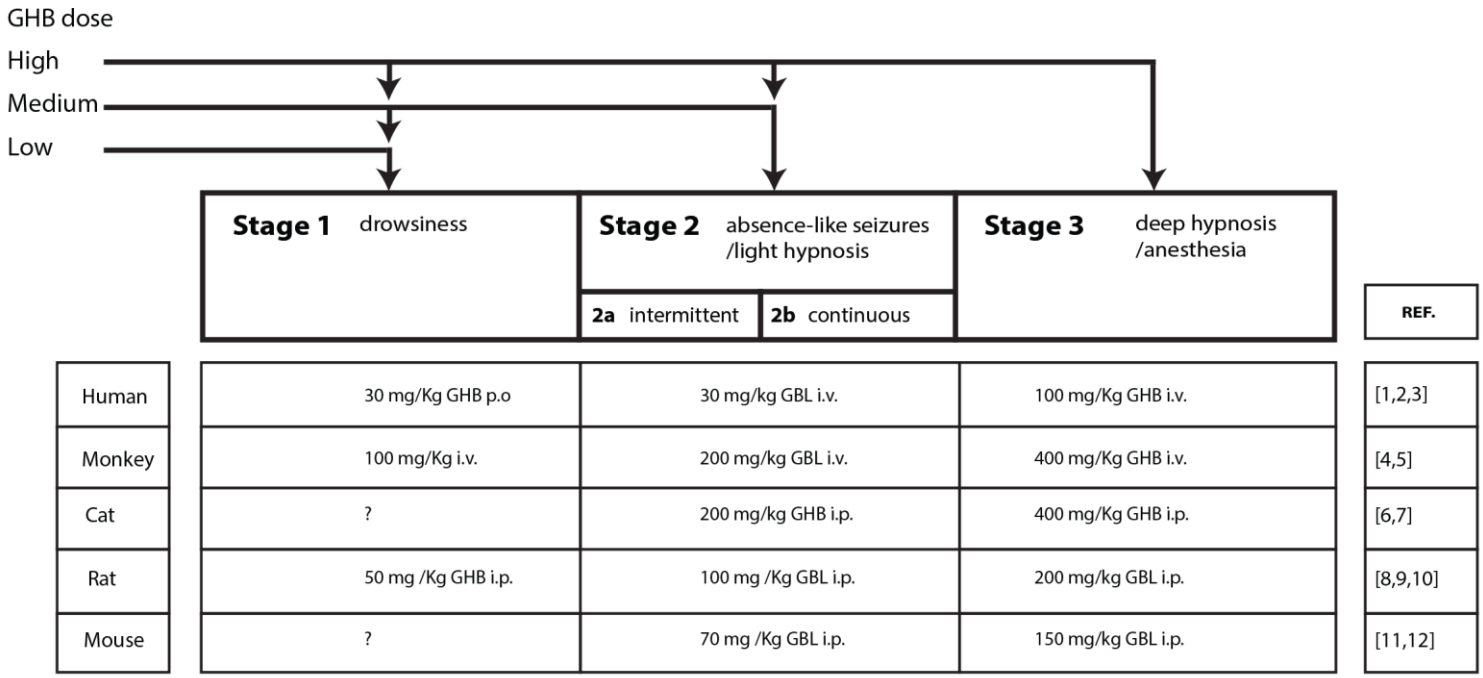

Figure 4.8. Systemic GHB administration induces three stages of activity that are distinguishable at the EEG and behavioural level. GHB (or its prodrug GBL) dose-dependently induces marked changes in the EEG and behaviour in various animal species (humans, monkeys, cats, rats and mice). These GHB-elicited activities can be grouped in 3 stages (top) that are reached in succession with increasing concentrations of GHB. The wearing off of the drug also follows the 3 stages but in an inverse order. The threshold dose to reach each stage is illustrated together with the route of administration. Low doses of GHB (stage 1) induce drowsiness and non-REM sleep. Medium doses of GHB induce a peculiar phenotype that is generally thought to mimic human absence seizures and/or light hypnosis, and can be divided in two substages (a and b). During stage 2a, intermittent EEG paroxysms emerge from a background of desynchronized EEG. During stage 2b (that is reached with the same threshold dose of stage 2a) there is a light hypnotic state, characterized by changes in body posture and decrease in muscle tone, while the EEG paroxysms become continuous. At high doses of GHB, a behavioural state of deep hypnosis/anaesthesia is reached (stage 3) which is accompanied by a burst suppression pattern in the EEG. p.o.: per os; i.v.: intravenous; i.p.: intraperitoneal; ?: data non available. [1] (Mamelak et al., 1977); [2] (Yamada et al., 1967); [3] (Schneider et al., 1963); [4] (Snead, 1978c); [5] (Tenney et al., 2004) ; [6] (Snead et al., 1976) ; [7] (Winters and Spooner, 1964); [8] (Monti et al., 1979); [9] (Godschalk et al., 1977) ; [10] (Snead, 1988); [11] (Kim et al., 2001) ; [12] (Ishige et al., 1996). Adapted from (Venzi et al., 2015).

The practice of defining the slow/delta waves as ASs seems to be driven more from the pharmacological profile of this evoked activity than from similarities to the human condition. It is striking that stage 2 GHB-evoked activities are abolished by ethosuximide and exacerbated by phenytoin. Nonetheless, given that 1) EEG paroxysms are devoid of a spike component, 2) the behavioural correlates are similar to hypnosis and, in humans, are accompanied by a feeling of drunkenness and reduced cognitive function (e.g. difficulty in performing mental arithmetic), and 3) the effects of anti-absence drugs against hypnotic drugs (and their EEG manifestations) have not been tested, it would be prudent to withhold judgment on whether, in primates, this stage actually models human ASs (**Table 4.3**).

In the cat, 3 Hz SW complexes, along with trains of spikes and isolated waves, are produced in stage 2. These activities bear morphological similarity to human SWDs (Snead et al., 1976), but unfortunately the sensitivity of this GHB-elicited activity to anti-absence and anti-convulsant drugs has not been tested.

In the rat, the intermittent spike and wave bursts of stage 2a have similar EEG morphology to human SWDs. Importantly, the motor behaviour of the rats is also indicative of an AS, i.e. freezing for the duration of the EEG paroxysm and the resumption of previous motor behaviour upon its termination. Assessing an impairment of consciousness in rats is even more challenging than it is in humans (Blumenfeld, 2012). Some strategies, such as comparing evoked potential during sleep/SWDs (Westerhuis et al., 1996), or looking at ictal stimulus processing (Drinkenburg and Schuurmans, 2003), have been performed in rat genetic models of ASs, but not in the GHB model. Moreover, the frequency of GHB-elicited SWDs is higher than that in humans. However, this feature is shared by all rat pharmacological and genetic models of ASs. The reason for this phenomenon is unclear but it has been suggested that it represents intrinsic inter-species differences (McQueen and Woodbury, 1975).

Stage 2b (i.e. continuous hypersynchrony) in rats was originally suggested not to model ASs. This conclusion was based on the fact that, behaviourally, the animals appear sedated (i.e. for several minutes rats are not moving), and therefore there is no evidence of interruption of a directed movement. Moreover, their posture (i.e. the animals are sitting quietly with their belly on the cage floor with a decreased muscle tone) is more suggestive of a hypnotic state than of ASs. Finally, the morphology of the EEG activity during stage 2b

is different from that of the intermittent bursts of spike and waves: their frequency is lower and less regular, and the spike component is often missing. It is striking though that both stage 2a and 2b in rats have the same pharmacological profile, i.e. they both respond to anti-absence drugs (**Table 4.2**). As mentioned previously, the effect of anti-absence drugs on the EEG and behaviours elicited by hypnotic drugs has never been tested, but there is some evidence that ETX can reduce the duration of pentobarbital-induced sleep in rats (Bachmann et al., 1988). On the basis of all these issues, therefore, we suggest that the more cautious interpretation at present is that, in rats, only stage 2a models ASs whilst stage 2b is more similar to sedation/hypnosis (**Table 4.3**).

In mice, stages 2a and 2b are less well defined than in rats and no study has clearly described the transition between intermittent bursts of spike and waves and continuous hypersynchrony and their respective behavioural correlates. Isolated spike and waves in mice, with sudden onset and termination, are sometimes difficult to discern (see figure 3A and 5D in ref (Kim et al., 2001; Schofield et al., 2009), respectively). Moreover, the pharmacological characterization of GHB-induced ASs in mice is still only partial and some differences to the rat GHB-model, such as the unresponsiveness of stage 2 GHB-elicited activities to valproate, have not been further investigated.

In conclusion, while the GHB-model in the rat has been characterized extensively, in other species many important aspects of this characterization are still missing. The fact that in all species the activities of stage 2 are defined as ASs is misleading, and this classification should be restricted to stage 2a in rats until further investigation is carried out in other species (**Table 4.3**).

Table 4.3 Comparison of stage 2 GHB-elicited activities and human ASs.

	EEG		**Behaviour**		**Pharmacological Profile**	
	Stage2a	Stage2b	Stage2a	Stage2b	Stage2a	Stage 2b
Human	+	-	?	-	?	?
Monkey	?	-	?	-	?	++
Cat	+++	+	+	-	?	?
Rat	++	+	+	-	+++	+++
Mouse	+	-	?	-	+	+

+: some degree of similarity to human ASs; ++: similar to human ASs; +++: closely matching human ASs; -: different from human ASs. See section 3 for further details. Adapted from (Venzi et al., 2015).

4.4.4 Summary of the re-evaluation of the GHB-model of ASs

In the final section of this chapter I provide a summary of my evaluation of the GHB-model of absence seizures and describe the rationale that guided further characterizing two aspects of this model that will be dealt with in the remaining chapters of this thesis: the activity of isolated thalamic neurons during ASs (Chapter 5) and the development of a seizure-classification algorithm (Chapter 6).

- **Only GHB-elicited stage 2a models ASs in the rat**

Both in rats and in mice, where the GHB-model has been extensively used, researchers tend to identify all activities evoked by a non-anaesthetic dose of GHB as ASs. I argue that this classification is incorrect as it lumps together activities that resemble ASs with others that represent a sedated/hypnotic state. Stage 2a in rats (Table 3), where the animals display SWDs accompanied by behavioural arrest, has been thoroughly characterized, in terms of EEG and behaviour, and has the same face validity as genetic AS models. Stage 2b, where the EEG paroxysm becomes continuous and is accompanied by changes in body posture and muscle tone that more closely resemble hypnosis than ASs, should be considered as a distinct phenomenon. This classification has important consequences for the practical use of the GHB-model. For instance in the experiment presented in section 4.3.1 the average duration of stage 2a (SWDs with behavioural arrest) was 4.4 ± 3.5 minutes (mean ± SD); the average total duration of the CSS, which we can now confidently classify as a hypnotic state, was 14.3 ± 11.4 minutes (mean ± SD). Therefore, the results of many studies are skewed towards the hypnotic effects of GHB rather than GHB-elicited ASs. Finally, the practice of considering stage 2a and stage 2b together seems to be driven mainly by pharmacological considerations. Undoubtedly, the unique pharmacological profile of ASs should contribute towards defining a model of ASs (as it defines the model predictive validity) (Table 2), but cannot be used as a substitute for EEG and behaviour that resembles, i.e. has face validity for, ASs. In this respect, a direct comparison, in the same animals, of the effect of ethosuximide, valproate, carbamazepine and phenytoin on the EEG and behaviour of GHB stage 2a and 2b vs sedation, hypnosis and natural slow wave sleep could be of great significance.

- **The GHB model in the mouse**

The GHB model in the mouse is not as well characterized as in the rat. In particular, i) the EEG of stage 2a appears to vary greatly between studies (Figure 1F2) and an EEG morphology with clear spikes is rarely observed; ii) as mentioned previously for the rat, in a model of ASs, SWDs should be accompanied by behavioural arrest: a prolonged lack of movements accompanied by a decrease of muscle tone and change in body posture (Meerlo et al., 2004; Vienne et al., 2010; Black et al., 2014), as observed in stage 2b in mice, is more reminiscent of an hypnotic state than ASs; iii) the pharmacological characterization of the GHB model in mice is incomplete (4.4.3.2.1). It is only by resolving these issues that we will be able to accept, with confidence, the GHB model in mice. Therefore much of the evidence on the role of T-type Ca^{2+} in the GHB-model, obtained in mice (see section 4.1), should be treated with caution.

- **Role of thalamus and cortex in the expression of GHB-elicited ASs and hypnosis**

Many studies suggest that the thalamus is a key area in the generation of GHB-elicited ASs. Various pre- and post-synaptic mechanisms have been described in TC neurons (section 1.4.2.1.5). In particular, GHB increases the tonic $GABA_A$ current, a key factor in the generation of ASs (Cope et al., 2009). Nonetheless, the activity of isolated thalamic neurons *in vivo* during GHB-elicited ASs (and hypnosis) is still unknown. Given that, except for this thesis, the only evidence available for the firing dynamics of thalamic neurons is in the mouse (Lee et al., 2014b), it is of pivotal importance to directly record from TC and NRT neurons *in vivo* during GHB-elicited ASs. Recording of thalamic neurons during these states, which also allow a direct comparison of neuronal activity during ASs and hypnosis, will be presented in Chapter 5.

- **EEG seizure properties in the GHB-model**

While it has been suggested that ASs in the GHB-model can be quantified in the same way as in polygenic rat models (Depaulis et al., 1989; Snead, 1992a), it appears from the literature that the information available for various seizure parameters, e.g. seizure length, morphology of SWDs, dominant frequency, etc) (**Table 4.1**) is scarce or contradictory. This may be, in part, due to a lack of consensus regarding which of the activities evoked by exogenous GHB administration represents an AS (Godschalk et al., 1977; Snead, 1984, 1988).

Moreover, current seizure detection methods for the GHB model have not been shown to be able to discriminate between sleep, hypnosis and ASs (Kim et al., 2001; Schofield et al., 2009). For this reason, in Chapter 6 I will describe the development of a novel seizure-classification algorithm capable of discriminating between hypnosis, sleep and ASs.

Chapter 5 Activity of thalamic neurons during GHB-elicited absence seizures and hypnosis

5.1 Introduction

Systemic administration of GBL elicits two types of activity: ASs and a hypnotic state (see section 4.4.4). Investigating the thalamic correlates of these drug-induced states could shed some light on their difference and would allow a direct comparison with the thalamic activity in GAERS during ASs. Moreover, characterizing the activity of thalamic neurons during GHB-elicited ASs is important *per se* in order to compare pharmacological to genetic ASs. Indeed, preliminary experiments from the lab in freely moving GAERS (McCafferty et al., 2012) have confirmed and expanded previous results obtained under neurolept anaesthesia (Pinault et al., 1998; Slaght et al., 2002). TC neurons were found to be silent or express single spikes for each SWC, while in NRT neurons burst firing was prevalent. These results are in stark contrast with those obtained *in vitro* which instead suggest burst firing in both TC and NRT neurons at each SWC (Bal et al., 1995a; McCormick and Contreras, 2001; Huguenard and McCormick, 2007).

There is no report of the activity of thalamic neurons after GHB administration *in vivo* but *in vitro* work suggests that GHB can facilitate intra-thalamic oscillations (which can be self-sustaining), although the cellular pacemaker(s) of this activity are unclear (Gervasi et al., 2003). Nonetheless, the relevance of oscillations described *in vitro* to *in vivo* ASs is debatable (Leresche et al., 2011).

Finally, notwithstanding the fact that GHB is recognized to have sedative/hypnotic properties (Winters and Kott, 1979; Entholzner et al., 1995; Carai et al., 2001), the effect GHB or other hypnotic drugs have on the firing dynamics of thalamic neurons are to the best of my knowledge unknown.

5.2 Methods

The methods employed in this chapter are described in Chapter 2.

5.3 Results

5.3.1 Data collection

In the attempt to record isolated units from the VB and NRT of freely moving Wistar rats, 4 rats were implanted with a silicon probe mounted on a microdrive. Out of the 4 animals, 1 was discarded because it presented brief spontaneous SWDs during the recovery period, which were still apparent up 10 days from the surgery. Furthermore, 2 animals were discarded because the GBL injection did not evoke any SWDs and/or the SNR in the EEG and units recording was too low to conclusively isolate units and define EEG behavioural states. Thus, the data presented in this chapter comes from one Wistar rat injected with 100mg/Kg GBL in 6 independent sessions. A minimum of 24 hours was waited in between two consecutive sessions. 34 isolated neurons were obtained in total, 24 of them were classified as NRT based on their burst signature during sleep (see section 2.4.5.3). 10 neurons were not classifiable as their bursts did not fit the NRT or TC signature and, in some cases, presented few bursts during sleep. For the NRT neurons 713 isolated SWDs with behavioural arrest, 141 hypnosis epochs, 115 light-sleep epochs, 369 active wakefulness epochs constituted the dataset analyzed in this chapter. Given the relatively small number of NRT neurons recorded and the variability in seizure properties in the GHB-model (see Chapter 6) the data was analyzed both as the distribution of events and the mean for each neuron when possible.

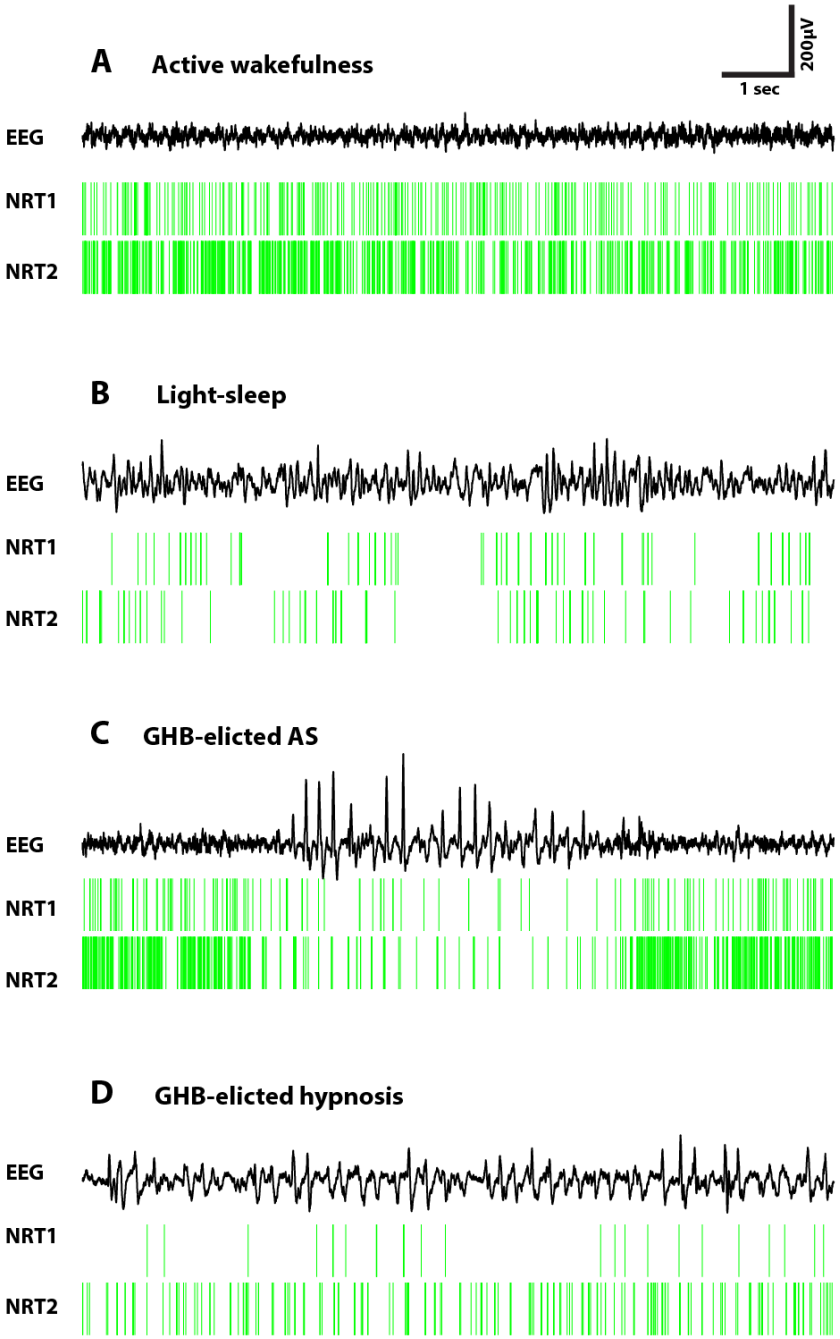

Figure 5.1. Activity of NRT neurons during different behavioural states. Simultaneous activity of two NRT neurons (raster plots, green) during active wakefulness (A), light-sleep (B), a GHB-elicited AS (C) and GHB-elicited hypnosis (D) an corresponding fronto-parietal EEG recording (black). It evident that both NRT neurons decrease their firing rate during light-sleep and the drug-elicited states compared to active-wakefulness.

5.3.2 Firing of NRT neurons during GHB-elicited ASs and hypnosis

5.3.2.1 NRT neurons decrease their firing rate during GHB-elicited ASs and hypnosis

Figure 5.1 illustrates the activity of 2 simultaneously recorded NRT neurons during active wakefulness and light-sleep prior to the injection (**Figure 5.1A-B**) of GBL and during a GHB-elicited ASs and GHB-elicited hypnosis (**Figure 5.1C-D**). As expected, the firing rate of NRT neurons during light-sleep is markedly decreased compared to active wakefulness. It can also be appreciated by visual inspection that during both GHB-elicited activities NRT neurons drastically decrease their firing rate compared to active wakefulness.

The quantitative results (**Figure 5.2**) are presented as distributions of epochs for each behavioural state (as opposed as averages for each neuron) to reflect the variability of seizure parameters in the GHB-model (see Chapter 6) and to have a better chance to capture possible differences in the distribution shape. Results are also summarized in **Table 5.1** and the analyzed statistically via two-sample Kolmogorov-Smirnov test in **Table 5.2**.

The total[3] firing rate during active wakefulness (median: 20.8 Hz; 10^{th} and 90^{th} percentiles: 8.9 and 34.4 Hz, respectively, $p<0.001$) was higher than during light-sleep (median: 6.6 Hz; 10^{th} and 90^{th} percentiles: 2.5 and 26.9 Hz, respectively, $p<0.001$), GHB-elicited ASs (median: 10.5 Hz; 10^{th} and 90^{th} percentiles: 3.9 and 25.6 Hz, respectively, $p<0.001$) and GHB-elicited hypnosis (median: 8.8 Hz; 10^{th} and 90^{th} percentiles: 4.0 and 24.4 Hz, respectively, $p<0.001$). No significant difference was found comparing the tonic firing rate of the drug-induced states amongst each other.

Keeping in mind the results of local block of T-type channels in the NRT (Chapter 4) it is interesting to look at the rates of burst firing (the activity more classically associated with T-type channels) and tonic and doublets firing during GHB-elicited ASs and hypnosis.

The burst rate during GHB-elicited ASs (median: 0.79 Hz; 10^{th} and 90^{th} percentiles: 0 and 3.1Hz, respectively) was marginally higher than during GHB-elicited hypnosis (median:

[3] Total firing is defined as tonic firing, plus bursts, plus doublets.

0.67 Hz; 10th and 90th percentiles: 0.13 and 2.9 Hz, respectively, $p<0.01$) and marginally lower than that of light-sleep (median: 0.87 Hz; 10th and 90th percentiles: 0.12 and 3.3 Hz, respectively, $p<0.001$). Burst firing during sleep and the drug-induced states was significantly higher than during active wakefulness (median: 0.24 Hz; 10th and 90th percentiles: 0 and 1.7 Hz, respectively, $p<0.001$ for all comparisons).

The tonic firing rate during active wakefulness (median: 15.3 Hz; 10th and 90th percentiles: 7.3 and 23.5 Hz, respectively, $p<0.001$) was instead found to be higher than during light-sleep (median: 2.1 Hz; 10th and 90th percentiles: 0.93 and 7.9 Hz, respectively, $p<0.001$), GHB-elicited ASs (median: 4.8 Hz; 10th and 90th percentiles: 2.0 and 9.1 Hz, respectively ,$p<0.001$) and GHB-elicited hypnosis (median: 4.5 Hz; 10th and 90th percentiles: 2.5 and 7.5 Hz, respectively, $p<0.001$).

Finally the doublet firing rate during GHB-elected ASs (median: 0.73 Hz; 10th and 90th percentiles: 0 and 2.3 Hz, respectively) was higher than during hypnosis (median: 0.66 Hz; 10th and 90th percentiles: 0.5 and 1.7 Hz, respectively, $p<0.001$); moreover it was lower than that of wakefulness (median: 1.2 Hz; 10th and 90th percentiles: 0.31 and 3.9 Hz, respectively, $p<0.001$) and higher than that of light-sleep (median: 0.43 Hz; 10th and 90th percentiles: 0.21 and 2.2 Hz, respectively, $p<0.001$).

A summary for the same parameters, averaged for each on the 24 NRT neurons, is presented in **Figure 5.3** and **Table 5.1**. No clear differences are apparent for indicators of central tendency (i.e. median) and spread (e.g. percentiles) of the distributions.

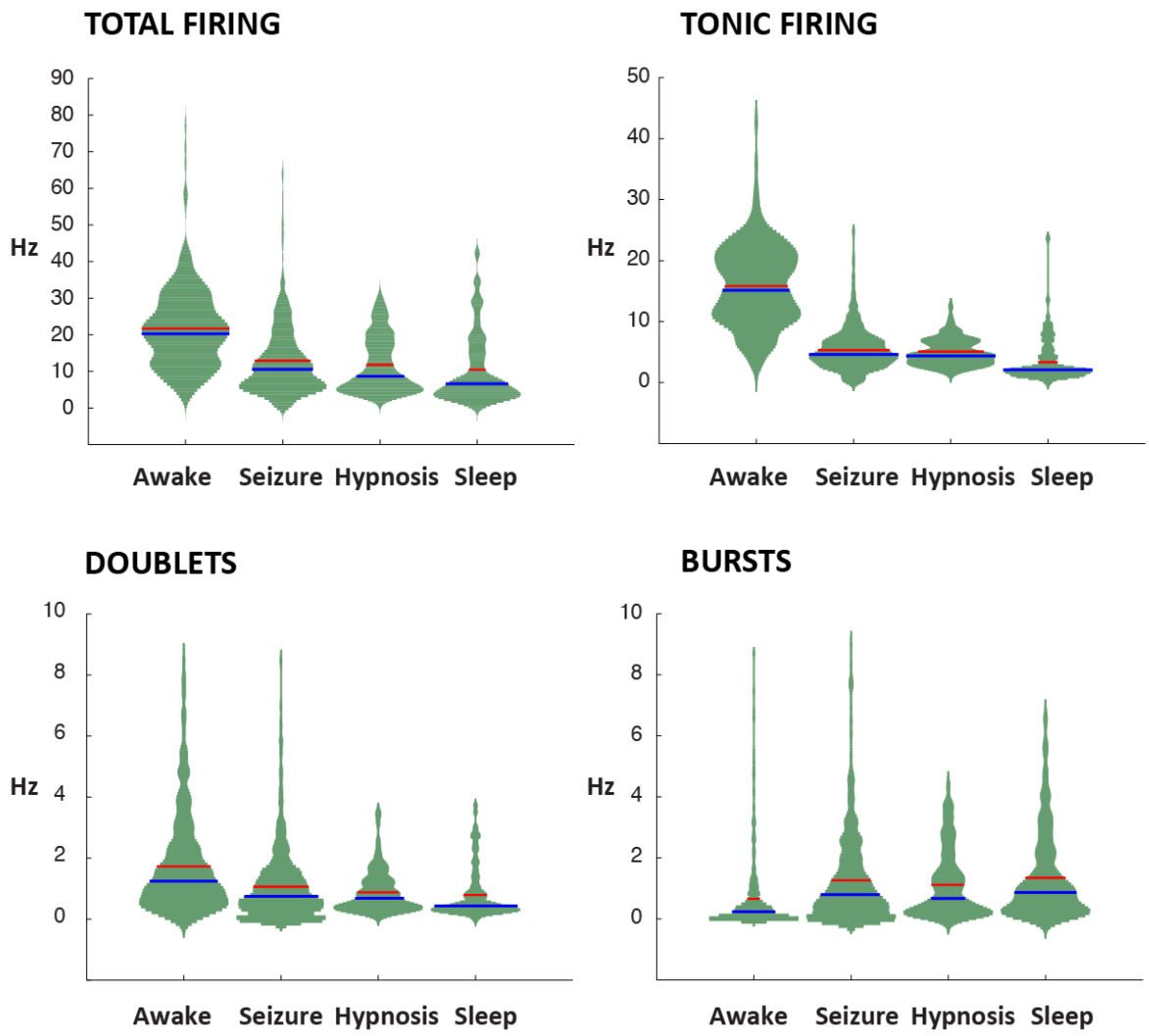

Figure 5.2 Distribution of firing outputs of NRT neurons during different behavioural states epochs. Violin plots (green) are smoothed histograms of the distribution of the different activities (A: total firing, B: tonic firing, C: doublets, D: bursts) of 24 NRT neurons for each event epoch (i.e. active wakefulness, n=369; light-sleep, n=115; GHB-elicited hypnosis; n=141; GHB-elicited ASs, n=713). Blue and red lines represent median and mean of the distributions, respectively.

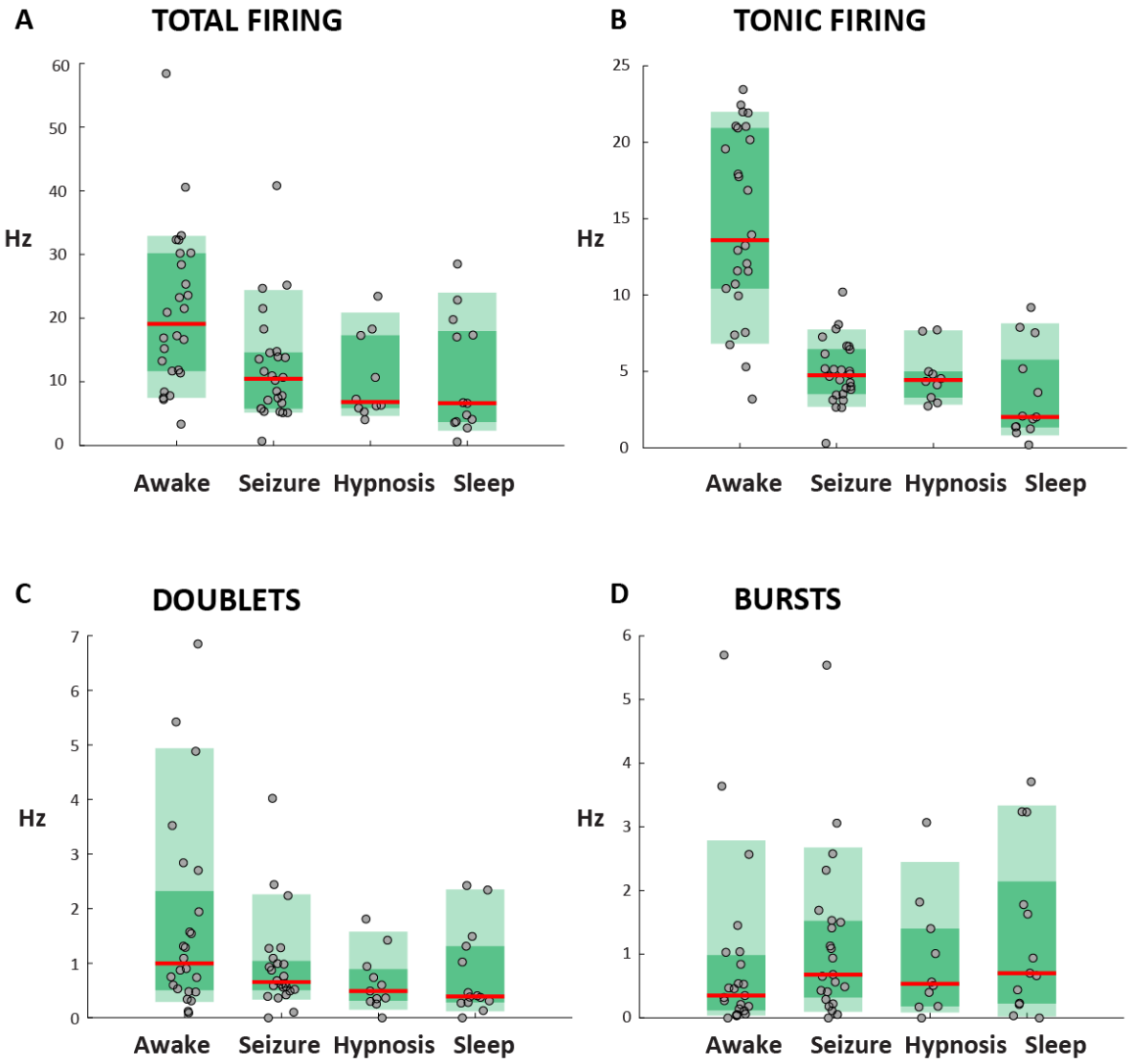

Figure 5.3 Distribution of firing outputs averaged for each NRT neuron. Box plots (green) of average activity of NRT neurons (A: total firing, B: tonic firing, C: doublets, D: bursts) during different behavioural states (i.e. active wakefulness, n=24; light-sleep, n=10; GHB-elicited hypnosis; n=13; GHB-elicited ASs, n=24), visually detected in the EEG. The red lines represent the medians; the dark-green and light-green shaded areas encompass the 25th to 75th percentiles and 10th and 90th percentiles of the distributions, respectively.

Table 5.1 Summary of NRT neuron activity during different behavioural states

Behavioural state	Firing Output	Event distribution				Neuronal Average			
		Median	10th Prct[a]	90th Prct	Mean ± SEM	Median	10th Prct	90th Prct	Mean ± SEM
Active Wakefulness	Total Firing	20.77	8.98	4.42	21.70±0.56	19.09	7.50	32.89	21.1±2.43
	Tonic firing	15.36	7.28	23.50	15.78±0.32	13.59	6.82	21.98	14.68±1.18
	Doublets	1.24	0.31	3.87	1.72±0.081	0.995	0.29	4.93	1.71±0.36
	Bursts	0.24	0.00	1.69	0.65±0.061	0.35	0.04	2.78	0.87±0.28
Light-sleep	Total Firing	6.61	2.47	26.90	10.47±0.90	6.63	2.31	24.00	10.69±2.54
	Tonic firing	2.10	0.93	7.94	3.39±0.30	2.01	0.83	8.15	3.43±0.83
	Doublets	0.43	0.21	2.26	0.79±0.075	0.4	0.24	2.36	0.86±0.22
	Bursts	0.87	0.12	3.36	1.34±0.13	0.82	0.16	3.38	1.4±0.38
GHB-elicited ASs	Total Firing	10.48	3.95	25.65	11.81±0.64	10.47	5.16	24.38	2.12±1.67
	Tonic firing	4.80	2.00	9.17	5.32±0.11	4.755	2.71	7.74	4.9±0.40
	Doublets	0.73	0.00	2.31	1.04±0.041	0.68	0.38	2.28	0.99±0.17
	Bursts	0.79	0.00	3.10	1.25±0.053	0.81	0.16	2.72	1.22±0.27
GHB-elicited hypnosis	Total Firing	8.86	4.00	24.39	12.83±0.36	6.810	4.67	20.87	10.47±2.13
	Tonic firing	4.54	2.53	7.47	4.92±0.17	4.445	2.84	7.68	4.71±0.55
	Doublets	0.66	0.25	1.73	0.87±0.055	0.68	0.38	2.28	0.99±0.17
	Bursts	0.67	0.13	2.88	1.12±0.091	0.56	0.10	2.57	1.01±0.31

[a]Prct: percentile.

Events: SWDs: n=713; hypnosis epochs= n=141; light-sleep epochs: n=115; active wakefulness epochs: n= 369. Neurons: active wakefulness, n=24; light-sleep, n=10; GHB-elicited hypnosis; n=13; GHB-elicited ASs, n=24.All values are in Hz.

Table 5.2 Statistical comparison of NRT neuron activity during different behavioural states

Total Firing				
	Awake	Seizure	Hypnosis	Sleep
Awake		<0.001	<0.001	<0.001
Seizure			ns	<0.001
Hypnosis				<0.01
Tonic Firing				
	Awake	Seizure	Hypnosis	Sleep
Awake		<0.001	<0.001	<0.001
Seizure			ns	<0.001
Hypnosis				<0.001
Doublets				
	Awake	Seizure	Hypnosis	Sleep
Awake		<0.001	<0.001	<0.001
Seizure			<0.01	<0.001
Hypnosis				<0.01
Bursts				
	Awake	Seizure	Hypnosis	Sleep
Awake		<0.001	<0.001	<0.001
Seizure			<0.01	<0.01
Hypnosis				ns

P-values of two-sample Kolmogorov-Smirnov tests. SWDs: n=713; hypnosis epochs= n=141; light-sleep epochs: n=115; active wakefulness epochs: n= 369.

5.3.2.2 NRT-spike-triggered EEG average distinguish different behavioural states while autocorrelograms do not

To further characterize the relationship between the EEG activity and NRT neuron firing rate the NRT spike-triggered EEG average was computed over a window of 1 second for the four behavioural states described above. The EEG averages for active wakefulness and light-sleep did not show any peaks, indicating no clear temporal association of the NRT spikes with the EEG activity (**Figure 5.4A**). In contrast, GHB-elicited ASs displayed 5 peaks on the EEG average, suggesting that NRT single spikes are temporally associated with 5Hz SWDs. Finally, NRT spikes in hypnosis also displayed a temporal association with the EEG, although at the lower frequency of 4Hz hypnotic activity.

To further explore neuronal rhythmicity during the 4 behavioural states, the mean autocorrelograms for NRT neurons were calculated over a window of 600ms. No clear peaks other then that at zero lag were visible at this time window for any behavioural state (**Figure 5.4B1**). At smaller time window (**Figure 5.4B2**) the different widths of the zero lag peaks became discernible. Whilst the autocorrelogram of active wakefulness was flat, the autocorrelograms of light-sleep, GHB-elicited ASs and hypnosis displayed a larger width (~10msec) indicative of enrichment in burst firing.

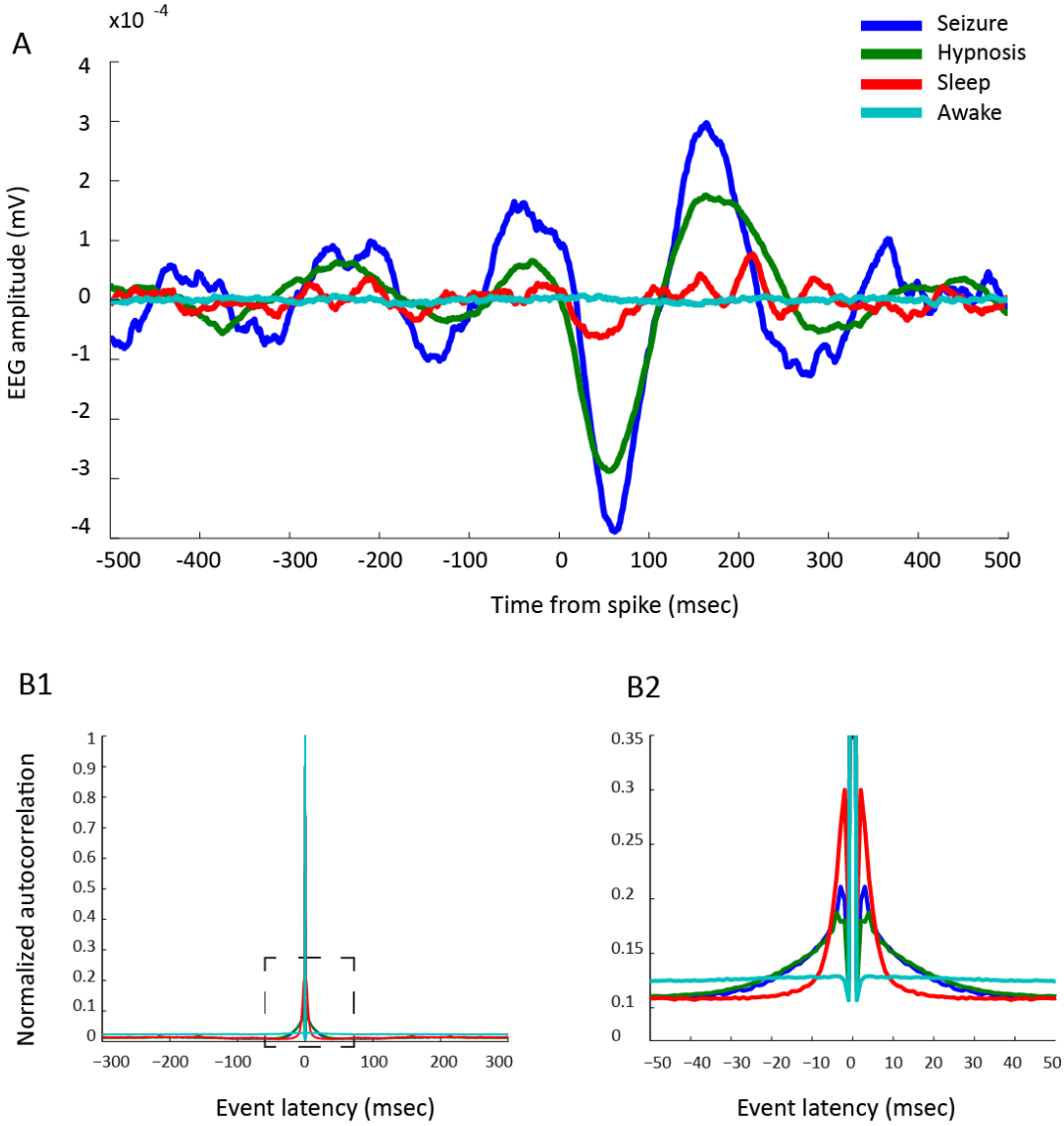

Figure 5.4. NRT spike-triggered EEG averages and average autocorrelograms of NRT neurons during different behavioural states. The NRT-spike-triggered EEG average (A) (computed over a one-second window, centered a zero for the NRT-spike occurrence), reveals a 5Hz rhythmicity for GHB-elicited ASs (blue) and 3-4Hz rhythmicity for GHB-elicited hypnosis (green). No clear peaks are evident for light-sleep (red) and active wakefulness (light-blue). The average autocorrograms (B) for NRT neurons reveal no evident rhythmicity over a 600 msec window reveal no periodicity for any behavioural states (B1). Closer inspection at 50 msec window (B2) shows that for GHB-elicited ASs and hypnosis and light-sleep have a larger width of the zero-lag peak, indicative of an enrichment of burst firing compared to active-wakefulness. NRT neurons: active wakefulness, n=24; light-sleep, n=10; GHB-elicited hypnosis; n=13; GHB-elicited ASs, n=24.

5.3.2.3 **Firing dynamics and temporal synchrony of NRT firing associated with SWCs**

Having characterized the firing output of NRT neurons during different behavioural states, GHB-elicited SWDs were investigated in more detail. The activity (e.g. silence, tonic firing, burst firing, doublets) of NRT neurons (n=21) was estimated for each SWC (**Figure 5.5**A).

The prevalent activity of NRT neurons in a given SWC was silence (median: 42.8%; 10th and 90th percentiles: 7.8% and 61.5%, respectively). Tonic firing was the second most common activity (median: 28.4%; 10th and 90th percentiles: 12.8% and 57.1%, respectively), followed by burst firing (median: 8.2%; 10th and 90th percentiles: 3.5% and 24.2%, respectively). Finally, doublets was the least frequent output of NRT neurons (median: 6.4%; 10th and 90th percentiles: 0% and 11.0%, respectively).

The low firing rate of NRT neurons and low occurrence of bursts during GHB-elicited ASs if further highlighted by expressing the rate of each type of activity per SWC. NRT neurons had a total of 2.4 spikes/SWC (10th and 90th percentiles: 1.3 and 5.2 respectively), 0.77 tonic spikes/SWC (10th and 90th percentiles: 0.5 and 1.4 respectively), 0.083 bursts/SWC (10th and 90th percentiles: 0.0072 and 0.26 respectively) and 0.049 doublets/SWC (10th and 90th percentiles: 0 and 0.087).

The firing output of NRT neurons appears to be weakly associated with the EEG peak (positive–going) of each SWC (n=21) (**Figure 5.6**). Although no sharp peaks were evident, NRT firing had a max +5 ms for total firing (**Figure 5.6A**), +10 ms for tonic firing (**Figure 5.6B**), and +5 ms for burst firing (**Figure 5.6C**).

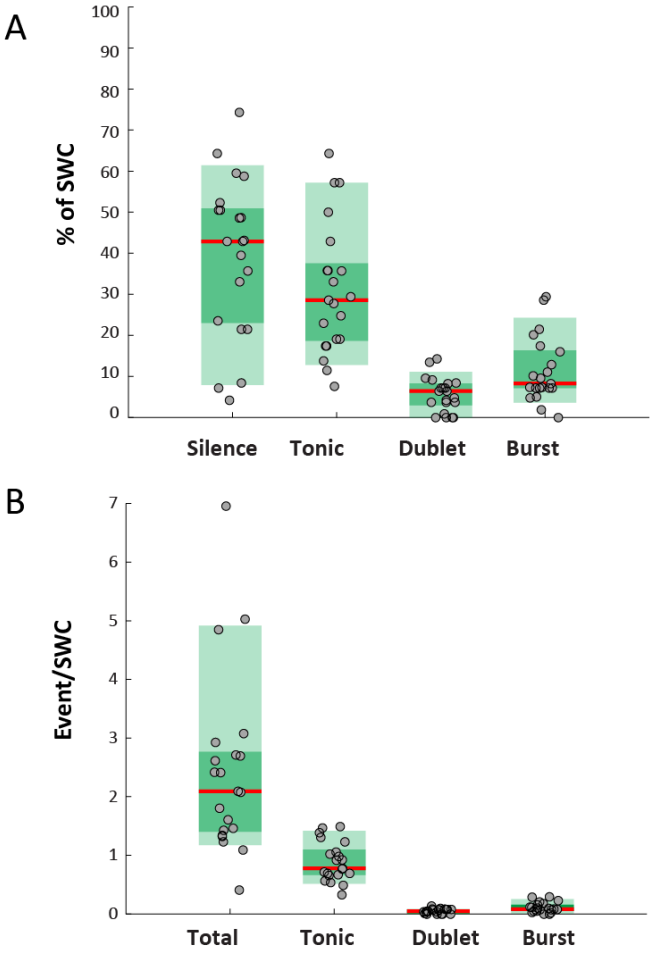

Figure 5.5 Analysis of NRT output per SWC. (A) SWCs are mostly accompanied by silence or tonic firing which make up ~70% of the output of NRT neurons (n=21), while burst and doublet firing are rare. (B) Rates of each of output expressed as number of events/SWC . The red lines represent the medians, the dark-green and light-green shaded areas encompass the 25th to 75th percentiles and 10th and 90th percentiles of the distributions, respectively.

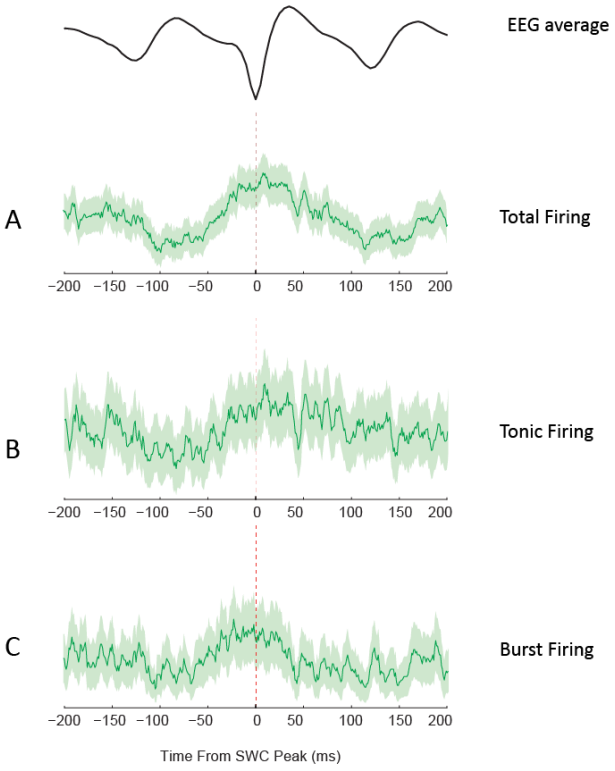

Figure 5.6 Association of NRT firing output with EEG SWC. NRT firing for total firing (A), tonic firing (B) and burst firing (C) appeared to be weakly associated with the EEG peak of each SWC (400 msec window, centered around positive-going EEG peak of a SWC, top) The dark-green line and light-green shaded areas represents the mean and SEM respectively (n=21).

5.4 Discussion

The experiments presented in this chapter contain the first *in vivo* recordings of thalamic neurons during GHB-elicited ASs and hypnosis and thus provide understanding of how GHB brings about these drug-induced states.

5.4.1 Summary of results

The results of this chapter are:

- GHB-elicited ASs and hypnosis are both characterized by a decrease in the firing rate of NRT neurons compared to active-wakefulness;
- The burst rate is increased during the drug induced states, compared to active-wakefulness, to a similar extent as during light-sleep;
- During GHB-elicited ASs, about 70% of SWCs are accompanied by either silence or a single action potential. Bursts firing occurs in less than 10% of SWCs.

5.4.2 Methodological considerations

Due to the technical probldms I encountered in these experiments (section 5.3.1), the data presented in this Chapter comes from one Wistar rat. The result of 6 different sessions with 6 independent GBL injections constituted the database analyzed. It cannot be excluded that repeated injections of GBL induced a bias in the results.

Because of the difficulty in maintaining stable extracellular recordings for a prolonged amount of time, the experimental protocol employed involved injecting GBL after 1) having found NRT neuron(s) whose amplitude had a sufficient SNR and 2) having collected enough sleep to then characterize the burst signature of the neuron as NRT or TC. For this reason, it was possible to record only short periods of light-sleep, preceding the drug injection.

Extracellular recordings during ictal activity are challenging because multiple neurons fire action potentials quasi-simultaneously. The ability to isolate individual neurons based on

PCA depends on the ability to record spike waveforms that are not distorted by noise or by the co-occurrence of multiple units firing (which would result in the summation of multiple voltage deflections). Indeed, during GHB-elicited ASs, multiunit activity, distorted by the presence of multiple overlapping peaks (generally dubbed 'hypersynchrony' (Schindler et al., 2007; Cymerblit-Sabba and Schiller, 2012)) was observed in multiple channels. As described in section 2.4.5.1, only neurons whose waveforms were not distorted during ASs were included in the dataset. This means that our dataset of NRT neuron could be biased towards certain neuron morphologies/orientations or neurons whose firing tended to be less synchronous with the EEG peak of SWDs.

5.4.3 NRT activity during GHB-elicited hypnosis: comparison to natural sleep and anaesthesia

Hypnotic drugs are well characterized at the level of their molecular targets, while the information on how they affect neuronal activity *in vivo*, especially in the thalamus, is still scarce (Rudolph and Antkowiak, 2004). While no information is available for GHB, human fMRI and PET studies suggest that hypnotic concentration of drugs such as propofol or etomidate decrease blood-flow in the thalamus (Fiset et al., 1999; Franks, 2008; Mhuircheartaigh et al., 2010), a change that is normally associated with a decrease in firing rates. In cats and rats, it is instead well known that anaesthetic concentration of ketamine or urethane hyperpolarize NRT neurons sufficiently to induce LTCP-mediated bursts, similarly to natural sleep (Marks and Roffwarg, 1993; Steriade et al., 1993a; Crabtree and Isaac, 2002; Llinás and Steriade, 2006).

It has been reported that, in the rat, the firing rate of NRT neurons during wakefulness is ~23Hz and decreases to ~18Hz during slow-wave sleep (Marks and Roffwarg, 1993). Indeed the authors posit that, differently from the cat (Domich et al., 1986), the mean firing rate of NRT neurons in rats does not distinguish between sleep and wakefulness. In my hands, the firing rate of NRT neurons of active wakefulness was 20.8 Hz, which decreased to 6.6Hz during light-sleep. This discrepancy could arise from the small population of NRT neurons sampled or from the fact the only light-sleep epochs could be recorded in my experimental conditions. Notably, the firing rates of NRT neurons of Wistar rats during active wakefulness and sleep are comparable to those of GAERS rats recorded in the same experimental conditions (20.4 and 11.1 Hz, respectively, Crunelli lab, unpublished).

The comparison of the firing rate of NRT neurons during GHB-elicited hypnosis is made difficult by the lack of a direct analysis of this parameter with other hypnotic agents. In

terms of the activity of thalamic neurons, one report showed that, in cats, anaesthetic concentration of propofol and etomidate produced ~50% decrease in the firing rate of TC neurons, although the activity of NRT neurons was not investigated (Andrada et al., 2012). Similarly, no information if available to compare the decrease in tonic firing and increase in burst firing observed during GHB-elicited hypnosis. Nonetheless, various studies have described NRT neurons increasing their burst firing and decreasing tonic firing doing natural-sleep and anaesthesia, two states that bear resemblance to hypnosis and sedation. (Steriade et al., 1993a, 1993b; Timofeev and Steriade, 1996).

5.4.4 NRT activity during GHB-elicited ASs: comparison with other models of ASs

The results presented in this chapter are the first investigation of the firing of NRT neurons during pharmacologically induced ASs in freely-moving animals.

While the activity of TC neurons during ASs is still controversial (Crunelli and Leresche, 2002; Steriade, 2005; Huguenard and McCormick, 2007), there is a good convergence of *in vivo* and *in vitro* work on what is the firing output of NRT neurons. *In vitro*, various studies support the idea that NRT neurons predominantly fire bursts during SWD-like oscillation in thalamic slices (Bal et al., 1995a; Sohal and Huguenard, 2003; Beenhakker and Huguenard, 2009).

To date, the most relevant information available on the activity on NRT neurons during ASs comes from *in vivo* studies under various anaesthetic regimens. The first indication of the activity of isolated NRT neurons during SWDs is found in a study investigating 2-4Hz SW-complexes that emerge, along with other 'fast-runs' (10-15Hz) oscillations, after ketamine-xylizine anaesthesia in the cat (Steriade and Contreras, 1995). Although the authors acknowledge that those paroxysmal oscillation are distinct from ASs (and the effect of anti-absence drugs on this oscillations has not being tested), they still bear some morphological similarity to SWDs. In those conditions, NRT neurons display burst firing synchronously to the spike of each EEG SWC. A similar conclusion was reached by a more recent study in a well-established model of ASs (Slaght et al., 2002). Intracellular recordings of NRT neurons in GAERS rats under neurolept-anaesthesia show that NRT neurons receive a barrage of EPSPs which generate a LTCP and associated high-frequency burst, synchronously with each EEG spike.

Nonetheless, neurolept-anaesthesia can profoundly alter neuronal excitability (Inoue et al., 1994; Mahon et al., 2001) and experimental ASs, which are defined as EEG SWDs coupled to behavioural arrest, can only be defined in the freely-moving condition. Indeed, recent experiments (Crunelli lab unpublished; see also (McCafferty et al., 2012) in freely-moving GAERS, using the same recording technique as that presented in this Chapter have shown that, differently from neurolept-anaesthesia, only a subset of NRT neurons fires burst during each SWC. Indeed, while globally silence (52.9% of SWCs) and tonic firing (33.0% of SWCs) make up the majority of the output of NRT neurons during ASs in GAERS, a subpopulation of NRT neurons (n=5/24) was found to fire bursts in 90% of SWCs. In the GHB model the firing output of NRT neurons appears to be similar to that of NRT neurons in GAERS in the freely-moving condition, although no population of NRT neurons firing at each SWC was identified. This discrepancy could reflect a lack of adequate sampling of the NRT in Wistar rats or intrinsic differences between the two models.

It is worth noting that the dialysis experiment of the T-type channel antagonist TTA-P2 in VB+NRT (section 4.3.3), which found no block of ASs, strongly supports the idea that T-type channel mediated bursts are not necessary for the expression of ASs in the GHB-model, therefore the relative paucity of bursts observed during ASs is not surprising. Moreover, independent of the type of firing output, it is possible that the NRT is not as important in the GHB-model as in genetic models of ASs. Indeed, lesions of the NRT, which fully block the generation in GAERS (Vergnes and Marescaux, 1992) only attenuate GHB-elicited ASs (Banerjee and Snead, 1994).

In addition to the content of the output, also the timing of the output of NRT neurons has highlighted important differences in ASs recorded under neurolept-anaesthesia and the case of ASs in freely moving animals. While Slaight et. al (2002) reported that, on average, NRT bursts occurred 19ms before the SWC peak, in my hands no clear peak was evident for burst firing in the SWC triggered average (nor in other types of activity). It should be noted that, given the non-stationarity of the seizure instantaneous frequency in the GHB-model (see Chapter 6), defining the synchrony of NRT unit activity with the EEG is not a trivial matter.

5.4.5 NRT activity during GHB-elicited ASs and hypnosis

The rates of tonic firing, bursts and doublets of NRT neurons do not discriminate between GHB-elicited ASs and hypnosis. Indeed, the firing parameters for these drug-induced states

are comparable to light-sleep and contrast to those of active wakefulness. This is not necessarily surprising because the rates of discharge are gross measure of neuronal activity. For instance in most models of ASs the firing rates of thalamic neurons as comparable during ASs and natural-sleep (Avoli et al., 1983; Steriade and Contreras, 1995; McCormick and Contreras, 2001), but this two types of activity are behaviourally, pharmacologically and mechanistically distinct.

Investigation of the timing of the discharge of NRT neurons revealed that over a one second window the firing of GHB-induced ASs was associated with an EEG oscillation at 5 Hz, while in the case of GHB-induced hypnosis the rhythmicity was 4Hz. In contrast, mean autocorrelograms did not show any rhythmicity for NRT neurons around 200-250ms where peaks for GHB-elicited ASs and hypnosis could have been expected (and that are apparent for GAERS NRT neurons during ASs). Nonetheless, it should be noted that GHB-elicited ASs are short compared to those GAERS (1.6±0.7 seconds compared to 17±10 seconds in GAERS (Danober et al., 1998)) and that the frequency of GHB-elicited ASs and hypnosis is much more broad than that of GAERS ASs (see Chapter 6 for quantitative analysis of this parameter): these factor may have made the detection of the signal periodicity with autocorrelograms very difficult.

Chapter 6 Development of a seizure classification algorithm for genetic and pharmacological absence seizures

6.1 Introduction

All activities evoked by GHB are traditionally classified as an ASs, but in the discussion of Chapter 4, I provided evidence that this is indeed not the case. Only a subset of GHB-elicited activities can be confidently classified as ASs while the majority of the activity evoked by GHB reflects a hypnotic state. The aim of this chapter is to develop a classification algorithm that is capable of identify ASs in the EEG signal and to differentiate them from hypnosis and sleep.

In the case of GHB-elicited ASs (keeping in mind the lack of distinction between ASs and hypnosis) several authors reported manual seizure detection (Depaulis et al., 1989; Snead, 1992a; Kim et al., 2001; Cheong et al., 2009) or manual detection based on an arbitrary threshold (Song et al., 2004; Zaman et al., 2011) e.g. events exceeding 2 SD of the mean of a control EEG period were detected and visually scored as “seizure” or “no seizure”. To the best of my knowledge only two studies have used a detection method based on the spectral properties of the GHB-elicited ASs and both employed the wavelet transform (Schofield et al., 2009; Bergstrom et al., 2013). The first study defined the 2–8 Hz as the frequency band specific for GHB-induced seizures with no further justification and without testing the selectivity of the method on other brain oscillations (e.g. NREM sleep) that occur in the same frequency band. Therefore, this detection method is conceptually similar to a threshold applied to a filtered trace. The second study is based on wavelet transform coupled to line length measures. While this detection method was reported to classify ASs with 99% accuracy and 91% precision (Bergstrom et al., 2013), the ability of the algorithm to discriminate SWDs from NREM sleep (and hypnosis) was not investigated.

Therefore, as a preliminary step to the development of automated detection algorithm for GHB-elicited activities, I sought to investigate the spectral properties of SWDs, hypnosis and NREM-sleep in order to define a set of parameters able to discriminate between them at the EEG level.

6.2 Methods

The methods employed in this chapter are described in Chapter 2, further details on the methodological development are provided in the Results section.

6.3 Results

6.3.1 Data collection

The dataset analyzed in this Chapter consists of fronto-parietal EEG recordings from GAERS rats (n=6), drug-naïve Wistar rats (n=8), and two separate groups of Wistar rats injected with either PTZ (25 mg/kg) (n=8) or GBL (100mg/kg) (n=8). In these animals different behavioural states were manually detected on the EEG traces according to the criteria defined in Chapter 2. These were: light NREM sleep (in drug-naïve Wistar rats and GAERS, hereafter referred to as "sleep"), SWDs (for GAERS: n=345, PTZ-model: n=1209 and GHB-model, n=123) and GHB-elicited hypnosis (n=16).

6.3.2 Instantaneous maximum frequency of different behavioural states in genetic and pharmacological models of ASs

In order to compare spontaneous SWDs in GAERS and drug-induced SWDs in the PTZ and GHB model, time-frequency plots were computed via the continuous wavelet transform (hereafter referred to as 'wavelet transform'). The same procedure was applied to sleep and GHB-elicited hypnosis. The instantaneous maximum frequency (F_{max}) was then computed in the range 1-10Hz and the data was binned in 100 equally spaced bins (**Figure 6.1**). It can be appreciated that the F_{max} peaks for PTZ and GAERS were around 7 Hz (GAERS: 7.0 ± 0.70 Hz; PTZ: 7.6 ± 0.94, mean and SD respectively). Instead GHB-elicited SWDs and hypnosis (SWDs: 5.1 ± 1.3 Hz; hypnosis: 4.3 ± 1.1 Hz) overlapped between each other and with sleep (3.4 ± 1.6 Hz). Therefore, while for GAERS and PTZ SWDs a detection algorithm could be developed simply based on a frequency threshold, the same could not apply to the case of GHB. To correctly identify GHB-elicited SWDs is necessary to resort to a finer analysis at the properties of SWDs.

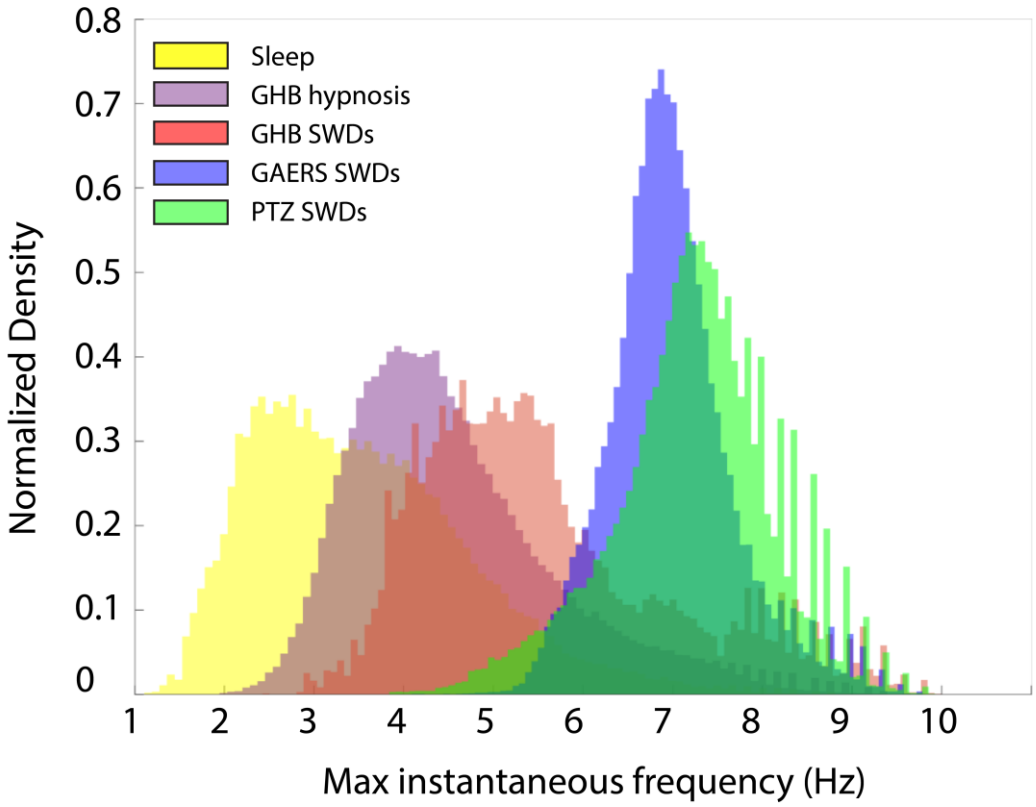

Figure 6.1. Instantaneous maximum frequency in different behavioural states in genetic and pharmacological models of AS. Histograms showing the distribution of the instantaneous maximum (max) frequency in the range 1-10Hz for GAERS, GHB and PTZ SWDs and light-NREM sleep (sleep) and GHB-elicited hypnosis.

6.3.3 Time-frequency representation of SWDs: harmonic ridge detection

A distinctive feature of SWDs that is revealed in the power spectrum is the presence of peaks representing the dominant (or fundamental) frequency and various harmonics that appear at whole multiples of the dominant frequency (Van Hese et al., 2009). These harmonic peaks arise from the spike component of the SWCs and, the sharper is the spike, the more harmonic peaks are found in the power spectrum (Akman et al., 2010; van Luijtelaar et al., 2011). For the purpose of the algorithm presented in this chapter only the properties of the first harmonic (i.e. at 14 Hz for a 7Hz SWD) are considered and will be discussed in some detail.

To illustrate this phenomenon, the wavelet transform of a 7 Hz synthetic SWDs [4] is compared to that of a typical GAERS SWDs (**Figure 6.2**). The average power spectrum (**Figure 6.2A,B**, right-hand side) shows two peaks at 7 and 14 Hz, representing the dominant frequency of each oscillation and its harmonic. The time-frequency plots similarly display the distribution of the power in two parallel horizontal lines, which are defined as the "ridges" of the time-frequency plot and contain most energy of the signal (Carmona et al., 1999; Iatsenko et al., 2013c). The identification of ridges in non-trivial (Zhang et al., 2003), indeed it can be observed that in a non-ideal SWD (from GAERS) (**Figure 6.2B**) the detection of the instantaneous F_{max} (black line) "jumps" between the dominant frequency and its harmonic due non-stationarities of the signal. The approach employed to correctly identify the ridges corresponding to the dominant frequency and its harmonic is based on the algorithms developed by Dima Iatsenko (Iatsenko et al., 2013a, 2013b, 2013c), optimized for the case of SWDs in the following way. This procedure involves three steps, which use the function "ecurve.m", freely available (see section 2.4.4), to extract the ridges from the signal after giving some constrains in order to identify the harmonics. First, the F_{max} in the range 1-10Hz is extracted from the signal (black line in **Figure 6.2B**). Second, the ridge is detected in upper and lower support regions around F_{max} (i.e. the ridge is following the regions of highest unimodal amplitude of the wavelet transform around F_{max}, Iatsenko et al., (2013c)). This extracts a ridge which is not

[4] For the remainder of this Chapter, the equations for the generation of synthetic signals, obtained as the summation of individual waveforms, are detailed in the Figure legend.

oscillating between the dominant frequency and its harmonic (compare the black lines in **Figure 6.2B** and **Figure 6.3B**). Third, the ridge of the harmonic is extracted (magenta line, **Figure 6.3A,B**) in the wavelet transform in the range 1-20Hz. This is done by detecting thehe regions of highest unimodal amplitude in the wavelet distribution that are present around twice the frequency of the ridge detected in the previous step (i.e. the black line in **Figure 6.3B**). It can be appreciated that during a SWDs the two ridges extracted are parallel, while interictally the ridge of the harmonic (magenta line in **Figure 6.3B**) is oscillating around the harmonic frequency because of the lack of concentration of spectral power at that frequency. Finally, the ridge extracting procedure generates three vectors (subsequently reconstructed via the function "rectfr.m"), containing the frequency, amplitude and phase of each ridge.

6.3.4 Harmonic coherence is a distinctive feature of SWDs

Given that experimental SWDs have different dominant frequencies, the relationship between the instantaneous phase of the ridge at the dominant frequency (Φ_D) and that of its harmonic (Φ_H) was further analyzed. Intuitively, if we consider two stationary oscillations one at twice the frequency of the other, those will be 2:1 frequency locked (i.e. $\Phi_H - 2\Phi_D$=constant), while otherwise a phase shift may appear over time. An illustration of this concept is presented in **Figure 6.4** for two sine waves, one of which has a slow phase drift. The strength of phase locking between two oscillations can be quantified as such:

$$Coherence = abs(mean(e^{i(\Phi H - 2\Phi D)}) \qquad \text{Equation 1}$$

Whereby the coherence between Φ_H and Φ_D (hereafter referred to as 'coherence') is defined as the absolute value of the mean difference between the instantaneous phases of the two ridges, in the notation of complex numbers. The coherence can vary between 0 and 1, with 1 representing oscillations that are in phase at all times. The concept of coherence can be readily applied to SWDs. Importantly, while artificial SWDs have coherence close to 1 in the absence of noise (**Figure 6.5A**), irregularity in the phase lock between the spikes and waves dramatically reduce the coherence of a signal (**Figure 6.5B**). This means that the coherence provides a useful measure of how regular a SWD is.

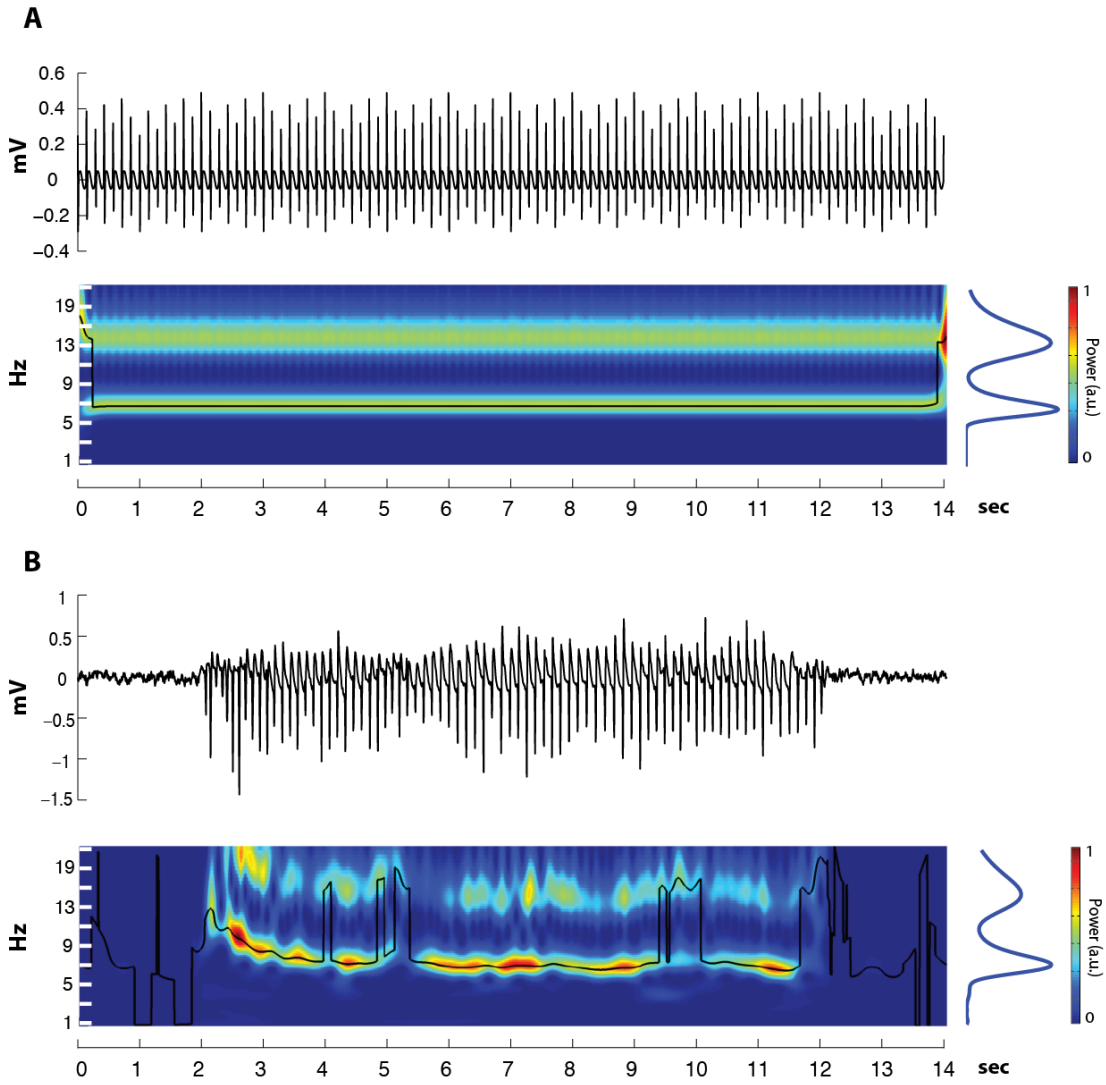

Figure 6.2. Instantaneous maximum frequency in synthetic and GAERS SWDs. (A) A synthetic SWD (top) obtained by summing a sine wave 0.5 sin (2π 7 t) to a positive going and a negative going train of triangular spikes obtained with the Matlab "pulsetran" function (width of the pulse 0.01 sec, amplitude 1 and -0.5, respectively). In wavelet transform of the signal (bottom) the energy is concentrated in two parallel lines, representing the dominant frequency of the signal and its harmonic (at 14Hz). The black line represents the instantaneous maximum frequency. The profile on right side of the figure is the mean of the wavelet power over time (i.e. the power spectrum). (B) GAERS SWDs emerging from a desynchronized EEG. Note how the instantaneous maximum fluctuates between the dominant frequency and its harmonic.

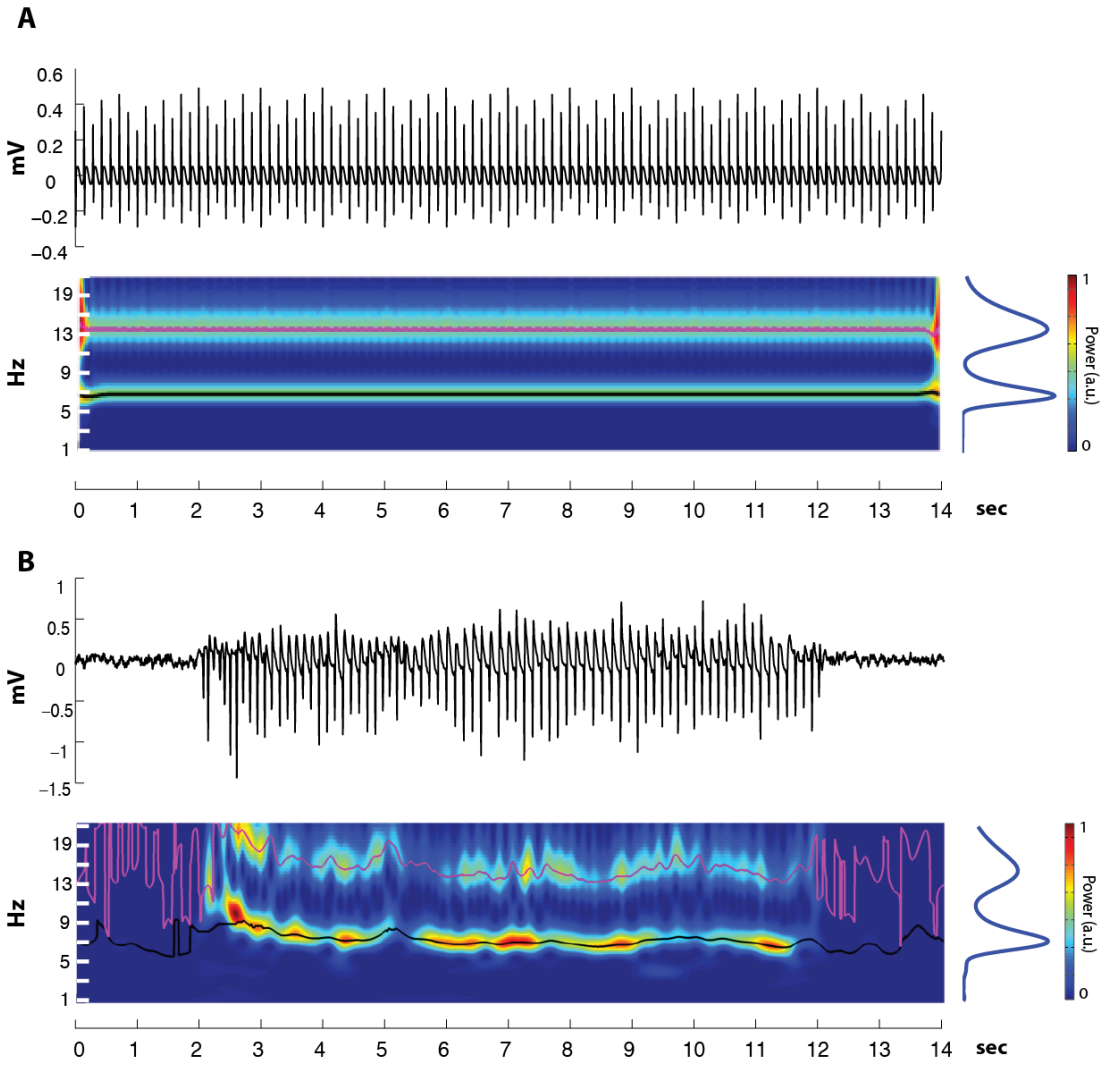

Figure 6.3 Ridge extraction algorithm: application to "real" and synthetic SWDs. The figure contains the same signals of Figure 6.2. The black and the magenta lines represent the ridges (i.e. lines that mark where in the a time-frequency plot most of the energy is concentrated) of the dominant frequency and its harmonic, respectively. Note how interictally (B) the ridge of the harmonic is not stationary as the algorithm fails to extract a stable ridge from an area with low energy. For a full description of the ridge detection algorithm see the main text.

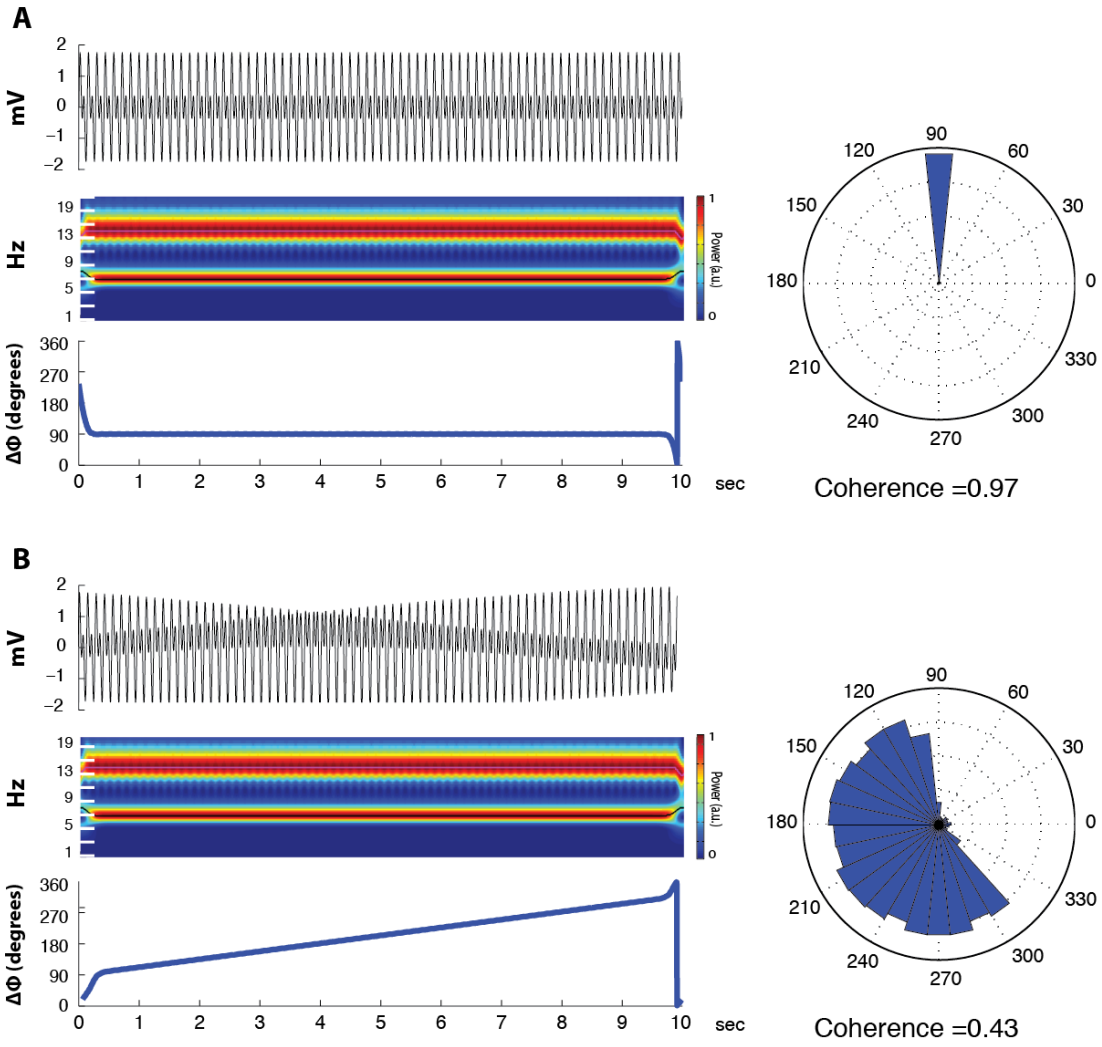

Figure 6.4 Coherence between signals oscillating at different frequency: effect of phase drift. (A) Ridge detection applied to a signal composed of two sine waves: sin (2π 7 t + Φ t) and sin (2π 14 t) with Φ=0. Note how the phase difference (ΔΦ, bottom plot) between the two ridges (7Hz and 14Hz, black and magenta lines in the middle panel) is constant across time. A histogram showing the distribution of the angle difference is shown on the right (rose plot) and the coherence (i.e. magnitude of mean angle difference vector, see main text) is reported on the bottom. (B) Ridge detection of a signal composed of two sine waves: sin (2π 7 t + Φ t) and sin (2π 14 t + Φ) with Φ=0.8. Introducing a slow phase drift in the signal (Φ t) does not change the wavelet spectrum (middle panel), but introduces a drift in the phase difference plot (bottom panel). This phase drift is reflected in a reduced coherence between the two oscillations.

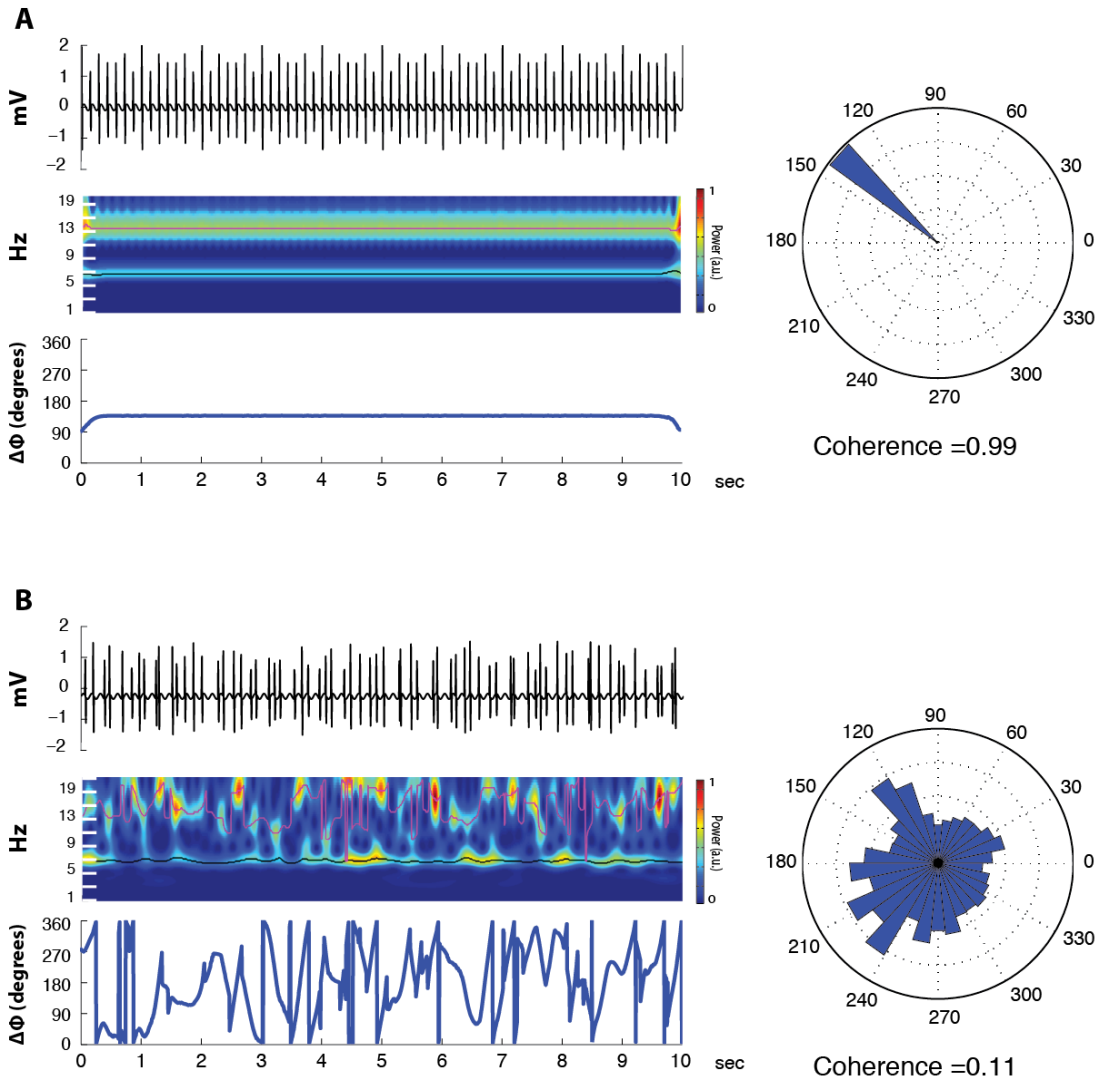

Figure 6.5. Coherence can be used to assess the regularity of SWDs. (A) A synthetic SWD (same parameters as that of Figure 6.2) has a coherence close to one, demonstrating that the coherence measure is also useful in the case of trains of SWCs as with sum of sine waves of harmonic frequency (compare to Figure 6.4). (B) The same synthetic signal as (A) but the position of each spike is now randomly distributed within each SWC (without changing the total number of spikes). The coherence of the signal drops to 0.11, illustrating that the coherence is sensitive to how orderly the spikes and waves occur (i.e. the phase of spikes and waves).

6.3.5 Classification of experimental ASs and other behavioural states according to their coherence

Having shown that the coherence is a useful descriptor of synthetic SWDs, I will now characterize experimental ASs, from the dataset described in section 6.3.1, via their coherence. Examples of GAERS (**Figure 6.6A**), PTZ (**Figure 6.6B**) and GHB SWDs (**Figure 6.7A,B**) are provided. From visual inspection of these figures it becomes evident that also in the case 'real' SWDs, the closer the coherence is to 1, the more the SWDs appear as a regular successions of SWCs, while missing spikes and drifts in the dominant frequency produce a lower coherence. GHB-elicited hypnosis, where no defined SWCs are present (i.e. EEG spikes are only occasionally locked to the wave, see section 4.3.1), has low coherence (**Figure 6.8A**). NREM sleep is also characterized by low coherence because of the lack of a stationary harmonic component (or spikes) (**Figure 6.8B**). The distribution of the coherence for various experimental seizures and behavioural states, plotted against the median of the dominant frequency ridge (extracted with the algorithm described above) for each event, is shown in **Figure 6.9**. The distributions of coherence and dominant frequency are summarized in **Table 6.1** and compared statistically in **Table 6.2**. While GAERS SWDs have tight distribution in term of coherence measure, pharmacological SWDs are more variable. Indeed although PTZ and GHB SWDs had a coherence significantly different from all other behavioural states, their coherence was not significantly different among each other. Only 19.6% of GHB SWDs have a coherence higher than the 10^{th} percentile of the coherence of GAERS SWDs, highlighting the low overlap of the two distributions. Nonetheless, GHB-elicited SWDs and hypnosis are even more separated, with only 12.5% of GHB-elicited hypnosis events having coherence higher than the 10^{th} percentile of that of GHB-elicited SWDs. In the case of SWDs, the coherence measure appears to be positively correlated to the dominant frequency, albeit only weakly (**Table 6.3**). This suggests that the two measures reflect largely independent features of SWDs.

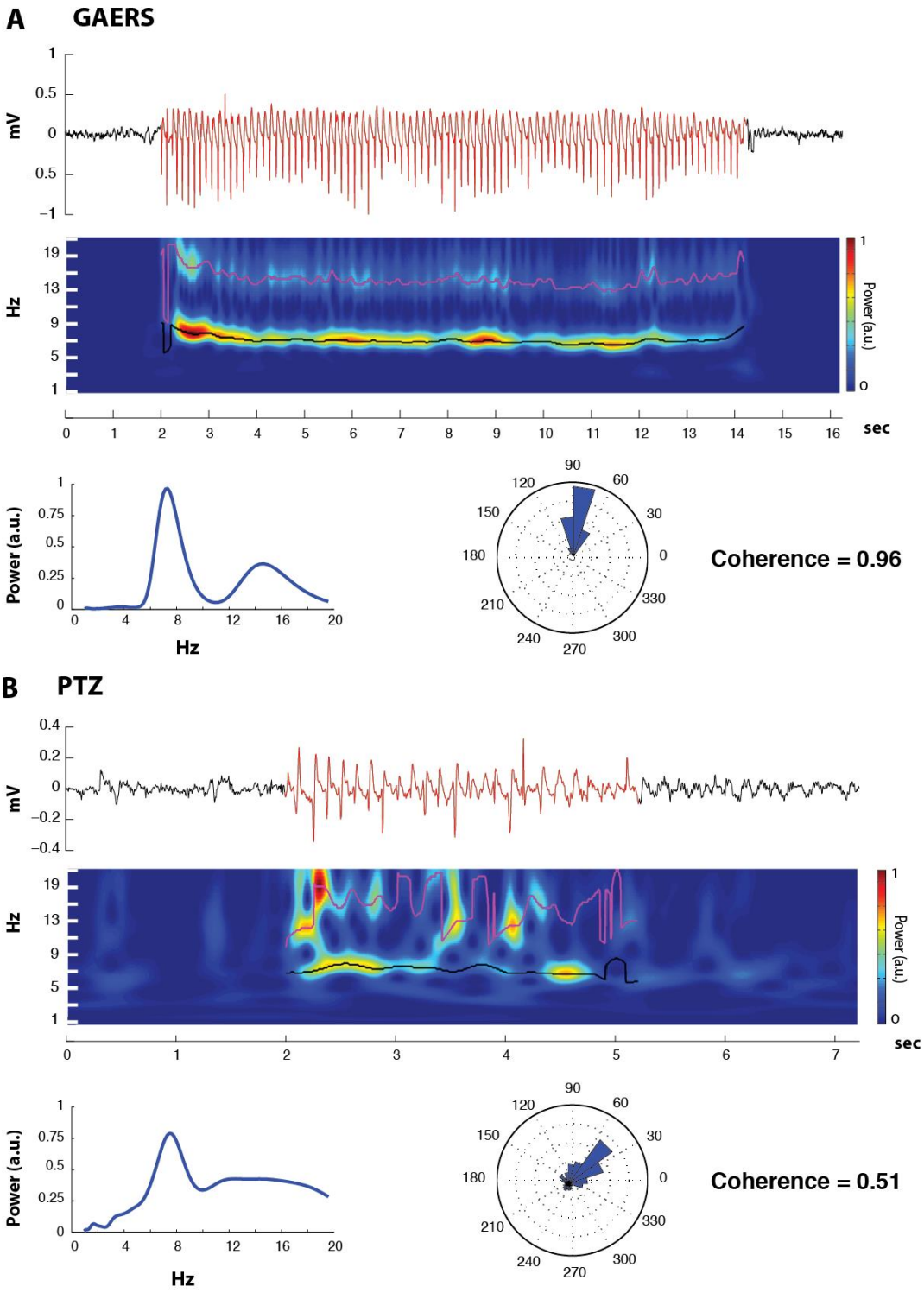

Figure 6.6. Coherence of GAERS and PTZ-induced SWDs. GAERS (A) and PTZ-elicited SWD (B). The top panel shows the SWDs (red) emerging from interictal EEG (black). The middle panel shows the wavelet transform of the EEG signal, and the two ridges (black and magenta lines) representing the dominant frequency of the SWD and its harmonic. The bottom panel shows on the left the power spectrum of the EEG signal, and, on the right, the rose plot of the phase difference between the ridges and the coherence. Note how a low coherence (B) also correlates with the lack of sharp harmonic peak in the power spectrum.

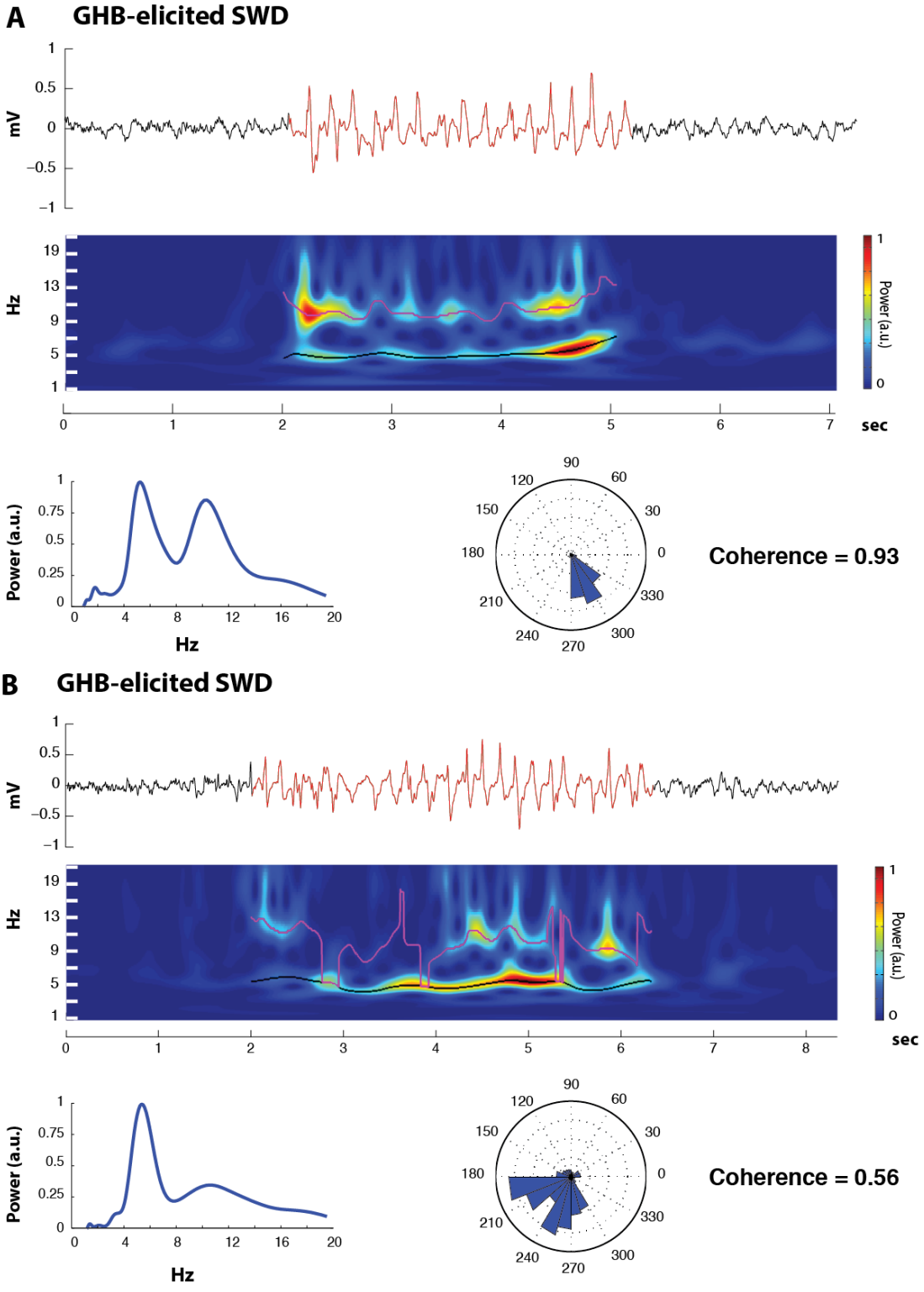

Figure 6.7. Coherence of GHB-elicited SWDs. Two GHB-elicited SWDs with a high (A) and low (B) coherence, both recorded from the same animal. For the description of the panels see the legend of Figure 6.6.

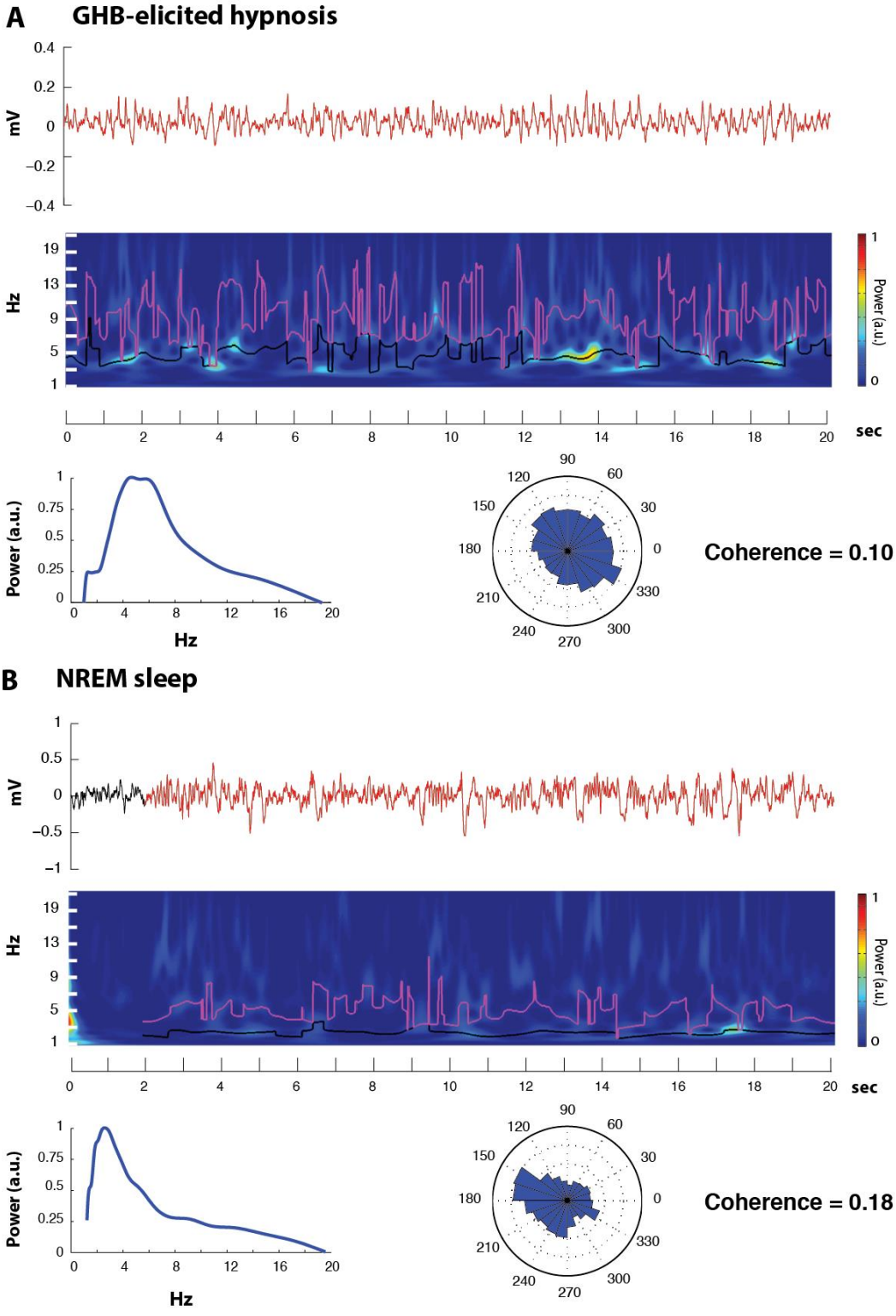

Figure 6.8. Coherence of GHB-elicited hypnosis and NREM sleep. GHB-elicited hypnosis and NREM sleep (only 20 seconds are shown for clarity), two states with a higher amplitude and synchrony compared to the active wakefulness control EEG, have a low coherence because of the lack of defined harmonics in their wavelet spectrum. For the description of the panels see the legend of Figure 6.6.

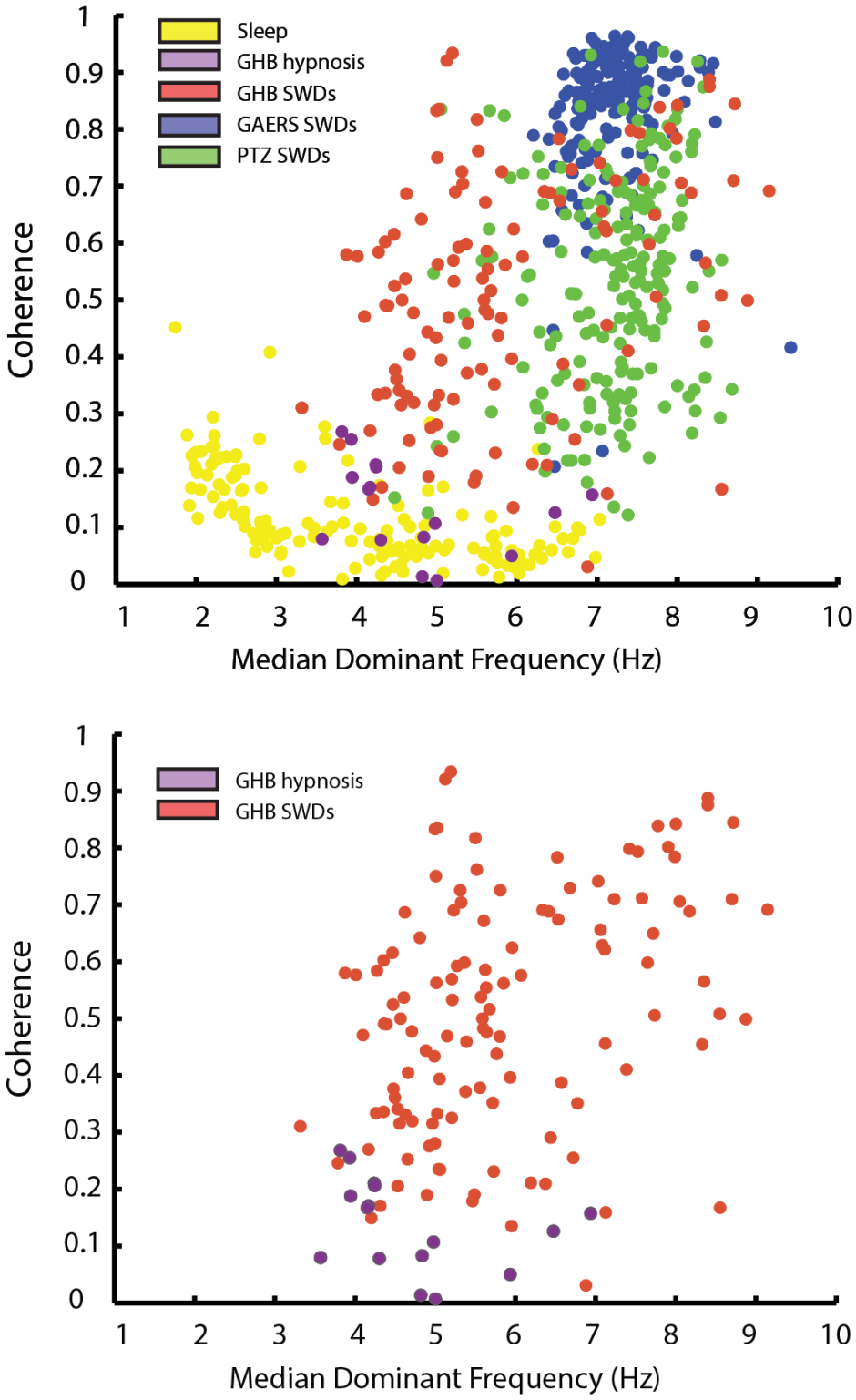

Figure 6.9 Dominant frequency vs coherence in different behavioural states for genetic and pharmacological models of ASs. Scatter plot coherence vs dominant frequency for GAERS, PTZ and GHB SWDs, and for GHB-elicited hypnosis and NREMs sleep. The bottom plot is a replica of the top plot only showing GHB-elicited activities in order to highlight the difference of the two activities evoked by the drug. For clarity only n=100 events (randomly selected) are presented in each group, except for GHB-elicited hypnosis (n=16).

Table 6.1 Summary of the coherence and dominant frequency different the behavioural states.

EEG state	Coherence				Dominant Frequency			
	Median	10th Prct[a]	90th Prct	Mean ± SEM	Median	10th Prct	90th Prct	Mean ± SEM
GAERS SWDs	0.86	0.68	0.93	0.82±0.12	7.10	6.65	7.69	7.2±0.48
PTZ SWDs	0.55	0.28	0.79	0.54±0.19	7.40	6.39	8.00	7.3±0.7
GHB SWDs	0.51	0.23	0.79	0.51±0.20	5.5	4.36	8.01	5.9±1.4
GHB hypnosis	0.14	0.02	0.25	0.14±0.08	4.3	3.83	6.42	4.7±1.0
NREM Sleep	0.10	0.04	0.24	0.12±0.08	3.8	2.21	6.01	3.9±1.4

[b]Prct: percentile. All frequency values are in Hz.

Table 6.2 Statistical comparison for the distributions of coherence and dominant frequency for different behavioural states.

		Coherence				
		GAERS SWD	PTZ SWD	GHB SWD	GHB hypnosis	Sleep
Dominant Frequency	GAERS SWD		P<0.001	P<0.001	P<0.001	P<0.001
	PTZ SWD	P<0.001		ns	P<0.001	P<0.001
	GHB SWD	P<0.001	P<0.001		P<0.001	P<0.001
	GHB hypnosis	P<0.001	P<0.001	P<0.001		ns
	Sleep	P<0.001	P<0.001	P<0.001	P<0.05	

Results of two-sample Kolmogorov-Smirnov tests. SWDs: GAERS: n=345, PTZ-model: n=1209 and GHB-model, n=123. GHB-elicited hypnosis: n=16; NREM sleep n=120.

Table 6.3 Correlation between coherence and dominant frequency

	Pearson's correlation	p-value
GAERS SWDs	0.18	<0.001
PTZ SWDs	0.17	<0.001
GHB SWDs	0.35	<0.001
GHB hypnosis	-0.34	ns
NREM Sleep	-0.55	<0.001

6.4 Discussion

6.4.1 Summary of results

In this chapter I presented an approach to classify SWDs and other EEG activities according to the phase relationship between their dominant frequency and its harmonic. The application of ridge detection to SWDs is novel, and to my knowledge, this is the first time that a measure of coherence has been used to classify experimental ASs. Importantly, this algorithm was first validated on synthetic signals and then applied to both genetic and pharmacological SWDs. It can be appreciated that, while GAERS SWDs have a tight distribution both in terms of their dominant frequency and coherence, pharmacological ASs exist on a broad spectrum for both parameters. Given that the frequency of SWDs is different between experimental and human ASs (see sections 1.2 and 1.4) it is important to develop new parameters able to discriminate SWDs according to their waveform regularity, rather than their peak frequency. In addition, I have shown that the coherence is a useful measure to discriminate GHB-elicited SWDs and hypnosis, and thus it could be incorporated in an automated seizure detection algorithm for the GHB-model, a tool that, as described in section 6.1, is still not available.

6.4.2 Methodological considerations

The first steps of the algorithm presented is this Chapter are based on the ridge detection methods developed by Dima Iatsenko (Iatsenko et al., 2013a, 2013b, 2013c). Other ridge detections methods have been developed and are freely available. For instance, WAVOS (Harang et al., 2012) contains a Matlab implementation of the "crazy climbers" algorithm, originally developed by Carmona et al. (1999) for ridge detection of noisy signals via simulated annealing (i.e. random walks). Although the ridge detection method present in WAVOS has been applied to detect patterns in circadian and genetic data (Meeker et al., 2011; Webb et al., 2012), the crazy climbers algorithm has a high computational cost. For instance, ridge detection in the SWDs presented in **Figure 6.2B** took less than 3 seconds on the machine employed (HP Z800, 8-core, 48GB RAM) for the analysis using the ridge

detection of Iatsenki et al. (2013c), while took ~20 minutes using the implementation of Harang et al. (2012).

Once the ridge of the dominant frequency and its harmonic are detected, various different measures of their relationship could be produced. The reason to concentrate on the Φ difference as opposed to the ratio of the frequencies or amplitudes of ridges was due to the consideration that, while having a frequency ratio of 2 is a necessary condition for a spike and wave (i.e. to produce a spike is necessary to sum two sine waves at harmonic frequency), the ΔΦ relationship is less predictable. This idea is illustrated in **Figure 6.4**: two sine waves of the same amplitude and frequency produce the same ridges on the time-frequency (compare **Figure 6.4A** and **Figure 6.4B**), but the introduction of a phase shift changes the ΔΦ measure. Therefore, ΔΦ stands a better chance to discriminate two similar SWDs than the frequency ratio (which always oscillates around 2) does. The ratio of the ridge amplitudes was not considered a good parameter because of the noise introduced by the waxing and waning pattern of real SWDs (see for instance **Figure 6.6** and **Figure 6.7**).

6.4.3 Application of the coherence measure to classify the EEG activities evoked by GHB

The results for the GHB-model indicate that the peak frequency is variable in this model of ASs and suggest that this variability is intrinsic to the model (at least in the rat), rather than dependent exclusively on the animal strain or dose of GHB employed (see **Table 4.1**). Indeed, the fact that a similar variability was not found in PTZ-elicited ASs, indicates that this variability is not a feature of pharmacologically induced ASs as a whole. The ability of GHB to induce both hypnosis/sedation and ASs could be responsible for this difference. Nonetheless, the modest correlation between dominant frequency and coherence (which can be considered an index of how much an oscillation is "spike-and-wavy") argues against the idea that the two states are on a spectrum and that a slowing of the EEG rhythm induces a conversion of SWDs to a hypnotic state. Indeed, GHB can elicit SWDs in he frequency range of 5 to 9 Hz with a coherence >0.7 (see **Figure 6.9**, bottom). Importantly, the coherence could be used to further compare the underlying neuronal activity of GAERS and GHB-elicited ASs (for instance measured via thalamic unit recordings such as those described in Chapter 5) only selecting SWDs with a similar coherence, thus gaining more insight on the similarity and differences of experimental ASs.

GHB-elicited hypnosis is characterized by a coherence that is similar to that of NREM sleep, clearly distinct from GHB-elicited SWDs. However, hypnosis is also distinct from NREM sleep in terms of its dominant frequency with a distribution that is shifted to higher frequencies (compare **Figure 6.1** and **Figure 6.9**). This suggests that drug-induced hypnosis and sleep underlie different EEG rhythms.

6.4.4 Limitations of the coherence measure and further characterization of the GHB-model of ASs

A limitation of the coherence measure is that it can only be applied to previously detected events. Various automated procedures could help making this process automatic, for instance applying an amplitude threshold on the EEG signal would split the recording into different events for which then the coherence could be separately calculated. In addition, the use behavioural measures (as detected via video monitoring or electromyogram, EMG) could help identifying automatically NREM sleep and hypnosis. Nonetheless, for the purpose of using the GHB-model to study ASs, it is sufficient to reliably separate SWDs from the remaining EEG signal. Therefore a threshold on the coherence (i.e. coherence > 0.3, see **Figure 6.9**) would be sufficient to correctly discriminate SWDs from hypnotic events. Moreover, by applying the same idea of measuring the instantaneous phase difference between dominant frequency and it harmonic, it would be possible to develop an algorithm that detects periods of stationary $\Delta\Phi$ (which underlie SWDs, see **Figure 6.5**) on the continuous EEG signal without previously epoching putative SWD events.

The fact that only ~20% of the GHB-elicited SWDs have a coherence overlapping the distribution of GAERS SWDs could be seen as a limitation of the GHB-model. Nonetheless, until the coherence measure is applied to humans ASs, there is no way to determine whether the high variability in the coherence of pharmacological models is a limitation or an advantage in these models in mimicking the human condition. For instance, it is worth noting the in human SWDs the spike component of the SWC is often reduced in amplitude or even missing, in particular towards the end of a SWD (Sogawa et al., 2009) (see also **Figure 1.1** and **Figure 4.7**A). This suggest that the coherence measure of human SWDs would be lower than in the case of GAERS SWDs.

Chapter 7 General discussion

7.1 Summary of major findings

The data presented in Chapter 3 of this thesis provides the first rigorous pharmacological investigation of the role of 5-$HT_{2A/C}$ receptors in the expression of ASs. In particular, pharmacological activation of 5-HT_{2C} receptors produces a transient, but drastic, block of ASs. This block of ASs is followed by a rebound increase in seizure length, which is likely to be caused by receptor desensitization and/or off-target effects of 5-HT_{2C} agonists. The effects of 5-HT_{2C} agonists are of translational relevance because the first 5-HT_{2C} agonist has recently been approved for human use (FDA, 2012). Activation of 5-HT_{2A} receptors also produces a block of ASs but this was only found with TCB-2, a compound that has hallucinogenic properties. 5-HT_{2A} antagonists, which have long been in the pipeline of pharmaceutical industries as anxiolytics, antipsychotics and sleep-promoting drugs, instead produce an increase in seizure length. The results above were initially applied to GAERS rats, and, in an attempt to replicate them in the GHB-model of ASs, it immediately became apparent that this pharmacological model does not exclusively produce ASs, but also results in a hypnotic state, previously unreported in the ASs literature.

Thus, the rest of this thesis has been devoted to further characterizing the GHB-model of ASs, in view of its wide application in studies with transgenic animals. The main result of this characterization is that GHB-elicited ASs are distinct at the level of both the EEG and of behaviour (Chapter 4). Therefore, the practice of classifying all activities evoked by GHB as ASs is incorrect and this calls into question results obtained with the GHB-model without considering such a distinction. The *in vivo* characterization of the thalamic activity of GHB-elicited ASs and hypnosis allowed us to further extend the comparison with genetic models of ASs (Chapter 5). Although, due to technical limitations, it was only possible to record the activity of NRT neurons, it is clear that both GHB-elicited ASs and hypnosis are characterized by a decrease in the total firing rate of NRT neurons and, in that respect, they are similar to NREM sleep. The difference between GHB-elicited ASs and hypnosis lies in the different association between the unit activity and the EEG, as highlighted by the NRT spike-triggered EEG average. This analysis of GHB-elicited ASs shed new light on the mechanism underlying the expression of ASs. Contrary to what was predicted by *in vitro* and *in vivo* experiments under neurolept anaesthesia, in freely moving animals burst firing

is found in the less than <10% of SWCs. The prevalent activity of NRT neurons during ASs is either silence or tonic firing. This may explain why thalamic application of the potent T-type channel antagonist, TTAP-2, does not affect GHB-elicited ASs (Chapter 4). Finally, the development of an algorithm to classify GHB-elicited ASs demonstrates that, at the EEG level, the spectral properties of SWDs can be used to discriminate hypnosis and SWDs (Chapter 6). Moreover, the measure of spectral coherence can be used in various experimental models of ASs to characterize SWDs according to their waveform regularity.

7.2 5-$HT_{2A/C}$ and ASs: is there an abnormality in their expression?

The results described in Chapter 3 show that 5-$HT_{2A/C}$ can modulate ASs, although the brain area(s) responsible for this activity remain unclear. Preliminary results on the modulation of the tonic $GABA_A$ current by 5-$HT_{2A/C}$Rs (section 3.1) indicated a thalamic site of action, a hypothesis that was not verified experimentally. Moreover, it remains uncertain if, in epileptic animals, abnormalities in 5-$HT_{2A/C}$Rs are involved in the pathophysiology of ASs. The fact that 5-HT_{2C}R knockout mice are more susceptible to a variety of convulsive seizures indicates that this may be a possibility. *In vitro* findings that 5-HT_{2A} antagonists have no effect on the tonic $GABA_A$ current in Wistars, but drastically decrease the tonic $GABA_A$ current in GAERS, instead point to a higher 5-HT2A activity in epileptic animals. In order to clarify this issue experimentally, a series of experiments were initiated, in collaboration with Cristiano Bombardi (University of Bologna, Italy), at the time of the writing of this thesis. Using immunocytochemistry, the expression of 5-HT_{2A}Rs and 5-HT_{2C}Rs was compared in the TC network of adult (P90) GAERS and NECs. Preliminary results show that both 5-HT_{2A}Rs and 5-HT_{2C}Rs are differentially expressed in GAERS (n=4) compared to NECs (n=4). In particular, the number of cells positive (for mm^2) for 5-HT_{2A}Rs in the S1po and in the VB is higher in GAERS compared to NECs (S1po: GAERS 4695.7 ± 519.4, NECs 3540 ± 187,4, $p<0.05$; VB: GAERS 722.3 ± 301.8, NECs 339.3 ± 78.4; $p<0.001$). This difference could explain the effects of 5-HT_{2A} antagonists, *in vitro,* mentioned above. In the case of 5-HT_{2C}Rs the relationship is, instead, reversed, with NECs having a higher number 5-HT_{2C} positive neurons compared to NECs (S1po: GAERS 2496.3 ± 192.4, NECs 3026 ± 197.1, $p<0.05$; VB: GAERS 612.2 ± 196, NECs 852.7 ± 272.2; $p<0.05$). No differential expression of 5-HT_{2C}Rs and 5-HT_{2A}Rs was observed in the NRT in GAERS compared to NECs. Although these preliminary results may indicate a role of 5-HT_{2A}Rs and 5-HT_{2C}Rs in the pathophysiology of ASs, it remains to be ascertained whether these changes in expression are a cause or a consequence of the ASs phenotype.

Immunohistochemistry experiments in animals at P14 and P20 (ages which precede the ASs phenotype) will help to clarify this issue.

7.3 GHB-elicited hypnosis: role of the thalamus

The fact that GHB is capable of producing ASs and a hypnotic state is not surprising. Indeed, the same is true for THIP, which induces ASs in rodents (see section 1.4.2), but also hypnosis/NREM sleep in both humans (Faulhaber et al., 1997; Hinton and Johnston, 2009) and rodents (Lancel and Faulhaber, 1996; Krogsgaard-Larsen et al., 2004).

Interestingly, while GHB and THIP are, respectively, a $GABA_B$ and a $GABA_A$ agonist, both drugs enhance the tonic $GABA_A$ inhibition in the thalamus (Belelli et al., 2005; Cope et al., 2009). In the case of GHB, this due to an indirect cross-talk between $GABA_B$Rs and extrasynptic $GABA_A$Rs (Connelly et al., 2013), whereas THIP is a direct agonist of extrasynaptic, δ-containing $GABA_A$Rs (Drasbek et al., 2007). In addition, low doses of anaesthetics (such as isofluorane and propofol), which have a sedative/hypnotic effect on humans, have also been shown to increase the tonic $GABA_A$ inhibition in the thalamus (Glykys and Mody, 2007; Jia et al., 2008). Therefore, it could be hypothesized that a common site of action for molecularly distinct hypnotics is the thalamus, specifically via an action on extrasynaptic $GABA_A$Rs.

7.4 NRT activity during GHB-elicited SWDs

The experiments presented in Chapter 5 represent the first recordings of NRT neurons in freely moving animals during pharmacological ASs. These results are in contrast to the current hypothesis about the type and timing of the output of NRT neurons during SWDs. The closest comparison available in the literature is with the activity of NRT neurons *in vivo* under neurolept anaesthesia in GAERS (Slaght et al., 2002), where NRT neurons, almost exclusively, fired bursts of action potentials associated with the EEG spikes of the SWD. In particular, the first action potential of the burst peaked at 18.7 ± 10.6 ms before the EEG spike. In my hands, the prevalence of single spikes or silence was also accompanied by a less defined association of neuronal firing to the EEG spike, with the probability of NRT neurons to fire between -25 and +25 ms (before and after the EEG spike) being roughly the same. Although my results have a small sample size, a similar difference in the firing of NRT neurons (i.e. paucity of burst firing during SWDs) has been

found for ASs recorded in freely moving GAERS compared to under neurolept anaesthesia (Crunelli lab, unpublished). Therefore, it is possible the neurolept anaesthesia regime (composed of fentalyl + haloperidol) is a major cause of the difference between the two *in vivo* conditions. Indeed, it has been shown that different regimes of neurolept anaesthesia can greatly influence neuronal excitability (Inoue et al., 1994). Another possibility is that the sample of NRT cells recorded was composed of a non-homogenous set of neurons projecting to various TC nuclei not limited to VB. This could influence the timing of neuronal output and, potentially, also the type of the activity expressed, although it is worth noting that, in the case of the experiment of Slaght (2002), the NRT neurons recorded were scattered across the DV extent of the nucleus, but they all expressed the same type of output. A better sampling of the NRT population, and increased sample size, are necessary before drawing a solid mechanistic conclusion on the activity of the whole NRT during GHB-elicited ASs.

7.4.1 Role of T-type channels in pharmacological ASs

The activity of TC neurons during GHB-elicited ASs is currently unknown. Nonetheless, considering the results of reverse microdialysis of TTA-P2 in TC (Chapter 4), and assuming a similar type of output to that of TC neurons in GAERS (Pinault et al., 1998), it is possible to speculate about the role of the T-current in the GHB-model. Evidence for a role of T-type channels expressed in TC neurons is only found in studies with a global block of the T-current in the CNS, either via pharmacological antagonism (Tringham et. al 2012; this thesis), knockout of Cav3.1 channels (Kim et al., 2001), or overexpression of Cav3.1 channels throughout the brain (Ernst et al., 2009). Experiments which locally block T-type channels in the TC neurons (Chapter 4) argue against an involvement of the T-current in the pathogenesis of ASs. The recording of NRT neurons *in vivo,* and the effect of the block of T-type channels in both VB and NRT, also provide clear evidence that T-type channel activity in the thalamus (at least in these nuclei) is not necessary for the expression of GHB-elicited ASs. Therefore, these results strongly suggest a role of cortical T-type channels in the initiation and propagation of GHB-elicited ASs, as has been already shown to be case for GAERS ASs (McCafferty et al., 2012). The *in vitro* hypothesis that, in both TC and NRT, neurons display burst firing as their major output (McCormick and Bal, 1997; McCormick and Contreras, 2001; Beenhakker and Huguenard, 2009) is incompatible with the current *in vivo* evidence. Although *in vitro* models of ASs have certainly aided understanding of what range of activities thalamic neurons are capable of expressing in physiological and pathophysiological contexts, the lack of a full neuronal connectivity (e.g

inputs from cortical cells) and neuromodulatory inputs in the thalamic slice preparation does not allow to ascertain whether any of these activities will be present in the intact animal.

7.5 Suggested future work

7.5.1 Further investigation of the location of 5-$HT_{2A/C}$Rs that modulate ASs

As mentioned in section 7.2 there is some preliminary evidence of abnormal expression of 5-$HT_{2A/C}$ in the TC network of GAERS, compared to non-epileptic animals. Therefore, it would interesting to ascertain if this abnormality is at least partly responsible for the ASs phenotype, and if there is a brain area where a local manipulation of 5-$HT_{2A/C}$ could recapitulate the results of systemic administration. The microdialysis approached used to investigate the role of these receptors in the thalamus has limitations due to the moderate selectivity of the compounds used (see section 3.4.2.5). Unfortunately, other selective compounds available have a poor solubility in aCSF (e.g. the selective 5-HT_{2C} agonists CP809101 and vabicaserin) and thus they are not appropriate for reverse microdialysis. Other approaches, such as RNA interference or microinjection of oligonucleotides (Van Oekelen et al., 2003b; Cohen, 2005), could be employed to test the role of a specific 5-HT2 receptor subtypes in the expression of ASs. Amongst the brain areas to target, the S1po, the initiation site of ASS in GAERS, would be an obvious choice.

7.5.2 Activity of TC and cortical neurons during GHB-elicited ASs

Our understanding of the mechanism of ASs expression in the GHB-model is incomplete. In particular, based on the results of this thesis, the first priority will be to record TC neurons, with the same technique employed in Chapter 5, and compare their activity to that found in freely moving GAERS. This would allow a direct comparison between two models of ASs and would further our understanding of the differences and similarities between genetic and pharmacological model of ASs. In particular, it would be of interest to record the activity of TC neurons from the VB, but also from other thalamic nuclei such as the mediodorsal and intralaminar, since lesions of these nuclei have no effect of GAERS ASs (Vergnes and Marescaux, 1992), but abolish GHB-elicited SWDs (Banerjee and Snead, 1994).

Recording of cortical neurons would also be of fundamental interest: the only available information on the activity of different cortical layers during GHB-elicited ASs is in striking contrast to the current notions on how ASs are generated and propagated (Crunelli and Leresche, 2002; Polack et al., 2007) since layer V and VI of the cortex were reported to be silent during GHB-induced ASs in the rat (Banerjee et al., 1993).

7.5.3 Development of an automated algorithm to detect SWDs in pharmacological and genetic models of ASs

The algorithm presented in Chapter 6 has shown that the coherence between the dominant frequency of a SWD and its harmonic is a useful tool to distinguish GHB-elicited ASs and hypnosis. Using the same principle it would be possible to define a time-varying measure of the relationship between the ridge of the dominant frequency and its harmonic, such as the instantaneous $\Delta\Phi$. It would be possible to identify SWDs based on the stationarity of their $\Delta\Phi$ and this method could be applied to all experimental (and human) ASs.

.

7.5.4 Characterization of the PTZ model

In recent years multiple studies have used the GHB-model to investigate the contribution of individual genes to expression of ASs. Given the limitations of this model, highlighted in this thesis, it is surprising that other pharmacological models, such as PTZ, remain much less well characterized. Like GHB, PTZ produces SWDs with highly variable coherence, but PTZ-elicited SWDs have a tight dominant frequency peak and are always isolated, with no EEG or behavioural indication of a hypnotic state. In addition, although GHB and PTZ both act on the GABAergic system, while GHB is $GABA_B$ agonist, PTZ is a weak $GABA_A$ antagonist. The different mechanism of action of the two drugs indicates that multiple independent mechanisms can produce ASs in a naïve animal. ASs evoked by the two models are not necessarily identical: indeed, an indication of the difference between GHB and PTZ has come from studies showing that transgenic mice can be resistant to PTZ, but not GHB-elicited ASs or vice versa (see section 1.4.2.1.3). Therefore, a more thorough characterization of PTZ would be useful for the field, because it would add another tool with which to investigate experimental ASs in transgenic animals without the confounding factor of the presence of a hypnotic state in addition to the ASs phenotype.

Appendix A Statistical tables

In this Appendix the full statistical output of the analysis in Chapter 3 is presented. The following notation will be used in the following tables:

% dec: percentage of decrease compared to the same period in the vehicle group. Negative values correspond to an increase.

p-value: p-value for Dunnet's multiple comparing post-hoc for a given treatment after conducting two-way ANOVA with drug and time as factors. *, $p<0.05$; **, $p<0.01$; ***, $p<0.001$; ****, $p<0.0001$; ns, not significant.

SME: post-hoc testing for the simple main effect (SME) of a given treatment over the 2-hour observation window. The percentage decrease also refers to the 2 hours post-injection.

20-120: 20 minutes bin window, e.g. 20 refers to 0 (injection) to 20 minutes post-injection, 40 refers to 20 minutes post-injection to 40 minutes post-injection and so on.

Table A.1 Summary statistics for lorcaserin

Dose-response lorcaserin						
dose (mg/kg)	0.3		3		10	
	% decrease	p-statistic	% decrease	p value	%diff	p statistic
CUMULATIVE TIME						
SME	16.5	ns	23.5	**	40.9	****
20	-12.5	ns	86.1	****	96.9	****
40	-16.4	ns	82.4	***	100.0	****
60	6.1	ns	5.6	ns	90.9	****
80	6.3	ns	-16.4	ns	59.8	*
100	-31.2	ns	-14.2	ns	-3.1	ns
120	-60.9	ns	-14.9	ns	-15.7	ns
LENGTH						
SME	-22.3	ns	-77.6	**	-36.4	****
20	-29.5	ns	55.5	ns	22.1	ns
40	-13.6	ns	31.9	ns	95.5	ns
60	-5.2	ns	-231.7	****	-9.1	ns
80	-19.6	ns	-139.7	***	-63.3	ns
100	-35.1	ns	-122.2	**	-71.0	ns
120	-31.4	ns	-99.1	*	-69.7	ns
NUMBER						
SME	2.3	ns	23.5	**	72.1	****
20	14.0	ns	73.1	***	96.8	****
40	-3.0	ns	77.2	****	98.9	****
60	9.9	ns	72.2	****	86.7	****
80	22.5	ns	49.4	*	67.9	**
100	0.8	ns	43.7	**	48.4	ns
120	-32.4	ns	40.6	ns	26.2	ns
Lorcaserin ± SB 242082						
	3mg/kg locaserin		3mg/kg lorcaserin + SB 242082 0.5mg/kg		SB 242082 0.5mg/kg	
	% decrease	p statistic	% decrese	p value	%diff	p statistic
CUMULATIVE TIME						
SME	18.2	*	-7.1	ns	1.2	ns
20	78.8	****	49.7	**	29.4	ns
40	63.2	***	13.2	ns	-18.8	ns
60	13.5	ns	-17.6	ns	-22.0	ns
80	-25.4	ns	-34.6	ns	15.0	ns
100	-69.1	**	-60.0	*	13.2	ns
120	3.2	ns	-26.8	ns	12.8	ns
LENGTH						
SME	-90.6	****	-52.0	***	-18.5	ns
20	-8.4	ns	11.8	ns	-6.3	ns
40	-128.7	**	-85.5	ns	-64.9	ns
60	-150.1	****	-69.4	ns	-30.3	ns
80	-154.2	****	-93.8	*	-8.0	ns
100	-88.8	*	-47.7	ns	-85.5	ns
120	-34.4	ns	-46.2	ns	-9.6	ns
NUMBER						
SME	56.2	****	27.6	****	17.5	***
20	80.2	****	43.9	***	30.9	*
40	86.8	****	55.8	****	29.5	**
60	64.6	****	32.1	*	8.1	ns
80	45.2	**	15.5	ns	22.9	ns
100	7.4	ns	-11.1	ns	55.8	ns
120	31.9	*	11.5	ns	21.7	ns

Table A.2 Summary statistics for CP809101

Dose-response CP809101						
mg/kg	0.3		3		10	
	% dec	p-value	% dec	p-value	% dec	p-value
CUMULATIVE TIME						
SME	-0.3	ns	24.4	***	78.2	****
20	23.1	ns	70.1	****	84.2	****
40	10.5	ns	57.0	***	89.8	****
60	15.7	ns	16.5	ns	144.8	**
80	-5.9	ns	-2.9	ns	79.6	**
100	-18.0	ns	-2.6	ns	72.4	**
120	-71.9	ns	-36.8	ns	62.7	ns
LENGTH						
SME	-14.9	*	-16.5	*	36.7	****
20	-3.8	ns	4.8	ns	28.1	ns
40	-9.0	ns	1.8	ns	45.6	ns
60	7.3	ns	-45.3	**	279.3	ns
80	-13.3	ns	-24.0	ns	27.0	ns
100	-60.0	***	-20.5	ns	40.7	ns
120	-14.3	ns	-23.0	ns	34.0	ns
NUMBER						
SME	10.7	ns	56.2	****	70.8	****
20	23.6	ns	80.2	****	78.1	****
40	17.2	ns	86.8	****	82.0	****
60	11.1	ns	64.6	****	157.4	***
80	11.0	ns	45.2	**	74.4	****
100	19.4	ns	7.4	ns	67.6	***
120	-43.4	ns	31.9	*	47.3	ns
CP809101 ± SB 242082						
	3mg/kg CP809101		3mg/kg CP809101 + SB 242082 0.5mg/kg		SB 242082 0.5mg/kg0	
	% dec	p-value	% dec	p-value	% dec	p-value
CUMULATIVE TIME						
SME	24.4	***	-9.5	ns	8.6	ns
20	70.1	****	45.8	**	38.5	**
40	57.0	***	22.1	ns	8.6	ns
60	16.5	ns	-35.4	*	9.0	ns
80	-2.9	ns	-34.6	ns	-5.5	ns
100	-2.6	ns	-23.8	ns	22.1	ns
120	-36.8	ns	-79.0	*	-38.5	ns
LENGTH						
SME	-16.5	*	19.4	**	-18.6	**
20	4.8	ns	7.7	ns	7.0	ns
40	1.8	ns	-7.4	ns	-18.4	ns
60	-45.3	**	-33.8	ns	0.1	ns
80	-24.0	ns	-29.4	ns	-44.7	*
100	-20.5	ns	-30.5	ns	-7.4	ns
120	-23.0	ns	-34.6	ns	-43.9	*
NUMBER						
SME	56.2	****	11.7	*	22.8	****
20	80.2	****	47.1	***	38.1	**
40	86.8	****	30.8	*	25.1	ns
60	64.6	****	4.6	ns	12.1	ns
80	45.2	**	-2.1	ns	25.9	ns
100	7.4	ns	5.1	ns	30.8	*
120	31.9	*	-30.7	ns	-5.8	ns

Table A.3 Summary statistics for TCB-2

Dose-response TCB-2						
mg/kg	0.03		0.3		3	
	% dec	p-value	% dec	p-value	% dec	p-value
CUMULATIVE TIME						
SME	14.1	*	76.8	****	97.3	****
20	34.4	**	94.9	***	97.1	****
40	-12.2	ns	96.4	***	100.0	****
60	24.2	ns	77.0	*	100.0	****
80	26.4	ns	67.3	ns	94.5	****
100	14.6	ns	41.0	ns	95.4	****
120	-16.9	ns	57.2	ns	95.1	***
LENGTH						
SME	-13.6	ns	1.1	ns	72.6	****
20	2.9	ns	57.2	ns	33.9	ns
40	-35.5	*	1.5	ns	100.0	NA
60	-7.9	ns	5.1	ns	100.0	NA
80	-3.2	ns	-7.3	ns	53.5	*
100	-22.1	ns	1.3	ns	66.3	***
120	-22.3	ns	7.1	ns	66.2	**
NUMBER						
SME	25.6	****	75.1	****	94.1	****
20	35.2	*	90.8	****	96.2	****
40	15.9	ns	96.2	****	100.0	****
60	28.3	*	83.3	****	100.0	****
80	29.1	ns	66.1	***	92.2	****
100	34.6	*	53.2	**	86.8	****
120	5.7	ns	58.2	**	86.7	***
TCB2 ± MDL11,939						
	0.3mg/kg TCB-2		0.3 mg/kg TCB-2 + MDL11,939 0.5mg/kg		MDL11,939 0.5 mg/kg	
	% dec	p-value	% dec	p-value	% dec	p-value
CUMULATIVE TIME						
SME	76.8	****	-8.9	ns	-37.6	***
20	94.9	***	4.9	ns	-18.4	ns
40	96.4	***	-0.8	ns	-57.7	*
60	77.0	*	-41.6	ns	-32.9	ns
80	67.3	ns	-10.0	ns	-64.4	*
100	41.0	ns	-15.8	ns	-0.8	ns
120	57.2	ns	9.9	ns	-25.2	ns
LENGTH						
SME	1.1	ns	-27.1	**	-29.0	**
20	57.2	ns	2.6	ns	-22.0	ns
40	1.5	ns	-22.0	ns	-32.6	ns
60	5.1	ns	-74.6	**	-27.2	ns
80	-7.3	ns	-27.2	ns	-36.3	ns
100	1.3	ns	-36.1	ns	-22.0	ns
120	7.1	ns	-12.3	ns	-31.9	ns
NUMBER						
SME	75.1	****	15.8	*	10.2	ns
20	90.8	****	3.3	ns	29.3	ns
40	96.2	****	12.6	ns	5.3	ns
60	83.3	****	17.5	ns	14.2	ns
80	66.1	***	13.0	ns	-11.2	ns
100	53.2	**	21.9	ns	12.6	ns
120	58.2	**	26.5	ns	11.9	ns

Table A.4 Summary statistics for Lisuride

Dose-response lisuride				
mg/kg	0.1		0.5	
	% dec	p-value	% dec	p-value
CUMULATIVE TIME				
SME	-31.9	*		
20	-78.7	ns	99.2	*
40	-19.6	ns	82.2	*
60	-19.4	ns	1554.0	ns
80	-35.2	ns	-12.3	ns
100	-36.1	ns	-55.2	ns
120	3.0	ns	-118.4	*
LENGTH				
SME	-26.9	*		
20	-1.7	ns	85.1	**
40	6.1	ns	44.2	ns
60	-12.8	ns	347.0	ns
80	-90.7	**	-19.1	ns
100	-54.3	ns	-55.2	ns
120	-17.1	ns	-101.9	**
NUMBER				
SME	-6.44	ns		ns
20	-66.7	ns	95.5	ns
40	-27.5	ns	47.0	ns
60	7.5	ns	-213.8	ns
80	26.2	ns	-22.0	ns
100	13.9	ns	-20.9	ns
120	9.0	ns	-12.9	ns

Lisuride ± MDL11,939						
	0.5 mg/kg lisuride		0.5 mg/kg lisuride + MDL11,939 0.5mg/kg		MDL11,939 0.5mg/kg0	
	% dec	p-value	% dec	p-value	% dec	p-value
CUMULATIVE TIME						
SME	8.4	ns	34.4	*	-22.8	ns
20	99.2	**	82.2	*	-40.3	ns
40	83.6	***	54.4	*	-13.9	ns
60	4.5	ns	-82.0	ns	-48.8	ns
80	-13.4	ns	-17.7	ns	-32.6	ns
100	-52.9	ns	59.3	ns	54.4	ns
120	-127.0	***	85.4	*	4.6	ns
LENGTH						
SME	-5.3	ns	49.0	***	-39.4	**
20	85.0	*	74.6	*	-46.1	ns
40	45.7	ns	56.2	ns	-32.4	ns
60	26.7	ns	47.4	ns	-31.3	ns
80	-18.3	ns	21.9	ns	-44.6	ns
100	-52.9	ns	20.4	ns	56.2	ns
120	-95.0	**	73.0	*	-27.7	ns
NUMBER						
SME	4.9	ns	-34.2	ns	5.2	ns
20	95.5	ns	60.4	ns	-3.7	ns
40	48.7	ns	-24.9	ns	10.0	ns
60	-56.2	ns	-257.2	****	-7.7	ns
80	-29.8	ns	-93.2	ns	13.3	ns
100	-25.0	ns	54.9	ns	-24.9	ns
120	-21.2	ns	56.0	ns	32.0	ns

Table A.5 Summary statistics for Vabicaserin

Dose-response Vabicaserin				
mg/kg	5		15	
	% dec	p-value	% dec	p-value
CUMULATIVE TIME				
SME	-30.9	***	8.3	ns
20	26.2	ns	49.9	*
40	-37.3	ns	60.0	**
60	-57.1	*	467.5	ns
80	-23.9	ns	-3.5	ns
100	-39.6	ns	-23.4	ns
120	-55.2	*	-62.6	*
LENGTH				
SME	-47.1	****	-62.9	****
20	-29.9	ns	-12.5	ns
40	-73.3	**	-19.2	ns
60	-94.7	**	-135.4	*
80	-32.1	ns	-95.2	***
100	-37.1	ns	-92.2	***
120	-23.8	ns	-85.9	**
NUMBER				
SME	11.6	ns	44.0	****
20	46.7	**	59.0	***
40	21.3	ns	71.6	****
60	16.8	ns	184.9	****
80	1.4	ns	38.8	**
100	-1.7	ns	28.2	*
120	-12.7	ns	9.9	ns

Table A.6 Summary statistics for M100907

Dose-response M100907				
mg/kg	0.5		3	
	% dec	p-value	% dec	p-value
CUMULATIVE TIME				
SME	-28.9	***	-21.6	*
20	-19.7	ns	3.5	ns
40	-27.2	ns	-36.6	ns
60	-36.0	ns	-413.3	ns
80	-45.6	ns	-30.9	ns
100	-17.7	ns	-31.9	ns
120	-30.3	ns	-11.4	ns
LENGTH				
SME	-58.2	****	-52.6	****
20	-63.6	**	-46.8	ns
40	-41.9	ns	-56.0	*
60	-98.0	***	-179.6	ns
80	-52.2	ns	-54.4	ns
100	-46.2	ns	-58.3	*
120	-39.0	ns	-45.9	ns
NUMBER				
SME	16.7	**	18.9	**
20	26.2	ns	28.9	ns
40	11.3	ns	14.4	ns
60	29.7	*	587.6	ns
80	5.8	ns	16.7	ns
100	25.2	ns	15.9	ns
120	2.7	ns	21.8	ns

Table A.7Summary statistics for Ro60-0175

Ro60-0175		
mg/kg	3	
	% dec	p-value
CUMULATIVE TIME		
SME	62.8	****
20	64.6	**
40	84.3	****
60	72.9	****
80	62.5	**
100	45.6	ns
120	28.8	ns
LENGTH		
SME	16.3	ns
20	39.6	ns
40	55.5	ns
60	25.1	ns
80	13.3	ns
100	-11.7	ns
120	-51.3	ns
NUMBER		
SME	8.528372561	****
20	17.7	ns
40	9.8	ns
60	0.4	ns
80	13.6	ns
100	-0.6	ns
120	8.0	ns

References

Aghajanian G, Liu R-J (2009) Serotonin (5-Hydroxytryptamine; 5-HT): CNS Pathways and Neurophysiology. In: Encyclopedia of Neuroscience, pp 715–722.

Aghajanian G., Marek G. (1997) Serotonin Induces Excitatory Postsynaptic Potentials in Apical Dendrites of Neocortical Pyramidal Cells. Neuropharmacology 36:589–599.

Aizawa M, Ito Y, Fukuda H (1997) Pharmacological profiles of generalized absence seizures in lethargic, stargazer and gamma-hydroxybutyrate-treated model mice. Neurosci Res 29:17–25.

Akman O, Demiralp T, Ates N, Onat FY (2010) Electroencephalographic differences between WAG/Rij and GAERS rat models of absence epilepsy. Epilepsy Res 89:185–193.

Akrawi WP, Drummond JC, Kalkman CJ, Patel PM (1996) A comparison of the electrophysiologic characteristics of EEG burst-suppression as produced by isoflurane, thiopental, etomidate, and propofol. J Neurosurg Anaesthesiol 8:40–46.

Alexander GM, Godwin DW (2006) Metabotropic glutamate receptors as a strategic target for the treatment of epilepsy. Epilepsy Res 71:1–22.

Alkire MT, Hudetz AG, Tononi G (2008) Consciousness and anaesthesia. Science (80-) 322:876–880.

Aloyo VJ, Berg K a, Spampinato U, Clarke WP, Harvey J a (2009) Current status of inverse agonism at serotonin2A (5-HT2A) and 5-HT2C receptors. Pharmacol Ther 121:160–173.

Amarillo Y, Zagha E, Mato G, Rudy B, Nadal MS (2014) The interplay of seven subthreshold conductances controls the resting membrane potential and the oscillatory behavior of thalamocortical neurons. J Neurophysiol 112:393–410.

Amzica F (2009) Basic physiology of burst-suppression. Epilepsia 50 Suppl 1:38–39.

Andrada J, Livingston P, Lee BJ, Antognini J (2012) Propofol and etomidate depress cortical, thalamic, and reticular formation neurons during anaesthetic-induced unconsciousness. Anaesth Analg 114:661–669.

Andrade R (2011) Serotonergic regulation of neuronal excitability in the prefrontal cortex. Neuropharmacology 61:382–386.

Applegate C, Tecott L (1998a) Global Increases in Seizure Susceptibility in Mice Lacking 5-HT 2C Receptors: A Behavioral Analysis. Exp Neurol 530:522–530.

Applegate CD, Tecott LH (1998b) Global increases in seizure susceptibility in mice lacking 5-HT2C receptors: a behavioral analysis. Exp Neurol 154:522–530.

Araneda R, Andrade R (1991) 5-Hydroxytryptamine2 and 5-hydroxytryptamine1A receptors mediate opposing responses on membrane excitability in rat association cortex. Neuroscience 40:399–412.

Ashby R, Kasser J, Wang V, Rr G, Ashby CR, Jiang LH, Kasser RJ, Wang RY (1990) Electrophysiological characterization of 5-hydroxytryptamine2 receptors in the rat medial prefrontal cortex. J Pharmacol Exp Ther 252:171–178.

Avanzini G, de Curtis M, Marescaux C, Panzica F, Spreafico R, Vergnes M (1992) Role of the thalamic reticular nucleus in the generation of rhythmic thalamo-cortical activities subserving spike and waves. J Neural Transm Suppl 35:85–95.

Avanzini G, de Curtis M, Panzica F, Spreafico R (1989) Intrinsic properties of nucleus reticularis thalami neurones of the rat studied in vitro. J Physiol 416:111–122.

Avoli M (1980) Electroencephalographic and pathophysiologic features of rat parenteral penicillin epilepsy. Exp Neurol 69:373–382.

Avoli M (2012) A brief history on the oscillating roles of thalamus and cortex in absence seizures. Epilepsia 53:779–789.

Avoli M, Gloor P, Kostopoulos G, Gotman J (1983) An analysis of penicillin-induced generalized spike and wave discharges using simultaneous recordings of cortical and thalamic single neurons. J Neurophysiol.

Bachmann K, Jahn D, Yang C, Schwartz J (1988) Ethosuximide disposition kinetics in rats. Xenobiotica 18:373–380.

Bagdy G, Kecskemeti V, Riba P, Jakus R (2007) Serotonin and epilepsy. J Neurochem 100:857–873.

Bai X, Vestal M, Berman R, Negishi M, Spann M, Vega C, Desalvo M, Novotny EJ, Constable RT, Blumenfeld H (2010) Dynamic time course of typical childhood absence seizures: EEG, behavior, and functional magnetic resonance imaging. J Neurosci 30:5884–5893.

Bal T, Krosigk M von, McCormick D (1995a) Role of the ferret perigeniculate nucleus in the generation of synchronized oscillations in vitro. J Physiol 483 (Pt 3:665–685.

Bal T, McCormick DA (1993) Mechanisms of oscillatory activity in guinea-pig nucleus reticularis thalami in vitro: a mammalian pacemaker. J Physiol 468:669–691.

Bal T, von Krosigk M, McCormick D a (1995b) Synaptic and membrane mechanisms underlying synchronized oscillations in the ferret lateral geniculate nucleus in vitro. J Physiol 483:641–663.

Bancaud J (1969) Physiopathogenesis of generalized epilepsies of organic nature (stereoencephalographic study). In: The Physiopathogenesis of the Epilepsies, pp 158–185.

Banerjee PK, Hirsch E, Snead OC, Iii CS (1993) gamma-Hydroxybutyric acid induced spike and wave discharges in rats: relation to high-affinity [3H]gamma-hydroxybutyric acid binding sites in the thalamus and cortex. Neuroscience 56:11–21.

Banerjee PK, Snead OC (1992) Involvement of excitatory amino acid mechanisms in gamma-hydroxybutyrate model of generalized absence seizures in rats. Neuropharmacology 31:1009–1019.

Banerjee PK, Snead OC (1995a) Thalamic NMDA receptors in the gamma-hydroxybutyrate model of absence seizures: a cerebral microinjection study in rats. Neuropharmacology 34:43–53.

Banerjee PK, Snead OC (1995b) Presynaptic gamma-hydroxybutyric acid (GHB) and gamma-aminobutyric acidB (GABAB) receptor-mediated release of GABA and glutamate (GLU) in rat thalamic ventrobasal nucleus (VB): a possible mechanism for the generation of absence-like seizures induced by GH. J Pharmacol Exp … 273:1534–1543.

Banerjee PK, Snead OC (1998) Neuroactive steroids exacerbate gamma-hydroxybutyric acid-induced absence seizures in rats. Eur J Pharmacol 359:41–48.

Banerjee PK, Snead OCC (1994) Thalamic mediodorsal and intralaminar nuclear lesions disrupt the generation of experimentally induced generalized absence-like seizures in rats. Epilepsy Res 17:193–205.

Bay T, Eghorn LF, Klein AB, Wellendorph P (2014) GHB receptor targets in the CNS: focus on high-affinity binding sites. Biochem Pharmacol 87:220–228.

Bean BP (2007) The action potential in mammalian central neurons. Nat Rev Neurosci 8:451–465.

Bearden LJ, Snead OC, Healey CT, Pegram G V (1980) Antagonism of gamma-hydroxybutyric acid-induced frequency shifts in the cortical EEG of rats by dipropylacetate. Electroencephalogr Clin Neurophysiol 49:181–183.

Bécamel C, Gavarini S, Chanrion B, Alonso G, Galéotti N, Dumuis A, Bockaert J, Marin P (2004) The serotonin 5-HT2A and 5-HT2C receptors interact with specific sets of PDZ proteins. J Biol Chem 279:20257–20266.

Beenhakker MP, Huguenard JR (2009) Neurons that fire together also conspire together: is normal sleep circuitry hijacked to generate epilepsy? Neuron 62:612–632.

Beierlein M (2014) Synaptic mechanisms underlying cholinergic control of thalamic reticular nucleus neurons. J Physiol 592:4137–4145.

Béïque J-C, Campbell B, Perring P, Hamblin MW, Walker P, Mladenovic L, Andrade R (2004) Serotonergic regulation of membrane potential in developing rat prefrontal cortex: coordinated expression of 5-hydroxytryptamine (5-HT)1A, 5-HT2A, and 5-HT7 receptors. J Neurosci 24:4807–4817.

Belelli D, Peden DR, Rosahl TW, Wafford K a, Lambert JJ (2005) Extrasynaptic GABAA receptors of thalamocortical neurons: a molecular target for hypnotics. J Neurosci 25:11513–11520.

Bercovici E, Cortez MA, Wang X, Snead OC (2006) Serotonin depletion attenuates AY-9944-mediated atypical absence seizures. Epilepsia 47:240–246.

Berg AT, Berkovic SF, Brodie MJ, Buchhalter J, Cross JH, van Emde Boas W, Engel J, French J, Glauser T a, Mathern GW, Moshé SL, Nordli D, Plouin P, Scheffer IE (2010) Revised terminology and concepts for organization of seizures and epilepsies: report of the ILAE Commission on Classification and Terminology, 2005-2009. Epilepsia 51:676–685.

Berg AT, Scheffer IE (2011) New concepts in classification of the epilepsies: entering the 21st century. Epilepsia 52:1058–1062.

Berg AT, Shinnar S, Levy SR, Testa FM, Smith-Rapaport S, Beckerman B (2000) How well can epilepsy syndromes be identified at diagnosis? A reassessment 2 years after initial diagnosis. Epilepsia 41:1269–1275.

Berg K a, Maayani S, Goldfarb J, Scaramellini C, Leff P, Clarke WP (1998) Effector pathway-dependent relative efficacy at serotonin type 2A and 2C receptors: evidence for agonist-directed trafficking of receptor stimulus. Mol Pharmacol 54:94–104.

Berg KA, Dunlop J, Sanchez T, Silva M, Clarke WP (2008) A Conservative, Single-Amino Acid Substitution in the Second Cytoplasmic Domain of the Human Serotonin2C Receptor Alters Both Ligand-Dependent and -Independent Receptor Signaling. J Pharmacol Exp Ther 324:1084–1092.

Berg KA, Stout BD, Cropper JD, Maayani S, Clarke WP, Health T, Antonio S (1999) Novel Actions of Inverse Agonists on 5-HT 2C Receptor Systems. 872:863–872.

Berger M, Gray J a, Roth BL (2009) The expanded biology of serotonin. Annu Rev Med 60:355–366.

Bergstrom R a, Choi JH, Manduca A, Shin H-S, Worrell G a, Howe CL (2013) Automated identification of multiple seizure-related and interictal epileptiform event types in the EEG of mice. Sci Rep 3:1483.

Berkovic SF, Howell RA, Hay DA, Hopper JL (1998) Epilepsies in twins: genetics of the major epilepsy syndromes. Ann Neurol 43:435–445.

Berman R, Negishi M, Vestal M, Spann M, Chung MH, Bai X, Purcaro M, Motelow JE, Danielson N, Dix-Cooper L, Enev M, Novotny EJ, Constable RT, Blumenfeld H (2010) Simultaneous EEG, fMRI, and behavior in typical childhood absence seizures. Epilepsia 51:2011–2022.

Berridge M (1998) Neuronal calcium signaling. Neuron 21:13–26.

Bessaïh T, Bourgeais L, Badiu CI, Carter DA, Toth TI, Ruano D, Lambolez B, Crunelli V, Leresche N (2006) Nucleus-specific abnormalities of GABAergic synaptic transmission in a genetic model of absence seizures. J Neurophysiol 96:3074–3081.

Bista P, Meuth SG, Kanyshkova T, Cerina M, Pawlowski M, Ehling P, Landgraf P, Borsotto M, Heurteaux C, Pape H-C, Baukrowitz T, Budde T (2012) Identification of the muscarinic pathway underlying cessation of sleep-related burst activity in rat thalamocortical relay neurons. Pflugers Arch 463:89–102.

Black SW, Morairty SR, Chen T-M, Leung AK, Wisor JP, Yamanaka A, Kilduff TS (2014) GABAB Agonism Promotes Sleep and Reduces Cataplexy in Murine Narcolepsy. J Neurosci 34:6485–6494.

Blackburn TP (2009) Serotonin (5-Hydroxytryptamine; 5-HT): Receptors. In: Encyclopedia of Neuroscience, pp 701–714.

Blume WT, Lüders HO, Mizrahi E, Tassinari C, van Emde Boas W, Engel J (2001) Glossary of descriptive terminology for ictal semiology: report of the ILAE task force on classification and terminology. Epilepsia 42:1212–1218.

Blumenfeld H (2005) Cellular and network mechanisms of spike-wave seizures. Epilepsia 46 Suppl 9:21–33.

Blumenfeld H (2012) Impaired consciousness in epilepsy. Lancet Neurol 11:814–826.

Blumenfeld H, Meador KJ (2014) Consciousness as a useful concept in epilepsy classification. Epilepsia:1–6.

Bockaert J, Claeysen S, Bécamel C, Dumuis A, Marin P (2006) Neuronal 5-HT metabotropic receptors: fine-tuning of their structure, signaling, and roles in synaptic modulation. Cell Tissue Res 326:553–572.

Bonnycastle DD, Giarman NJ, Paasonen MK (1957) Anticonvulsant compounds and 5-hydroxytryptamine in rat brain. Br J Pharmacol Chemother 12:228–231.

Bradley PB, Engel G, Feniuk W, Fozard JR, Humphrey PP, Middlemiss DN, Mylecharane EJ, Richardson BP, Saxena PR (1986) Proposals for the classification and nomenclature of functional receptors for 5-hydroxytryptamine. Neuropharmacology 25:563–576.

Brickley SG, Mody I (2012) Extrasynaptic GABAA Receptors: Their Function in the CNS and Implications for Disease. Neuron 73:23–34.

Bromidge SM, Duckworth M, Forbes IT, Ham P, King FD, Thewlis KM, Blaney FE, Naylor CB, Blackburn TP, Kennett GA, Wood MD, Clarke SE (1997) 6-Chloro-5-methyl-1-[[2-[(2-methyl-3-pyridyl)oxy]-5-pyridyl]carbamoyl]- indoline (SB-242084): the first selective and brain penetrant 5-HT2C receptor antagonist. J Med Chem 40:3494–3496.

Bruno RM, Sakmann B (2006) Cortex is driven by weak but synchronously active thalamocortical synapses. Science 312:1622–1627.

Budde T, Munsch T, Pape H-C (1998) Distribution of L-type calcium channels in rat thalamic neurones. Eur J Neurosci 10:586–597.

Budde T, Sieg F, Braunewell K-H, Gundelfinger ED, Pape H-C (2000) Ca2+-Induced Ca2+ Release Supports the Relay Mode of Activity in Thalamocortical Cells. Neuron 26:483–492.

Burgess DL, Jones JM, Meisler MH, Noebels JL (1997) Mutation of the Ca2+ Channel β Subunit Gene Cchb4 Is Associated with Ataxia and Seizures in the Lethargic (lh) Mouse. Cell 88:385–392.

Buzsaki G (1991) The thalamic clock: emergent network properties. Neuroscience 41:351–364.

Cain SM, Snutch TP (2010) Contributions of T-type calcium channel isoforms to neuronal firing. Channels (Austin) 4:475–482.

Carai M a, Colombo G, Brunetti G, Melis S, Serra S, Vacca G, Mastinu S, Pistuddi a M, Solinas C, Cignarella G, Minardi G, Gessa GL (2001) Role of GABA(B) receptors in the sedative/hypnotic effect of gamma-hydroxybutyric acid. Eur J Pharmacol 428:315–321.

Carbone E, Lux HD (1984) A low voltage-activated, fully inactivating Ca channel in vertebrate sensory neurones. Nature 310:501–502.

Carmona RA, Hwang WL, B T (1999) Multi-Ridge Detection and Time-Frequency Reconstruction. IEEE Trans Biomed Eng 47:480–492.

Carter LP, Koek W, France CP (2006) Lack of effects of GHB precursors GBL and 1,4-BD following i.c.v. administration in rats. Eur J Neurosci 24:2595–2600.

Carter LP, Koek W, France CP (2009) Behavioral analyses of GHB: receptor mechanisms. Pharmacol Ther 121:100–114.

Cavaccini A, Yague JG, Errington AC, Crunelli V, Di Giovanni G (2012) Opposite effects of thalamic 5-HT2A and 5-HT2C receptor activation on tonic GABA-A inhibition: implications for absence epilepsy. In: SfN. New Orleans.

Cavdar S, Bay HH, Yildiz SD, Akakin D, Sirvanci S, Onat F (2014) Comparison of numbers of interneurons in three thalamic nuclei of normal and epileptic rats. Neurosci Bull 30:451–460.

Celada P, Puig MV, Artigas F (2013) Serotonin modulation of cortical neurons and networks. Front Integr Neurosci 7:25.

Chaurasia CS (1999) In vivo microdialysis sampling: theory and applications. Biomed Chromatogr 13:317–332.

Chaves J, Sander JW (2005) Seizure aggravation in idiopathic generalized epilepsies. Epilepsia 46 Suppl 9:133–139.

Chen KC, Höistad M, Kehr J, Fuxe K, Nicholson C (2002) Quantitative dual-probe microdialysis: Mathematical model and analysis. J Neurochem 81:94–107.

Chen Y, Lu J, Pan H, Zhang Y, Wu H, Xu K, Liu X, Jiang Y, Bao X, Yao Z, Ding K, Lo WHY, Qiang B, Chan P, Shen Y, Wu X (2003) Association between genetic variation of CACNA1H and childhood absence epilepsy. Ann Neurol 54:239–243.

Cheong E, Shin H-S (2013a) T-type Ca^{2+} channels in absence epilepsy. Biochim Biophys Acta 1828:1560–1571.

Cheong E, Shin H-S (2013b) T-type Ca2+ channels in normal and abnormal brain functions. Physiol Rev 93:961–992.

Cheong E, Shin H-S (2014) T-type Ca2+ channels in absence epilepsy. Pflugers Arch 466:719–734.

Cheong E, Zheng Y, Lee K, Lee J, Kim S, Sanati M, Lee S, Kim YSY-S, Shin H-SHS (2009) Deletion of phospholipase C β4 in thalamocortical relay nucleus leads to absence seizures. Proc Natl Acad Sci 106:21912.

Chipaux M, Vercueil L, Kaminska A, Mahon S, Charpier S (2013) Persistence of cortical sensory processing during absence seizures in human and an animal model: evidence from EEG and intracellular recordings. PLoS One 8:e58180.

Coenen a M, Drinkenburg WH, Inoue M, van Luijtelaar EL (1992) Genetic models of absence epilepsy, with emphasis on the WAG/Rij strain of rats. Epilepsy Res 12:75–86.

Coenen a ML, Van Luijtelaar ELJM (2003) Genetic animal models for absence epilepsy: a review of the WAG/Rij strain of rats. Behav Genet 33:635–655.

Cohen CJ, McCarthy RT, Barrett PQ, Rasmussen H (1988) Ca channels in adrenal glomerulosa cells: K+ and angiotensin II increase T-type Ca channel current. Proc Natl Acad Sci U S A 85:2412–2416.

Cohen H (2005) Anxiolytic effect and memory improvement in rats by antisense oligodeoxynucleotide to 5-hydroxytryptamine-2A precursor protein. Depress Anxiety 22:84–93.

Connelly WM, Fyson SJ, Errington AC, McCafferty CP, Cope DW, Di Giovanni G, Crunelli V (2013) GABAB Receptors Regulate Extrasynaptic GABAA Receptors. J Neurosci 33:3780–3785.

Constantinople CM, Bruno RM (2013) Deep cortical layers are activated directly by thalamus. Science 340:1591–1594.

Cope DW, Di Giovanni G, Fyson SJ, Orbán G, Errington AC, Lorincz ML, Gould TM, Carter DA, Crunelli V (2009) Enhanced tonic GABAA inhibition in typical absence epilepsy. Nat Med 15:1392–1398.

Cope DW, Hughes SW, Crunelli V (2005) GABAA receptor-mediated tonic inhibition in thalamic neurons. J Neurosci 25:11553–11563.

Cornea-Hébert V, Riad M, Wu C, Singh SK, Descarries L (1999) Cellular and subcellular distribution of the serotonin 5-HT2A receptor in the central nervous system of adult rat. J Comp Neurol 409:187–209.

Cortez MA, Snead OC (2006) Pharmacologic Models of Generalized Absence Seizures in Rodents. In: Models of Seizures and Epilepsy, pp 111–126. Academic Press.

Coulon P, Budde T, Pape H-C (2012) The sleep relay--the role of the thalamus in central and decentral sleep regulation. Pflugers Arch 463:53–71.

Coupar IM, Desmond P V, Irving HR (2007) Human 5-HT(4) and 5-HT(7) receptor splice variants: are they important? Curr Neuropharmacol 5:224–231.

Crabtree J, Isaac J (2002) New intrathalamic pathways allowing modality-related and cross-modality switching in the dorsal thalamus. J Neurosci 46:1–31.

Craig PJ, Beattie RE, Folly EA, Banerjee MD, Reeves MB, Priestley J V, Carney SL, Sher E, Perez-Reyes E, Volsen SG (1999) Distribution of the voltage-dependent calcium channel alpha1G subunit mRNA and protein throughout the mature rat brain. Eur J Neurosci 11:2949–2964.

Crandall SR, Govindaiah G, Cox CL (2010) Low-threshold Ca2+ current amplifies distal dendritic signaling in thalamic reticular neurons. J Neurosci 30:15419–15429.

Crunelli V, Cope DW, Terry JR (2011) Transition to absence seizures and the role of GABA(A) receptors. Epilepsy Res 97:283–289.

Crunelli V, David F, Lőrincz ML, Hughes SW (2015) The thalamocortical network as a single slow wave-generating unit. Curr Opin Neurobiol 31:72–80.

Crunelli V, Emri Z, Leresche N (2006) Unravelling the brain targets of gamma-hydroxybutyric acid. Curr Opin Pharmacol 6:44–52.

Crunelli V, Hughes SW (2010) The slow (<1 Hz) rhythm of non-REM sleep: a dialogue between three cardinal oscillators. Nat Neurosci 13:9–17.

Crunelli V, Leresche N (2002) Childhood absence epilepsy: genes, channels, neurons and networks. Nat Rev Neurosci 3:371–382.

Crunelli V, Tóth TI, Cope DW, Blethyn K, Hughes SW (2005) The "window" T-type calcium current in brain dynamics of different behavioural states. J Physiol 562:121–129.

Currier RD, Kooi KA, Saidman LJ (1963) PROGNOSIS OF "PURE" PETIT MAL; A FOLLOW-UP STUDY. Neurology 13:959–967.

Cymerblit-Sabba A, Schiller Y (2012) Development of hypersynchrony in the cortical network during chemoconvulsant-induced epileptic seizures in vivo. J Neurophysiol 107:1718–1730.

Dahlstroem A, Fuxe K (1964) EVIDENCE FOR THE EXISTENCE OF MONOAMINE-CONTAINING NEURONS IN THE CENTRAL NERVOUS SYSTEM. I. DEMONSTRATION OF MONOAMINES IN THE CELL BODIES OF BRAIN STEM NEURONS. Acta Physiol Scand Suppl:SUPPL 232:1–55.

Danober L, Depaulis A, Vergnes M, Marescaux C (1995) Mesopontine cholinergic control over generalized non-convulsive seizures in a genetic model of absence epilepsy in the rat. Neuroscience 69:1183–1193.

Danober L, Deransart C, Depaulis A, Vergnes M, Marescaux C (1998) Pathophysiological mechanisms of genetic absence epilepsy in the rat. Prog Neurobiol 55:27–57.

Danober L, Vergnes M, Depaulis A, Marescaux C (1994) Nucleus basalis lesions suppress spike and wave discharges in rats with spontaneous absence-epilepsy. Neuroscience 59:531–539.

David F, Schmiedt JT, Taylor HL, Orban G, Di Giovanni G, Uebele VN, Renger JJ, Lambert RC, Leresche N, Crunelli V (2013) Essential thalamic contribution to slow waves of natural sleep. J Neurosci 33:19599–19610.

De Deurwaerdère P, Navailles S, Berg K a, Clarke WP, Spampinato U (2004) Constitutive activity of the serotonin2C receptor inhibits in vivo dopamine release in the rat striatum and nucleus accumbens. J Neurosci 24:3235–3241.

Deleuze C, David F, Béhuret S, Sadoc G, Shin H-S, Uebele VN, Renger JJ, Lambert RC, Leresche N, Bal T (2012) T-type calcium channels consolidate tonic action potential output of thalamic neurons to neocortex. J Neurosci 32:12228–12236.

Deleuze C, Huguenard JR (2006) Distinct electrical and chemical connectivity maps in the thalamic reticular nucleus: potential roles in synchronization and sensation. J Neurosci 26:8633–8645.

Deng F, Price MG, Davis CF, Mori M, Burgess DL (2006) Stargazin and other transmembrane AMPA receptor regulating proteins interact with synaptic scaffolding protein MAGI-2 in brain. J Neurosci 26:7875–7884.

Depaulis A, Luijtellar G van (2006) Genetic Models of Absence Epilepsy in the Rat. In: Models of Seizures and Epilepsy, pp 233 – VI. Elsevier.

Depaulis A, Snead OC, Marescaux C, Vergnes M (1989) Suppressive effects of intranigral injection of muscimol in three models of generalized non-convulsive epilepsy induced by chemical agents. Brain Res 498:64–72.

Desîlets-Roy B, Varga C, Lavallée P, Deschênes M (2002) Substrate for cross-talk inhibition between thalamic barreloids. J Neurosci 22:RC218.

Dezsi G, Ozturk E, Stanic D, Powell KL, Blumenfeld H, O'Brien TJ, Jones NC (2013) Ethosuximide reduces epileptogenesis and behavioral comorbidity in the GAERS model of genetic generalized epilepsy. Epilepsia 54:1–9.

Di Giovanni G, Di Matteo V, Pierucci M, Benigno A, Esposito E (2006) Central serotonin2C receptor: from physiology to pathology. Curr Top Med Chem 6:1909–1925.

Di Matteo V, De Blasi A, Di Giulio C, Esposito E (2001) Role of 5-HT2C receptors in the control of central dopamine function. Trends Pharmacol Sci 22:229–232.

DiMario FJ, Clancy RR (1988) Paradoxical precipitation of tonic seizures by lorazepam in a child with atypical absence seizures. Pediatr Neurol 4:249–251.

Doherty J, Hattox S, Snead O, Roth R (1978) Identification of endogenous gamma-hydroxybutyrate in human and bovine brain and its regional distribution in human, guinea pig and rhesus monkey brain. J Pharmacol Exp Ther.

Domich L, Oakson G, Steriade M (1986) Thalamic burst patterns in the naturally sleeping cat: a comparison between cortically projecting and reticularis neurones. J Physiol 379:429–449.

Doyle J, Ren X, Lennon G, Stubbs L (1997) Mutations in the Cacnl1a4 calcium channel gene are associated with seizures, cerebellar degeneration, and ataxia in tottering and leaner mutant mice. Mamm Genome 8:113–120.

Drasbek KR, Hoestgaard-jensen K, Jensen K (2007) Modulation of Extrasynaptic THIP Conductances by GABA A -Receptor Modulators in Mouse Neocortex. :2293–2300.

Dreyfus FM, Tscherter A, Errington AC, Renger JJ, Shin H-S, Uebele VN, Crunelli V, Lambert RC, Leresche N (2010) Selective T-type calcium channel block in thalamic neurons reveals channel redundancy and physiological impact of I(T)window. J Neurosci 30:99–109.

Drinkenburg W, Schuurmans M (2003) Information Processing During Spike–Wave Discharges. Behav Brain:1–10.

Drinkenburg WHIM, Schuurmans MLEJ, Coenen AML, Vossen JMH, van Luijtelaar ELJM (2003) Ictal stimulus processing during spike-wave discharges in genetic epileptic rats. Behav Brain Res 143:141–146.

Dudley MW, Wiech NL, Miller FP, Carr AA, Cheng HC, Roebel LE, Doherty NS, Yamamura HI, Ursillo RC, Palfreyman MG (1988) Pharmacological effects of MDL 11,939: A selective, centrally acting antagonist of 5-HT2 receptors. Drug Dev Res 13:29–43.

Dunlop J, Watts S, Barrett J (2011) Characterization of vabicaserin (SCA-136), a selective 5-hydroxytryptamine 2C receptor agonist. J Pharmacol Exp Ther.

Egan CT, Herrick-Davis K, Miller K, Glennon R a, Teitler M (1998) Agonist activity of LSD and lisuride at cloned 5HT2A and 5HT2C receptors. Psychopharmacology (Berl) 136:409–414.

Emri Z, Antal K, Crunelli V (1996) Gamma-hydroxybutyric acid decreases thalamic sensory excitatory postsynaptic potentials by an action on presynaptic GABAB receptors. Neurosci Lett 216:121–124.

Engel J (2001) A proposed diagnostic scheme for people with epileptic seizures and with epilepsy: report of the ILAE Task Force on Classification and Terminology. Epilepsia 42:796–803.

Entholzner E, Mielke L, Pichlmeier R, Weber F, Schneck H (1995) [EEG changes during sedation with gamma-hydroxybutyric acid]. Anaesthesist 44:345–350.

Ernst WL, Zhang Y, Yoo JW, Ernst SJ, Noebels JL (2009) Genetic enhancement of thalamocortical network activity by elevating alpha 1g-mediated low-voltage-activated calcium current induces pure absence epilepsy. J Neurosci 29:1615–1625.

Errington AC, Cope DW, Crunelli V (2011) Augmentation of Tonic GABA(A) Inhibition in Absence Epilepsy: Therapeutic Value of Inverse Agonists at Extrasynaptic GABA(A) Receptors. Adv Pharmacol Sci 2011:790590.

Errington AC, Hughes SW, Crunelli V (2012) Rhythmic dendritic Ca2+ oscillations in thalamocortical neurons during slow non-REM sleep-related activity in vitro. J Physiol 590:3691–3700.

Errington AC, Renger JJ, Uebele VN, Crunelli V (2010) State-dependent firing determines intrinsic dendritic Ca2+ signaling in thalamocortical neurons. J Neurosci 30:14843–14853.

Etter L, Mulley JC, Heron SE, Wallace RH, Gecz J, Dibbens LM (2011) “Blinders, phenotype, and fashionable genetic analysis”: setting the record straight for epilepsy! Epilepsia 52:1757–1758.

Fantegrossi WE, Murnane KS, Reissig CJ (2008) The behavioral pharmacology of hallucinogens. Biochem Pharmacol 75:17–33.

Fariello RG, Golden GT (1987) The THIP-induced model of bilateral synchronous spike and wave in rodents. Neuropharmacology 26:161–165.

Farrant M, Kaila K (2007) The cellular, molecular and ionic basis of GABAA receptor signalling. Prog Brain Res 160:59–87.

Farrant M, Nusser Z (2005) Variations on an inhibitory theme: phasic and tonic activation of GABA(A) receptors. Nat Rev Neurosci 6:215–229.

Faulhaber J, Steiger A, Lancel M (1997) The GABA A agonist THIP produces slow wave sleep and reduces spindling activity in NREM sleep in humans. Psychopharmacology (Berl) 130:285–291.

FDA (2010) FDA Briefing Document NDA 22529 Lorqess (lorcaserin hydrochloride).

FDA (2012) FDA Briefing Document NDA 22529 Lorcaserin Hydrochloride.

Fedulova SA, Kostyuk PG, Veselovsky NS (1985) Two types of calcium channels in the somatic membrane of new-born rat dorsal root ganglion neurones. J Physiol 359:431–446.

Feldmeyer D (2012) Excitatory neuronal connectivity in the barrel cortex. Front Neuroanat 6:24.

Feldmeyer D, Brecht M, Helmchen F, Petersen CCH, Poulet JF a, Staiger JF, Luhmann HJ, Schwarz C (2013) Barrel cortex function. Prog Neurobiol 103:3–27.

Fink H, Morgenstern R (1985) Locomotor effects of lisuride: a consequence of dopaminergic and serotonergic actions. Psychopharmacology (Berl) 85:464–468.

Fiset P, Paus T, Daloze T, Plourde G, Meuret P, Bonhomme V, Hajj-Ali N, Backman SB, Evans a C (1999) Brain mechanisms of propofol-induced loss of consciousness in humans: a positron emission tomographic study. J Neurosci 19:5506–5513.

Fisher R, Boas W, Blume W, Elger C (2005) Epileptic seizures and epilepsy: definitions proposed by the International League Against Epilepsy (ILAE) and the International Bureau for Epilepsy (IBE). … 46:1698–1699; author reply 1701–1702.

Fisher RS, Prince DA (1977) Spike-wave rhythms in cat cortex induced by parenteral penicillin. II. Cellular features. Electroencephalogr Clin Neurophysiol 42:625–639.

Fletcher CF, Lutz CM, O'Sullivan TN, Shaughnessy JD, Hawkes R, Frankel WN, Copeland NG, Jenkins NA (1996) Absence epilepsy in tottering mutant mice is associated with calcium channel defects. Cell 87:607–617.

Fletcher PJ, Chintoh AF, Sinyard J, Higgins G a (2004) Injection of the 5-HT2C receptor agonist Ro60-0175 into the ventral tegmental area reduces cocaine-induced locomotor activity and cocaine self-administration. Neuropsychopharmacology 29:308–318.

Fletcher PJ, Grottick AJ, Higgins GA (2002) Differential effects of the 5-HT(2A) receptor antagonist M100907 and the 5-HT(2C) receptor antagonist SB242084 on cocaine-induced locomotor activity, cocaine self-administration and cocaine-induced reinstatement of responding. Neuropsychopharmacology 27:576–586.

Fletcher PJ, Tampakeras M, Sinyard J, Slassi A, Isaac M, Higgins GA (2009) Characterizing the effects of 5-HT(2C) receptor ligands on motor activity and feeding behaviour in 5-HT(2C) receptor knockout mice. Neuropharmacology 57:259–267.

Fox MA, French HT, LaPorte JL, Blackler AR, Murphy DL (2010) The serotonin 5-HT(2A) receptor agonist TCB-2: a behavioral and neurophysiological analysis. Psychopharmacology (Berl) 212:13–23.

Frank MG, Stryker MP, Tecott LH (2002) Sleep and sleep homeostasis in mice lacking the 5-HT2c receptor. Neuropsychopharmacology 27:869–873.

Franks NP (2008) General anaesthesia: from molecular targets to neuronal pathways of sleep and arousal. Nat Rev Neurosci 9:370–386.

Friedman A, Gutnick MJ (1987) Low-threshold calcium electrogenesis in neocortical neurons. Neurosci Lett 81:117–122.

Fuentealba P, Steriade M (2005) The reticular nucleus revisited: intrinsic and network properties of a thalamic pacemaker. Prog Neurobiol 75:125–141.

Gaddum JH, Picarelli ZP (1957) Two kinds of tryptamine receptor. Br J Pharmacol Chemother 12:323–328.

Garcia EE, Smith RL, Sanders-Bush E (2007) Role of G(q) protein in behavioral effects of the hallucinogenic drug 1-(2,5-dimethoxy-4-iodophenyl)-2-aminopropane. Neuropharmacology 52:1671–1677.

Gervasi N, Monnier Z, Vincent P, Paupardin-Tritsch D, Hughes SW, Crunelli V, Leresche N (2003) Pathway-specific action of gamma-hydroxybutyric acid in sensory thalamus and its relevance to absence seizures. J Neurosci 23:11469–11478.

Gharedaghi MH, Seyedabadi M, Ghia J-E, Dehpour AR, Rahimian R (2014) The role of different serotonin receptor subtypes in seizure susceptibility. Exp brain Res 232:347–367.

Giaretta D, Avoli M, Gloor P (1987) Intracellular recordings in pericruciate neurons during spike and wave discharges of feline generalized penicillin epilepsy. Brain Res 405:68–79.

Giorgetti M, Tecott LH (2004) Contributions of 5-HT(2C) receptors to multiple actions of central serotonin systems. Eur J Pharmacol 488:1–9.

Glauser T a, Cnaan A, Shinnar S, Hirtz DG, Dlugos D, Masur D, Clark PO, Adamson PC (2013) Ethosuximide, valproic acid, and lamotrigine in childhood absence epilepsy: initial monotherapy outcomes at 12 months. Epilepsia 54:141–155.

Glauser T a, Cnaan A, Shinnar S, Hirtz DG, Dlugos D, Masur D, Clark PO, Capparelli E V, Adamson PC (2010) Ethosuximide, valproic acid, and lamotrigine in childhood absence epilepsy. N Engl J Med 362:790–799.

Glauser T, Ben-Menachem E, Bourgeois B, Cnaan A, Chadwick D, Guerreiro C, Kalviainen R, Mattson R, Perucca E, Tomson T (2006) ILAE treatment guidelines: evidence-based analysis of antiepileptic drug efficacy and effectiveness as initial monotherapy for epileptic seizures and syndromes. Epilepsia 47:1094–1120.

Gloor P (1968) Generalized cortico-reticular epilepsies. Some considerations on the pathophysiology of generalized bilaterally synchronous spike and wave discharge. Epilepsia 9:249–263.

Glykys J, Mody I (2007) Activation of GABAA receptors: views from outside the synaptic cleft. Neuron 56:763–770.

Godschalk M, Dzoljic M, Bonta I (1976) Antagonism of gamma-hydroxybutyrate-induced hypersynchronization in the ECoG of the rat by anti-petit mal drugs. Neurosci Lett 3.

Godschalk M, Dzoljic M, Bonta I (1977) Slow wave sleep and a state resembling absence epilepsy induced in the rat by gamma-hydroxybutyrate. Eur J Pharmacol 44:105–111.

González-Maeso J, Ang RL, Yuen T, Chan P, Weisstaub N V, López-Giménez JF, Zhou M, Okawa Y, Callado LF, Milligan G, Gingrich JA, Filizola M, Meana JJ, Sealfon SC (2008) Identification of a serotonin/glutamate receptor complex implicated in psychosis. Nature 452:93–97.

González-Maeso J, Sealfon SC (2009) Agonist-trafficking and hallucinogens. Curr Med Chem 16:1017–1027.

González-Maeso J, Weisstaub N V, Zhou M, Chan P, Ivic L, Ang R, Lira A, Bradley-Moore M, Ge Y, Zhou Q, Sealfon SC, Gingrich JA (2007) Hallucinogens recruit specific cortical 5-HT(2A) receptor-mediated signaling pathways to affect behavior. Neuron 53:439–452.

Groenewegen HJ, Witter MP (2004) Thalamus. In: The Rat Nervous System, pp 407–453. Elsevier.

Guberman A, Gloor P, Sherwin AL (1975) Response of generalized penicillin epilepsy in the cat to ethosuximide and diphenylhydantoin. Neurology 25:785–64.

Guyon A, Leresche N (1995) Modulation by different GABAB receptor types of voltage-activated calcium currents in rat thalamocortical neurones. J Physiol 485 (Pt 1:29–42.

Hagiwara S, Ozawa S, Sand O (1975) Voltage clamp analysis of two inward current mechanisms in the egg cell membrane of a starfish. J Gen Physiol 65:617–644.

Halász P, Terzano MG, Parrino L (2002) Spike-wave discharge and the microstructure of sleep-wake continuum in idiopathic generalised epilepsy. Neurophysiol Clin 32:38–53.

Hannon J, Hoyer D (2008) Molecular biology of 5-HT receptors. Behav Brain Res 195:198–213.

Harang R, Bonnet G, Petzold LR (2012) WAVOS: a MATLAB toolkit for wavelet analysis and visualization of oscillatory systems. BMC Res Notes 5:163.

Harris K, Henze D (2000) Accuracy of tetrode spike separation as determined by simultaneous intracellular and extracellular measurements. J Neurophysiol.

Harris RM, Hendrickson AE (1987) Local circuit neurons in the rat ventrobasal thalamus--a GABA immunocytochemical study. Neuroscience 21:229–236.

Hazan L, Zugaro M, Buzsáki G (2006) Klusters, NeuroScope, NDManager: A free software suite for neurophysiological data processing and visualization. J Neurosci Methods 155:207–216.

Heisler L, Chu H, Tecott L (1998) Epilepsy and obesity in serotonin 5-HT2C receptor mutant mice. Ann N Y Acad Sci.

Hempelmann A, Cobilanschi J, Heils A, Muhle H, Stephani U, Weber Y, Lerche H, Sander T (2007) Lack of evidence of an allelic association of a functional GABRB3 exon 1a promoter polymorphism with idiopathic generalized epilepsy. Epilepsy Res 74:28–32.

Hernández-Cruz A, Pape HC (1989) Identification of two calcium currents in acutely dissociated neurons from the rat lateral geniculate nucleus. J Neurophysiol 61:1270–1283.

Heron SE, Khosravani H, Varela D, Bladen C, Williams TC, Newman MR, Scheffer IE, Berkovic SF, Mulley JC, Zamponi GW (2007a) Extended spectrum of idiopathic generalized epilepsies associated with CACNA1H functional variants. Ann Neurol 62:560–568.

Heron SE, Sanchez L, Scheffer IE, Berkovic SF, Mulley JC (2007b) Association studies and functional validation or functional validation alone? Epilepsy Res 74:237–238.

Herrmann WM, Horowski R, Dannehl K, Kramer U, Lurati K (1977) Clinical Effectiveness of Lisuride Hydrogen Maleate: A Double-Blind Trial Versus Methysergide. Headache J Head Face Pain 17:54–60.

Higgins G a, Fletcher PJ (2003) Serotonin and drug reward: focus on 5-HT2C receptors. Eur J Pharmacol 480:151–162.

Higgins G a, Sellers EM, Fletcher PJ (2013a) From obesity to substance abuse: therapeutic opportunities for 5-HT2C receptor agonists. Trends Pharmacol Sci 34:560–570.

Higgins G a, Silenieks LB, Lau W, de Lannoy I a M, Lee DKH, Izhakova J, Coen K, Le a D, Fletcher PJ (2013b) Evaluation of chemically diverse 5-HT_2c receptor agonists on behaviours motivated by food and nicotine and on side effect profiles. Psychopharmacology (Berl) 226:475–490.

Higgins G a, Silenieks LB, Rossmann A, Rizos Z, Noble K, Soko AD, Fletcher PJ (2012) The 5-HT2C receptor agonist lorcaserin reduces nicotine self-administration, discrimination, and reinstatement: relationship to feeding behavior and impulse control. Neuropsychopharmacology 37:1177–1191.

Higgins GA, Ouagazzal AM, Grottick AJ (2001) Influence of the 5-HT(2C) receptor antagonist SB242,084 on behaviour produced by the 5-HT(2) agonist Ro60-0175 and the indirect 5-HT agonist dexfenfluramine. Br J Pharmacol 133:459–466.

Hinton T, Johnston G (2009) Anxiolytic and Hypnotic Drugs Acting on Ionotropic GABA Receptors. Encycl Neurosci.

Höcht C, Opezzo J, Taira C (2007) Applicability of reverse microdialysis in pharmacological and toxicological studies. … Pharmacol Toxicol … 55:3–15.

Hofmann F, Biel M, Flockerzi V (1994) Molecular basis for Ca2+ channel diversity. Annu Rev Neurosci 17:399–418.

Holmes MD, Brown M, Tucker DM (2004) Are “generalized” seizures truly generalized? Evidence of localized mesial frontal and frontopolar discharges in absence. Epilepsia 45:1568–1579.

Horita H, Uchida E, Maekawa K (1991) Circadian rhythm of regular spike-wave discharges in childhood absence epilepsy. Brain Dev 13:200–202.

Hoyer D, Hannon JP, Martin GR (2002) Molecular, pharmacological and functional diversity of 5-HT receptors. Pharmacol Biochem Behav 71:533–554.

Hoyer D, Martin G (1997) 5-HT receptor classification and nomenclature: towards a harmonization with the human genome. Neuropharmacology 36:419–428.

Hu RQ, Banerjee PK, Snead OC (2000) Regulation of gamma-aminobutyric acid (GABA) release in cerebral cortex in the gamma-hydroxybutyric acid (GHB) model of absence seizures in rat. Neuropharmacology 39:427–439.

Hu RQ, Cortez MA, Man HY, Roder J, Jia Z, Wang YT, Snead OC (2001) Gamma-hydroxybutyric acid-induced absence seizures in GluR2 null mutant mice. Brain Res 897:27–35.

Hu X, Dong J, Wang X, Wu T, Yang L, Lu X (2011) Localization of epileptic foci in Children with childhood absence epilepsy by magnetoencephalography combined with synthetic aperture magnetometry. J Biomed Res 25:259–265.

Hughes S, Cope D, Blethyn K, Crunelli V (2002) Cellular Mechanisms of the Slow (<1 Hz) Oscillation in Thalamocortical Neurons In Vitro. Neuron 33:947–958.

Hughes S, Lörincz M, Cope D (2004) Synchronized oscillations at α and θ frequencies in the lateral geniculate nucleus. Neuron 42:253–268.

Hughes SW, Cope DW, Tóth TI, Williams SR, Crunelli V (1999) All thalamocortical neurones possess a T-type Ca2+ “window” current that enables the expression of bistability-mediated activities. J Physiol 517 (Pt 3:805–815.

Hughes SW, Crunelli V (2005) Thalamic mechanisms of EEG alpha rhythms and their pathological implications. Neuroscientist 11:357–372.

Hughes SW, Errington A, Lorincz ML, Kékesi K a, Juhász G, Orbán G, Cope DW, Crunelli V (2008) Novel modes of rhythmic burst firing at cognitively-relevant frequencies in thalamocortical neurons. Brain Res 1235:12–20.

Huguenard JR (1996) Low-threshold calcium currents in central nervous system neurons. Annu Rev Physiol 58:329–348.

Huguenard JR, Coulter DA, Prince DA (1991) A fast transient potassium current in thalamic relay neurons: kinetics of activation and inactivation. J Neurophysiol 66:1304–1315.

Huguenard JR, McCormick D a (2007) Thalamic synchrony and dynamic regulation of global forebrain oscillations. Trends Neurosci 30:350–356.

Huguenard JR, Prince D a (1992) A novel T-type current underlies prolonged Ca(2+)-dependent burst firing in GABAergic neurons of rat thalamic reticular nucleus. J Neurosci 12:3804–3817.

Humphrey PPA, Hartig P, Hoyer D (1993) A proposed new nomenclature for 5-HT receptors. Trends Pharmacol Sci 14:233–236.

Huotari a.-M (2004) Evoked EEG patterns during burst suppression with propofol. Br J Anaesth 92:18–24.

Iatsenko D, McClintock P, Stefanovska A (2013a) Linear and synchrosqueezed time-frequency representations revisited. Part I: Overview, standards of use, related issues and algorithms. arXiv Prepr arXiv.

Iatsenko D, McClintock P, Stefanovska A (2013b) Linear and synchrosqueezed time-frequency representations revisited. Part II: Resolution, reconstruction and concentration. arXiv Prepr arXiv.

Iatsenko D, McClintock P, Stefanovska A (2013c) On the extraction of instantaneous frequencies from ridges in time-frequency representations of signals. arXiv Prepr arXiv.

Imbrici P, Jaffe SL, Eunson LH, Davies NP, Herd C, Robertson R, Kullmann DM, Hanna MG (2004) Dysfunction of the brain calcium channel CaV2.1 in absence epilepsy and episodic ataxia. Brain 127:2682–2692.

Ingram EM, Tessler S, Bowery NG, Emson PC (2000) Glial glutamate transporter mRNAs in the genetically absence epilepsy rat from Strasbourg. Brain Res Mol Brain Res 75:96–104.

Inoue M, Ates N, Vossen JM, Coenen a M (1994) Effects of the neuroleptanalgesic fentanyl-fluanisone (Hypnorm) on spike-wave discharges in epileptic rats. Pharmacol Biochem Behav 48:547–551.

Inoue M, Duysens J, Vossen JM, Coenen AM (1993) Thalamic multiple-unit activity underlying spike-wave discharges in anaesthetized rats. Brain Res 612:35–40.

Isaac M (2005) Serotonergic 5-HT2C receptors as a potential therapeutic target for the design antiepileptic drugs. Curr Top Med Chem 5:59–67.

Ishige K, Aizawa M, Ito Y, Fukuda H (1996) gamma-Butyrolactone-induced absence-like seizures increase nuclear CRE- and AP-1 DNA-binding activities in mouse brain. Neuropharmacology 35:45–55.

Jahnsen H, Llinás R (1984) Electrophysiological properties of guinea-pig thalamic neurones: an in vitro study. J Physiol 349:205–226.

Jakus R, Graf M, Juhasz G, Gerber K, Levay G, Halasz P, Bagdy G (2003) 5-HT2C receptors inhibit and 5-HT1A receptors activate the generation of spike-wave discharges in a genetic rat model of absence epilepsy. Exp Neurol 184:964–972.

Jallon P, Loiseau P, Loiseau J (2001) Newly diagnosed unprovoked epileptic seizures: presentation at diagnosis in CAROLE study. Coordination Active du Réseau Observatoire Longitudinal de l' Epilepsie. Epilepsia 42:464–475.

Jensen K, Mody I (2001) GHB depresses fast excitatory and inhibitory synaptic transmission via GABA(B) receptors in mouse neocortical neurons. Cereb Cortex 11:424–429.

Jia F, Yue M, Chandra D, Homanics GE, Goldstein P a, Harrison NL (2008) Isoflurane is a potent modulator of extrasynaptic GABA(A) receptors in the thalamus. J Pharmacol Exp Ther 324:1127–1135.

Jones EG (2002) Thalamic circuitry and thalamocortical synchrony. Philos Trans R Soc Lond B Biol Sci 357:1659–1673.

Jones EG (2009) Synchrony in the interconnected circuitry of the thalamus and cerebral cortex. Ann N Y Acad Sci 1157:10–23.

Jones NC, O'Brien TJ, Powell KL (2011) Morphometric changes and molecular mechanisms in rat models of idiopathic generalized epilepsy with absence seizures. Neurosci Lett 497:185–193.

Jones NC, Salzberg MR, Kumar G, Couper A, Morris MJ, O'Brien TJ (2008) Elevated anxiety and depressive-like behavior in a rat model of genetic generalized epilepsy suggesting common causation. Exp Neurol 209:254–260.

Jouvenceau A, Eunson LH, Spauschus A, Ramesh V, Zuberi SM, Kullmann DM, Hanna MG (2001) Human epilepsy associated with dysfunction of the brain P/Q-type calcium channel. Lancet 358:801–807.

Kammermeier PJ, Jones SW (1997) High-voltage-activated calcium currents in neurons acutely isolated from the ventrobasal nucleus of the rat thalamus. J Neurophysiol 77:465–475.

Kang J-Q, Kang J, Macdonald RL (2004) The GABAA receptor gamma2 subunit R43Q mutation linked to childhood absence epilepsy and febrile seizures causes retention of alpha1beta2gamma2S receptors in the endoplasmic reticulum. J Neurosci 24:8672–8677.

Kantor S, Jakus R, Molnar E, Gyongyosi N, Toth A, Detari L, Bagdy G (2005) Despite similar anxiolytic potential, the 5-hydroxytryptamine 2C receptor antagonist SB-242084 [6-chloro-5-methyl-1-[2-(2-methylpyrid-3-yloxy)-pyrid-5-yl carbamoyl] indoline] and chlordiazepoxide produced differential effects on electroencephalogram power. J Pharmacol Exp Ther 315:921–930.

Kaupmann K, John F, Wellendorph P, Mombereau C, Sansig G, Klebs K, Schmutz M, Froestl W, Putten H Van Der, Mosbacher J, Bra H, Waldmeier P, Bettler B, Cryan JF, van der Putten H, Bräuner-Osborne H (2003) Specific gamma-hydroxybutyrate-binding sites but loss of pharmacological effects of gamma-hydroxybutyrate in GABA(B)(1)-deficient mice. Eur J Neurosci 18:2722–2730.

Kehne JH, Baron BM, Carr AA, Chaney SF, Elands J, Feldman DJ, Frank RA, van Giersbergen PL, McCloskey TC, Johnson MP, McCarty DR, Poirot M, Senyah Y, Siegel BW, Widmaier C, Chaney F, Johnson P, Feldman J, Roussel M (1996) Preclinical characterization of the potential of the putative atypical antipsychotic MDL 100,907 as a potent 5-HT2A antagonist with a favorable CNS safety profile. J Pharmacol Exp Ther 277:968–981.

Kennard JTT, Barmanray R, Sampurno S, Ozturk E, Reid CA, Paradiso L, D'Abaco GM, Kaye AH, Foote SJ, O'Brien TJ, Powell KL (2011) Stargazin and AMPA receptor membrane expression is increased in the somatosensory cortex of Genetic Absence Epilepsy Rats from Strasbourg. Neurobiol Dis 42:48–54.

Kennett GA, Wood MD, Bright F, Trail B, Riley G, Holland V, Avenell KY, Stean T, Upton N, Bromidge S, Forbes IT, Brown AM, Middlemiss DN, Blackburn TP (1997) SB 242084, a selective and brain penetrant 5-HT2C rec eptor antagonist. Neuropharmacology 36:609–620.

Killory BD, Bai X, Negishi M, Vega C, Spann MN, Vestal M, Guo J, Berman R, Danielson N, Trejo J, Shisler D, Novotny EJ, Constable RT, Blumenfeld H (2011) Impaired attention and network connectivity in childhood absence epilepsy. Neuroimage 56:2209–2217.

Kim D, Song I, Keum S, Lee T, Jeong MJ, Kim SS, McEnery MW, Shin HS (2001) Lack of the burst firing of thalamocortical relay neurons and resistance to absence seizures in mice lacking alpha(1G) T-type Ca(2+) channels. Neuron 31:35–45.

Kim U, Sanchez-Vives M, McCormick D (1997) Functional dynamics of GABAergic inhibition in the thalamus. Science (80-) 278:130–134.

Kimura A, Imbe H, Donishi T, Tamai Y (2007) Axonal projections of single auditory neurons in the thalamic reticular nucleus: implications for tonotopy-related gating function and cross-modal modulation. Eur J Neurosci 26:3524–3535.

Kimura A, Stevenson PL, Carter RN, MacColl G, French KL, Paul Simons J, Al-Shawi R, Kelly V, Chapman KE, Holmes MC, Atsuko Kimura PLSRNCGMKLFJPSRA-SVKKECMCH (2009) Overexpression of 5-HT2C receptors in forebrain leads to elevated anxiety and hypoactivity. Eur J Neurosci 30:299–306.

Kleinschmidt S, Mertzlufft F (1995) Gamma-hydroxybutyric acid--significance for anaesthesia and intensive care medicine?. Anasthesiol Intensivmed Notfallmed Schmerzther 30:393–402.

Krogsgaard-Larsen P, Frølund B, Liljefors T, Ebert B (2004) GABA(A) agonists and partial agonists: THIP (Gaboxadol) as a non-opioid analgesic and a novel type of hypnotic. Biochem Pharmacol 68:1573–1580.

Krout KE, Belzer RE, Loewy AD (2002) Brainstem projections to midline and intralaminar thalamic nuclei of the rat. J Comp Neurol 448:53–101.

Kulik A, Nakadate K, Nyiri G, Notomi T, Malitschek B, Bettler B, Shigemoto R, Nyíri G (2002) Distinct localization of GABA(B) receptors relative to synaptic sites in the rat cerebellum and ventrobasal thalamus. Eur J Neurosci 15:291–307.

Kumaresan S, David J, Joseph T (2000) Comparative profiles of sodium valproate and ethosuximide on electro-behavioural correlates in gamma-hydroxybutyrate and pentylenetetrazol induced absence seizures in rats. Indian J Physiol Pharmacol 44:411–418.

Kurrasch-Orbaugh DM, Parrish JC, Watts VJ, Nichols DE (2003) A complex signaling cascade links the serotonin2A receptor to phospholipase A2 activation: the involvement of MAP kinases. J Neurochem 86:980–991.

Kurrasch-orbaugh DM, Watts VALJ, Barker EL, Nichols DE (2003) Phospholipase C and Phospholipase A 2 Signaling Pathways Have Different Receptor Reserves. 304:229–237.

Laborit G, KIND A, DE LEON REGIL C (1961) 220 cases of anaesthesia in neurosurgery with sodium 4-hydroxybutyrate. Presse Med 69:1216–1217.

Laborit H (1964) Sodium 4-hydroxybutyrate. Int J Neuropharmacol 3:433–451.

Laborit H, Jouany JM, Gerard J, Fabiani F (1960) Generalities concerning the experimental study and clinical use of gamma hydroxybutyrate of Na. Agressologie 1:397–406.

Lachance-Touchette P, Martin C, Poulin C, Gravel M, Carmant L, Cossette P (2010) Screening of GABRB3 in French-Canadian families with idiopathic generalized epilepsy. Epilepsia 51:1894–1897.

Lam Y-W, Sherman SM (2007) Different topography of the reticulothalmic inputs to first- and higher-order somatosensory thalamic relays revealed using photostimulation. J Neurophysiol 98:2903–2909.

Lam Y-W, Sherman SM (2011) Functional organization of the thalamic input to the thalamic reticular nucleus. J Neurosci 31:6791–6799.

Lambert RC, Bessaïh T, Crunelli V, Leresche N (2014) The many faces of T-type calcium channels. Pflugers Arch 466:415–423.

Lancel M, Faulhaber J (1996) The GABAA agonist THIP (gaboxadol) increases non-REM sleep and enhances delta activity in the rat. Neuroreport 7:2241–2245.

Lannes B, Micheletti G, Vergnes M, Marescaux C, Depaulis a, Warter JM (1988) Relationship between spike-wave discharges and vigilance levels in rats with spontaneous petit mal-like epilepsy. Neurosci Lett 94:187–191.

Lannes B, Vergnes M, Marescaux C, Depaulis A, Micheletti G, Warter JM, Kempf E (1991) Lesions of noradrenergic neurons in rats with spontaneous generalized non-convulsive epilepsy. Epilepsy Res 9:79–85.

Lapierre O, Montplaisir J, Lamarre M, Bedard M a (1990) The effect of gamma-hydroxybutyrate on nocturnal and diurnal sleep of normal subjects: further considerations on REM sleep-triggering mechanisms. Sleep 13:24–30.

Lee S-C, Patrick SL, Richardson K a., Connors BW (2014a) Two Functionally Distinct Networks of Gap Junction-Coupled Inhibitory Neurons in the Thalamic Reticular Nucleus. J Neurosci 34:13170–13182.

Lee SE, Lee J, Latchoumane C, Lee B, Oh S-J, Saud ZA, Park C, Sun N, Cheong E, Chen C-C, Choi E-J, Lee CJ, Shin H-S (2014b) Rebound burst firing in the reticular thalamus is not essential for pharmacological absence seizures in mice. Proc Natl Acad Sci U S A.

Lennox WG (1960) Epilepsy and Related Disorders (Brown L, ed). Boston, MA.

Leresche N, Lambert RCR, Errington ACA, Crunelli V (2011) From sleep spindles of natural sleep to spike and wave discharges of typical absence seizures: is the hypothesis still valid? Museum 463:201–212.

Letts VA, Felix R, Biddlecome GH, Arikkath J, Mahaffey CL, Valenzuela A, Bartlett FS, Mori Y, Campbell KP, Frankel WN (1998) The mouse stargazer gene encodes a neuronal Ca2+-channel gamma subunit. Nat Genet 19:340–347.

Leysen J (2004) 5-HT2 Receptors. Curr Drug Targets-CNS Neurol …:11–26.

Li Q, Kuhn CM, Wilson W a, Lewis D V (2007) Effects of gamma hydroxybutyric acid on inhibition and excitation in rat neocortex. Neuroscience 150:82–92.

Li Q-H, Nakadate K, Tanaka-Nakadate S, Nakatsuka D, Cui Y, Watanabe Y (2004) Unique expression patterns of 5-HT2A and 5-HT2C receptors in the rat brain during postnatal development: Western blot and immunohistochemical analyses. J Comp Neurol 469:128–140.

Liang J, Zhang Y, Wang J, Pan H, Wu H, Xu K, Liu X, Jiang Y, Shen Y, Wu X (2006) New variants in the CACNA1H gene identified in childhood absence epilepsy. Neurosci Lett 406:27–32.

Lin C, Lu S, Schmechel D (1985) Glutamic acid decarboxylase immunoreactivity in layer IV of barrel cortex of rat and mouse. J Neurosci 5:1934–1939.

Lingenhoehl K, Brom R, Heid J, Beck P, Froestl W, Kaupmann K, Bettler B, Mosbacher J (1999) Gamma-hydroxybutyrate is a weak agonist at recombinant GABA(B) receptors. Neuropharmacology 38:1667–1673.

Liu S, Bubar MJ, Lanfranco MF, Hillman GR, Cunningham K a (2007) Serotonin2C receptor localization in GABA neurons of the rat medial prefrontal cortex: implications for understanding the neurobiology of addiction. Neuroscience 146:1677–1688.

Liu XB, Jones EG (1999) Predominance of corticothalamic synaptic inputs to thalamic reticular nucleus neurons in the rat. J Comp Neurol 414:67–79.

Liu XB, Warren RA, Jones EG (1995) Synaptic distribution of afferents from reticular nucleus in ventroposterior nucleus of cat thalamus. J Comp Neurol 352:187–202.

Liu Z, Vergnes M, Depaulis A, Marescaux C (1992) Involvement of intrathalamic GABAb neurotransmission in the control of absence seizures in the rat. Neuroscience 48:87–93.

Livingston S, Torres I, Pauli LL, Rider R V (1965) Petit mal epilepsy. Results of a prolonged follow-up study of 117 patients. JAMA 194:227–232.

Llinás R, Jahnsen H (1982) Electrophysiology of mammalian thalamic neurones in vitro. Nature 297:406–408.

Llinás R, Yarom Y (1981) Electrophysiology of mammalian inferior olivary neurones in vitro. Different types of voltage-dependent ionic conductances. J Physiol 315:549–567.

Llinás RRR, Steriade M (2006) Bursting of thalamic neurons and states of vigilance. J Neurophysiol 95:3297–3308.

Loiseau P, Pestre M, Dartigues JF, Commenges D, Barberger-Gateau C, Cohadon S (1983) Long-term prognosis in two forms of childhood epilepsy: typical absence seizures and epilepsy with rolandic (centrotemporal) EEG foci. Ann Neurol 13:642–648.

Long M a, Landisman CE, Connors BW (2004) Small clusters of electrically coupled neurons generate synchronous rhythms in the thalamic reticular nucleus. J Neurosci 24:341–349.

Lorincz ML, Kékesi KA, Juhász G, Crunelli V, Hughes SW (2009) Temporal framing of thalamic relay-mode firing by phasic inhibition during the alpha rhythm. Neuron 63:683–696.

Lüttjohann A, Fabene PF, van Luijtelaar G (2009) A revised Racine's scale for PTZ-induced seizures in rats. Physiol Behav 98:579–586.

Mahon S, Deniau JM, Charpier S (2001) Relationship between EEG potentials and intracellular activity of striatal and cortico-striatal neurons: an in vivo study under different anaesthetics. Cereb Cortex 11:360–373.

Maitre M (1997) The gamma-hydroxybutyrate signalling system in brain: organization and functional implications. Prog Neurobiol 51.

Mamelak M, Escriu JM, Stokan O (1977) The effects of gamma-hydroxybutyrate on sleep. Biol Psychiatry 12:273–288.

Manning JPA, Richards DA, Leresche N, Crunelli V, Bowery NG (2004) Cortical-area specific block of genetically determined absence seizures by ethosuximide. Neuroscience 123:5–9.

Marcus RJJ, Winters WDD, Mori K, Spooner CEE (1967) EEG and behavioral comparison of the effects of gamma-hydroxybutyrate, gamma-butyrolactone and short chain fatty acids in the rat. Int J Neuropharmacol 6:175–185.

Marescaux C, Vergnes M, Depaulis A (1992a) Genetic absence epilepsy in rats from Strasbourg--a review. J Neural Transm Suppl 35:37–69.

Marescaux C, Vergnes M, Depaulis A (1992b) Neurotransmission in rats' spontaneous generalized nonconvulsive epilepsy. Epilepsy Res Suppl 8:335–343.

Markram H, Sakmann B (1994) Calcium transients in dendrites of neocortical neurons evoked by single subthreshold excitatory postsynaptic potentials via low-voltage-activated calcium channels. Proc Natl Acad Sci U S A 91:5207–5211.

Marks G, Roffwarg H (1993) Spontaneous activity in the thalamic reticular nucleus during the sleep/wake cycle of the freely-moving rat. Brain Res 623:241–248.

Marquis K., Dunlop J, Ramamoorthy2 S, Beyer CE, Lin Q, Brennan J, Piesla MJ, Ashby CR, Harrison2 B, Magolda2 RM, Pangalos N, Stack G, Rosenzweig-Lipson S (2014) SCA-136: a novel 5-HT2C receptor agonist possessing atypical antipsychotic-like effects in preclinical models. In, pp 2–3.

Martin CBP, Hamon M, Lanfumey L, Mongeau R (2014) Controversies on the role of 5-HT(2C) receptors in the mechanisms of action of antidepressant drugs. Neurosci Biobehav Rev 42:208–223.

Martin JR, Bös M, Jenck F, Moreau J, Mutel V, Sleight AJ, Wichmann J, Andrews JS, Berendsen HH, Broekkamp CL, Ruigt GS, Köhler C, Delft AM (1998) 5-HT2C receptor agonists: pharmacological characteristics and therapeutic potential. J Pharmacol Exp Ther 286:913–924.

Masson J, Emerit MB, Hamon M, Darmon M (2012) Serotonergic signaling: multiple effectors and pleiotropic effects. Wiley Interdiscip Rev Membr Transp Signal 1:685–713.

Mathivet P, Bernasconi R (1997) Binding characteristics of γ-hydroxybutyric acid as a weak but selective GABAB receptor agonist. Eur J Neurosci 321:67–75.

Matricardi S, Verrotti A, Chiarelli F, Cerminara C, Curatolo P (2014) Current advances in childhood absence epilepsy. Pediatr Neurol 50:205–212.

Matteo V Di, Giovanni G Di, Mascio M Di, Esposito E (1999) SB 242084, a selective serotonin2C receptor antagonist, increases dopaminergic transmission in the mesolimbic system. Neuropharmacology 38:1195–1205.

McCafferty CP, David F, Venzi M, Giovanni G Di, Orban G, Uebele VN, Renger3 JJ, Lamber4 R, Leresche N, Crunelli V (2012) T-type calcium channels of cortical but not thalamocortical neurons are necessary for absence seizures. In: SfN.

McCormick D a, Bal T (1997) Sleep and arousal: thalamocortical mechanisms. Annu Rev Neurosci 20:185–215.

McCormick D a, Contreras D (2001) On the cellular and network bases of epileptic seizures. Annu Rev Physiol 63:815–846.

McCormick DA (1992) Neurotransmitter Actions in the Thalamus and Cerebral Cortex. J Clin Neurophysiol 9:212.

McCormick DA, Huguenard JR (1992) A model of the electrophysiological properties of thalamocortical relay neurons. J Neurophysiol 68:1384–1400.

McCormick DA, Pape HC (1990) Properties of a hyperpolarization-activated cation current and its role in rhythmic oscillation in thalamic relay neurones. J Physiol 431:291–318.

McCormick DA, Prince DA (1987) Actions of acetylcholine in the guinea-pig and cat medial and lateral geniculate nuclei, in vitro. J Physiol 392:147–165.

McCormick DA, Prince DA (1988) Noradrenergic modulation of firing pattern in guinea pig and cat thalamic neurons, in vitro. J Neurophysiol 59:978–996.

McCormick DA, Wang Z (1991) Serotonin and noradrenaline excite GABAergic neurones of the guinea-pig and cat nucleus reticularis thalami. J Physiol 442:235–255.

McKay BE, McRory JE, Molineux ML, Hamid J, Snutch TP, Zamponi GW, Turner RW (2006) Ca(V)3 T-type calcium channel isoforms differentially distribute to somatic and dendritic compartments in rat central neurons. Eur J Neurosci 24:2581–2594.

McLean TH, Parrish JC, Braden MR, Marona-Lewicka D, Gallardo-Godoy A, Nichols DE (2006) 1-Aminomethylbenzocycloalkanes: conformationally restricted hallucinogenic phenethylamine analogues as functionally selective 5-HT2A receptor agonists. J Med Chem 49:5794–5803.

McQueen JK, Woodbury DM (1975) Attempts to produce spike-and-wave complexes in the electrocorticogram of the rat. Epilepsia 16:295–299.

Meeker K, Harang R, Webb AB, Welsh DK, Doyle FJ, Bonnet G, Herzog ED, Petzold LR (2011) Wavelet measurement suggests cause of period instability in mammalian circadian neurons. J Biol Rhythms 26:353–362.

Meeren H (2005) Evolving concepts on the pathophysiology of absence seizures: the cortical focus theory. Arch … 62.

Meeren HKM, Pijn JPM, Van Luijtelaar ELJM, Coenen AML, Lopes da Silva FH (2002) Cortical focus drives widespread corticothalamic networks during spontaneous absence seizures in rats. J Neurosci 22:1480–1495.

Meerlo P, Westerveld P, Turek FW, Koehl M (2004) Effects of gamma-hydroxybutyrate (GHB) on vigilance states and EEG in mice. Sleep 27:899–904.

Meerts C, Absalom A (2013) Anxiolytics, sedatives and hypnotics. Anaesth Intensive Care Med 14:355–360.

Meis S, Biella G, Pape HC (1996) Interaction between low voltage-activated currents in reticular thalamic neurons in a rat model of absence epilepsy. Eur J Neurosci 8:2090–2097.

Meltzer HY, Roth BL (2013) Lorcaserin and pimavanserin: emerging selectivity of serotonin receptor subtype-targeted drugs. J Clin Invest 123:4986–4991.

Mendelson WB (2002) BASIC MECHANISMS OF SEDATIVE / HYPNOTICS. In: Neuropsychopharmacology: The Fifth Generation of Progress. Edited.

Merlo D, Mollinari C, Inaba Y, Cardinale A, Rinaldi AM, D'Antuono M, D'Arcangelo G, Tancredi V, Ragsdale D, Avoli M (2007) Reduced GABAB receptor subunit expression and paired-pulse depression in a genetic model of absence seizures. Neurobiol Dis 25:631–641.

MESULAM M, MUFSON E, WAINER B, LEVEY A (1983) Central cholinergic pathways in the rat: An overview based on an alternative nomenclature (Ch1–Ch6). Neuroscience 10:1185–1201.

Meuth S, Budde T (2003) Contribution of TWIK-related acid-sensitive K+ channel 1 (TASK1) and TASK3 channels to the control of activity modes in thalamocortical neurons. J … 23:6460–6469.

Meyer HS, Wimmer VC, Hemberger M, Bruno RM, de Kock CPJ, Frick A, Sakmann B, Helmstaedter M (2010a) Cell Type-Specific Thalamic Innervation in a Column of Rat Vibrissal Cortex. Cereb Cortex:2287–2303.

Meyer HS, Wimmer VC, Oberlaender M, de Kock CPJ, Sakmann B, Helmstaedter M (2010b) Number and Laminar Distribution of Neurons in a Thalamocortical Projection Column of Rat Vibrissal Cortex. Cereb Cortex:2277–2286.

Mhuircheartaigh RN, Rosenorn-Lanng D, Wise R, Jbabdi S, Rogers R, Tracey I (2010) Cortical and Subcortical Connectivity Changes during Decreasing Levels of Consciousness in Humans: A Functional Magnetic Resonance Imaging Study using Propofol. J Neurosci 30:9095–9102.

Micheletti G, Warter JM, Marescaux C, Depaulis A, Tranchant C, Rumbach L, Vergnes M (1987) Effects of drugs affecting noradrenergic neurotransmission in rats with spontaneous petit mal-like seizures. Eur J Pharmacol 135:397–402.

Millan MJ, Maiofiss L, Cussac D, Audinot V, Boutin J-A, Newman-Tancredi A (2002) Differential actions of antiparkinson agents at multiple classes of monoaminergic receptor. I. A multivariate analysis of the binding profiles of 14 drugs at 21 native and cloned human receptor subtypes. J Pharmacol Exp Ther 303:791–804.

Millan MJ, Marin P, Bockaert J, Mannoury la Cour C (2008) Signaling at G-protein-coupled serotonin receptors: recent advances and future research directions. Trends Pharmacol Sci 29:454–464.

Millan MJ, Peglion JL, Lavielle G, Perrin-Monneyron S (1997) 5-HT2C receptors mediate penile erections in rats: actions of novel and selective agonists and antagonists. Eur J Pharmacol 325:9–12.

Miller LE (2013) Lorcaserin for weight loss: insights into US Food and Drug Administration approval. J Acad Nutr Diet 113:25–30.

Miner LAH, Backstrom JR, Sanders-Bush E, Sesack SR (2003) Ultrastructural localization of serotonin2A receptors in the middle layers of the rat prelimbic prefrontal cortex. Neuroscience 116:107–117.

Mishra AM, Ellens DJ, Schridde U, Motelow JE, Purcaro MJ, DeSalvo MN, Enev M, Sanganahalli BG, Hyder F, Blumenfeld H (2011) Where fMRI and Electrophysiology Agree to Disagree: Corticothalamic and Striatal Activity Patterns in the WAG/Rij Rat. J Neurosci 31:15053–15064.

Monckton JE, McCormick DA (2002) Neuromodulatory role of serotonin in the ferret thalamus. J Neurophysiol 87:2124–2136.

Monti JM, Altier H, D'Angelo L (1979) The effects of the combined administration of gamma-hydroxybutyrate and diazepam on sleep parameters in the rat. J Neural Transm 45:177–183.

Monti JM, Jantos H (2006) Effects of the serotonin 5-HT2A/2C receptor agonist DOI and of the selective 5-HT2A or 5-HT2C receptor antagonists EMD 281014 and SB-243213, respectively, on sleep and waking in the rat. Eur J Pharmacol 553:163–170.

Monti JM, Jantos H (2010) The Role of 5-HT2A/2C Receptors in Sleep and Waking. In: 5-HT2C Receptors in the Pathophysiology of CNS Disease, pp 393–412. Humana Press.

Morabito M V, Abbas AI, Hood JL, Kesterson RA, Jacobs MM, Kump DS, Hachey DL, Roth BL, Emeson RB (2010) Mice with altered serotonin 2C receptor RNA editing display characteristics of Prader-Willi syndrome. Neurobiol Dis 39:169–180.

Morairty SR, Hedley L, Flores J, Martin R, Kilduff TS (2008) Selective 5HT2A and 5HT6 receptor antagonists promote sleep in rats. Sleep 31:34–44.

Moreno JL, Holloway T, Albizu L, Sealfon SC, González-Maeso J (2011) Metabotropic glutamate mGlu2 receptor is necessary for the pharmacological and behavioral effects induced by hallucinogenic 5-HT2A receptor agonists. Neurosci Lett 493:76–79.

Moreno JL, Muguruza C, Umali A, Mortillo S, Holloway T, Pilar-Cuéllar F, Mocci G, Seto J, Callado LF, Neve RL, Milligan G, Sealfon SC, López-Giménez JF, Meana JJ, Benson DL, González-Maeso J (2012) Identification of three residues essential for 5-hydroxytryptamine 2A-metabotropic glutamate 2 (5-HT2A·mGlu2) receptor heteromerization and its psychoactive behavioral function. J Biol Chem 287:44301–44319.

Motelow JE, Blumenfeld H (2009) Functional neuroimaging of spike-wave seizures. Methods Mol Biol 489:189–209.

Moya PR, Berg KA, Gutiérrez-Hernandez MA, Sáez-Briones P, Reyes-Parada M, Cassels BK, Clarke WP (2007) Functional selectivity of hallucinogenic phenethylamine and phenylisopropylamine derivatives at human 5-hydroxytryptamine (5-HT)2A and 5-HT2C receptors. J Pharmacol Exp Ther 321:1054–1061.

Neher E, Sakaba T (2008) Multiple roles of calcium ions in the regulation of neurotransmitter release. Neuron 59:861–872.

Nevado-Holgado AJ, Marten F, Richardson MP, Terry JR (2012) Characterising the dynamics of EEG waveforms as the path through parameter space of a neural mass model: application to epilepsy seizure evolution. Neuroimage 59:2374–2392.

Ngomba RT, Santolini I, Salt TE, Ferraguti F, Battaglia G, Nicoletti F, van Luijtelaar G (2011) Metabotropic glutamate receptors in the thalamocortical network: strategic targets for the treatment of absence epilepsy. Epilepsia 52:1211–1222.

Nichols CD, Sanders-bush E (2001) Serotonin Receptor Signaling and Hallucinogenic Drug Action. 2:73–79.

Nichols DE (2004) Hallucinogens. Pharmacol Ther 101:131–181.

Nichols DE, Nichols CD (2008) Serotonin Receptors. Chem Rev:1614–1641.

Nicolelis MMAL, Fanselow EEE (2002) Thalamcortical optimization of tactile processing according to behavioral state. Nat Neurosci 5:517–524.

Niedermeyer E (1972) The Generalized Epilepsies: A Clinical Electroencephalographical Study. Charles C Thomas.

Nilius B, Hess P, Lansman JB, Tsien RW (1985) A novel type of cardiac calcium channel in ventricular cells. Nature 316:443–446.

Noebels JL (1999) Single-gene models of epilepsy. Adv Neurol 79:227–238.

Noebels JL (2006) Models of Seizures and Epilepsy. In: Models of Seizures and Epilepsy, pp 223–232. Elsevier.

Ogino S, Nagakura Y, Tsukamoto M, Watabiki T, Ozawa T, Oe T, Shimizu Y, Ito H (2013) Systemic administration of 5-HT(2C) receptor agonists attenuates muscular hyperalgesia in reserpine-induced myalgia model. Pharmacol Biochem Behav 108:8–15.

Oh SW et al. (2014) A mesoscale connectome of the mouse brain. Nature 508:207–214.

Ohno Y, Sofue N, Imaoku T, Morishita E, Kumafuji K, Sasa M, Serikawa T (2010) Serotonergic Modulation of Absence-Like Seizures in Groggy Rats: a Novel Rat Model of Absence Epilepsy. J Pharmacol Sci 114:99–105.

Oostenveld R, Fries P, Maris E, Schoffelen J-M (2011) FieldTrip: Open source software for advanced analysis of MEG, EEG, and invasive electrophysiological data. Comput Intell Neurosci 2011:156869.

Orban G, David F, Di Giovanni G, Cope DW, Bowles, Uebele VN, Renger JJ, Lambert RC, Leresche N, Crunelli V (2010) Block of T-type calcium channels of thalamocortical neurones by TTA-P2 does not suppress absence seizures. In: SfN. San Diego.

Panayiotopoulos C (2008) Typical absence seizures and related epileptic syndromes: assessment of current state and directions for future research. Epilepsia:2131–2139.

Panayiotopoulos CP (1999) Typical absence seizures and their treatment. Arch Dis Child 81:351–355.

Panayiotopoulos CP (2001) Treatment of typical absence seizures and related epileptic syndromes. Paediatr Drugs 3:379–403.

Pape H-C, Munsch T, Budde T (2004) Novel vistas of calcium-mediated signalling in the thalamus. Pflugers Arch 448:131–138.

Pape HC, Budde T, Mager R, Kisvárday ZF (1994) Prevention of Ca(2+)-mediated action potentials in GABAergic local circuit neurones of rat thalamus by a transient K+ current. J Physiol 478 Pt 3:403–422.

Parker a P, Agathonikou a, Robinson RO, Panayiotopoulos CP (1998) Inappropriate use of carbamazepine and vigabatrin in typical absence seizures. Dev Med Child Neurol 40:517–519.

Parri H, Crunelli V (1998) Sodium current in rat and cat thalamocortical neurons: role of a non-inactivating component in tonic and burst firing. J Neurosci 18:854–867.

Paxinos G, Watson C (1997) The rat Brain in Stereotaxic Coordinates. Blackwell Publishing.

Pazos A, Hoyer D, Palacios JM (1984) The binding of serotonergic ligands to the porcine choroid plexus: characterization of a new type of serotonin recognition site. Eur J Pharmacol 106:539–546.

Pedreira C, Martinez J, Ison MJ, Quian Quiroga R (2012) How many neurons can we see with current spike sorting algorithms? J Neurosci Methods 211:58–65.

Penfield W, Jasper H (1947) Highest level seizures. Res Publ Ass Res Nerv Ment Dis 26:252–271.

Perez-Reyes E (1999) Three for T: molecular analysis of the low voltage-activated calcium channel family. Cell Mol Life Sci 56:660–669.

Perez-Reyes E (2003) Molecular physiology of low-voltage-activated t-type calcium channels. Physiol Rev 83:117–161.

Perez-Reyes E, Cribbs LL, Daud A, Lacerda AE, Barclay J, Williamson MP, Fox M, Rees M, Lee JH (1998) Molecular characterization of a neuronal low-voltage-activated T-type calcium channel. Nature 391:896–900.

Peroutka SJ, Snyder SH (1979) Multiple serotonin receptors: differential binding of [3H]5-hydroxytryptamine, [3H]lysergic acid diethylamide and [3H]spiroperidol. Mol Pharmacol 16:687–699.

Pinault D (2004) The thalamic reticular nucleus: structure, function and concept. Brain Res Brain Res Rev 46:1–31.

Pinault D, Leresche N, Charpier S, Deniau J-MM, Marescaux C, Vergnes M, Crunelli V (1998) Intracellular recordings in thalamic neurones during spontaneous spike and wave discharges in rats with absence epilepsy. J Physiol 509 (Pt 2:449–456.

Plock N, Kloft C (2005) Microdialysis--theoretical background and recent implementation in applied life-sciences. Eur J Pharm Sci 25:1–24.

Polack P-O, Guillemain I, Hu E, Deransart C, Depaulis A, Charpier S (2007) Deep layer somatosensory cortical neurons initiate spike-and-wave discharges in a genetic model of absence seizures. J Neurosci 27:6590–6599.

Popa D, Léna C, Fabre V, Prenat C, Gingrich J, Escourrou P, Hamon M, Adrien J (2005) Contribution of 5-HT2 receptor subtypes to sleep-wakefulness and respiratory control, and functional adaptations in knock-out mice lacking 5-HT2A receptors. J Neurosci 25:11231–11238.

Posner EB, Mohamed K, Marson AG (2005) Ethosuximide, sodium valproate or lamotrigine for absence seizures in children and adolescents. Cochrane database Syst Rev:CD003032.

Powell KL, Cain SM, Ng C, Sirdesai S, David LS, Kyi M, Garcia E, Tyson JR, Reid C a, Bahlo M, Foote SJ, Snutch TP, O'Brien TJ (2009) A Cav3.2 T-type calcium channel point mutation has splice-variant-specific effects on function and segregates with seizure expression in a polygenic rat model of absence epilepsy. J Neurosci 29:371–380.

Powell KL, Kyi M, Reid C a, Paradiso L, D'Abaco GM, Kaye a H, Foote SJ, O'Brien TJ (2008) Genetic absence epilepsy rats from Strasbourg have increased corticothalamic expression of stargazin. Neurobiol Dis 31:261–265.

Prince DA, Farrell D (1969) "Centrencephalic" spike-wave discharges following parenteral penicillin injection in the cat. Neurology 19:309–310.

Puig MV, Celada P, Díaz-mataix L, Artigas F (2003) In Vivo Modulation of the Activity of Pyramidal Neurons in the Rat Medial Prefrontal Cortex by 5-HT 2A Receptors : Relationship to Thalamocortical Afferents. Cereb Cortex:870–882.

Puig MV, Watakabe A, Ushimaru M, Yamamori T, Kawaguchi Y (2010) Serotonin modulates fast-spiking interneuron and synchronous activity in the rat prefrontal cortex through 5-HT1A and 5-HT2A receptors. J Neurosci 30:2211–2222.

Quesney LF, Gloor P, Kratzenberg E, Zumstein H (1977) Pathophysiology of generalized penicillin epilepsy in the cat: the role of cortical and subcortical structures. I. Systemic application of penicillin. Electroencephalogr Clin Neurophysiol 42:640–655.

Quesseveur G (2012) 5-HT2 ligands in the treatment of anxiety and depression. Expert Opin Drug Discov:1–25.

Rateau Y, Ropert N (2006) Expression of a functional hyperpolarization-activated current (Ih) in the mouse nucleus reticularis thalami. J Neurophysiol 95:3073–3085.

Richards DA, Lemos T, Whitton PS, Bowery NG (1995) Extracellular GABA in the ventrolateral thalamus of rats exhibiting spontaneous absence epilepsy: a microdialysis study. J Neurochem 65:1674–1680.

Rijn C Van, Weyn B, Coenen A (1993) Effects of lamotrigine on absence seizures in rats. Polish J … 46:467–470.

Roth BL (2011) Irving Page Lecture: 5-HT(2A) serotonin receptor biology: interacting proteins, kinases and paradoxical regulation. Neuropharmacology 61:348–354.

Roth R, Delgado J, Giarman N (1966) γ-butyrolactone and γ-hydroxybutyric acid-II. The pharmacologically active form. Int J Neuropharmacol 5:421–428.

Roth R, Giarman N (1966) γ-Butyrolactone and γ-hydroxybutyric acid-I. Distribution and metabolism. Biochem Pharmacol I:1333–1348.

Rousseau A-F, Ledoux D, Sabourdin N, Richard P, Damas P, Constant I (2012) Clinical sedation and bispectral index in burn children receiving gamma-hydroxybutyrate. Paediatr Anaesth 22:799–804.

Rudolf G, Bihoreau MT, Godfrey RF, Wilder SP, Cox RD, Lathrop M, Marescaux C, Gauguier D (2004) Polygenic control of idiopathic generalized epilepsy phenotypes in the genetic absence rats from Strasbourg (GAERS). Epilepsia 45:301–308.

Rudolph U, Antkowiak B (2004) Molecular and neuronal substrates for general anaesthetics. Nat Rev Neurosci 5:709–720.

Sadleir LG, Farrell K, Smith S, Connolly MB, Scheffer IE (2006) Electroclinical features of absence seizures in childhood absence epilepsy. Neurology 67:413–418.

Sarkisova K, van Luijtelaar G (2011) The WAG/Rij strain: a genetic animal model of absence epilepsy with comorbidity of depression [corrected]. Prog Neuropsychopharmacol Biol Psychiatry 35:854–876.

Schiff ND (2008) Central thalamic contributions to arousal regulation and neurological disorders of consciousness. Ann N Y Acad Sci 1129:105–118.

Schindler K, Leung H, Elger CE, Lehnertz K (2007) Assessing seizure dynamics by analysing the correlation structure of multichannel intracranial EEG. Brain 130:65–77.

Schmid CL, Raehal KM, Bohn LM (2008) Agonist-directed signaling of the serotonin 2A receptor depends on beta-arrestin-2 interactions in vivo. Proc Natl Acad Sci U S A 105:1079–1084.

Schneider J, Thomalske G, Trautmann P, Smolarz R, Sabbagh R (1963) The EEG behavior of humans and animals subjected to the progressive action of sodium 4-hydroxybutyrate. Agressologie 4:55–70.

Schofield CM, Kleiman-Weiner M, Rudolph U, Huguenard JR (2009) A gain in GABAA receptor synaptic strength in thalamus reduces oscillatory activity and absence seizures. Proc Natl Acad Sci U S A 106:7630–7635.

Senatore a, Guan W, Spafford JD (2014) Cav3 T-type channels: regulators for gating, membrane expression, and cation selectivity. Pflugers Arch 466:645–660.

Senatore A, Zhorov BS, Spafford JD (2012) Cav3 T-type calcium channels. Wiley Interdiscip Rev Membr Transp Signal 1:467–491.

Sherman SM (2001) Tonic and burst firing: dual modes of thalamocortical relay. Trends Neurosci 24:122–126.

Sherman SM (2004) Interneurons and triadic circuitry of the thalamus. Trends Neurosci 27:670–675.

Sherman SM (2005) Thalamic relays and cortical functioning. Prog Brain Res 149:107–126.

Sherman SM (2007) The thalamus is more than just a relay. Curr Opin Neurobiol 17:417–422.

Sherman SM, Guillery RW (2002) The role of the thalamus in the flow of information to the cortex. Philos Trans R Soc Lond B Biol Sci 357:1695–1708.

Sherman SM, Guillery RW (2006) Exploring the thalamus.

Shipe WD et al. (2008) Design, synthesis, and evaluation of a novel 4-aminomethyl-4-fluoropiperidine as a T-type Ca2+ channel antagonist. J Med Chem 51:3692–3695.

Sitnikova E, van Luijtelaar G (2004) Cortical control of generalized absence seizures: effect of lidocaine applied to the somatosensory cortex in WAG/Rij rats. Brain Res 1012:127–137.

Siuciak J a, Chapin DS, McCarthy S a, Guanowsky V, Brown J, Chiang P, Marala R, Patterson T, Seymour P a, Swick A, Iredale P a (2007) CP-809,101, a selective 5-HT2C agonist, shows activity in animal models of antipsychotic activity. Neuropharmacology 52:279–290.

Slaght SJ, Leresche N, Deniau J-M, Crunelli V, Charpier S (2002) Activity of thalamic reticular neurons during spontaneous genetically determined spike and wave discharges. J Neurosci 22:2323–2334.

Smith MI, Piper DC, Duxon MS, Upton N (2002) Effect of SB-243213, a selective 5-HT2C receptor antagonist, on the rat sleep profile: A comparison to paroxetine. Pharmacol Biochem Behav 71:599–605.

Snead OC (1978a) Gamma hydroxybutyrate in the monkey. II. Effect of chronic oral anticonvulsant drugs. Neurology 28:643–648.

Snead OC (1978b) Gamma hydroxybutyrate in the monkey. III. Effect of intravenous anticonvulsant drugs. Neurology 28:1173–1178.

Snead OC (1978c) Gamma hydroxybutyrate in the monkey. I. Electroencephalographic, behavioral, and pharmacokinetic studies. Neurology 28:636–642.

Snead OC (1982) An investigation of the relationship between the dopaminergic and electroencephalographic effects of gamma-butyrolactone. Neuropharmacology 21:539–543.

Snead OC (1984) Ontogeny of gamma-hydroxybutyric acid. II. Electroencephalographic effects. Brain Res 317:89–96.

Snead OC (1988) gamma-Hydroxybutyrate model of generalized absence seizures: further characterization and comparison with other absence models. Epilepsia 29:361–368.

Snead OC (1990) The ontogeny of GABAergic enhancement of the gamma-hydroxybutyrate model of generalized absence seizures. Epilepsia 31:363–368.

Snead OC (1991) The γ-hydroxybutyrate model of absence seizures: correlation of regional brain levels of γ-hydroxybutyric acid and γ-butyrolactone with spike wave discharges. Neuropharmacology 30:161–167.

Snead OC (1992a) Pharmacological models of generalized absence seizures in rodents. J Neural Transm Suppl 35:7–19.

Snead OC (1992b) Evidence for GABAB-mediated mechanisms in experimental generalized absence seizures. Eur J Pharmacol 213:343–349.

Snead OC (1996a) Relation of the [3H] gamma-hydroxybutyric acid (GHB) binding site to the gamma-aminobutyric acidB (GABAB) receptor in rat brain. Biochem Pharmacol 52:1235–1243.

Snead OC (1998) Ganaxolone, a selective, high-affinity steroid modulator of the gamma-aminobutyric acid-A receptor, exacerbates seizures in animal models of absence. Ann Neurol 44:688–691.

Snead OC (2002) Gamma-hydroxybutyrate and Absence Seizure Activity. In: Gamma-Hydroxybutyrate: Pharmacological and Functional Aspects, pp 132–149.

Snead OC, Banerjee PKP, Burnham M, Hampson D (2000) Modulation of absence seizures by the GABA(A) receptor: a critical rolefor metabotropic glutamate receptor 4 (mGluR4). J Neurosci 20:6218–6224.

Snead OC, Bearden LJ, Pegram V (1980) Effect of acute and chronic anticonvulsant administration on endogenous gamma-hydroxybutyrate in rat brain. Neuropharmacology 19:47–52.

Snead OC, Depaulis A, Banerjee PK, Hechler V, Vergnes M (1992) The GABAA receptor complex in experimental absence seizures in rat: an autoradiographic study. Neurosci Lett 140:9–12.

Snead OC, Hechler V, Vergnes M, Marescaux C, Maitre M (1990) Increased gamma-hydroxybutyric acid receptors in thalamus of a genetic animal model of petit mal epilepsy. Epilepsy Res 7:121–128.

Snead OC, Hosey LC (1985) Exacerbation of seizures in children by carbamazepine. N Engl J Med 313:916–921.

Snead OC, Morley BJ (1981) Ontogeny of gamma-hydroxybutyric acid. I. Regional concentration in developing rat, monkey and human brain. Brain Res 227:579–589.

Snead OC, Yu RK, Huttenlocher PR (1976) Gamma hydroxybutyrate. Correlation of serum and cerebrospinal fluid levels with electroencephalographic and behavioral effects. Neurology 26:51–56.

Snead OCC (1996b) Antiabsence seizure activity of specific GABA B and gamma-hydroxybutyric acid receptor antagonists. Pharmacol Biochem Behav 53:73–79.

Sogawa Y, Moshe S, Shinnar S, Dlugos D, Conry J, Cnaan A, Glauser T (2009) Petit-mal sonata: predominant EEG seizure patterns in childhood absence epilepsy (CAE).

Sohal VS, Huguenard JR (2003) Inhibitory interconnections control burst pattern and emergent network synchrony in reticular thalamus. J Neurosci 23:8978–8988.

Song I, Kim D, Choi S, Sun M, Kim Y, Shin H-S (2004) Role of the alpha1G T-type calcium channel in spontaneous absence seizures in mutant mice. J Neurosci 24:5249–5257.

Spreafico R, Mennini T, Danober L, Cagnotto A, Regondi MC, Miari A, De Blas A, Vergnes M, Avanzini G (1993) GABAA receptor impairment in the genetic absence epilepsy rats from Strasbourg (GAERS): an immunocytochemical and receptor binding autoradiographic study. Epilepsy Res 15:229–238.

Steriade M (1999) Brainstem activation of thalamocortical systems. Brain Res Bull 50:391–392.

Steriade M (2004) Acetylcholine systems and rhythmic activities during the waking-sleep cycle. Prog Brain Res 145:179–196.

Steriade M (2005) Sleep, epilepsy and thalamic reticular inhibitory neurons. Trends Neurosci 28:317–324.

Steriade M (2006) Grouping of brain rhythms in corticothalamic systems. Neuroscience 137:1087–1106.

Steriade M, Contreras D (1995) Relations between cortical and thalamic cellular events during transition from sleep patterns to paroxysmal activity. J Neurosci 15:623–642.

Steriade M, Contreras D, Curró Dossi R, Nuñez A (1993a) The slow (< 1 Hz) oscillation in reticular thalamic and thalamocortical neurons: scenario of sleep rhythm generation in interacting thalamic and neocortical networks. J Neurosci 13:3284–3299.

Steriade M, McCormick DA, Sejnowski TJ (1993b) Thalamocortical oscillations in the sleeping and aroused brain. Science 262:679–685.

Stout BD, Clarke WP, Berg KA (2002) Rapid desensitization of the serotonin(2C) receptor system: effector pathway and agonist dependence. J Pharmacol Exp Ther 302:957–962.

Sun Y-G, Pita-Almenar JD, Wu C-S, Renger JJ, Uebele VN, Lu H-C, Beierlein M (2013) Biphasic cholinergic synaptic transmission controls action potential activity in thalamic reticular nucleus neurons. J Neurosci 33:2048–2059.

Talley EM, Cribbs LL, Lee JH, Daud A, Perez-Reyes E, Bayliss DA (1999) Differential distribution of three members of a gene family encoding low voltage-activated (T-type) calcium channels. J Neurosci 19:1895–1911.

Tanaka M, Olsen RW, Medina MT, Schwartz E, Alonso ME, Duron RM, Castro-Ortega R, Martinez-Juarez IE, Pascual-Castroviejo I, Machado-Salas J, Silva R, Bailey JN, Bai D, Ochoa A, Jara-Prado A, Pineda G, Macdonald RL, Delgado-Escueta A V (2008) Hyperglycosylation and reduced GABA currents of mutated GABRB3 polypeptide in remitting childhood absence epilepsy. Am J Hum Genet 82:1249–1261.

Tecott L, Sun L, Akana S (1995) Eating disorder and epilepsy in mice lacking 5-HT2c serotonin receptors. Nature.

Tenney J, Glauser T (2013) The current state of absence epilepsy: can we have your attention? Epilepsy Curr 13:135–140.

Tenney JR, Duong TQ, King JA, Ludwig R, Ferris CF (2003) Corticothalamic modulation during absence seizures in rats: a functional MRI assessment. Epilepsia 44:1133–1140.

Tenney JR, Marshall PC, King JA, Ferris CF (2004) fMRI of generalized absence status epilepticus in conscious marmoset monkeys reveals corticothalamic activation. Epilepsia 45:1240–1247.

Tennigkeit F, Schwarz DW, Puil E (1998) Modulation of bursts and high-threshold calcium spikes in neurons of rat auditory thalamus. Neuroscience 83:1063–1073.

Thomas RH, Berkovic SF (2014) The hidden genetics of epilepsy-a clinically important new paradigm. Nat Rev Neurol 10:283–292.

Thompson AJ, Lummis SCR (2006) 5-HT3 receptors. Curr Pharm Des 12:3615–3630.

Thomsen W, Grottick A (2008) Lorcaserin, a novel selective human 5-hydroxytryptamine2C agonist: in vitro and in vivo pharmacological characterization. J Pharmacol Exp Ther.

Tian M, Macdonald RL (2012) The intronic GABRG2 mutation, IVS6+2T->G, associated with childhood absence epilepsy altered subunit mRNA intron splicing, activated nonsense-mediated decay, and produced a stable truncated γ2 subunit. J Neurosci 32:5937–5952.

Timofeev I, Steriade M (1996) Low-frequency rhythms in the thalamus of intact-cortex and decorticated cats. J Neurophysiol 76:4152–4168.

Tokuda S, Kuramoto T, Tanaka K, Kaneko S, Takeuchi IK, Sasa M, Serikawa T (2007) The ataxic groggy rat has a missense mutation in the P/Q-type voltage-gated Ca2+ channel alpha1A subunit gene and exhibits absence seizures. Brain Res 1133:168–177.

Touret M, Parrot S, Denoroy L, Belin M-F, Didier-Bazes M (2007) Glutamatergic alterations in the cortex of genetic absence epilepsy rats. BMC Neurosci 8:69.

Tracey D (2004) Somatosensory System. In: The Rat Nervous System, pp 797–815. Elsevier.

Tringham E, Powell KL, Cain SM, Kuplast K, Mezeyova J, Weerapura M, Eduljee C, Jiang X, Smith P, Morrison J-L, Jones NC, Braine E, Rind G, Fee-Maki M, Parker D, Pajouhesh H, Parmar M, O'Brien TJ, Snutch TP (2012) T-Type Calcium Channel Blockers That Attenuate Thalamic Burst Firing and Suppress Absence Seizures. Sci Transl Med 4:121ra19–ra121ra19.

Tsakiridou E, Bertollini L, de Curtis M, Avanzini G, Pape HC (1995) Selective increase in T-type calcium conductance of reticular thalamic neurons in a rat model of absence epilepsy. J Neurosci 15:3110–3117.

Tscherter A, David F, Ivanova T, Deleuze C, Renger JJ, Uebele VN, Shin H-S, Bal T, Leresche N, Lambert RC (2011) Minimal alterations in T-type calcium channel gating markedly modify physiological firing dynamics. J Physiol 589:1707–1724.

Tucker DM, Brown M, Luu P, Holmes MD (2007) Discharges in ventromedial frontal cortex during absence spells. Epilepsy Behav 11:546–557.

Ulrich D, Huguenard JR (1996) GABAB receptor-mediated responses in GABAergic projection neurones of rat nucleus reticularis thalami in vitro. J Physiol 493 (Pt 3:845–854.

Upton N, Stean T, Middlemiss D, Blackburn T, Kennett G (1998) Studies on the role of 5-HT2C and 5-HT2B receptors in regulating generalised seizure threshold in rodents. Eur J Pharmacol 359:33–40.

Urban JJD, Clarke WPW, von Zastrow M, Nichols DE, Kobilka B, Weinstein H, Javitch JA, Roth BL, Christopoulos A, Sexton PM, Miller KJ, Spedding M, Mailman RB (2007) Functional selectivity and classical concepts of quantitative pharmacology. J Pharmacol Exp Ther 320:1–13.

Vacher H, Mohapatra DP, Trimmer JS (2008) Localization and targeting of voltage-dependent ion channels in mammalian central neurons. Physiol Rev 88:1407–1447.

Van Cauter E, Plat L, Scharf MB, Leproult R, Cespedes S, L'Hermite-Balériaux M, Copinschi G (1997) Simultaneous stimulation of slow-wave sleep and growth hormone secretion by gamma-hydroxybutyrate in normal young Men. J Clin Invest 100:745–753.

Van de Bovenkamp-Janssen MC, van der Kloet JC, van Luijtelaar G, Roubos EW (2006) NMDA-NR1 and AMPA-GluR4 receptor subunit immunoreactivities in the absence epileptic WAG/Rij rat. Epilepsy Res 69:119–128.

Van Hese P, Martens J-P, Waterschoot L, Boon P, Lemahieu I (2009) Automatic detection of spike and wave discharges in the EEG of genetic absence epilepsy rats from Strasbourg. IEEE Trans Biomed Eng 56:706–717.

Van Luijtelaar EL, Coenen AM (1986) Two types of electrocortical paroxysms in an inbred strain of rats. Neurosci Lett 70:393–397.

Van Luijtelaar G, Sitnikova E, Littjohann A (2011) On the origin and suddenness of absences in genetic absence models. Clin EEG Neurosci 42:83–97.

Van Oekelen D, Luyten WHM. ML, Leysen JE (2003a) 5-HT2A and 5-HT2C receptors and their atypical regulation properties. Life Sci 72:2429–2449.

Van Oekelen D, Megens A, Meert T, Luyten WHML, Leysen JE (2003b) Functional study of rat 5-HT2A receptors using antisense oligonucleotides. J Neurochem 85:1087–1100.

Van Raay L, Jovanovska V, Morris MJ, O'Brien TJ (2012) Focal administration of neuropeptide Y into the S2 somatosensory cortex maximally suppresses absence seizures in a genetic rat model. Epilepsia 53:477–484.

Vandecasteele M, M S, Royer S, Belluscio M, Berényi A, Diba K, Fujisawa S, Grosmark A, Mao D, Mizuseki K, Patel J, Stark E, Sullivan D, Watson B, Buzsáki G (2012) Large-scale recording of neurons by movable silicon probes in behaving rodents. J Vis Exp:e3568.

Vanover KE, Davis RE (2010) Role of 5-HT2A receptor antagonists in the treatment of insomnia. Nat Sci Sleep 2:139–150.

Varela C, Sherman SM (2007) Differences in response to muscarinic activation between first and higher order thalamic relays. J Neurophysiol 98:3538–3547.

Varela C, Sherman SM (2009) Differences in response to serotonergic activation between first and higher order thalamic nuclei. Cereb Cortex 19:1776–1786.

Venzi M, Di Giovanni G, Crunelli V (2015) A critical evaluation of the gamma-hydroxybutyrate (GHB) model of absence seizures. CNS Neurosci Ther.

Vergnes M, Boehrer A, Simler S, Bernasconi R, Marescaux C (1997) Opposite effects of GABAB receptor antagonists on absences and convulsive seizures. Eur J Pharmacol 332:245–255.

Vergnes M, Marescaux C (1992) Cortical and thalamic lesions in rats with genetic absence epilepsy. J Neural Transm Suppl 35:71–83.

Vergnes M, Marescaux C, Boehrer A, Depaulis A (1991) Are rats with genetic absence epilepsy behaviorally impaired? Epilepsy Res 9:97–104.

Vergnes M, Marescaux C, Micheletti G, Reis J, Depaulis A, Rumbach L, Warter JM (1982) Spontaneous paroxysmal electroclinical patterns in rat: a model of generalized non-convulsive epilepsy. Neurosci Lett 33:97–101.

Vienne J, Bettler B, Franken P, Tafti M (2010) Differential effects of GABAB receptor subtypes, {gamma}-hydroxybutyric Acid, and Baclofen on EEG activity and sleep regulation. J Neurosci 30:14194–14204.

Von Krosigk M, Bal T, McCormick DA (1993) Cellular mechanisms of a synchronized oscillation in the thalamus. Science 261:361–364.

Wahl-Schott C, Biel M (2009) HCN channels: structure, cellular regulation and physiological function. Cell Mol Life Sci 66:470–494.

Wakamori M, Yamazaki K, Matsunodaira H, Teramoto T, Tanaka I, Niidome T, Sawada K, Nishizawa Y, Sekiguchi N, Mori E, Mori Y, Imoto K (1998) Single tottering mutations responsible for the neuropathic phenotype of the P-type calcium channel. J Biol Chem 273:34857–34867.

Wallace RH, Marini C, Petrou S, Harkin L a, Bowser DN, Panchal RG, Williams D a, Sutherland GR, Mulley JC, Scheffer IE, Berkovic SF (2001) Mutant GABA(A) receptor gamma2-subunit in childhood absence epilepsy and febrile seizures. Nat Genet 28:49–52.

Warter JMJ, Vergnes M, Depaulis A, Tranchant C, Rumbach L, Micheletti G, Marescaux C, Recherche G De, Nerveuse DP, Neurologique C, Civil H (1988) Effects of drugs affecting dopaminergic neurotransmission in rats with spontaneous petit mal-like seizures. Neuropharmacology 27:269–274.

Webb AB, Taylor SR, Thoroughman KA, Doyle FJ, Herzog ED (2012) Weakly circadian cells improve resynchrony. Sporns O, ed. PLoS Comput Biol 8:e1002787.

Weber ET, Andrade R (2010) Htr2a Gene and 5-HT(2A) Receptor Expression in the Cerebral Cortex Studied Using Genetically Modified Mice. Front Neurosci 4.

Weisstaub N V, Zhou M, Lira A, Lambe E, González-Maeso J, Hornung J-P, Sibille E, Underwood M, Itohara S, Dauer WT, Ansorge MS, Morelli E, Mann JJ, Toth M, Aghajanian G, Sealfon SC, Hen R, Gingrich JA (2006) Cortical 5-HT2A receptor signaling modulates anxiety-like behaviors in mice. Science 313:536–540.

Welsh SE, Kachelries WJ, Romano a G, Simansky KJ, Harvey J a (1998) Effects of LSD, ritanserin, 8-OH-DPAT, and lisuride on classical conditioning in the rabbit. Pharmacol Biochem Behav 59:469–475.

Werry TD, Loiacono R, Sexton PM, Christopoulos A (2008) RNA editing of the serotonin 5HT2C receptor and its effects on cell signalling, pharmacology and brain function. Pharmacol Ther 119:7–23.

West AE, Chen WG, Dalva MB, Dolmetsch RE, Kornhauser JM, Shaywitz AJ, Takasu MA, Tao X, Greenberg ME (2001) Calcium regulation of neuronal gene expression. Proc Natl Acad Sci U S A 98:11024–11031.

Westerhuis MMF, Coenen AML, Van Luijtelaar ELJM (1996) Tone discrimination during sleep-wake states and spike-wave discharges in rats. Sleep-Wake Res 7:155–159.

Westmijse I, Ossenblok P, Gunning B, van Luijtelaar G (2009) Onset and propagation of spike and slow wave discharges in human absence epilepsy: A MEG study. Epilepsia 50:2538–2548.

Wild J, Prekopcsak Z, Sieger T, Novak D, Jech R (2012) Performance comparison of extracellular spike sorting algorithms for single-channel recordings. J Neurosci Methods 203:369–376.

Williams D (1953) A study of thalamic and cortical rhythms in petit mal. Brain 76:50–69.

Williams SR, Tóth TI, Turner JP, Hughes SW, Crunelli V (1997a) The “window” component of the low threshold Ca2+ current produces input signal amplification and bistability in cat and rat thalamocortical neurones. J Physiol 505 (Pt 3:689–705.

Williams SR, Turner JP, Crunelli V (1995) Gamma-hydroxybutyrate promotes oscillatory activity of rat and cat thalamocortical neurons by a tonic GABAB, receptor-mediated hyperpolarization. Neuroscience 66:133–141.

Williams SR, Turner JP, Hughes SW, Crunelli V (1997b) On the nature of anomalous rectification in thalamocortical neurones of the cat ventrobasal thalamus in vitro. J Physiol 505 (Pt 3:727–747.

Wimmer VC, Bruno RM, de Kock CPJ, Kuner T, Sakmann B (2010) Dimensions of a Projection Column and Architecture of VPM and POm Axons in Rat Vibrissal Cortex. Cereb Cortex:2265–2276.

Winters WD, Kott KS (1979) Continuum of sedation, activation and hypnosis or hallucinosis: A comparison of low dose effects of pentobarbital, diazepam or gamma-hydroxybutyrate in the cat. Neuropharmacology 18:877–884.

Winters WD, Spooner CE (1964) A neurophysiological comparison of gamma-hydroxybutyrate with pentobarbital in cats. Electroencephalogr Clin Neurophysiol 18:287–296.

Winters WD, Spooner CE (1965) Various seizure activities following gamma-hydroxybutyrate. Int J Neuropharmacol 4:197–200.

Wolak DJ, Thorne RG (2013) Diffusion of macromolecules in the brain: implications for drug delivery. Mol Pharm 10:1492–1504.

Yadav P, Kroeze W, Farrell M, Roth B (2011) Antagonist functional selectivity: 5-HT2A serotonin receptor antagonists differentially regulate 5-HT2A receptor protein level in vivo. J Pharmacol … 339:99–105.

Yalçın O (2012) Genes and molecular mechanisms involved in the epileptogenesis of idiopathic absence epilepsies. Seizure 21:79–86.

Yamada Y, Yamamoto J, Fujiki A, Hishikawa Y, Kaneko Z (1967) Effect of butyrolactone and gamma-hydroxybutyrate on the EEG and sleep cycle in man. Electroencephalogr Clin Neurophysiol 22:558–562.

Zaman T, Lee K, Park C, Paydar A, Choi JH, Cheong E, Lee CJ, Shin H-S (2011) Cav2.3 channels are critical for oscillatory burst discharges in the reticular thalamus and absence epilepsy. Neuron 70:95–108.

Zhang Z, Ren Z, Huang W (2003) A novel detection method of motor broken rotor bars based on wavelet ridge. IEEE Trans Energy Convers 18:417–423.

Zhou FM, Hablitz JJ (1999) Activation of serotonin receptors modulates synaptic transmission in rat cerebral cortex. J Neurophysiol 82:2989–2999.

Zhou Q, Godwin DW, O'Malley DM, Adams PR (1997) Visualization of calcium influx through channels that shape the burst and tonic firing modes of thalamic relay cells. J Neurophysiol 77:2816–2825.